1-1-1987

Surface and interface chemistry of poly(tetrafluoroethylene)/

Christine A. Costello
University of Massachusetts Amherst

Surface and Interface Chemistry of Poly(tetrafluoroethylene)

A Dissertation Presented

By

Christine A. Costello

Submitted to the Graduate School of the
University of Massachusetts in partial fulfillment
of the requirements for the degree of

Doctor of Philosophy

May, 1987

Polymer Science and Engineering

Surface and Interface Chemistry of Poly(tetrafluoroethylene)

A Dissertation Presented

By

Christine A. Costello

Approved as to style and content by:

Thomas J. McCarthy, Chairperson of Committee

David A. Tirrell, Member

C. Peter Lillya, Member

Edwin L. Thomas, Department Head
Polymer Science and Engineering

Acknowledgements

I would like to thank my advisor, Professor Thomas McCarthy for the "butt loads" of enthusiasm, inspiration, and encouragement he provided throughout the course of this work. I also would like to thank the members of my committee, Professors Tirrell and Lillya for their help during my graduate career.

Thanks are also due to Dave Waldman for obtaining the Raman spectra in this thesis and for discussion concerning the results. Also, I would like to thank Menas Vratsanos for help in obtaining the SEI micrographs and tensile experiment data.

The talents of the glass-blowing lab are also greatly appreciated. Gordon, Larry, and Tim were extremely helpful in the design of glassware used for this research.

The members of the McCarthy group also deserve special recognition, not only for putting up with me over the past four years, but also for their help and friendship, especially through "explosive" times.

Finally, I would like to thank my parents and Rich for the their love and encouragement throughout the course of this work. Without their patience and understanding, completing this dissertation would have been impossible.

Abstract

Surface and Interface Chemistry of Poly(tetrafluoroethylene)

May, 1987

Christine A. Costello

B.S., Carnegie-Mellon University
Ph.D., University of Massachusetts at Amherst

Directed by: Professor Thomas J. McCarthy

Poly(tetrafluoroethylene) (PTFE) was surface-modified using the potassium salt of benzoin dianion in DMSO, yielding a reactive carbonaceous surface product (PTFE-C). The physical, chemical, and electronic properties of the new surface were investigated. The depth of reaction, determined gravimetrically, could be controlled from 150 Å to ~15,000 Å by varying reaction time. ESCA data, SEI micrographs and contact angle measurements indicated a physically heterogeneous reaction. UV-vis, CPMAS NMR, and ATR-IR spectroscopies indicated the presence of an extended conjugated system of sp, sp^2, and sp^3 carbons plus the existence of mobile unpaired spins. ATR-IR and Raman spectroscopy also indicated that hydrogen was incorporated into PTFE-C from the reaction solvent, DMSO, and also from water used during the workup. A series of deuterated derivatives PTFE-C indicated that a <u>trans</u> polyacetylene-like component and fluoroolefin structure was also present. PTFE-C was shown to be an electronic conductor when doped with iodine; conductivities on the order of $10^1\ \Omega^{-1}cm^{-1}$ were achieved, depending on the reaction depth.

The reactivity of PTFE-C was exploited to introduce a wide range

of organic functional groups to PTFE surfaces. These functionalized surfaces were characterized by XPS, ATR-IR, and contact angle measurements. PTFE-C was easily halogenated with either bromine or chlorine, forming PTFE-Br and PTFE-Cl. PTFE-OH was prepared by hydroboration of PTFE-C followed by treatment with H_2O_2/NaOH. The radically initiated reaction of maleic anhydride with PTFE-C yielded PTFE-COOH. Reaction of PTFE-Br with ammonia yielded PTFE-NH_2.

Metal-polymer interfaces were investigated by vapor depositing copper onto a PTFE-SH substrate prepared from the reaction of PTFE-Cl with tetrabutylammmonium thiolate. Peel force measurements indicated increased adhesion for PTFE-C and PTFE-SH.

Table of Contents

List of Tables

List of Figures

List of Schemes and Equations

Chapter I

Introduction

This introductory section will include a brief description of the motivation for this research followed by a statement of thesis objectives. The remaining sections will provide background on the chemistry and surface modification of poly(tetrafluoroethylene), latent conducting polymers, and metal-polymer interfaces. Finally, the surface analytical techniques employed in this research will be described.

Surface and Interface Chemistry of Poly(tetrafluoroethylene)

The need for the development of organic polymer surface chemistry as a scientific discipline is paramount. Phenomena such as wetting, wear, and adhesion of these materials is largely dependent on the chemistry at their surface and their interfaces.[1] Although there has been a tremendous development in surface analytical techniques in the past few years, the role of organic chemistry at polymer interfaces remains relatively unexplored. The reason for this is simple: general synthetic methods for the functionalization of polymer surfaces have not been developed. Only with well-defined surfaces can structure-property relationships be addressed.

We chose polytetrafluoroethylene (PTFE) as a substrate for a number of reasons. First, PTFE is a chemically resistant polymer; chemical transformations of functional groups attached at its surface would not affect the bulk material. Second, PTFE is easily cleaned by solvent extraction, remaining clean under ambient conditions without the use of high vacuum systems. Third, changing the wetting, adsorption, and

adhesive properties of PTFE by specific functionalization would have immediate applications in a number of areas. For example, the electronics industry is especially interested in problems related to adhesion of PTFE to metals. Metallization of PTFE would be directly applicable to the packaging technology of integrated circuits.[2] In the area of medical technology, PTFE is widely used in prostheses, sutures, and vascular grafts. Acute inflammatory reactions caused by foreign polymeric materials are believed to be caused by specific interactions of proteins at the surface of these materials.[3-5] Thus, an intimate knowledge of PTFE surface structure-property relationships should contribute to understanding problems related to its biocompatability.

Statement of thesis objectives

The primary goal of this research was to study the surface and interface chemistry of poly(tetrafluoroethylene) (PTFE). The investigation revolved around the development of a new surface modification of PTFE using benzoin dianion, which produces a reactive surface product (PTFE-C).[6] This reaction was applied to the areas of PTFE-surface functionalization, conducting polymers, and metal-polymer interfaces. The first objective of this research was the investigation of the physical and chemical properties of PTFE-C. Based on the results of the first phase of the work, the electronic properties have been investigated and we have shown that the synthesis of PTFE-C is a viable route to an electrically conducting polymer surface derived from a processable insulating material. The third objective of this research

was to introduce specific surface functionality to PTFE: hydroxyl, amino, and carboxylic acid groups. Our strategy for PTFE surface functionalization involves multistep procedures based on the reactive PTFE-C surface substrate. This reactive substrate is treated with a variety of organic reagents, effecting the introduction of specific

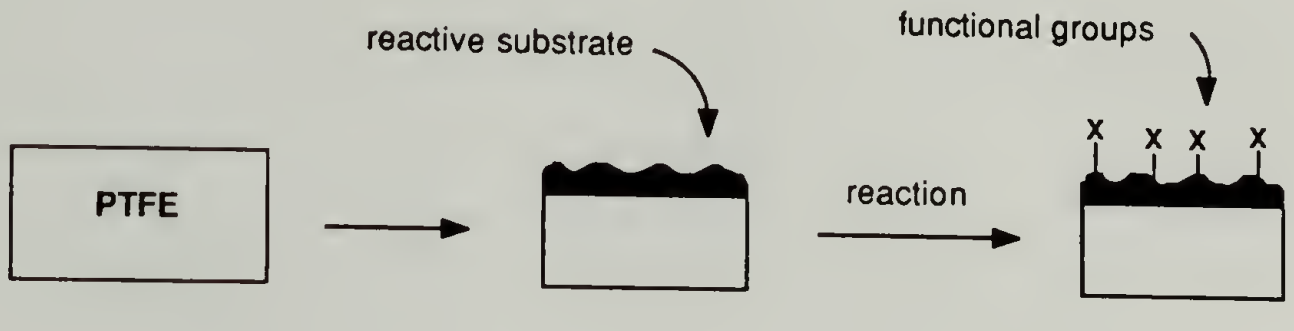

functionality. The final objective was a preliminary investigation of the structure/property relationships of a functionalized PTFE surface vapor deposited metal interface. Specifically, we investigated means of introducing sulfur functionality to PTFE surfaces via PTFE-C and studied its effect on copper-PTFE adhesion as measured by peel force measurements.

Chemistry of Polytetrafluoroethylene

Polytetrafluoroethylene is a highly crystalline, thermally stable polymer often noted for its excellent mechanical, surface, and electrical properties.[7] It is an entirely linear polymer with a room temperature density of 2.0 and 2.3 g/cm^3 for the amorphous and crystalline portions respectively. PTFE, usually synthesized by radical emulsion polymerization, is available as a granular resin (specific surface area 2-4 m^2/g), a colloidal aqueous dispersion, or a fine powder obtained by

coagulation of this dispersion (specific surface area 10-14 m^2/g). The molecular weight of the polymer is difficult to measure since PTFE is insoluble in all solvents below 300°C[8]; radioactive ^{35}S labeling experiments yielded M_n values from 400,000 to 8,900,000.[9] PTFE shows two first order transitions at 19°C and 30°C.[10] Below 19°C, a zig-zag conformation exists with a twist of 180° per 13 carbon atoms and a repeat distance of 16.9 Å. Above 19°C, the molecule shows a slight untwisting to a conformation with a 180° twist per 15 CF_2 groups and a repeat distance of 19.5 Å. This "room temperature" transition is important to a range of mechanical and viscoelastic properties.[11]

The unusual properties PTFE exhibits are consequences of its perfluorocarbon structure. Carbon-fluorine bonds are strong (116 kcal/mol)[12]; in addition, the small size of the fluorine atom aids in forming a tight protective sheath around the carbon backbone of the polymer chain. Larger substituents induce steric crowding, precluding formation of a regular, smooth skeleton; smaller substituents create gaps in the sheath. Thus reactivity of PTFE is inhibited by both the strength of the C-F bond and the physical nature of the polymer chain. In addition, intermolecular forces in PTFE are low compared to those for most polymers.[13]

One direct result of this perfluorocarbon structure is its unusual chemical inertness, even at high temperatures. Chemically, PTFE is a highly oxidized form of carbon; the most facile reaction should be reduction. The literature indicates that PTFE is reactive towards strong reducing agents, particularly alkali metals. Jansta describes a black lithium-intercalated carbon compound, $C_{4.75}Li$, which forms when PTFE is

treated with lithium amalgams.[14,15] XPS studies of this material indicate that it is reactive towards oxygen, water, nitrous oxide, ammonia, and sulfur.[16,17] EPR measurements show that the product possesses paramagnetic character.[18,19]

PTFE is similarly reduced with solutions of sodium or lithium napthalide in THF. Nelson reported enhanced adhesive bond strength with the "carbonaceous" layer formed during reduction.[20] XPS studies of this surface indicate that it is composed of only carbon and oxygen. The presence of unsaturation was demonstrated by its derivatization with bromine.[21]

Electrochemically generated intermediates are also effective reducing agents for PTFE. For example, when tetrabutylammonium tetrafluoroborate in DMF is used as an electrolyte (with or without added naphthalene) in the electrolysis of PTFE, the characteristic black carbonaceous intercalation product forms, producing a species with stoichiometry $-(-C_n-)^{-}R_4N^{+}$ where n=4-16.[22,23] The electrochemical reduction is highly anisotropic, depending on the orientation of the polymer chains at the surface which is induced by processing conditions.[24]

PTFE Surface Modifications

The surface free energy of PTFE (19 dyn/cm) is one of the lowest of any known solid material; as a result, few liquids spread on it. Because of this, much reseach has been directed at raising the surface energy. Numerous applications of PTFE exist in which its surface properties are

altered while bulk properties remain unchanged. Surface modification of PTFE can be achieved by many methods. Ion bombardment[25-27] produces topographical and chemical changes in PTFE surfaces. Plasma treatments[28] have also been utilized. Neither method introduces specific functional groups to the surface.

The most popular chemical means of PTFE surface modification are the reductions previously described. Numerous examples of the use of sodium naphthalide "etching" solution for the enhancement of PTFE wettability are found in the literature.[29,30] PTFE has also been modified by adsorption of iron pentacarbonyl followed by in situ oxidation[31]; contact angle changes indicate a change in surface properties.[32]

We originally intended to employ the product of alkali metal reductions of PTFE as the reactive substrate in our scheme for PTFE functionalization. During the course of these investigations, we discovered a milder reduction of PTFE which produced a more reactive surface substrate. Treatment of PTFE with a solution of benzoin and potassium t-butoxide in DMSO, produces a metallic gold-colored carbonaceous material. Although the mechanism is not understood, it is believed to occur via electron transfer from benzoin dianion.[33] This carbon-based polymer is reactive towards a variety of reagents, making possible the introduction of a wide range of functionality to PTFE surfaces.

Metal Polymer Interfaces

One of the more direct applications of this thesis research is in the study of metal-polymer adhesion. The nature of chemical bonding at

metal/polymer interfaces is the subject of much investigation, particularly in the field of electronics.[34] In microelectronics, thin dielectric films are needed to provide electrical isolation within and between stacked layers of metal in the multilevel structures needed for current microelectronics packaging. PTFE exhibits excellent dielectric properties for this application and has the added advantage of processibility. Poor adhesion to vapor deposited metals such as copper precludes its use in this application; vapor-deposition of copper on PTFE film forms interfaces which exhibit failure in mechanical peel force testing.[35]

Problems related to polymer metallization can be approached in a manner similar to that of polymer or small molecule adsorption to metals. Recent work indicates that inducing specific interactions enhances polymer or small molecule adsorption to metal substrates. For example, Regen[36] has demonstrated the spontaneous adsorption of thiol terminated phospholipids to gold from solution, taking advantage of specific sulfur-gold interactions. Thiol-endcapped anionically polymerized polystyrene is adsorbed to gold from THF solution in contrast to the unendcapped material.[37] Extension of this type of work to metallization of polymer surfaces may not be justified; adsorption from solution involves not only specific polymer interactions with the surface substrate, but also polymer interactions with the solvent.[38] Nevertheless, the literature contains many examples in which specific interactions (complex formation or covalent bonds) are utilized in order to enhance adhesion to vapor deposited metal. For example, polystyrene exposed to atomic oxygen in an electron beam exhibits better adhesion to vapor deposited copper, nickel,

and chromium than untreated films.[39,40] The role of oxygen-metal bond formation was substantiated by following in situ metal vapor deposition by XPS. Similar experiments on interactions of transition metals with polyimide surfaces have been reported. Cr and Ni were shown to react with carbonyl groups in the polyimide[41] but Ag and Cu were not

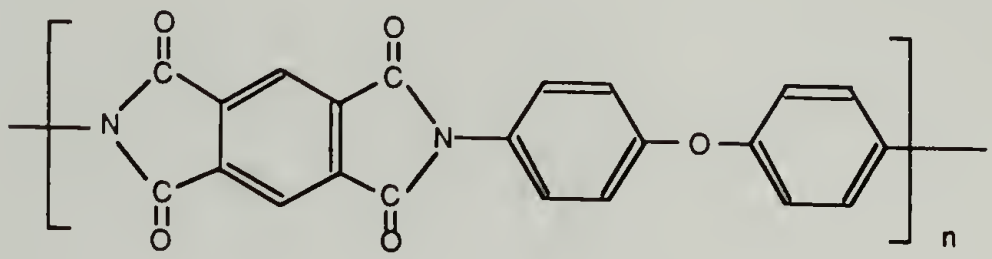

reactive as shown by XPS.[42] The reaction of aluminum vapor with polyimide surfaces has also been studied by XPS and UPS[43] and has been found to involve specific interactions with the carbonyl oxygen. Specific interactions of titanium vapor with polyimide were shown to vary depending on the extent of Ti surface coverage. At low coverage of Ti there is preferential binding between Ti metal and the carbonyl oxygen of the polyimide; as the coverage is increased, Ti-C bond formation predominates.[44]

Reactions of metal vapors with PTFE have been reported. Roberts has shown evidence for the chemical bonding of aluminum and titanium to PTFE. Evolution of a new F_{1s} peak in the XPS spectrum of a vapor deposited PTFE film was attributed to a new chemical species effecting metal/polymer joint strength.[45] Wheeler, however attributed the changes in XPS spectra to species resulting from x-irradiation damage incurred during XPS measurement.[46] It was also shown by the mass spectrum of the gas evolved during irradiation that the PTFE chains are heavily branched or cross-

linked and it was assumed that enhanced adhesion must be due to the reaction of metal vapors with these structures, even though there was no direct evidence for their existence.[47]

Though the methods and tools for probing metal-polymer interfaces have been well developed, work directed towards developing structure/property relationships is incomplete. In particular, the syntheses and characterization of polymer surfaces containing specific functional groups have not been investigated in relation to mechanical testing of the metal-polymer interface. We decided to carry out preliminary experiments in this area. The reactive surface resulting from the benzoin dianion reduction with PTFE is capable of transformation to numerous types of specific surface functionality. The introduction of sulfur functionality would enhance interactions with vapor deposited copper through Cu-S bond formation.[48] Recent work indicates that thiol groups in CH_3SH adsorb irreversibly to clean copper surfaces, losing hydrogen at 300K to form Cu-S-CH_3 bonds.[49]

Adhesive joint strength is routinely measured by peel force measurements. In these experiments, a ribbon of metal is vapor deposited on the polymer surface. The ribbon is "peeled" from the surface and the adhesive force of the joint monitored using an Instron instrument. Peel force measurements are made using various geometries:

The validity of equating this peel force with the true force of adhesion has been questioned,[50-51] but the method is still widely used.

Latent Conducting Polymers

Organic conducting polymers based on a conjugated backbone structure have been a recent research focus from both the application and theoretical points of view. The archetypical compound is polyacetylene, which upon appropriate oxidation or reduction exhibits conductivity near that of metals.[52] Although theoretically interesting, practical application of polyacetylene and other conjugated systems is limited: the inflexible planar arrangement of extended conjugation responsible for high conductivity is also responsible for the insolubility and infusibility that the polymers possess.

Solutions to this processing problem have been attempted; most attempts involve modification of the original material to a more soluble form. For example, random copolymers of acetylene with other acetylenic monomers have been synthesized.[53-55] Although solubility of these copolymers increased, the conjugation length was altered by deviations in planarity of the molecule due to the randomness of the copolymeration; poorly conducting materials resulted. Attempts at block copolymerization were made by "anionic to Zieglar-Natta transformations", producing polystyrene-polyacetylene block copolymers,[56,57] but conductivity results are not reported. Polyacetylene blocks have also been grafted from polyisoprene; the lack of conductivity observed for these polymers was attributed to the dilute nature of the polyacetylene block in the total

polymer matrix.[58]

Another solution involves the synthesis of latent conducting polymers: polymers that when reacted in some fashion (usually pyrolysis or elimination) yield extended conjugated forms. Once the precursor is processed into the desired form, it is reacted to form the intractable conducting material. Early attempts using this methodology met with limited success. Polyacetylenes synthesized by base catalyzed elimination of polyvinylchloride and polyvinylidine chloride yielded extended conjugated systems exhibiting semiconductive behavior.[59,60] More successful examples of this strategy include the Feast synthesis of polyacetylene shown below. It has been shown that by varying experimental conditions, polyacetylenes with a range of morphologies and densities can be prepared.[61,62]

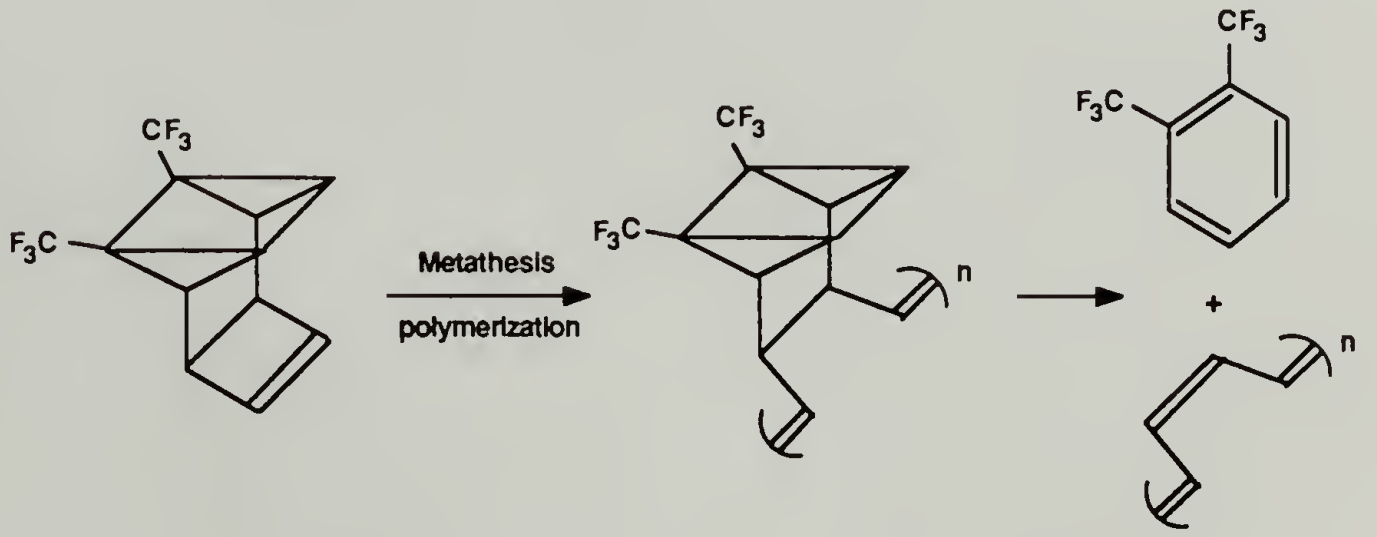

Conducting carbonaceous materials have also been prepared from the pyrolysis of polyacrylonitrile.[63] The materials exhibit graphite-like conductivity attributed to the formation of doubly conjugated ladder structures shown below:

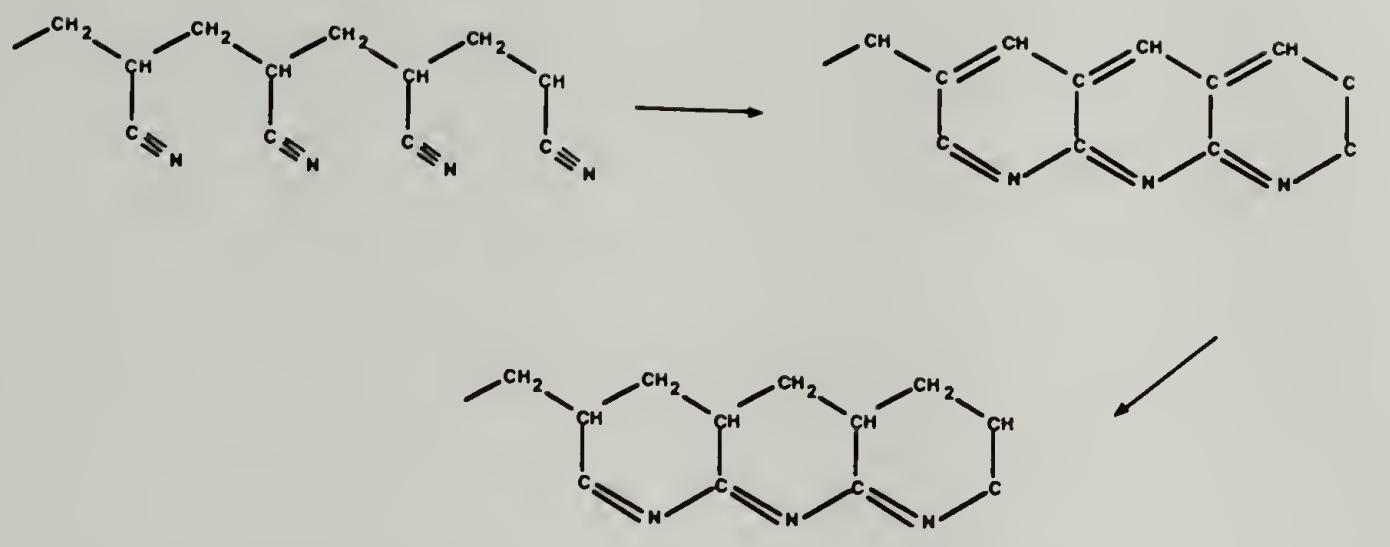

High molecular weight poly(p-phenylene vinylene) (PPV) has been synthesized via a water soluble precursor polyelectrolyte.[64,65] Hoffman elimination of **1** yielded PPV which softens during thermal treatment

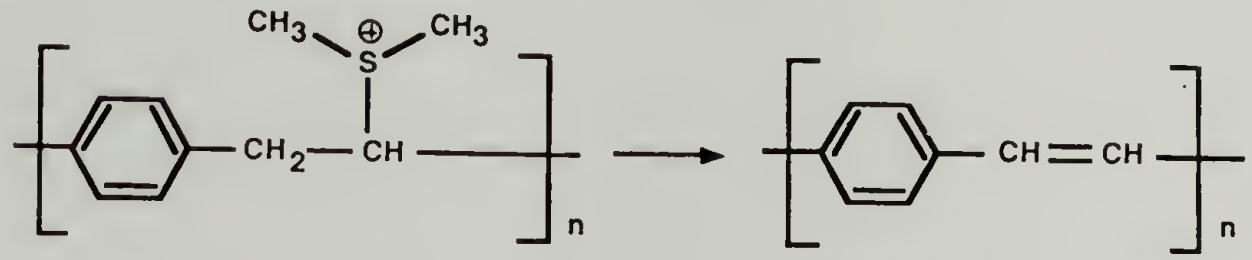

allowing stretching of the film to draw ratios of up to 15. Orienting the films during processing yielded conductivities of up to 2800 $\Omega^{-1}cm^{-1}$ in AsF_5 doped samples.[66]

The alkali metal and electrochemical reductions of PTFE described above are particularly important to the work presented in this thesis. Some discrepancies appear in the literature concerning the electronic conductivity of the carbonaceous product. For example, Yoshino reports that the electrical conductivity of lithium napthalide reduced PTFE is 10^{-5}-10^{-4} $\Omega^{-1}cm^{-1}$.[67] Nelson[68], Brewis[69], and Varma[70] however, find no conductivity for sodium napthalide reduced PTFE. Barker reports pristine

films from electrochemical reduction exhibit resistances between 10^{-1}-10^{-2} $\Omega^{-1}cm^{-1}$; the resistance increases by several orders of magnitude when the film is exposed to air, water, or, methanol.[71] We believe these data are inconsistent because 1) the salts from the reductions were not removed: ionic contributions to conductivity were not addressed and 2) the reactions were not consistently run in inert environments. Guzdar has found that while THF-rinsed sodium napthalide reduced PTFE films (synthesized under inert conditions) conduct electricity ($\sigma = 10^{-9}$-$10^{-5}\Omega^{-1}cm^{-1}$, depending on the depth of reaction), those washed in deoxygenated water exhibit no conductivity.[72] The conductivity other workers find in these materials, then, must be due to the presence of alkali metal fluoride salts which may be intercalated in the reduced layer.

Our interest in this area lies in the preparation of conducting materials from processable precursors and in the case of this research, PTFE. Our initial chemical characterization results indicated that PTFE-C produced by PTFE reduction with benzoin dianion is an extended conjugated system, capable of electronic conduction.[73] One objective of this thesis research was to study this material as an electronic conductor.

Surface Analytical Techniques

The following section briefly outlines the surface analytical techniques used in this research. The methods most frequently used were

contact angle, XPS or ESCA spectroscopy, attenuated total reflectance (ATR) infrared spectroscopy, and gravimetric analysis.

Contact Angles

Contact angle measurements yield information on the outer few angstroms of a surface. In this research, dynamic contact angles, i.e. advancing and receding, were measured using water as the probe fluid. The water drop is advanced across the surface using a Gilmont syringe fitted in a Rame Hart contact angle goniometer. The advancing contact angle is the angle θ_a indicated. The receding contact angle is measured by withdrawing water from the drop while simultaneously measuring the

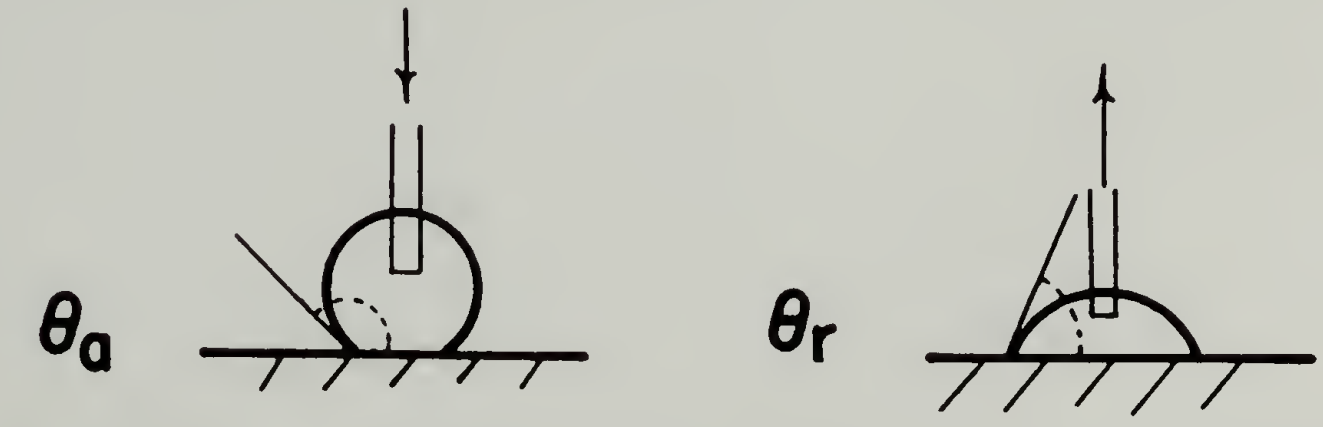

angle θ_r indicated. Low energy surfaces exhibit large contact angles (>90°), while high energy surfaces exhibit small contact angles (<90°). Some workers report equilibrium contact angles which are obtained after waiting some time for the liquid to remain stationary with respect to the solid.[74] The validity of such measurements is questionable since it has been shown that the liquid is actually evaporating; the liquid surface retracts and values close to receding values are measured as "equilibrium values."[75]

Contact angle hysteresis ($\theta_a - \theta_r$) is an important parameter

yielding information on surface roughness and chemical heterogeneity.[76] Surface roughening affects advancing and receding contact angles if the advancing contact angle on the smooth surface is above 86°.[77] There is no effect if contact angles on the smooth surface are between 60° and 80°; yet when θ_a and θ_r are below 60°, surface roughening decreases these values. There are indications that the relative amounts of low vs. high surface free energy components can be discerned by contact angle reproducibility. Poor reproducibility is observed in advancing contact angles when only a few percent of low surface free energy material is present in the outer few angstroms of the solid surface. Small amounts of high surface free energy material render poor reproducibility in receding angle values.[78]

Gravimetric Analysis

Gravimetric analysis can be used to monitor polymer surface reactions.[79] To gain useful information from this technique, one needs to know certain details about the chemical transformations such as the stoichiometry and the specificity of the reaction. The assumptions used in gravimetric analysis should be corroborated by independent chemical or spectroscopic analysis. When a reasonable amount of information is known about the nature of the chemical transformation, the gravimetric data can be related to the depth of the surface modification. For surface selective reactions, the relative mass changes are usually miniscule compared to the total mass of the polymer samples. To insure the

accuracy of the gravimetric analysis it is necessary to use sensitive analytical balances, sample geometries with high surface area/volume ratios (such as thin films or powders), and careful washing techniques.

The ideal polymer subtrate for gravimetric analysis must not be swollen by solvents or reagents; extensive swelling makes it impossible to remove these chemicals by evacuation. It is not desirable to heat the polymer under vacuum to remove excess solvent or reagent, since functional group migration into the bulk can occur at elevated temperature, making them inaccessible for subsequent surface reactions.[80]

The major disadvantage of gravimetric analysis of polymer surfaces is that it is extremely time consuming; samples must be dried on a vacuum line over a period of up to several weeks until constant weights are attained upon 3 consecutive weighings taken 24 hours apart. It may take months, then, to follow a sequence of reactions gravimetrically. Static charge buildup also causes problems, but can be remedied by introducing a polonium source to the balance and by neutralizing the charge on the polymer with a Zerostat anti-static gun.

Attenuated Total Reflectance Infrared Spectroscopy (ATR-IR)

For the organic chemist, transmission infrared spectroscopy provides a method for rapid identification and quantitation of functional groups. Internal reflection spectroscopy, described in detail by Harrick,[81,82] extends this technique to polymer surfaces. Reflection is measured from the interface between the sample surface and a high refractive index optical element yielding spectra very similar to absorption spectra. In the experiment, the IR beam establishes a standing wave in the crystal whose intensity falls off exponentially in the polymer. The depth of penetration (d_p) is the distance required for the electric field amplitude to fall to e^{-1} of its value at the surface of the sample.

$$d_p = \frac{\lambda_o}{2\pi n_1(\sin^2\theta - n^2_{21})^{1/2}}$$

where θ = angle of incidence between the radiation beam and the normal to the surface.

λ_o = wavelength of the radiation.

$$n_{21} = n_2/n_1 = \frac{\text{refractive index of the sample}}{\text{refractive index of the optical element}}$$

From the equation, it is obvious that the depth of penetration is linearly dependent on the wavelength of radiation; unlike the absorption spectrum, bands become more intense at increasing wavelength since it is representative of a larger sampling depth. Also, d_p decreases as the

angle of incidence of the radiation increases, or if the refractive index of the crystal increases, or the refractive index of the sample falls. For PTFE (n=1.35) on a 45° KRS5 crystal, d_p is 5170 Å at 3000 cm^{-1} and 10,300 Å at 1500 cm^{-1}.

Major disadvantages of ATR-IR as a surface analytical tool lie in the large sampling depths for analysis. Also, it is not very amenable to quantitative analysis since intensities of absorptions are not reproducible sample-to-sample due to variations in clamping pressure against the crystal. Methods have been developed for quantitative analysis[83] using band ratioing as an internal standard. It should also be noted that for optimal spectral contrast, the refractive indices of the sample and the crystal should be as nearly equal as possible.

X-ray Photoelectron Spectroscopy (XPS)

XPS, also referred to as Electron Spectroscopy for Chemical Analysis (ESCA), is a popular technique applied to the analysis of polymer surfaces. In this experiment, a sample is irradiated with monochromatic soft x-rays (usually either MgKα or AlKα) in an ultra-high vacuum chamber. The photons are absorbed and electrons emitted with kinetic energy given by:

$$KE = hv - BE - \theta_s$$

where hv is the energy of the photon, BE is the binding energy of the

atomic orbital from which the electron originates and θ_s is the spectrometer work function. The electrons leaving the sample are detected by an analyzer according to their kinetic energy; the XPS spectrum is a plot of the number of electrons emitted versus their respective binding energy.

Even though the mean free path of the incident photons is $\sim 10^{-4}$, the mean free path of the emitted electrons, which is dependent on kinetic energy, is much less; values are dependent on the nature of the material and usually range from 7-41 Å at a kinetic energy of 1000 eV. Efforts to obtain mean free paths in organic materials are more difficult and the results are irreproducible. The most consistent data were obtained by vapor deposition of known thicknesses of poly (p-xylylene) polymer films. Escape depths of 14 Å, 22 Å, 23 Å, and 29 Å for electrons of kinetic energy 969 eV, 1170 eV, 1202 eV, and 1403 eV respectively were obtained.[84] Thus, XPS provides a truly surface-selective technique for the investigation of polymer surfaces.

The binding energy can be considered as an ionization energy of the atom for a given shell; since there are often many shells for a given atom, there is a variety of binding energies associated with a given element. Standard spectra and charts containing each element's photoelectron lines are tabulated[85], facilitating qualitative analysis of a polymer surface. In addition, each ionization process has a different probability of occurence, referred to as photoelectric cross-section. Using the software from the PE 5000 series ESCA, the atomic percentage of any constituent of a sample is given by[86]

$$\%AC \text{ for element } X = \frac{\dfrac{I_x}{S_x T_x}}{\sum_{i=1}^{N} \dfrac{I_i}{S_i T_i}} \times 100$$

where n = number of regions (elements) surveyed

I = peak area of the 5 point smooth, baseline corrected data

S = peak area sensitivity factor

T = total acquisition time per data point

Values of S have been tabulated[85,86] for most elements. The determination of S includes consideration of photoelectric cross-sections corrected for the mean free path dependence on the kinetic energy. Quantitative analysis is usually accurate within 10-20% except when samples are physically or chemically heterogeneous. The value of S in transition metals, unlike that in other elements, varies depending on chemical state, making quantitative analysis difficult for these elements.

References

1. D.T. Clark and W.J. Feast, "Polymer Surfaces", Wiley-Interscience, New York, 1978.

2. G.M. Sessler, J.E. West, F.W. Ryan, and H. Schonhorn, J. Appl. Poly. Sci., **17**, 3199 (1973).

3. H.E. Kambic, S. Murabayashi, and Y. Nose, Chem. Eng. News, **15**, 31 (April 14, 1986).

4. S.R. Hanson, L.A. Harker, B.D. Rattner, and A.S. Hoffmann, J. Lab. Clin. Med., **95**, 289 (1980).

5. J.D. Andrade and V. Hlady, Adv. Poly. Sci., **79**, 1 (1986).

6. C.A. Costello and T.J. McCarthy, Macromolecules, **17**, 2942 (1984).

7. L.A. Wall, "Fluoropolymers", Wiley-Interscience, New York, 1972.

8. D.I. McCane in "Encyclopedia of Polymer Science and Technology", Vol. 13, Wiley, New York, (1970) p. 623.

9. K.L. Berry and J.H. Peterson, J. Am. Chem. Soc., **73**, 5195 (1951).

10. K.L. Berry and H.K. Starkweather, Adv. Poly. Sci., **2** 465 (1961).

11. G.P. Koo and R.D. Andrews, Poly. Eng. Sci., **9**, 268 (1969).

12. J. March, "Advanced Organic Chemistry", McGraw Hill, New York, p. 28.

13. See references 8 and 10.

14. J. Jansta and F.P. Dousek, Electochemical Acta, **18**, 673 (1973).

15. J. Jansta and F.P. Dousek, Carbon, **24**, 61 (1986).

16. L. Kavan, Z. Bastl, F.P. Dousek, and J. Jansta, Carbon, **22**, 77 (1984).

17. L. Kavan and F.P. Dousek, Carbon, **24**, 61 (1986).

18. L. Kavan, J. Klima, and M. Pseidlova, Carbon, **18**, 433 (1980).

19. See reference 17.

20. E.R. Nelson, T.J. Kilduff and A.A. Benderly, Ind. Eng. Chem., **50**, 329 (1958).

21. V.H. Brecht, F. Mayer, and H. Binder, Die Angew. Makro. Chem., **33**, 89 (1973).

22. D.M. Brewis, R.H. Dahm, and M.B. Konieczko, Die Angew. Makro. Chem., **43**, 191 (1975).

23. D.J. Barker, D.M. Brewis, R.H. Dahm, and L.R.J. Hoy, Polymer, **19**, 856 (1978).

24. D.J. Barker, D.M. Brewis, R.H. Dahm, and L.R.J. Hoy, J. Mat. Sci., **14**, 749 (1979).

25. R. Michael and D. Stalik, J. Vac. Sci. Tech., **A4**, 1861 (1986).

26. See reference 2.

27. R.H. Hansen and H. Schonhorn, Polymer Letters, **4**, 203 (1966).

28. A.K. Sharma and H. Yasuda, J. Vac. Sci. Tech., **21**, 994 (1982).

29. O. Cada and J. Spasova, Adhaesion, **23**, 18 (1979).

30. M. Yasaka, Japan Kokai Tokkyo Koho, JP 7953173 (1979).

31. R. Baumhardt-Nito, S.E. Galembeck, I. Joekes, and F. Galembeck, J. Poly. Sci. Chem. Ed., **19**, 819 (1981).

32. F. Galembeck, J. Poly. Sci. Poly. Lett., **15**, 107 (1977).

33. See reference 6.

34. K.L. Mittal, J. Vac. Sci. Tech., **13**, 19 (1976).

35. J. Park, C.A. Costello, T.J. McCarthy, unpublished results, this laboratory.

36. T. Diem, B. Czajka, B. Weber, and S.L. Regen, J. Am. Chem. Soc., **108**, 6094 (1986).

37. J.M. Stouffer and T.J. McCarthy, A.C.S. Prep. Poly. Chem. Div., **27**, (2) 242 (1986).

38. A.T. Hubbard, Acc. Chem. Res., **13**, 177 (1980).

39. J.M. Burkstrand, Appl. Phys. Lett., **33**, 5 (1978).

40. J.M. Burkstrand, J. Vac. Sci. Tech., **16**, 1072 (1979).

41. N.J. Chou and C.H. Tang, J. Vac. Sci. Tech., **A2**, 751 (1984).

42. N.J. Chou, D.W. Dong, J. Kim, and A.C. Liu, J. Elec. Soc., Solid State Tech., **131** 2335 (1984).

43. P.S. Ho, P.O. Hahn, J.W. Bartha, G.W. Rubloff, F.K. Leboues, and B.D. Silvermann, J. Vac. Sci. Tech., **A3**, 739 (1985).

44. F.S. Ohuchi and S.C. Freilich, J. Vac. Sci. Tech., **A4**, 1039 (1986).

45. R.F. Roberts and H. Schonhorn, Am. Chem. Soc. Div. Poly. Chem. Prep., **16**, 146 (1975).

46. D.R. Wheeler and S.V. Pepper, J. Vac. Sci. Tech., **20** 442 (1982).

47. D.R. Wheeler and S.V. Pepper, J. Vac. Sci. Tech., **20**, 226 (1982).

48. F.A. Cotton and G.F. Wilkinson, "Advanced Inorganic Chemistry", Interscience, New York, 1972, p. 906.

49. B.A. Sexton and G.L. Nyberg, Surface Science, **165**, 251 (1986).

50. J.J. Bikerman, "The Science of Adhesive Joints", Academic Press, New York, 1961, p. 182.

51. J.J. Bikermann, J. Appl. Phys., **28**, 1484 (1957).

52. J.C.W. Chien, "Polyacetylene, Chemistry, Physics, and Materials Science", Academic Press, New York, 1984.

53. J.C.W. Chien, G.E. Wnek, F.E. Karasz, J.A. Hirsch, Macromolecules, **14** 479 (1981).

54. W. Deits, P. Cukor, M. Rubner, and H. Japson, Synth. Metal, **4**, 199 (1982).

55. W. Deits, P. Cukor, M. Rubner, and H. Japson, Poly. Prep. Am. Chem. Soc., Div. Poly. Chem., **22**, 197 (1981).

56. M.E. Galvin and G.E. Wnek, Mol. Cryst. Liq. Cryst., **117**, 33 (1985).

57. F.S. Bates and G.L. Baker, J. de Physique, Colloque, **C3**, supplement au no. 6 Tome **44**, C3 (1983).

58. G.L. Baker and F.S. Bates, Macromolecules, **17** 2619 (1984).

59. F.F. He and H. Kise, J. Polym. Sci, Polym. Chem. Ed., **21** 1729 (1983).

60. E. Tsuchida, C. Shih, I. Shinohara and S. Kambara, J. Polym. Sci.:Pt.A, **2**, 3347 (1964).

61. J.H. Edwards and W.J. Feast, Polymer, **21**, 595 (1980).

62. J.H. Edwards, W.J. Feast and D.C. Bott, Polymer, **25**, 395 (1984).

63. K. Matsumura, J. Tsukamoto, A. Takahashi, and K. Sakoda, Mol. Cryst. Liq. Cryst., **121**, 329 (1985).

64. R.A. Wessling and R.G. Zimmerman, U.S. Patents 3,401,152 and 3,706,677.

65. F.E. Karasz, J.D. Capistran, D.R. Gagnon, and R.W. Lenz, Mol. Cryst. Liq. Cryst., **118**, 327 (1985).

66. I. Murase, T. Ohnishi, T. Noguchi, M. Hirooka, and S. Murakami, Mol. Cryst. Liq. Cryst., **118** 333 (1985).

67. K. Yoshino, S. Yanagida, T. Sakai, T. Azuma, Y. Iniushi, and H. Sakurai, Jpn. J. Appl. Phys., **21**, L301 (1982).

68. E.R. Nelson, T.J. Kilduff, and A.A. Benderly, Ind. Eng. Chem., **50**, 329 (1958).

69. D.M. Brewis, R.H. Dahm, and M.B. Konieczko, Makromol. Chem., **43**, 191 (1975).

70. A.J. Varma, J.P. Jog, and V.M. Nadkarni, Makromol. Chem. Rapid Commun., **1983**, 715.

71. D.J. Barker, D.M. Brewis, R.H. Dahm, L.R. Hoy, Polymer, **19**, 856 (1978).

72. Z. Guzdar, unpublished results, this laboratory.

73. C.A. Costello and T.J. McCarthy, Macromolecules, **18**, 2087 (1985).

74. S.R. Holmes-Farley, R.H. Reamey, T.J. McCarthy, J. Deutch, and G.M. Whitesides, Langmuir, **1**, 725 (1985).

75. L.S. Penn and B. Miller, J. Coll. Int. Sci., **77** 574 (1980).

76. A.W. Adamson, "Physical Chemistry of Surfaces, 4th Edition", Wiley-Interscience, New York, 1982, p. 341.

77. H.J. Busscher, A.W.J. Van Pelt, P. DeBeer, H.P. DeJong, and J. Arends, Colloids and Surfaces, **9**, 319 (1984).

78. R.E. Johnson and R.H. Dettre, "Surface and Colloid Science", Vol. 2, (Matijevic, ed.), Wiley-Interscience, New York, 1969.

79. J.A. Bonafini, A.J. Dias, Z.A. Guzdar, and T.J. McCarthy, J. Poly. Sci: Polym. Lett. Ed., **23**, 33 (1985).

80. E.M. Cross and T.J. McCarthy, unpublished results, this laboratory.

81. N.J. Harrick, "Internal Reflection Spectroscopy", Harrick Scientific Corporation, New York, 1979.

82. N.J. Harrick, J. Opt. Soc. Amer., **55**, 851 (1965).

83. F.M. Mirambella, J. Polym. Sci.:Polym. Phys. Ed., **20**, 2309 (1982).

84. C.J. Powell Surface Science, **44**, 29 (1974).

85. C.D. Wagner, W.M. Riggs, L.E. Davis, J.F. Moulder, and G.E. Muilenberg (Editor), "Handbook of X-ray Photoelectron Spectroscopy", Perkin-Elmer Corporation, Eden Prairie, Minnesota, 1979.

86. "Technical Manual: 5000 Series ESCA Systems", Perkin-Elmer, Physical Electronics Division, Eden Prairie, Minnesota. p. 4-30.

Chapter II

Experimental Procedure

Synthetic Methods

This section gives information relating to the procedures and techniques employed in the synthesis of PTFE-C and functionalized PTFE-C surfaces.

Inert atmosphere techniques

For most of the work described in this section, the manipulation of air sensitive solids, solutions, and gases is necessary to carry out the desired transformations. It became apparent as the work progressed that special precautions had to be taken to avoid contamination of films by adventitious hydrocarbons (present in the laboratory atmosphere) and silicone greases (from ground glass joints).

A comprehensive treatment of inert atmosphere techniques and apparatus is given in D.F. Shriver's book "The Manipulation of Air-Sensitive Compounds"[1]. Technical bulletins such as "How to Use Ace No-Air Glassware"[2] published by the Ace Glass Corporation, And "Handling Air-Sensitive Reagents"[3], published by the Aldrich Chemical Company, provide descriptions of techniques relating to synthesis of air-sensitive compounds. All experiments were conducted under an atmosphere of nitrogen unless otherwise noted. Prepurified grade nitrogen (Linde) was further purified by passage through columns of indicating Drierite (anhydrous calcium sulfate), phosphorous pentoxide, and BASF BTS catalyst (finely divided copper on inert support) to remove any water and oxygen, respectively. In general, liquids were transferred via cannula between

flasks by applying a slight positive pressure of nitrogen on the source flask while maintaining the receiving flask at atmospheric pressure. Solids which are sensitive to water and/or oxygen exposure were stored and manipulated in a Vacuum Atmospheres glove box. Air sensitive materials that could react with and deactivate the BTS catalyst in the drying train of the glove box were handled in a glove bag.

The vacuum line used throughout the course of this work is depicted in Figure 2.1. Solids were prepared for reaction by weighing them into flasks with $14/20 female joints and sealing with a #25 Suba-Seal (Aldrich). They were then evacuated and flushed with nitrogen using the needle connected to the luer-lock adapter pictured in the figure.

Reactions on polymer films were carried out in modified Schlenk tubes (Figure 2.2). PTFE stopcocks were used instead of ground glass joints whenever possible to avoid contamination by stopcock grease. These tubes were evacuated and flushed in a manner similar to that described above.

Virgin polymer films were stored in a clean vacuum oven at room temperature. To avoid contamination, the vacuum oven was used exclusively for the storage of virgin films. Samples were periodically checked for contamination by XPS and gravimetric analysis.

Solvents were stored under nitrogen in flasks depicted in Figure 2.2. When maintained under a positive nitrogen pressure, the flasks provide good protection from oxygen for approximately 1 month.

Some purified solid compounds and liquids in Schlenk-type storage flasks were stored in "Ball" canning jars containing Drierite as a dessicant. These jars provide an effective and inexpensive method of dry

Figure 2.1

Vacuum manifold used for air sensitive compound manipulation. Oblique valves attached to luer-lock needle adapters facilitated preparation of solids under nitrogen.

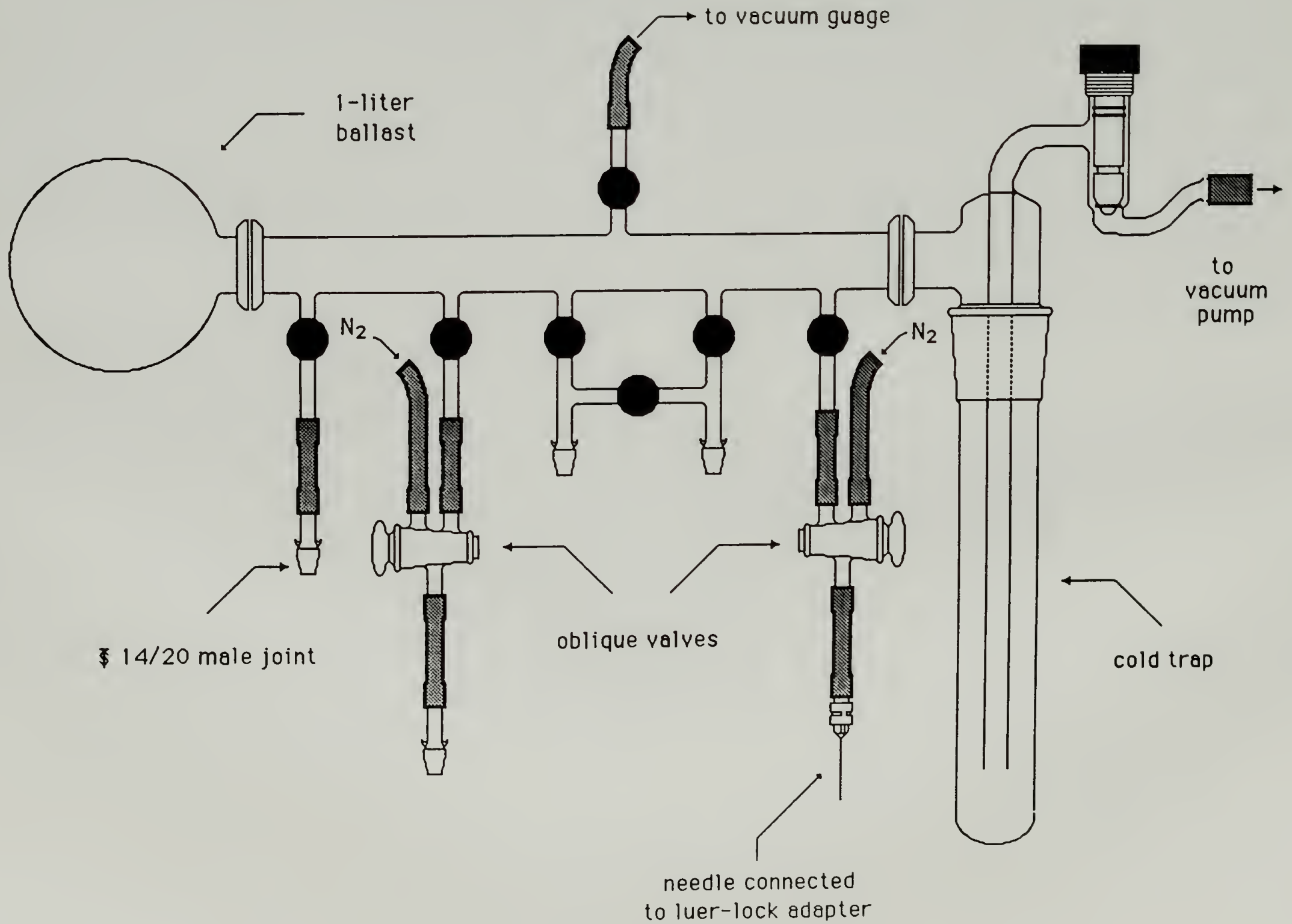
to vacuum guage
1-liter ballast
N2
N2
to vacuum pump
$ 14/20 male joint
oblique valves
cold trap
needle connected to luer-lock adapter

Figure 2.2

Schlenk reaction tube and solvent storage flask.

The distinguishing features of these tubes were the o-ring joints and Teflon stopcocks which alleviated contamination from silicone grease used in conventional ground glass joints and stopcocks.

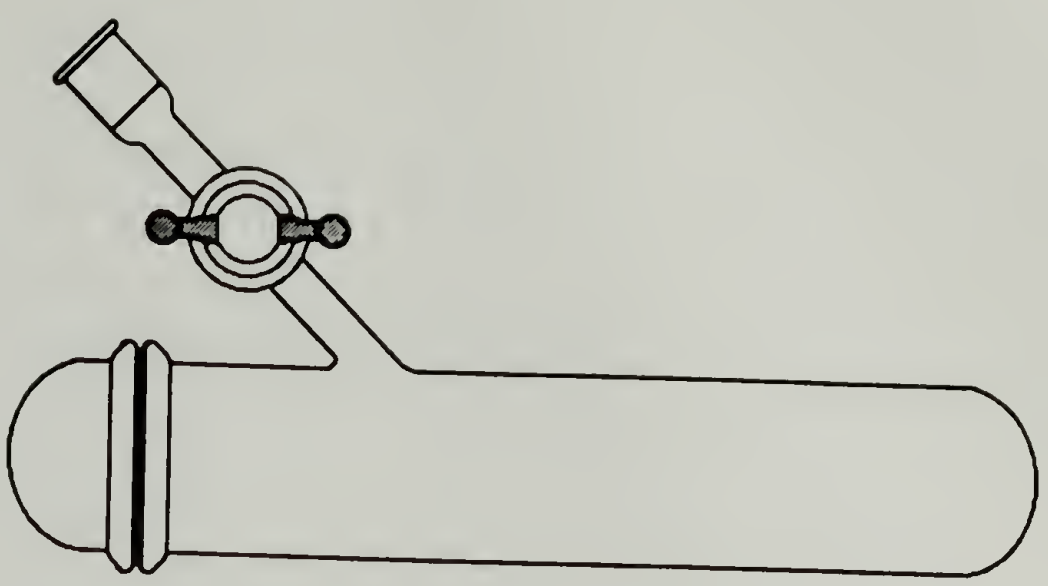

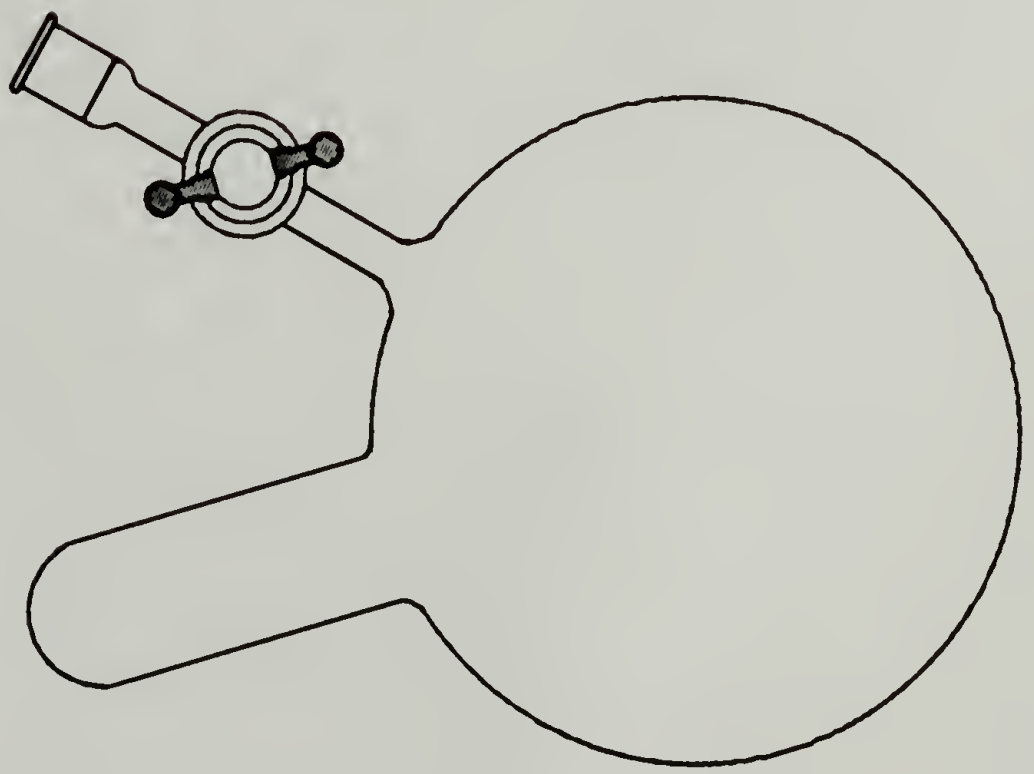

storage.

Purification of solvents

Dimethylsulfoxide (DMSO) (Aldrich) was stirred over calcium hydride (Aldrich) while sparging nitrogen through the suspension for about 1 hour, then distilled at reduced pressure and stored under nitrogen.

Tetrahydrofuran (American Burdick and Jackson, spectrophotometric grade, containing no inhibitors) was purified by distillation under nitrogen from sodium benzophenone dianion.

Heptane (Fisher, spectrophotometric grade) was distilled from sodium benzophenone dianion. Since the dianion is not soluble in heptane, bis (2-methoxyethyl)ether (Aldrich) (approximately 10% v/v) was added to solubilize the dianion.

Water was purified by double distillation in a Gilmont still followed by deoxygenation by purging with nitrogen for 1 hour per each 100 ml. Alternatively, water could be purified by distillation at reduced pressure. Either deoxygenation method was suitable for the work described.

Dichloromethane (Fisher, spectrophotometric grade) was purified by distillation under nitrogen from phosphorous pentoxide.

Carbon tetrachloride (Fisher, spectrophotometric grade) was distilled under nitrogen from phosphorous pentoxide.

Ethanol (Pharmco, dehydrated) was refluxed over magnesium turnings under nitrogen for 6 hours, then distilled under nitrogen. Ethanol used in ESCA tagging reactions was purified by distillation from from 2,4-dinitrophenylhydrazine to remove carbonyl impurities, followed by

fractional distillation under nitrogen.

N-methylpyrrolidinone (Eastman, spectrophotometric grade) was distilled under reduced pressure from phosphorous pentoxide and stored under nitrogen.

Dimethylformamide (Fisher, spectrophotometric grade) was distilled under reduced pressure from barium oxide and stored under nitrogen.

Mesitylene (Aldrich) was distlled from calcium hydride under reduced pressure and stored under nitrogen.

Benzene (Aldrich) was distilled from calcium hydride and stored under nitrogen.

Purification of reagents

Polytetrafluoroethylene film (Commercial Plastics/Dupont Teflon - 5 mils in thickness), PTFE powder (Polysciences #1344, 500 micron chromatographic), and PTFE films (Berghoff - 1/16" thickness) were extracted in a Soxhlet extractor with THF for 24h, then dried in a vacuum oven (10^{-3} torr) at 60°C. Drying was continued until successive weighings of the sample were within $\pm$ 0.001 mg.

Benzoin (Aldrich) was recrystallized twice to a constant melting point of 133.5-134.0 °C from 95% EtOH and stored in a dessicator.

Potassium t-butoxide (Aldrich) was sublimed using the apparatus depicted in Figure 2.3. Crude potassium t-butoxide was packed into the bottom of the Schlenk tube, then glass wool was packed on top. The tube

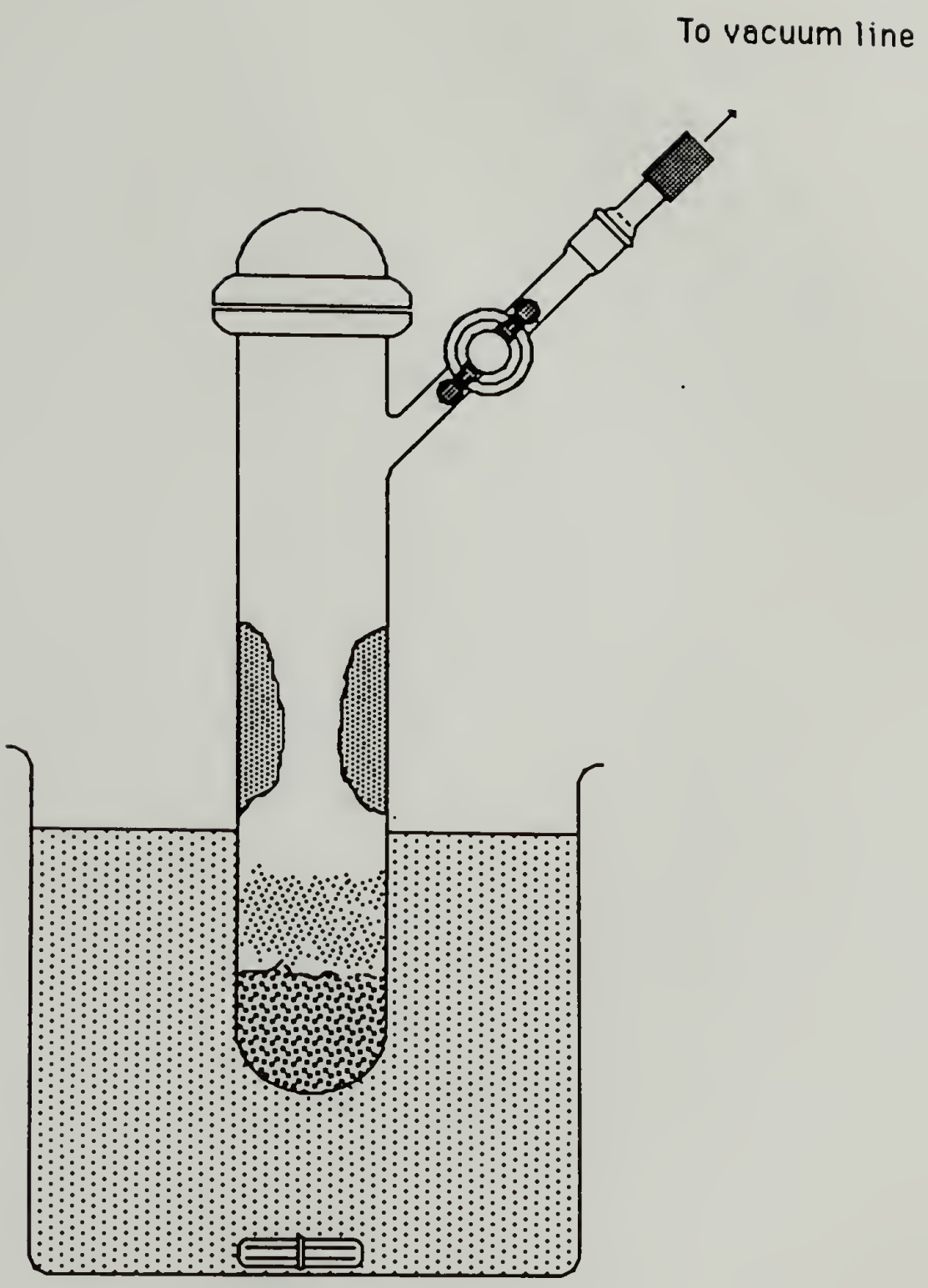

Figure 2.3

Sublimation of potassium t-butoxide. Base was sublimed at 165°C (silicone oil bath temperature) onto the walls of the Schlenk reaction flask.

was then immersed in a silicon oil bath until the level of the oil was just above the glass wool. When the oil bath was heated to 165°C (higher temperatures cause extensive degradation) under full vacuum (10^{-3} torr), the base condensed on the wall of the tube above the oil immersion level. Typically, about 8-12 hours were required to collect 3-5 g of pure base. After sublimation, the purified base was stored and manipulated in the glove box.

Chlorine (Linde) was passed through a fine sintered glass filter packed with glass wool to remove particulate matter. The gas was transferred through PTFE tubing fitted with stainless steel Swagelock adapters and a stainless steel needle.

Bromine (Fisher) was dissolved in CCl_4 (0.2M) and degassed on the vacuum line using three successive freeze-pump-thaw cycles. The solution was stored under nitrogen in the dark at 4°C.

Maleic anhydride (Aldrich) was recrystallized twice from chloroform and stored in a dessicator filled with indicating Drierite.

2,2'-Azobisisobutyronitrile (Aldrich) was recrystallized twice from methanol and stored in a dessicator filled with indicating Drierite at 4°C.

Ammonia (USX) was condensed under a nitrogen stream onto sodium in a Schlenk tube cooled to -76°C, then warmed to room temperature and distilled into a receiving trap cooled to -196°C.

Trifluoroacetic anhydride (Alfa) was degassed on the vacuum line using three successive freeze-pump-thaw cycles and stored under nitrogen.

Trifluoroacetic acid (Aldrich) was degassed on the vacuum line using

three successive freeze-pump-thaw cycles and stored under nitrogen.

Heptafluorobutyryl chloride (Alfa) was distilled at reduced pressure trap-to-trap and stored under nitrogen.

Pyridine (Aldrich) was distilled under nitrogen from calcium hydride.

Succinic anhydride (Aldrich) was sublimed at 1 mm of Hg pressure (oil bath at 98°C) and stored in the glovebox.

Pentafluorobenzaldehyde (Aldrich) was degassed on the vacuum line by three successive freeze-pump-thaw cycles and stored under nitrogen.

Acetic acid (Aldrich) was distilled from phosphorous pentoxide under nitrogen.

Dimethyacetylenedicarboxylate (Aldrich) was washed with 2N $NaCO_3$, then with calcium chloride. It was dried over $MgSO_4$, distilled at reduced pressure, and stored under nitrogen.

Oxalyl chloride (Aldrich) was distilled under nitrogen.

Formic Acid (Aldrich) was deoxygenated on the vacuum line by three successive freeze-pump-thaw cycles, then stored under nitrogen.

Benzaldehyde-d_6 (ICN Biomedicals) was washed with 10% $NaCO_3$ in D_2O, dried over $MgSO_4$ and distilled at reduced pressure through a short path column. The pure benzaldehyde-d_6 was stored under nitrogen at 4°C in the dark.

Thiolacetic acid (Aldrich) was distilled at reduced pressure trap-to-trap and stored under nitrogen.

Ethanethiol (Aldrich) was distilled at reduced pressure trap-to-trap and stored under nitrogen.

Carbon disulfide. Carbon disulfide (Aldrich) was shaken first with

mercury, then with cold saturated $HgCl_2$ solution, then finally with cold saturated $KMnO_4$. After drying over phosporous pentoxide, it was distilled under nitrogen and stored at 4°C in the dark.

Benzoyl peroxide (Aldrich) was recrystallized by dissolving it in chloroform and then adding an equal volume of methanol to the solution. The crystals were collected on a Buchner funnel and stored at 4°C in the dark.

3,5-Dintrobenzoyl chloride (Aldrich) was recrystallized from petroleum ether (fraction boiling at 50°C).

Sulfur dichloride (Aldrich) was purified by the method outlined below. As received, sulfur dichloride exists as an equilibrium mixture of sulfur dichloride, sulfur monochloride, and chlorine gas. Since the equilibrium concentrations of sulfur monochloride and chlorine are appreciable, especially at the boiling point of sulfur dichloride, distillation is ineffective at separating the components. Roser and Whitt[4] have reported a procedure whereby the sulfur dichloride is stabilized by the addition of either PCl_3 or PCl_5 during fractional distillation into a cooled receiving flask (-78°C). Using the distillation apparatus depicted in Figure 2.4, a solution of approximately 5 ml PCl_3 in 70 ml SCl_2 was poured into the pot by introduction through the thermometer joint. A stream of nitrogen was continuously blown over the system. When the system was heated to reflux up the helix packed column, but not above the thermometer bulb, chlorine gas was evolved and carried from the system by the nitrogen stream. By visual inspection it was obvious when all the chlorine was depleted from the system.

Figure 2.4

Distillation of sulfur dichloride. Sulfur dichloride stabilized with PCl_3 was refluxed up the glass helix-filled column. Chlorine was entrained by a stream of nitrogen until it was visually depleted. The sulfur dichloride was then fractionally distilled into a Schlenk tube equilibrated at -78^{o}C containing a PTFE-C film.

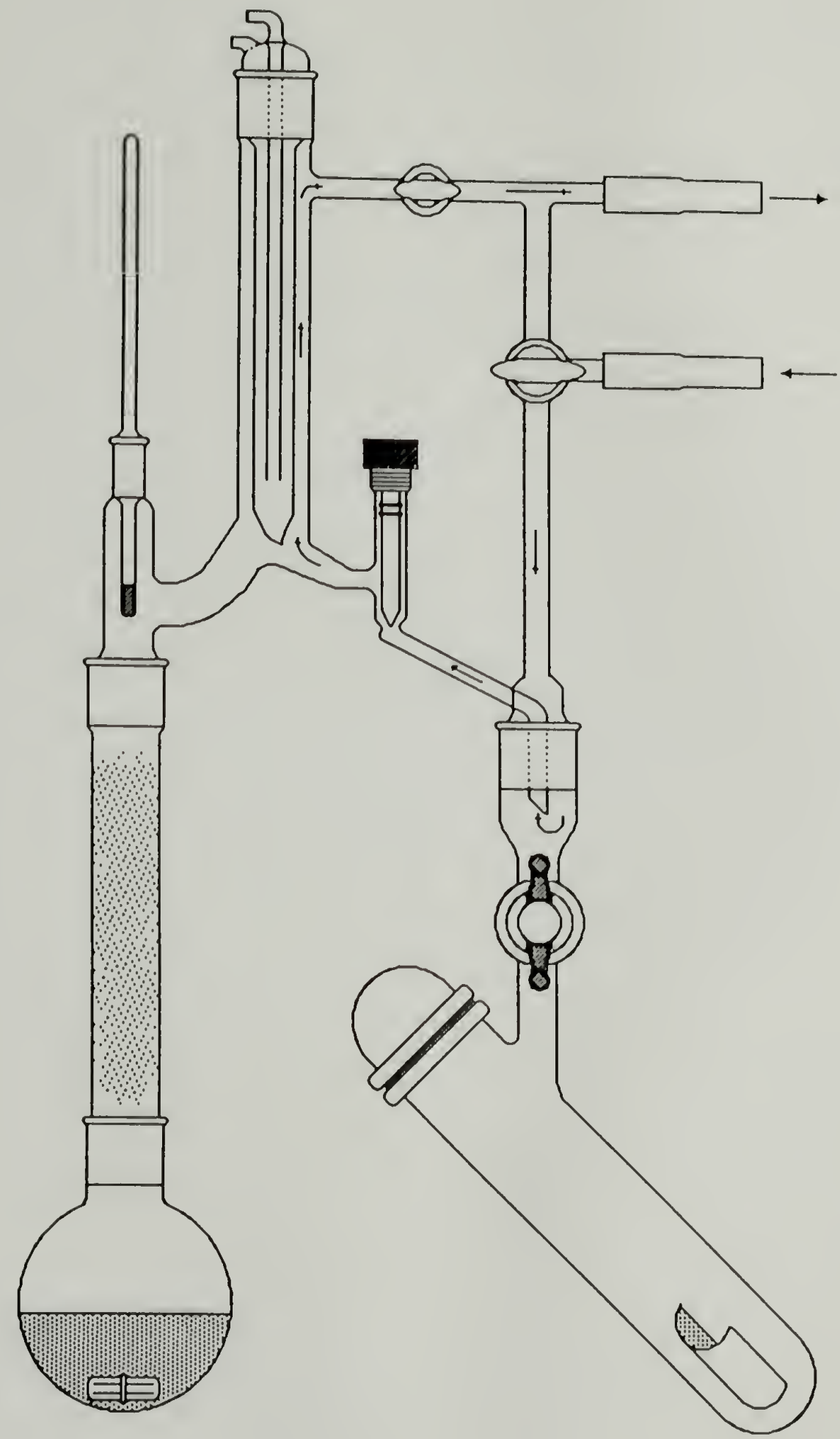

Increasing the heating rate affected the distillation rate of sulfur dichloride, which was collected onto a film contained in a cooled Schlenk tube. For some experiments, the sulfur dichloride was collected in a cooled receiving flask containing cyclooctene and PCl_3.

Styrene (Aldrich) was distilled from calcium hydride at reduced pressure and stored under nitrogen.

Other reagents used without further purification. The following reagents were used as received:

Borane-tetrahydrofuran complex (1.0M, Aldrich)
Aluminum chloride in nitrobenzene (Aldrich)
Sodium hydrogen sulfide (Alfa)
Tetrabutylammonium bromide (Aldrich)
Hydrogen peroxide (30% VWR)
Sulfuric acid (concentrated, Fisher)
Carbonyldiimidazole (Sigma)
Tetracyanoethylene (Aldrich)
Potassium chlorate (Alfa)
2,5-Dichlorophenylhydrazine (Aldrich)
2,4-Dinitrophenylhydrazine (Aldrich)
p-iodoaniline (Aldrich)
Chromium trioxide (Fisher)
Ammonium hydroxide (Fisher)
Sulfur (Fisher)
Methyllithium (1.7M in ether, Aldrich)
Calcium hydride (Aldrich)
m-chloroperbenzoic acid (MCPBA) (Aldrich)
Naphthalene (Aldrich)

Instrumentation and Techniques Employed

This section describes the instrumentation used to carry out characterization of polymer surfaces and the specific techniques employed in sample preparation and handling.

Gravimetric analysis. Gravimetric analyses were performed with a Cahn 29 electrobalance stabilized against static charging with a polonium source. PTFE samples (1 cm x 1 cm) were stored in a Schlenk tube under vacuum (10^{-3} torr) until just prior to weighing. They were removed with tweezers, cleaned of dust by blowing Freon (Dust-off, Polysciences) over them, and charge neutralized with a Zerostat anti-static instrument (Aldrich). The balance is accurate to $\pm 0.2 \mu g$; we estimate that our results are accurate to $\pm 1 \mu g$. It is important to remove all traces of volatile material from the bulk of the sample for accurate gravimetric results. Generally, samples were pumped down until a constant mass was obtained on three consecutive weighings taken 24 hours apart. In most cases, constant mass was achieved in a few days, but in some instances several weeks of pumping were necessary. Several PTFE films of known mass were stored with experimental samples and were weighed at the same time to check for possible contamination in storage and handling. In some cases where functional group migration was not a concern, gentle heating was used to accelerate the removal of excess solvent.

Elongation and scanning electron microscopy. Tensile specimens were cut from ASTM "dogbone" patterns, extracted, and reduced as described below for 12 hours. Control samples and PTFE-C were elongated with an Instron TT-BM tensile tester to 300% elongation. Samples were gold sputter-coated and secondary electron images were obtained using an ETEC autoscan scanning electron microscope.

Solid-state CPMAS NMR. A 10 cm X 10 cm PTFE film sample was reduced as described on page 54 for six days, rolled up and inserted into the

Kel-F spinner under nitrogen. Spectra were obtained on an IBM/Bruker 200-AF instrument with solids accessory operating cross-polarized with matching Hartmann/Hahn conditions at 50 KHz. The protons were irradiated with a 90^{o} pulse for 5 microseconds. The contact time (cross polarization) was 2 milliseconds. 5081 scans were collected.

Contact angle measurements. Contact angle measurements were obtained with a Rame-Hart telescopic goniometer equipped with a Gilmont syringe. Doubly distilled water was used as the probe fluid in all measurements. The pH of the water varied from 5 to 7, but no variation of contact angle was found within this range. Dynamic advancing and receding angles were determined by measuring the angle formed between the polymer surface and the tangent of the air/drop interface at the surface while adding (advancing) and withdrawing (receding) water to and from the drop (Figure 2.5). It should be noted that the 5 mil PTFE films used contained grain lines formed during processing. Contact angles of virgin PTFE measured against this grain tended to skip while those measured with the direction of the grain were reproducible.

X-ray photoelectron spectroscopy. XPS spectra were obtained on a Perkin Elmer-Physical Electronics 5100 ESCA spectrometer. Spectra were obtained using a MgK source at 15kV and 300 watts power. The pressure in the analysis chamber was 10^{-8} to 10^{-9} torr during data acquisition. The chemical shifts reported are approximate as the spectra were not corrected for sample charging. Survey spectra, atomic composition data, and high resolution spectra were recorded with pass energies of 89.95,

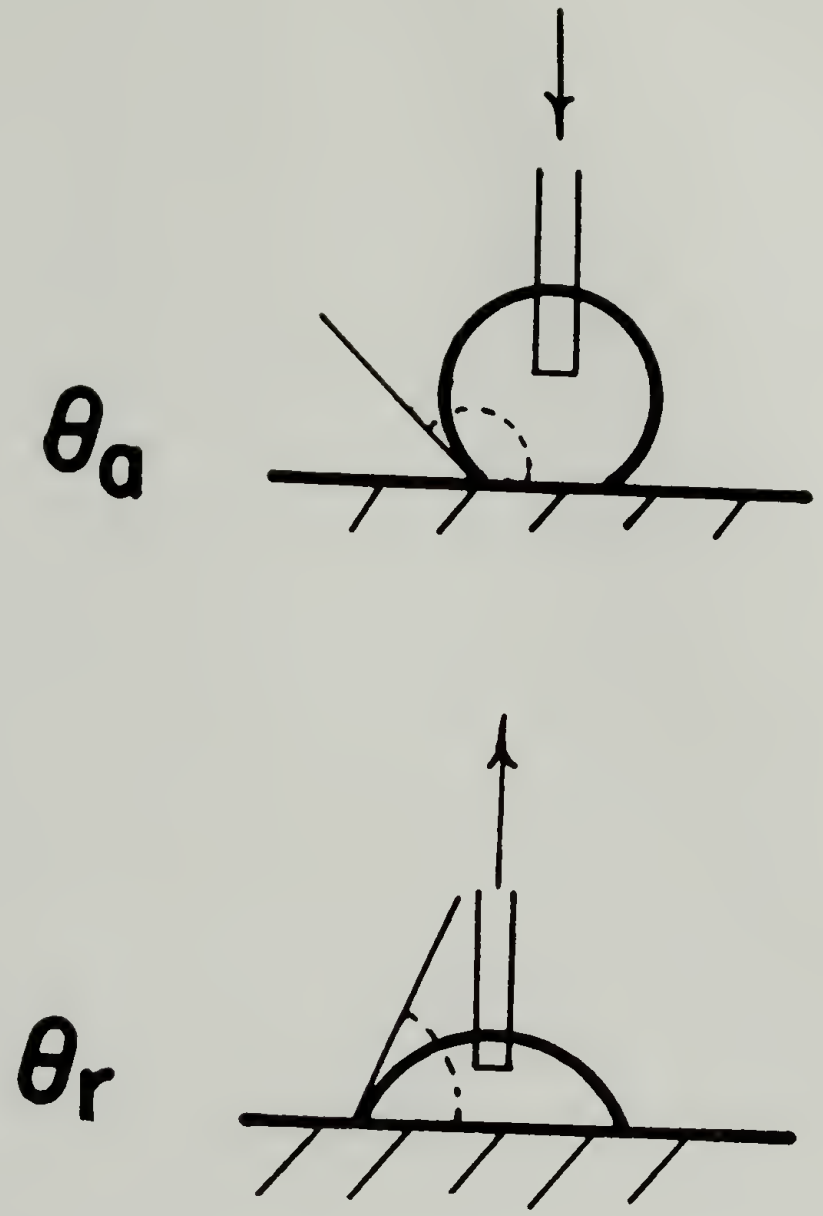

Figure 2.5

Contact angle measurements. Advancing and receding contact angles of water on a smooth surface are depicted.

71.52, and 7.44 eV, respectively. The samples were mounted in the glove box and transferred to the nitrogen-purged antechamber using Schlenk technique. Atomic composition data was determined using the instrument's computer and programmed sensitivity values.

Attenuated total reflectance IR spectroscopy. ATR-IR spectra were obtained using either an IBM-98, Perkin Elmer 283, or IBM-32 spectrometer and a 45° KRS-5 (thallium bromide iodide) crystal. The spectra recorded on the IBM-98 were obtained under vacuum and ratioed against the spectrum of the crystal backed with aluminum foil. It was necessary to accumulate 512 to 2000 scans to obtain acceptable signal to noise ratios. Spectra recorded on the Perkin Elmer 283 or the IBM-32 were obtained under nitrogen. Spectra recorded on the IBM-32 were ratioed against spectra of the crystal.

Raman spectroscopy. Raman spectra were recorded on a Jobin-Yvon Ramanor H6 25 laser Raman Spectrometer with argon (5145 Å) and helium (6328 Å) lasers. Reduced samples were transferred in the glove box to glass tubes which were then sealed under vacuum. Figure 2.6 depicts the glassware used for sealing tubes under vacuum.

EPR spectroscopy. EPR spectra were obtained with a Varian E109 Spectrometer with a TE-102 cavity. Reduced powders were packed into quartz EPR tubes in the glovebox and sealed under vacuum as is pictured in Figure 2.6. Variable temperature EPR data were obtained using a liquid nitrogen-cooled cavity warmed to the desired temperature by the heater contained in the spectrometer.

UV-vis spectroscopy. UV-vis spectra were recorded using a Perkin-Elmer Lambda 3A spectrophotometer. Two 5 mil PTFE films were selected so

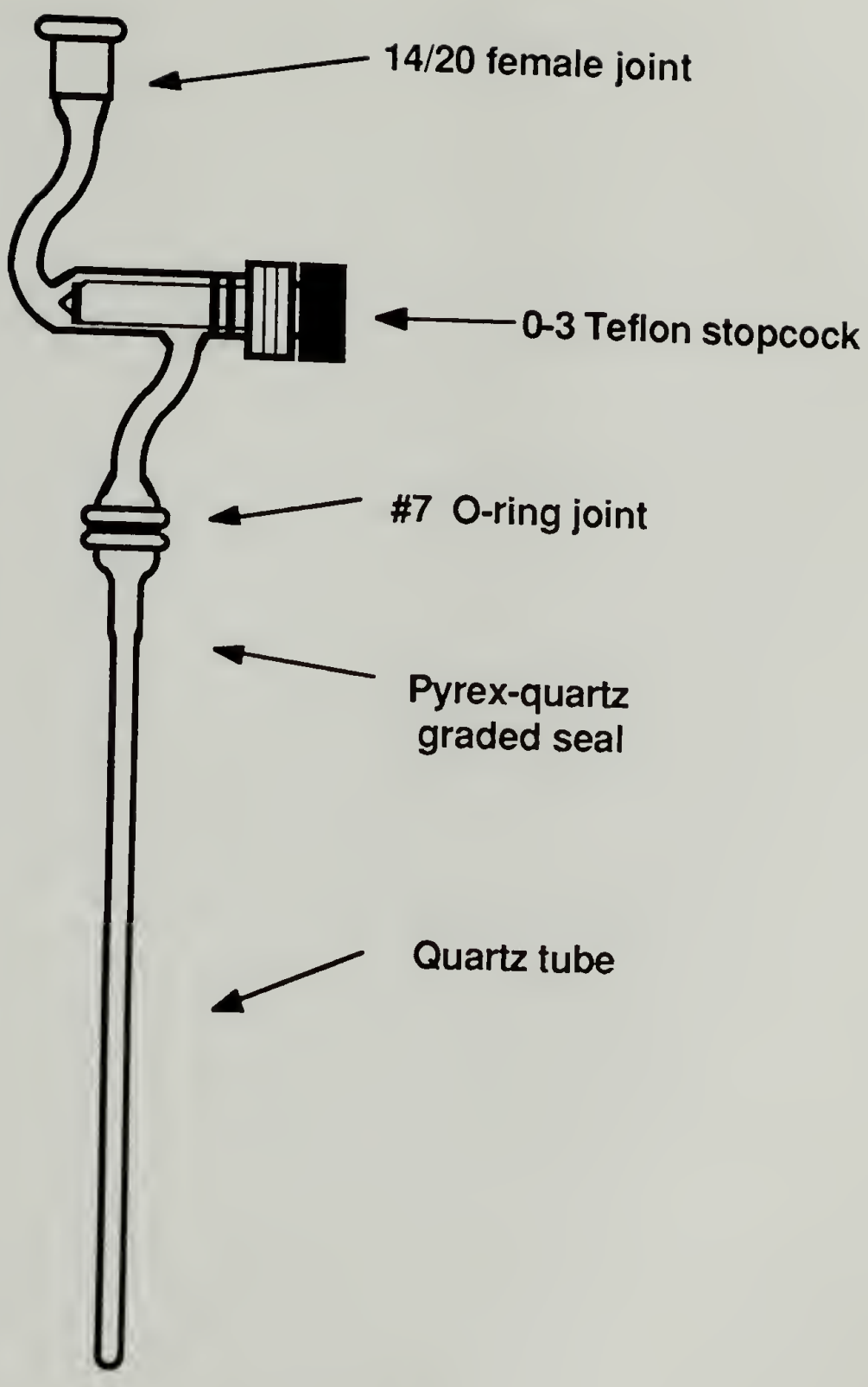

Figure 2.6

Tubes used for sealing Raman and EPR samples.

Tubes for Raman samples were regular Pyrex glass;

those for EPR samples were quartz.

that a flat baseline was exhibited when one was placed in the sample beam and one in the reference beam. After one of the film samples was reduced for 8 hours, its spectrum was recorded in air with the unreacted film in the reference beam.

Electrical conductivity measurements.

This section describes the techniques used to measure the electronic conductivity of PTFE-C and doping methods. Most of the procedures are based on techniques which are used widely in the field of conducting polymers.

Determination of conductivity

The conductivity of a solid material can be determined by measuring the resistance of a sample of known dimensions. The sample resistance is inversely proportional to the cross sectional area of the sample perpendicular to the direction of the current flow and is directly proportional to the distance that the current traverses. If the resistance of the sample is multiplied by the cross sectional area and then divided by the distance the current travels, then the <u>resistivity</u> of the sample is obtained. The resistivity is a physical quantity which is characteristic of a material and independent of the sample geometry. The conductivity of the material is the reciprocal of the resistivity.

The conductivity of PTFE-C was measured in an apparatus depicted in Figure 2.7. The films were mounted to free-standing platinum wires with conducting cement made of colloidal graphite in methyl ethyl ketone (Electrodag 502, Acheson). Figure 2.8 depicts a close-up view of a

mounted polymer film. It is important that no cement be applied between the two wires. Electrical contact was made through copper wires immersed in pools of mercury that surrounded the point where the platinum wires fed through the glass fingers. The resistance was measured on a Fluka multimeter and the conductivity determined by the following formula:

$$\sigma = \frac{\text{length}}{\text{width (cm) x thickness (cm) x resistance } (\Omega)}$$

The length **l** between the wires was taken to be the distance of current travel through the sample. The thickness of the conductor was taken to be the depth of reaction as determined by gravimetric analysis. (See Results and Discussion) The length **l**, and width **w** were measured with a vernier caliper.

Doping Methods.

Doping experiments were carried out in the apparatus depicted in Figure 2.7. PTFE-C films were mounted in the glove box with Electrodag which was deoxygenated by three freeze-pump-thaw cycles. Iodine, dried by trap-to-trap azeotopic distillation with dry heptane, was cooled to -196°C and evacuated for 0.5 hour immediately before every doping experiment. After the chamber containing the mounted film was evacuated for 1 hour, the resistance of the pristine PTFE-C was measured. The conductivity apparatus was then closed from the vacuum and the film was exposed to the iodine vapor. Resistance readings were then taken every 5 minutes until a minimum value was obtained. In most cases, this occurred within 30 minutes. On doping, PTFE-C changes in appearance from metallic

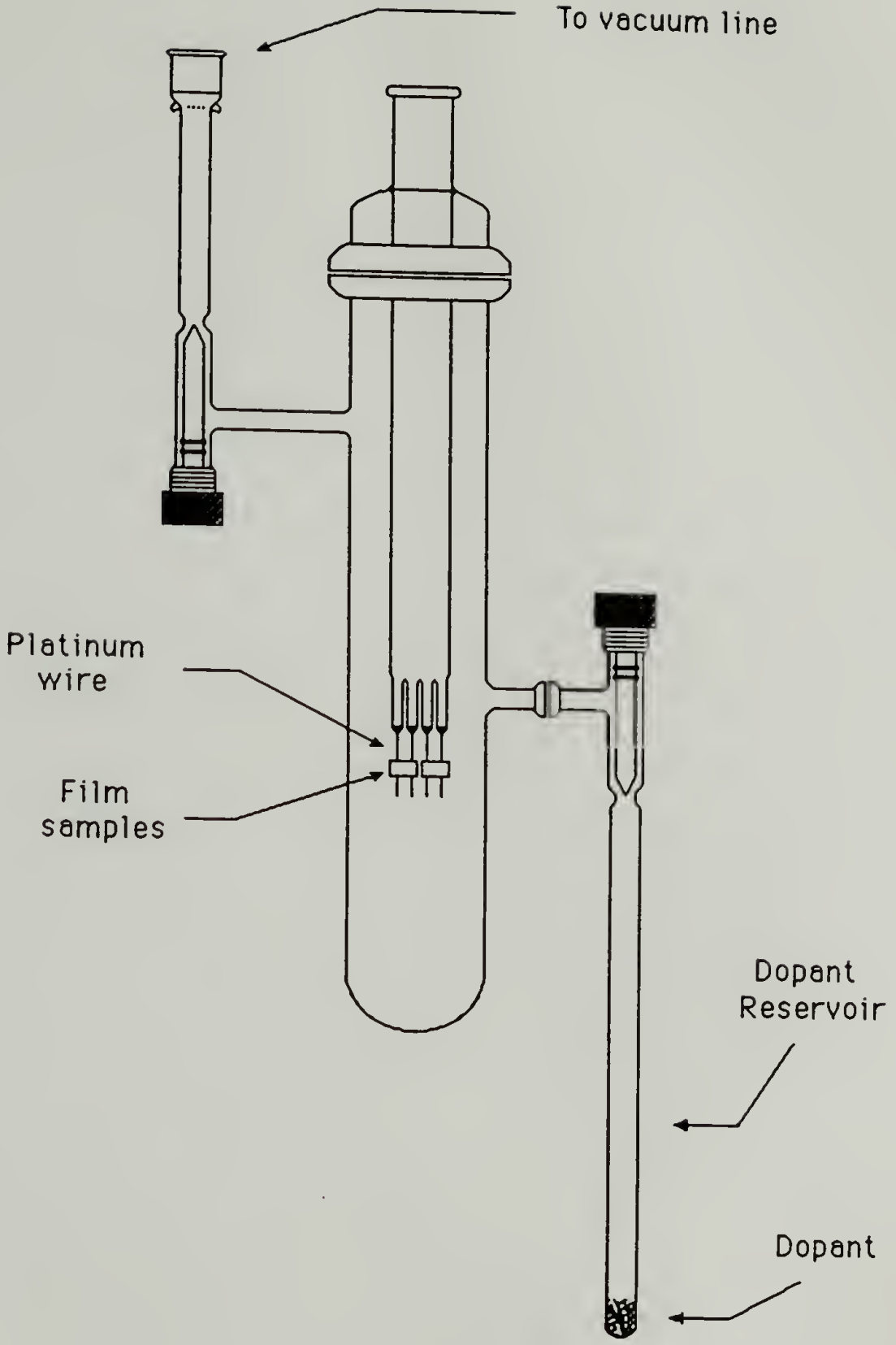

Figure 2.7

Apparatus for measuring conductivity of PTFE-C film samples. Resistance was measured as the sample was doped with iodine.

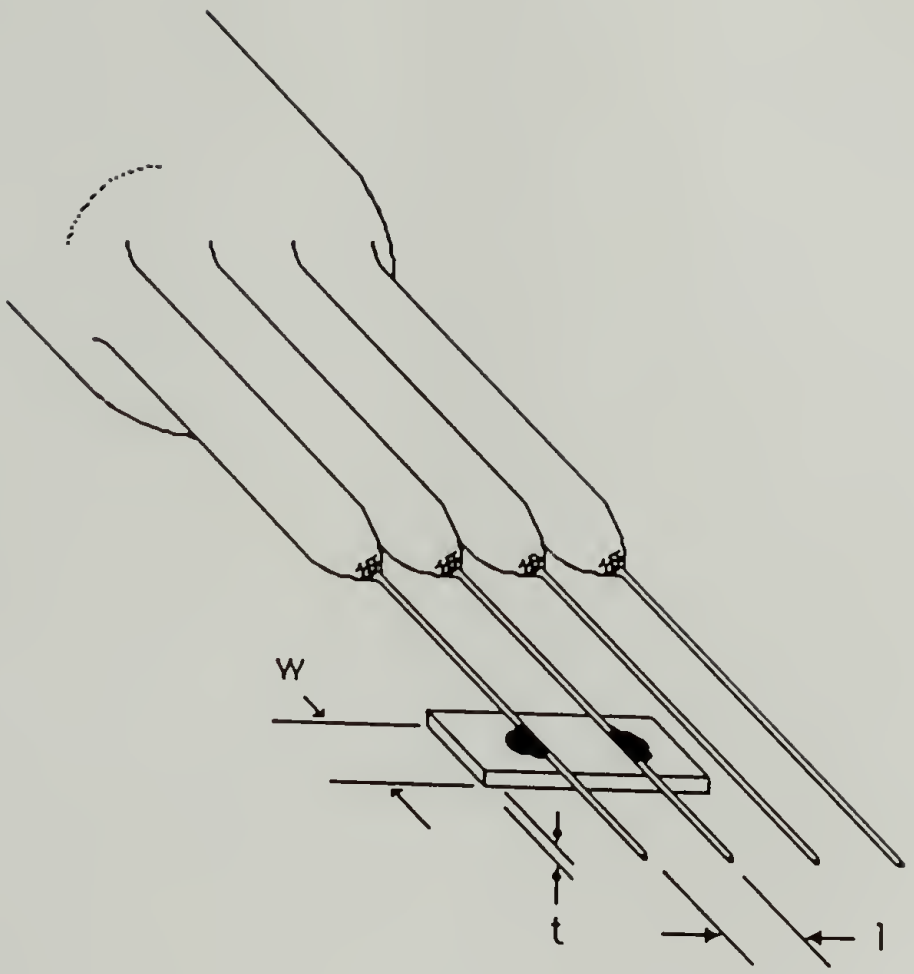

Figure 2.8

Close-up view detailing mounting of a film to the platinum wires. Cross sectional area was measured using the dimensions shown; the current path was taken to be the distance between the wires.

gold to metallic black.

After completion of the doping experiment, the doped films were removed for oxidation and gravimetric analysis. The PTFE-C and residual Electrodag were removed by oxidation with a solution of potassium chlorate in sulfuric acid. After oxidation, the films were washed with copious amounts of water and THF and evacuated to a constant weight.

Temperature dependence of conductivity

The temperature dependence of conductivity is often given by the Arrhenius expression

$$\sigma = \sigma_o + \exp[E_{act}/kT]$$

where sigma is the conductivity, T is the temperature in Kelvins, and k is the Boltzmann constant (8.61×10^{-5} eV/K). Taking the log of both sides, the expression

$$0.414 \log \sigma = \text{constant} + 0.414\ E_{act}(1/T)$$

is obtained. If the conduction process follows the Arrenhius relationship, then its energy of activation can be calculated from the slope of a plot of log σ versus 1/T.

The temperature dependence of conductivity of PTFE-C was measured using a Helitran (Air Products model #LT-3-110) liquid transfer refrigerator using a modified model WMX DMV-1 vacuum shroud containing the two-probe conductivity apparatus. Since the equipment configuration

made it impossible to dope the sample while mounted on the Helitran, it was necessary to perform the doping prior to taking conductivity measurements. Doping was carried out in the apparatus pictured in Figure 2.9. In these doping experiments, iodine was introduced into the sample chamber for 1.5 hours and the excess iodine pumped off overnight. The doped film was mounted on the Helitran two-probe apparatus in the glove box. The entire apparatus was then evacuated for 6 hours before making the conductivity measurements. The system was cooled to -196°C, and resistance recorded when the sample reached thermal equilibrium (as indicated by constant resistance reading). The system was heated in 20° increments, taking resistance readings only when thermal equilibrium was obtained. In most cases, it took approximately one hour for equilibrium to be reached.

Iodine doping of PTFE-C for iodine uptake experiments. (IV:57) Iodine uptake by PTFE-C films was measured by gravimetric analysis. PTFE-C films (reduced for 12 hours) measuring 2 x 3 inches were doped with iodine for 0.5 hours in the apparatus pictured in Figure 2.9. The excess dopant was removed by cooling the dopant reservoir with a liquid nitrogen trap. The films were then weighed at ambient conditions. After oxidation by potassium chlorate in sulfuric acid, the films were rinsed in water and THF, then pumped down to a constant mass in order to determine iodine uptake per mole of PTFE lost in the reduction.

Sodium naphthalide/THF doping of PTFE-C (IV:19) Napthalene (0.50 g) was weighed into a 200 ml round bottom flask, evacuated and flushed with nitrogen three times, then dissolved in 100 ml THF which was introduced by cannula. Sodium was cut into another round bottom flask which was

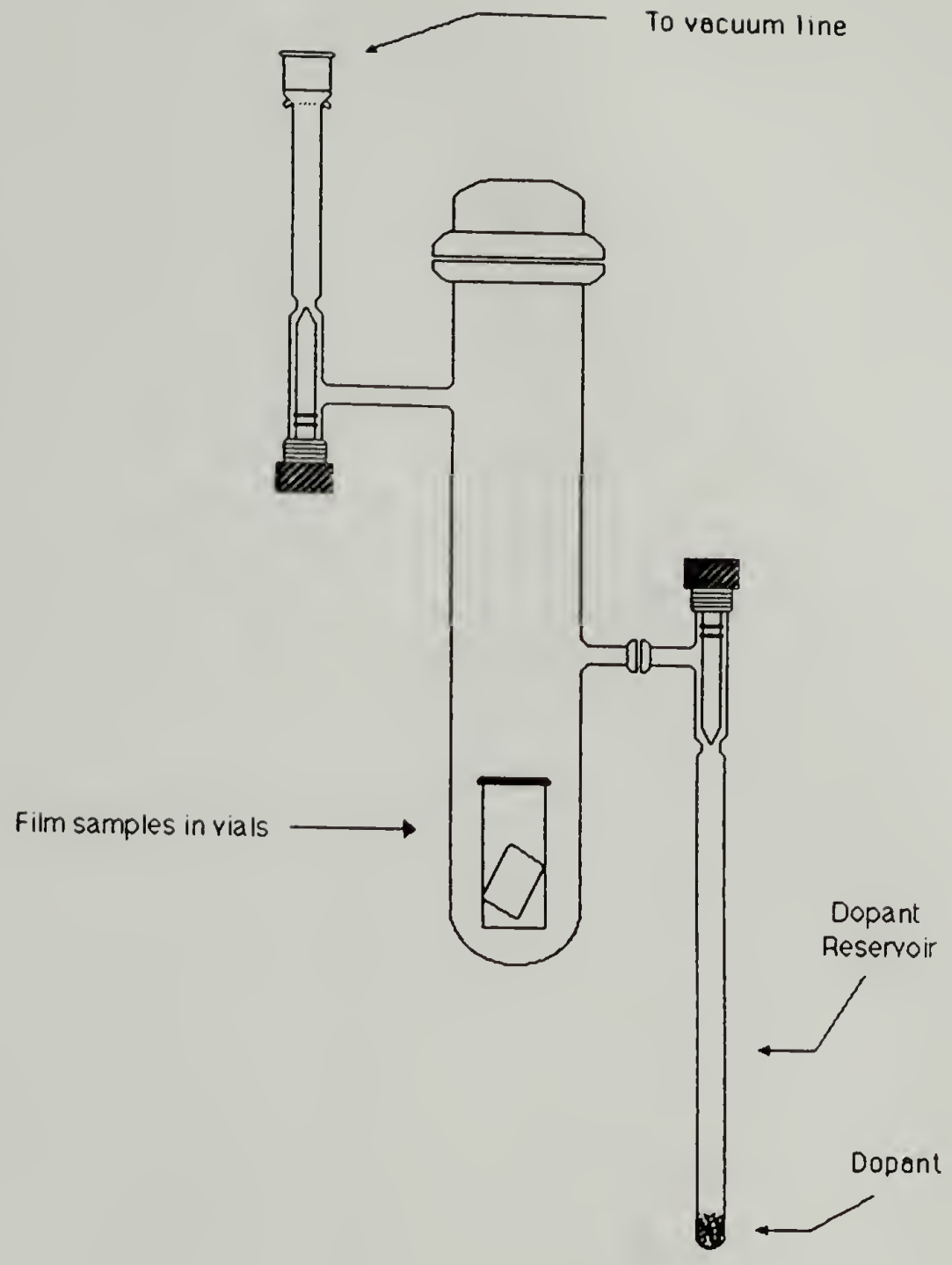

Figure 2.9

Doping apparatus for iodine uptake experiments. Gaseous iodine was introduced to the chamber with PTFE-C films contained in vials.

sufficiently purged with nitrogen. The sodium was washed 5 times with dry heptane and then the napthalene solution was transferred onto the sodium via cannula. After approximately 5 minutes, the solution turned green. The mixture was then stirred for 5 hours under nitrogen.

The doping procedure was carried out in a glove bag. A film sample of PTFE-C was dipped into a flask containing 50 ml of the sodium napthalide solution. The PTFE-C film immediately turned black. The film was rinsed in THF and mounted to the conductivity apparatus in the same manner as for iodine doping. The sample was evacuated in the conductivity apparatus prior to taking measurments.

Preparation of Modified PTFE Surfaces

This section describes the preparation of reduced PTFE (PTFE-C) derivatized surfaces. It should be noted that the preparation of the different surfaces is carried out with PTFE reduced at what may seem to be inconsistent depths. These depths of reaction were chosen to match the sensitivity of the various characterization techniques used to confirm the presence of the functional groups introduced. This point is addressed in more detail in the Results and Discussion section.

Preparation of benzoin dianion reduced PTFE (PTFE-C). (II:61-66)

Benzoin (0.27 g, 1.3 mmol) was weighed into a flask, which was sealed with a septum secured with a copper wire, and evacuated and flushed 3 times with nitrogen. DMSO (5 ml) was transferred to the flask containing the benzoin via cannula. Likewise, 1.0 g (8.9 mmol) of potassium t-butoxide was weighed in the glove box, evacuated and flushed with nitrogen and dissolved in 30 ml of DMSO. The benzoin solution was transferred via cannula with rapid stirring to the base solution. A dark purple solution immediately formed, indicative of the benzoin dianion. The solution was transferred via cannula to a Schlenk tube containing the PTFE films which had been evacuated and flushed with nitrogen and equilibrated in an oil bath at 50°C for at least 1 hour. For gravimetric analysis, 1 cm x 1 cm films were used; for XP spectroscopy 1.5 cm x 2.0 cm films were employed. The reaction was allowed to proceed for various lengths of time while maintaining a positive pressure of nitrogen. Throughout the course of the reaction, the color of the reaction solution

changes from purple to red. At the completion of the reaction, the solution was cannulated from the films; the films were then washed with five 10 ml portions of DMSO until the supernatant liquid was colorless (normally 4 washes were sufficient) Washing entailed transferring pure solvent via cannula onto the film followed by agitation for 30-60 sec intervals on the Vortex-Genie. The solvent was then transferred from the film via cannula. The PTFE appeared very dark purple-black at this point. The film was then washed with ten 10 ml portions of water. When the first portion of water was transferred onto the film it developed a lustrous gold appearance. After sufficient water washing, the film was rinsed with five 10 ml portions of THF and two 10 ml portions of heptane (for XPS analysis). Nitrogen was blown over the film for a few minutes to remove solvents and then the films were evacuated at 10^{-3} torr. The films varied in color, depending on the depth of reaction: reactions run for short times yielded films which were purple in color; more extensive reaction times yielded gold films.

PTFE powder was reduced in a similar manner. Approximately 100 mg of powder was weighed into a Schlenk tube and evacuated, flushed and equilibrated as described above. The reaction yielded black powder, which when viewed with a magnifying glass looked like gold rocks. Care had to be taken so that the powder was sufficiently washed; it tended to collect on the sides of the Schlenk tube.

PTFE-C preparation in THF. (III:73;77) Potassium t-butoxide (2.0 g, 17.8 mmol) was dissolved in 30 ml THF under nitrogen. A solution of benzoin (0.27 g, 1.3 mmol) in THF was then transferred to the base solution; a deep red-orange color developed. This dianion solution was

transferred into a Schlenk tube containing two pieces of PTFE and equilibrated in a 50°C oil bath. The films were allowed to react for 20 hours and the reaction solution (which now contained some precipitate) was transferred from the film. The films were washed in water (10 X 10 ml) then in THF (5 X 10 ml) and pumped down for gravimetric analysis. PTFE films prepared in THF had a few light purple patchy spots on them.

PTFE-C preparation in DMF. (III:75) The reaction was carried out in DMF following the procedure outlined above for the reaction in DMSO. A solution of benzoin (27 g, 1.3 mmol) in 5 ml DMSO was added to a solution of potassium t-butoxide (4.0 g, 35.6 mmol, as received from Aldrich) in 30 ml DMSO. After reaction of this dianion solution (which was a deep purple color, similar to that in DMSO) with the film and appropriate washings, the PTFE-C films were very faint purple in color. They were evacuated for gravimetric analysis.

PTFE preparation in NMP. (III:77) The reaction was carried out as that described in DMF for 24 hours. The reacted films were purple-gold, similar to those produced in DMSO. This film was evacuated for gravimetric analysis.

PTFE preparation in THF/DMSO. (III:79) Benzoin (0.27 g, 17.8 mmol) in 5 ml THF was added to a solution of 2.0g (17.8 mmol) potassium t-butoxide and 5 ml DMSO in 30 ml THF under a nitrogen atmosphere. The reaction solution, which had a much deeper red color than in the case described above for the reaction in THF alone, was transferred onto a PTFE film in a Schlenk tube under nitrogen which had been equilibrated in a 50°C oil bath. The film was reacted for 3 days, the solution removed,

and the film (black in color) washed in THF (5 X 10 ml) and then water (10 X 10 ml), and then THF again (5 X 10 ml). The film was pumped down for gravimetric analysis.

Oxidation of PTFE-C with $KClO_3/H_2SO_4$. (II:87;107;113;115 III:101;105;121) Film samples of PTFE-C were oxidized with a sulfuric acid solution of potassium chlorate (1 g $KClO_3$ in 50 ml H_2SO_4) at room temperature in an open flask for gravimetric analysis and XP spectroscopy. Oxidized film samples were washed with copious amounts of water and then THF and dried under vacuum at 60°C to a constant weight.

Air oxidation of PTFE-C (PTFE-O). (III:9) PTFE-C samples (2 day reduction) were exposed to ambient laboratory atmosphere for 4 weeks, turning from gold to brown to pale yellow. Before obtaining XP spectra, films were washed with THF and heptane, and then dried under vacuum overnight.

Chlorination of PTFE-C (PTFE-Cl). (III:21; V:121;125) A PTFE-C film sample was equilibrated at 0°C for 30 minutes under nitrogen in a Schlenk tube. The tube was flushed with chlorine for several minutes and then closed with a slight positive chlorine pressure and kept in the dark at 0°C for two hours. The film color turns from gold to white. The tube was flushed with nitrogen, washed with methylene chloride (2 X 10 ml) and dried under vacuum overnight.

Bromination of PTFE-C (PTFE-Br). (IV:93;103;105;113) Bromine (10 ml of 0.2M in CCl_4) was transferred via cannula to a Schlenk tube containing a film sample of PTFE-C at 0°C in the dark under nitrogen. After 11 hours, the bromine solution was removed and the yellow-white film sample was rinsed with copious amounts of CCl_4, methylene chloride,

heptane, and THF in this order and dried under vacuum overnight.

Reaction of PTFE-C with MCPBA in EtOH. (III:15) MCPBA (0.5 g, 2.9 mmol) was dissolved in 30 ml EtOH and the solution transferred onto a PTFE-C film in a Schlenk tube under nitrogen. The reaction proceeded at 4°C in the dark for 2 days. After the reaction period, the solution was removed and the films were washed in copious amounts of EtOH and then THF and pumped overnight at 10^{-3} torr.

Reaction of PTFE-C with MCPBA in glacial acetic acid. (III:19) A PTFE-C film was reacted in a solution of MCPBA (1.0 g, 5.8 mmol) in glacial acetic acid (25 ml) following the procedure above.

Polymerization of styrene from the surface of PTFE-C. (IV:91) A PTFE-C film was sealed in a crown-capped glass pressure bottle in a glove bag filled with nitrogen. Styrene (2 ml) was dissolved in benzene (15 ml) under nitrogen and transferred onto the film. Two ml of 4.3×10^{-2}M AIBN solution was injected and the "pop bottle" was placed in a 65°C oil bath overnight. The following day, the film was extracted at ambient conditions in THF and pumped down to a constant weight.

Hydroboration and subseqent oxidation of PTFE-C (PTFE-OH). (VI:9;11;15;17;21;27;31;37;39) Borane-THF complex (10 ml of 1.0M) was transferred to a Schlenk tube containing a PTFE-C film sample at room temperature under nitrogen. As the film reacted, it lost its luster and turned from gold to pale purple. After 12 hours, the borane solution was removed, the film was washed with THF (5 X 10 ml), and water (10 ml) was added. Sodium hydroxide solution (10 ml of 3M) was introduced followed by the slow addition of 10 ml of 30% hydrogen peroxide. The tube was

immersed in an ice bath for 3 hours. The solution was then removed and the film was washed with copious amounts of dilute NaOH, water, dilute HCl, water, THF and heptane in this order and dried under vacuum overnight.

Reaction of PTFE-OH with trifluoroacetic anhydride (PTFE-$OCOCF_3$). (VI:9;15) A PTFE-OH film was treated with 1 ml of trifluoroacetic anhydride in 9 ml THF under nitrogen at room temperature overnight. The solution was removed and the film was rinsed with THF and then heptane and dried under vacuum overnight.

Reaction of PTFE-OH with trichloroacetyl isocyanate. (VI:39) Trichloroacetylisocyanate (1 ml) was dissolved in 9 ml of THF under nitrogen and transferred onto a PTFE-OH film. The reaction was allowed to proceed for 24 hours under nitrogen at room temperature; the solution was removed and the films were washed in copious amounts of THF and heptane and evacuated overnight.

Reaction of PTFE-OH with 2,5-dichlorophenylhydrazine. (VI:43) 2,5-Dichlorophenylhydrazine (0.115 g, 0.65 mmol) and 1 ml water were dissolved in 16 ml EtOH under nitrogen and transferred via cannula onto a PTFE-OH film. Concentrated HCl (1 ml) was added via a Teflon cannula and the reaction was allowed to proceed at room temperature overnight. The solution was removed and the film was washed in EtOH, heptane, and THF and evacuated overnight.

Reaction of PTFE-OH with heptafluorobutyryl chloride (PTFE-$OCOC_3F_7$). (VI:39) A film sample of PTFE-OH was treated with 1 ml of HFBC and 1 drop pyridine in 9 ml THF under nitrogen at room temperature for 24 hours. The solution was removed and the film sample was rinsed with

ethanol, THF and then heptane and dried under vacuum overnight.

Reaction of PTFE-C with sodium hypochlorite. (II:81;107;113;115, VI:25) A sample of PTFE-C film (24 hour reduction) was placed in a beaker containing 50 ml of sodium hypochlorite (30%) and reacted for 24 hours. The film was then rinsed with copious amounts of water, and then THF and dried overnight under vacuum.

Diels-Alder reaction of maleic anhydride with PTFE-C. (VI:35;71;73;79) Maleic anhydride (0.60 g, 6.1 mmol) was weighed into a round bottom flask and evacuated and flushed with nitrogen three times. After dissolution in 15 ml of THF, the maleic anhydride solution was transferred onto two PTFE-C films and reacted for 24 hours at 50°C under nitrogen. At the end of the reaction period, the reaction solution was removed and the films were washed in THF (5 X 10 ml), heptane (2 X 10 ml), and then THF (5 X 10 ml) and evacuated overnight. One of the reacted films was hydrolyzed by heating it in water overnight under nitrogen in a Schlenk tube. It was then washed in THF and heptane and evacuated overnight.

Koch-Haaf reaction of PTFE-C. (VI:45) Formic acid (1 ml) was added to 5 ml concentrated H_2SO_4 via a Teflon cannula under nitrogen. Upon addition, the solution began to effervesce. It was then added to a Schlenk tube containing 2 PTFE-C films (reduced 12 hours) at room temperature. Additional formic acid (4 ml) was added and the tube was placed in an oil bath at 35°C overnight. The acid solution was removed and the films were washed in copious amounts of H_2O, 1N NaOH, THF, and heptane and evacuated overnight.

Hydroboration and subsequent CrO_3 oxidation of PTFE-C (VI:63;65;67;69;71) Borane-THF complex (10 ml, 1.0 M) was transferred via cannula into a Schlenk tube containing a PTFE-C film (reduced 12 hours) under nitrogen and reacted for 24 hours. The solution was removed, the film was rinsed in copious amounts of THF, and then equilibrated to 0°C. CrO_3/H_2SO_4 (4 ml of 8N) was introduced by pipette (a stream of nitrogen was blown over the film) and the reaction was allowed to proceed for 20 minutes. The oxidized film was washed in air in 3% H_2SO_4, and then H_2O and methylene chloride and evacuated overnight.

Attempted preparation of PTFE-polyethylene by hydroboration of PTFE-C followed by protonolysis with acetic acid. (VI:101) A PTFE-C film (1.25 hour reduction) was treated with borane-THF complex (10 ml 1M) under nitrogen in a Schlenk tube for 24 hours. The complex was removed and the film was washed in THF. A solution of 0.60 ml acetic diluted to 10 ml with THF was then added to the film and reacted overnight under nitrogen. The next day, the solution was removed and the film was washed in EtOH, H_2O, THF, and heptane and evacuated overnight.

Synthesis of maleic acid. (VI:73) Maleic acid was synthesized by a literature method.[5] Water (4.0 g, 0.22 mole) was added to maleic anhydride (19.61g, 0.17 mole) in a 500 ml Erlenmeyer flask. The mixture was heated on a hot plate until the maleic anhydride melted and a homogeneous solution formed. The flask was removed from the hot plate, covered with a watch glass, and allowed to stand for 2 days at room temperature, yielding a solid, white precipitate. The product was recrystallized in 150 ml of water yielding white crystals, which were repeatedly washed in benzene and evacuated to dryness. The product was

further purified by sublimation, yielding a product which melted at 132°C.

Photochemically initiated radical addition of formic acid to PTFE-C (VI:81) A solution of 0.0435 g (0.26 mmol) AIBN, 1 ml formic acid and 9 ml THF was prepared under nitrogen and transferred via Teflon cannula onto a PTFE-C film (reduced for 10 minutes) in a jacketed quartz Schlenk tube under nitrogen. The tube was irradiated (Rayonet Photochemical Reactor, 254 nm lamps) for 2 hours. The acid solution was removed and the film was washed in copious amounts of THF and heptane and evacuated overnight.

Thermally initiated radical addition of formic acid to PTFE-C (VI:79) The analogous thermal reaction was run using the same concentrations of reactants outlined above at 50°C for 12 hours. Reacted films were washed in THF and heptane and evacuated overnight.

Radical addition of acetic acid to PTFE-C. (VI:83) AIBN (0.04 g, 0.30 mmol) was dissolved in 10 ml of acetic acid and the solution was transferred via cannula onto a reduced PTFE film in a Schlenk reflux tube (Figure 2.10) and refluxed for 1.5 hours under nitrogen. The acid was removed and the film was washed in copious amounts of THF and heptane and evacuated overnight.

Friedel-Crafts reaction of oxalylchloride with PTFE-C. (VI:81) $AlCl_3$ (5.0 ml of 1M solution in nitrobenzene) was transferred onto a PTFE-C film (reduced for 6 hours) in a Schlenk tube under nitrogen and equilibrated at 50°C (oil bath temperature). Oxalyl chloride (1 ml) was then transferred onto the film. Since there was no sign of reaction

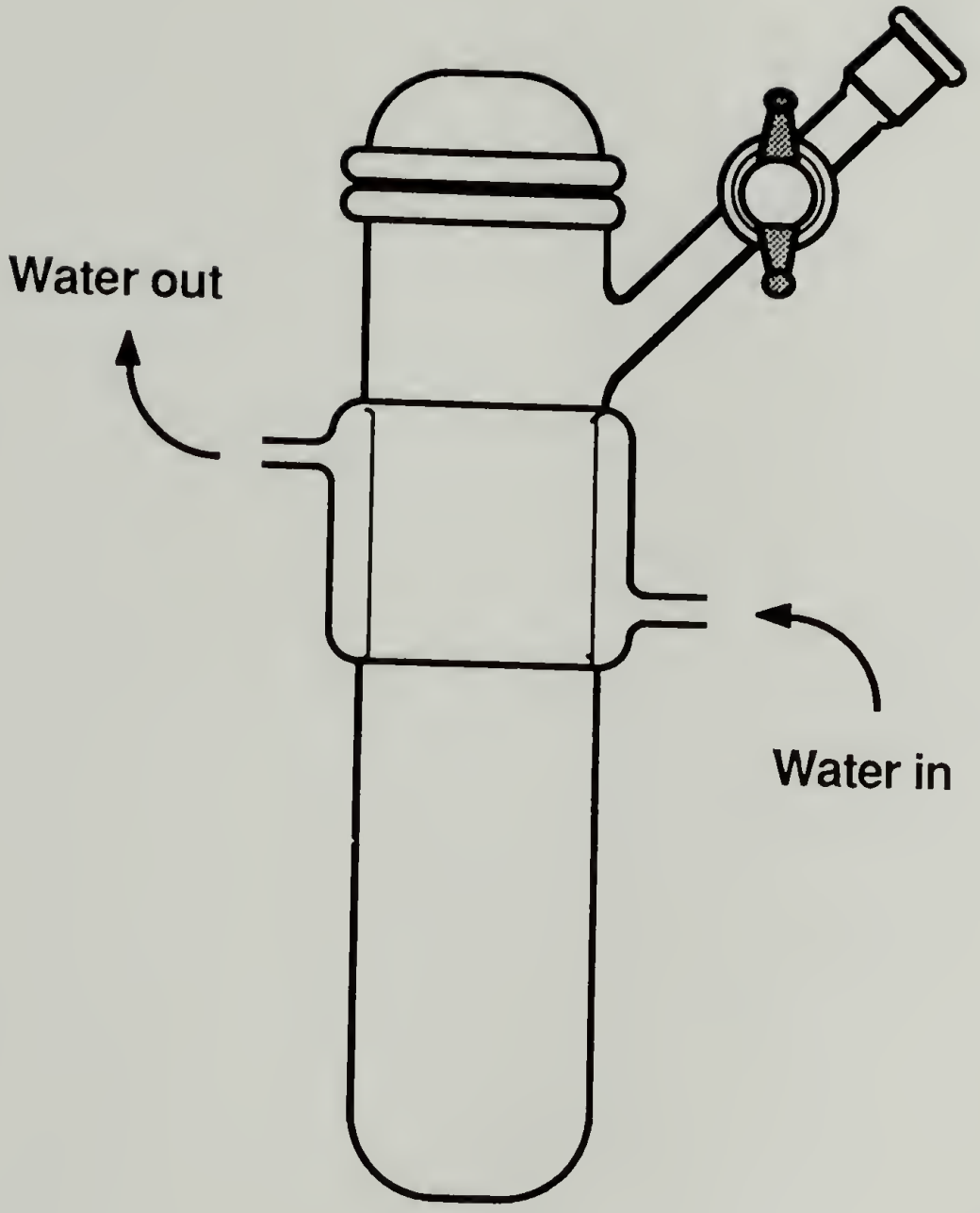

Figure 2.10

Schlenk refluxing tube.

after 2 hours under these conditions, the film was reacted overnight. The following day, the film was rinsed in copious amounts of benzene and THF. Water (15 ml) containing a few mls of concentrated HCl was added. The film was washed in water, THF, and heptane and evacuated overnight. The film did not appear to have reacted.

Reaction of PTFE-C with tetracyanoethylene. (VI:83;85) Tetracyanoethylene (0.15 g, 1.17mmol) was dissolved in 10 ml THF under nitrogen and transferred via cannula onto a PTFE-C film (15 minute reduction). The reaction proceeded overnight at room temperature. An attempted hydrolysis of any nitrile groups present was made under acid catalyzed conditions (5 ml HCl: 2 ml H_2O) at reflux for 0.5 hour and for 12 hours. The films were washed in water, THF, and then heptane and evacuated overnight.

Reaction of maleic acid with PTFE-C. (VI:85) Maleic acid (0.5 g, 4.3 mmol) was dissolved in 10 ml THF under nitrogen and transferred onto a PTFE-C film (reduced 15 minutes) in a Schlenk refluxing tube (Figure 2.10). The film was refluxed overnight and then washed in THF and heptane and evacuated overnight.

Reaction of PTFE-C with dimethylacetylenedicarboxylate. (VI:75) Dimethylacetylenedicarboxylate (1 ml) was dissolved in 9 ml THF under nitrogen and transferred onto a reduced PTFE film (10 minute reduction) in a Schlenk tube. The tube was placed in a 55°C oil bath and reacted overnight. The next day, the film was washed with copious amounts of THF, and then heptane and evacuated overnight.

Reaction of PTFE-C with succinic anhydride. (VI:107;109) Succinic

anhydride (0.15 g, 5 mmol) was weighed into a Schlenk tube containing a PTFE-C film in the glove box. THF (10 ml) was transferred into the tube and the reaction proceeded at room temperature overnight. The following day the solution was removed; the films were then refluxed in a Schlenk reflux tube in methylene chloride overnight. After refluxing, the methylene chloride was removed, the films were washed in THF and heptane and evacuated overnight.

Reaction of PTFE-C with maleic anhydride and subsequent hydrolysis. (VI:87;91;115) A PTFE-C film was placed in a jacketed Schlenk reaction tube with maleic anhydride (0.50g, 5.1 mmol), AIBN (0.15g, 9.1 mmol), and 5 ml THF under nitrogen. The tube was photolyzed (Rayonet Photochemical temperature bath) for 2 hours. At the end of the reaction period, the film was washed with THF (5 X 10 ml), and then transferred to a reflux tube in the glove box. Trifluoroacetic acid (0.5 ml) and water (9.5 ml) were added and refluxed for 24 hours. After refluxing, the film was washed in water, THF, and heptane (for XPS) and dried under vacuum overnight.

Reaction of PTFE-COOH with carbonyldiimidazole. (VI:87;91;99;111;115) A solution of 0.20 g (1.2 mmol) carbonyldiimidazole in 10 ml THF was transferred to a Schlenk tube containing a PTFE-COOH film and reacted overnight at room temperature. The following day, the solution was removed and the film sample was washed with copious amounts of THF and then heptane and dried under vacuum overnight.

Reaction of PTFE-anhydride with ammonia. (VI:97) Approximately 0.5 ml ammonia was distilled trap-to-trap into a tube containing a PTFE-

anhydride film at -196°C. The tube was sealed under vacuum, warmed to room temperature, and reacted for 5 days. At the end of the reaction period, the tube was broken in a nitrogen-filled glove bag and the film was placed in a Schlenk tube. The film was flushed with nitrogen, washed with copious amounts of EtOH and THF, extracted overnight in methylene chloride, and then evacuated overnight.

Reaction of PTFE–C with Ammonia. (VI:93) Ammonia was distilled trap-to-trap onto a PTFE-C film (reduced 16 hours) in a glass tube. The tube was sealed under vacuum and when cool, placed in a 150°C sand bath for 1 week. The tube was then opened in a nitrogen filled glove bag, and the film was placed in a Schlenk tube. The film was flushed with nitrogen, washed in EtOH, THF, and then heptane and evacuated overnight.

Hydroboration of PTFE–C followed by reaction with ammonium hydroxide and sodium hypochlorite. (VI:71) A PTFE-C film was treated with borane-THF complex as previously described. After washing the hydroborated film with THF, it was cooled to 0°C. Ammonium hydroxide (4.9 ml of a 2.05M solution in water) was added followed by the dropwise addition of sodium hypochlorite (15 ml of a 5% solution in water). The reaction was allowed to proceed for 25 minutes, and then the solution was removed and the film was rinsed in water, dilute HCl, water, THF, and then heptane in this order and evacuated overnight.

Preparation of PTFE–NH_2. (VI:89;91;93;95;101;105;111;117) A PTFE-C film (1 hour reduction) was brominated (2 hours). Ammonia (approximately 0.5 ml) was trap-to-trap distilled into a tube containing the PTFE-Br film at -196°C. The tube was sealed under vacuum and allowed to warm to

room temperature. On warming, the yellow PTFE-Br films became purple/brown in color. The reaction was allowed to proceed for 7 hours; the films were then transferred to a Schlenk tube in a nitrogen filled glove bag, where they were washed with ethanol, THF, and heptane in this order and evacuated overnight.

Reaction of PTFE-NH_2 with pentafluorobenzaldehyde (PFB). Pentafluorobenzaldehyde (0.5 ml, transferred at 50°C via cannula) was diluted to 10 ml with THF and transferred to a Schlenk tube containing a PTFE-NH_2 film under nitrogen. The reaction was allowed to proceed for 24 hours. After the reaction, the PFB solution was removed and the film was rinsed with copious amounts of THF and heptane, and then evacuated overnight.

Reaction of PTFE-NH_2 with trichloroacetylchloride. (VI:93;97;103) A solution of 0.5 ml trichloroacetylchloride in 9 ml THF was made under nitrogen and transferred onto a PTFE-NH_2 film in a Schlenk tube under nitrogen. The film was reacted overnight; the following day, the trichloroacetylchloride solution was removed and the film was washed in copious amounts of THF and heptane and then evacuated overnight.

Reaction of PTFE-Cl and PTFE-Br with $NBu_4^+SH^-$ (PTFE-SH). (V:95;97;107;109;111;115;117;127) PTFE-Cl and PTFE-Br film samples were treated with a solution of sodium hydrogen sulfide (0.45 g, 7.95 mmol) and tetrabutylammonium bromide (0.23 g, 0.71 mmol) in water under nitrogen at 80°C (for PTFE-Cl) and room temperature (for PTFE-Br) for 2 hours. After the reaction, the solutions were removed and the film samples were washed with water, THF, and then dried under vacuum overnight.

Reaction of PTFE-SH with 3,5-dinitrobenzoyl chloride. (V:117;135;139). A solution of 0.055 g (0.25 mmol) 3,5-dinitrobenzoyl chloride and a few drops of pyridine in 20 ml THF was transferred onto a PTFE-SH film and allowed to react for 10 minutes at room temperature under nitrogen. The DNBC solution was initially clear, but turned yellow when added to the film. After the reaction period, the DNBC solution was removed and the film washed in copious amounts of THF and heptane, and then evacuated overnight.

Reaction of PTFE-SH with heptafluorobutyrylchloride. (V:139) The reaction of PTFE-SH with HFBC was carried out in the same manner as that for PTFE-OH (see above).

Reaction of PTFE-C with sulfur dichloride. (V:129;131) Sulfur dichloride was distilled onto a PTFE-C film (10 minute reduction) (a few drops of PCl_3 were added to the film to stabilize the SCl_2) at various temperatures. Reactions were also run with 0.5 ml cyclooctene added to the PTFE-C film in order to scavenge any chlorine formed. In these cases, the sulfur dichloride was distilled into a Schlenk flask containing a few drops of PCl_3 and the cyclooctene at -78°C. The reaction solution was <u>immediately</u> transferred onto films equilibrated to the desired temperature. After 1 hour, the PTFE-C films appeared white and there was a considerable orange precipitate present; the films were washed in copious amounts of CCl_4, methylene chloride and THF, yielding samples suitable for XPS analysis.

Thermal and photochemical reaction of PTFE-C with thiolacetic acid and AIBN (PTFE-$SCOCH_3$) and subsequent hydrolysis.

(V:73;75;79;81;83;87;89;137) A solution of 0.1339 g AIBN in 10 ml thiolacetic acid was introduced to a Schlenk tube containing two PTFE-C films (10 minute reduction time). The tube was either heated at 40°C for 19 hours or photolyzed (Rayonet Photochemical Reactor, 354 nm) at 12°C for 12 hours. The solution was then removed and the film sample was washed with copious amounts of THF and dried under vacuum overnight. Base-catalyzed hydrolysis was carried out by heating the film sample at 60°C for 12 hours in a solution of 2.91 g (52 mmol) KOH in 20 ml water. After this time, the base solution was removed and the film sample washed with copious amounts of water, THF and then heptane and dried under vacuum overnight.

Reaction of PTFE-C with ethanethiol. (IV:63) Ethanethiol (5 ml) was transferred onto a PTFE-C film (12 hour reduction) in a Schlenk tube. The reaction was allowed to proceed for 12 hours under nitrogen at room temperature. The ethanethiol was removed and the film was washed with copious amounts of EtOH and THF and evacuated overnight.

Base catalyzed addition of ethanethiol to PTFE-C. (IV:63) Ethanethiol (5 ml) was added to KOH (0.1 g, 2.5 mmol), transferred onto a PTFE-C film (12 hour reduction) and reacted for 10 days. The yellow reaction solution was removed and the film was washed with copious amounts of EtOH and THF. The film was pumped down to constant weight before obtaining the ATR-IR spectrum.

Acid catalyzed reaction of ethanethiol. (IV:77) One drop of concentated H_2SO_4 and 2 ml of ethanethiol were dissolved in 15 ml of DMSO and transferred onto a PTFE-C film (12 hour reduction). The reaction was allowed to proceed for 12 hours, and then the reaction solution was

removed. The film was then extracted in THF (micro-soxhlet extractor) under nitrogen overnight. The film was pumped down to a constant weight for ATR-IR spectroscopy and gravimetric analysis.

Radical addition of ethanethiol to PTFE-C (IV:85) Ethanethiol (4 ml) was transferred via cannula onto a PTFE-C film (12 hour reduction). AIBN (1 ml of a 4.3 X 10^{-2}M solution in methanol) was injected and the tube was placed in a 65°C oil bath for 8 hours. After the reaction, the film was extracted overnight (micro-Soxhlet extractor) and then pumped down to a constant weight. An analogous reaction was carried out using photochemical initiation (IV:87). PTFE-C films, ethanethiol (4 ml) and AIBN (2 ml of 4.3 x 10^{-2}M solution in methanol) were transferred under nitrogen to a quartz tube. The tube was irradiated (Rayonnet Photochemical Reactor, 354nm lamps) for 12 hours. After the reaction, the films were extracted and then evacuated to a constant weight.

Reaction of PTFE-C with elemental sulfur. (IV:69;79;81) A film sample of PTFE-C and sulfur (1.13 g, 35 mmol) were placed in a round bottom flask fitted with a condenser and purged with nitrogen. Mesitylene (20 ml) was transferred via cannula to dissolve the sulfur; the mixture was then heated at reflux under nitrogen for 16 hours. The mixture initially appeared yellow, but became deep orange-red as the reaction proceeded. Following completion of the reaction, the PTFE-S film was extracted under nitrogen (micro-Soxhlet extractor) overnight in either benzene or toluene, and then evacuated to a constant weight before obtaining ATR-IR spectra and gravimetric data.

Reaction of PTFE-C with CS_2. (V:51;59) A PTFE-C film was suspended

above CS_2 (5 ml) in the quartz jacketed flask pictured in Figure 2.11. A film was hung on a glass hook, which was suspended from a nichrome wire which was threaded through a #29 Suba-Seal septum. The apparatus was assembled in the glove box to avoid oxygen contamination of PTFE-C. The CS_2 was transferred into the flask, making certain that no liquid came in contact with the film. The tube was then irradiated for 2 hours (Rayonnet Photochemical reactor, 254 nm lamps) maintaining the jacket temperature at 25° C. At the end of the reaction period, the liquid, which had turned yellow during the reaction, was removed via cannula; the film was transferred in a nitrogen-filled glovebag to a Schlenk tube, and then blown with a stream of nitrogen and evacuated overnight.

Preparation of PTFE-S for peel-testing. (IV:105, V:141) Since the sample geometry for peel testing neccessitated the use of 2 x 2 inch square sheets of PTFE, the quantity of reagents used in the reduction was increased so that the total solution volume was 50 ml. Unfortunately, with this large PTFE sample, the film tended to curl upon itself when extracted in THF, causing inhomogeneous reduction. Nevertheless, the PTFE-C films were reacted with sulfur in mesitylene at reflux for 2 days and separate sets were extracted in either toluene or benzene, and then evacuated for 1 week to remove all excess solvents. The films were sealed in glass pressure tubes with crown caps under nitrogen and then transported to IBM for peel testing.

For the second round of peel tests, it was decided that shorter reduction times were warranted and that samples should be kept rigorously air-free. It was also desirable to maintain a flat surface (uncurled from THF extraction) in order to facilitate peel testing. In order to

Figure 2.11

Apparatus for generation of atomic sulfur from CS_2 and subseqent reaction with a PTFE-C film. The film is suspended above the liquid CS_2 contained in a quartz jacketed flask. Irradiation of the liquid with 254 nm UV lamps generated atomic sulfur in the gas phase which reacted with the film.

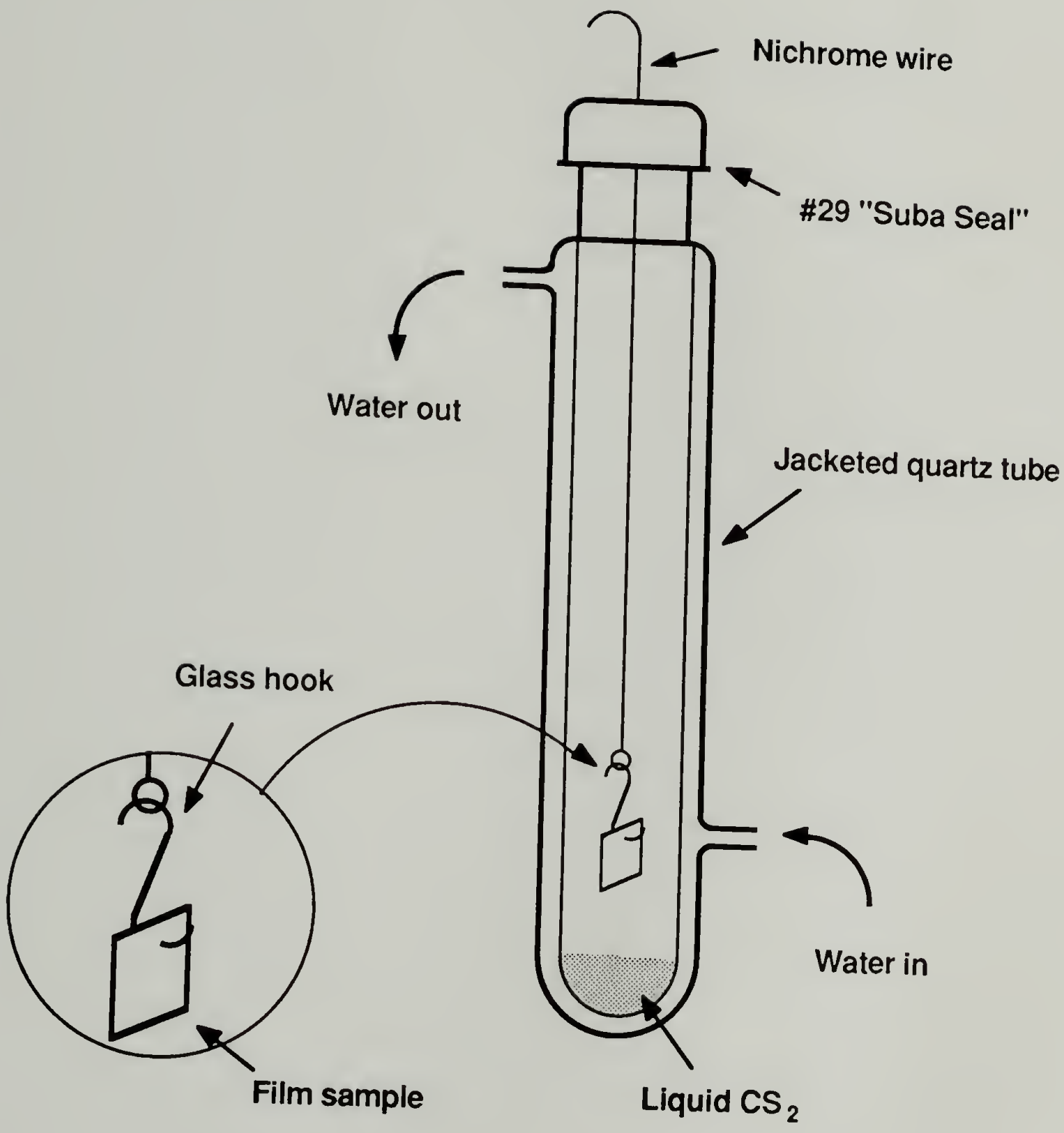
Nichrome wire
#29 "Suba Seal"
Water out
Jacketed quartz tube
Glass hook
Water in
Film sample
Liquid CS_2

meet these requirements, 1 x 4 x 1/16 inch PTFE sheets were cut and reduced for 20 minutes (The amount of reagents was adjusted so that the total volume of reducing solution was 40 ml). The PTFE-C sheets were treated with chlorine and reacted with $Bu_4N^+SH^-$ as described above, with a total solution volume of 40 ml. The films were too large to seal in conventional glass tubes, so they were loaded (in the glove box) in the tube pictured in Figure 2.12, which was fitted with a rubber stopper with purging tubes. While maintaining a steady flow of nitrogen, the tubes were constricted on a lathe in the glass shop. When constricted, the tubes were easily sealed under vacuum and then transported to IBM for peel testing.

Preparation of deuterated benzoin. (VI:58;61) Benzoin-d_{12} was prepared from benzaldehyde-d_6 via benzoin condensation in CH_3CH_2OD according to a literature procedure[6]. A 65 ml round-bottomed flask fitted with a condenser and containing 0.4g NaCN was purged with nitrogen. Ethanol-OD (10 cc) and D_2O (4 ml) were added to the flask. Benzaldehyde-d_6 (3.5 ml) was then added and the mixture was heated to reflux followed by continued heating for 0.5 hours under nitrogen atmosphere (The reaction mixture was light orange at this point). At the end of the reaction period, the heat was removed and the flask was cooled with an ice bath. Crystals of product fell out of solution within 0.5 hour; they were collected by filtration, recrystallized in ethanol-OD and dried under vacuum. The melting point (uncorrected) of the product was 129°C over a 0.5°C range. The infrared spectrum showed slight benzoin-h_{12} contamination.

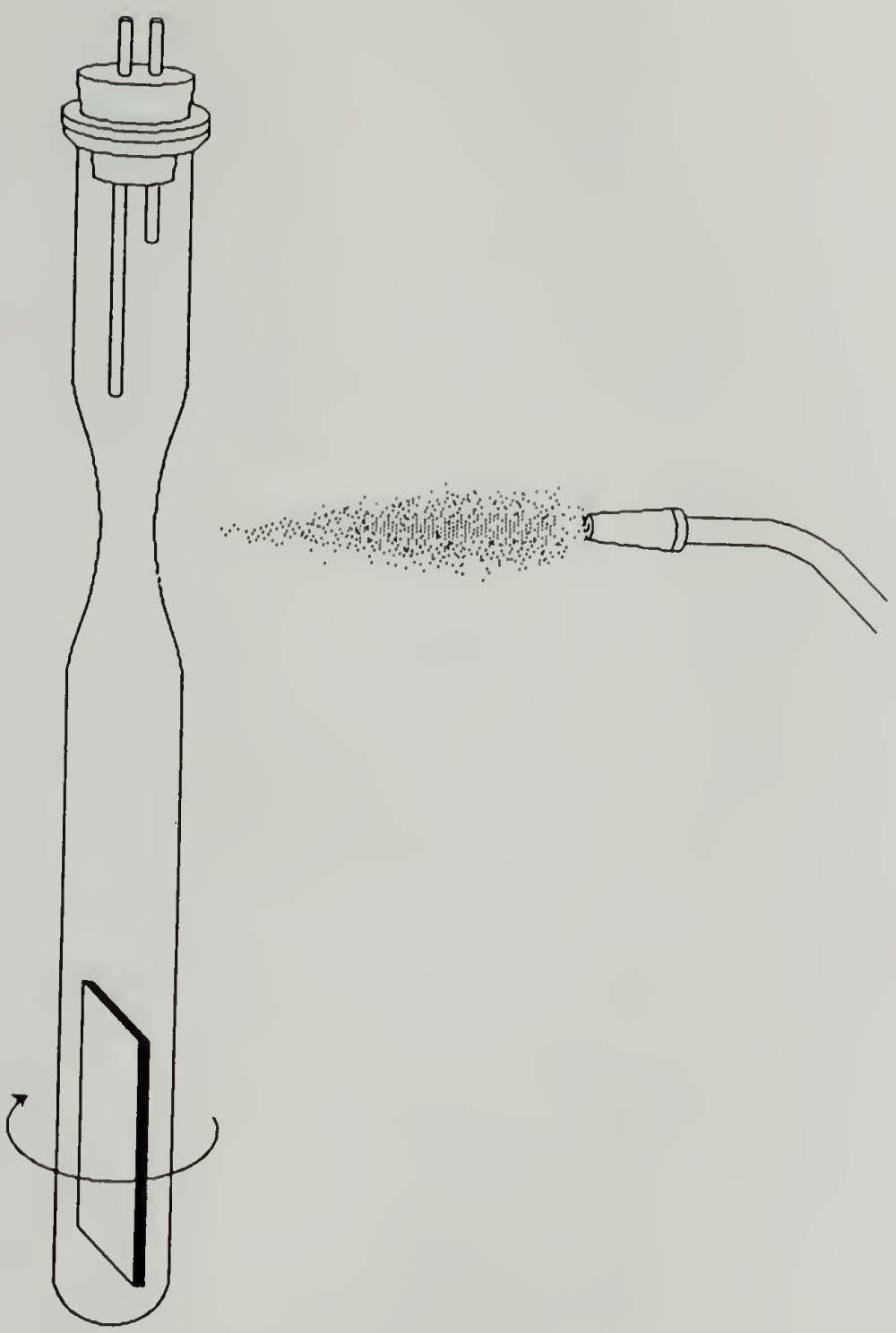

Figure 2.12

Sample preparation for peel force measurements.

References

1. D.F. Shrivers, "The Manipulation of Air-Sensitive Compounds", New York, McGraw-Hill, (1969).

2. "How to Use Ace No-Air Glassware", Bulletin Number 570, Ace Glass Incorporated, Vineland, New Jersey (1983).

3. Technical Information Bulletin Number AL-134, Aldrich Chemical Company, Milwaukee, Wisconsin (1983).

4. R.J. Roser and F.R. Whitt, J. Appl. Chem., **10**, 229 (1960).

5. Gilman, H. (Editor), "Organic Synthesis: Collective Volume I", Wiley, New York, (1932) p. 94.

6. Gilman, H. (Editor), "Organic Synthesis: Collective Volume I", Wiley, New York, (1932) p. 64.

Chapter III

Results and Discussion

When PTFE films are exposed to solutions of benzoin dianion generated from benzoin and excess potassium t-butoxide in DMSO at 50°C, a reaction is visible to the eye: PTFE changes from white to metallic gold. Control experiments using DMSO, DMSO/benzoin, and DMSO/base solutions under identical conditions render no reaction. Shorter reaction times yield purple-colored films; as the reaction proceeds, films begin to appear lustrous gold. It should be noted that the gold color is obtained only <u>after</u> H_2O is added in the workup to rinse the films; the reaction solution alone produces deep black-purple films. This important observation will be dealt with later in the discussion on chemical structure. Processing history of the polymer does not affect the reaction as PTFE powders, tape, and Goretex are all affected by the reagent. All of these forms turn gold on reaction except high surface area powders, which appear black to the naked eye, but on 10X magnification, appear gold.

The overall reaction is consistent with reduction of PTFE to a carbon-based polymer (Scheme 3.1):

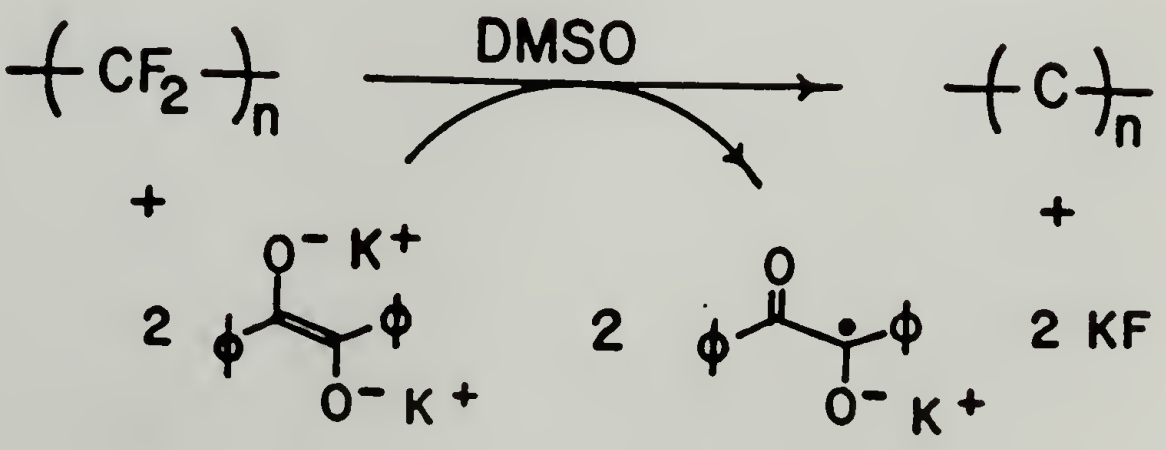

We assume the potassium salt of the dianion, a well studied species,[1] is the reducing agent. Although it is reported that the reaction of benzoin with base in DMSO yields the semidione:[2]

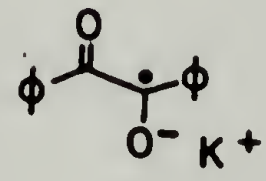

we did not observe the characteristic ESR spectrum of this species,[3] probably due to our inert preparation conditions. Although details of the reaction mechanism have not been thoroughly investigated, we presume that fluoride is removed by electron transfer to PTFE. Efforts at quantitation of fluoride ion using a specific ion probe were plagued by interference from the highly basic reaction solution. Characterization of the carbon-based layer, however, substantiates our assumptions.

Solvent effects on the reaction were monitored by visual inspection and gravimetric analysis. In the reaction in DMSO, PTFE films lose mass by loss of fluoride ion. Treatment of reduced films with NaOCl or $H_2SO_4/KClO_3$ effectively removes the reduced layer, with accompanying mass loss, exposing the underlying PTFE surface. Thus, if the PTFE films lose mass during the reaction sequence (reduction --> oxidation), then it can be assumed reaction has taken place.

The preparation of benzoin dianion in THF using 1.0g base/0.27g benzoin yields a deep red-orange solution which did not effect reaction of PTFE film by visual inspection. When the amount of base was doubled, a 2 day reaction period yielded films possessing barely noticeable reacted spots. Upon addition of a small amount of DMSO (14% v/v), the reaction proceeds as it does in DMSO. Reactions using N-

methylpyrrolidone as solvent produced gold films, while the occurrence of reaction in DMF (24 hour reaction period) was questionable. The mass changes on reaction, expressed as % mass change from that of the original film are given in Table 3.1.

Table 3.1

Solvent Effects on Reduction.

Solvent	[base]/[benzoin]	% Mass change	Reduction by visual inspection
THF	7.02	+ 0.0297	no
THF	14.04	+ 0.0648	maybe
DMF	28.08	+ 0.0043	maybe
NMP	28.08	- 0.2483	yes
THF/DMSO	14.04	- 0.4433	yes

In each case, mass losses definitely indicated when reaction has taken place. The reaction appears to be most facile in polar aprotic solvents possessing a slightly acidic proton, such as NMP and DMSO.

Physical Characterization

Surface Topography

The surface morphology of virgin PTFE films is rough on a sub-micron scale, due to the processing conditions. In practice, PTFE films are produced by skiving the film from a cylinder[4] of PTFE formed from compression of PTFE powder. This process yields regular grain lines on the surface which are visible in the SEI micrograph in Figure 3.1(a). On

Figure 3.1

SEI micrographs of virgin PTFE (a), reduced PTFE (b), and reduced-then-oxidized PTFE (C). The surface topology changes upon reduction and oxidation of reduced films show the corrosive nature of the reaction.

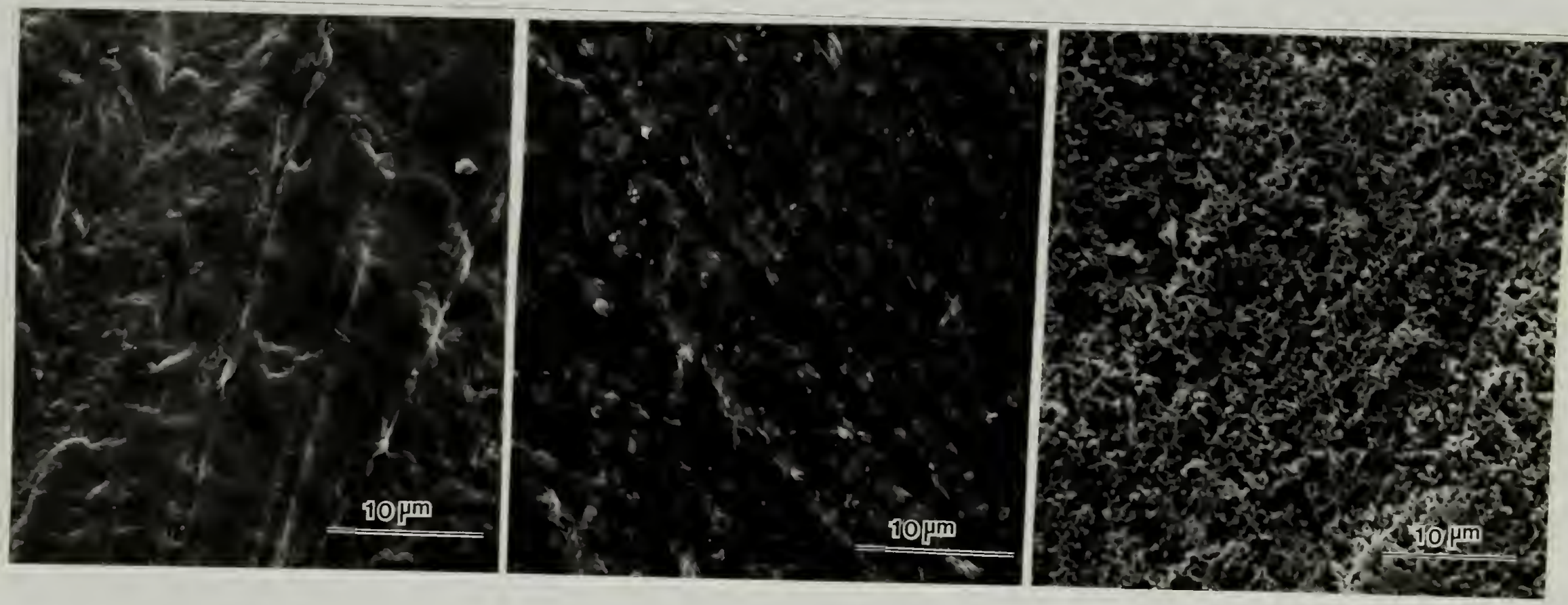
10μm
10μm
10μm

reduction, the roughness is amplified and grain lines are still visible. (Figure 3.1(b)) When this reduced layer is oxidized by $H_2SO_4/KClO_3$, the surface becomes extremely pitted, indicating that the reaction is highly corrosive (Figure 3.1(c)). All information related to the grain of the film is lost.

Contact angle measurements yield data consistent with the SEI micrographs. Advancing and receding contact angles measured on virgin PTFE confirm the anisotropy demonstrated in figure 3.1. When the water drop is advanced perpendicular to the grain of the film, it tends to skip and drag across the surface; mesurements made parallel to the grain are reproducible ($\theta_a = 121\pm2$; $\theta_r = 89\pm2$). Contact angles on extensively reduced films, however, skip badly regardless of direction. Since surface roughness (by SEI micrographs) has not increased, the skipping must be attributed to chemical heterogeneity produced by the reaction or developed during measurement. Contact angles of reduced-then-oxidized films, regardless of extent of reduction, skip too badly to obtain intelligible data. This result is a manifestation of the extremely pitted surface (Figure 3.1(c)).

When fluoride is eliminated during reduction, carbon bond lengths are shortened by development of unsaturation and crosslinking, forming a new type of surface material. When ASTM dogbone samples of PTFE are elongated to 300% of their original length on the Instron, changes consistent with the creation of a new surface layer are evident. Figure 3.2 shows micrographs of (a) virgin PTFE, (b) virgin PTFE elongated to 300%, (c) PTFE-C, and (d) PTFE-C elongated to 300%. When PTFE is

Figure 3.2

SEI micrographs taken during elongation experiments. See text for details.

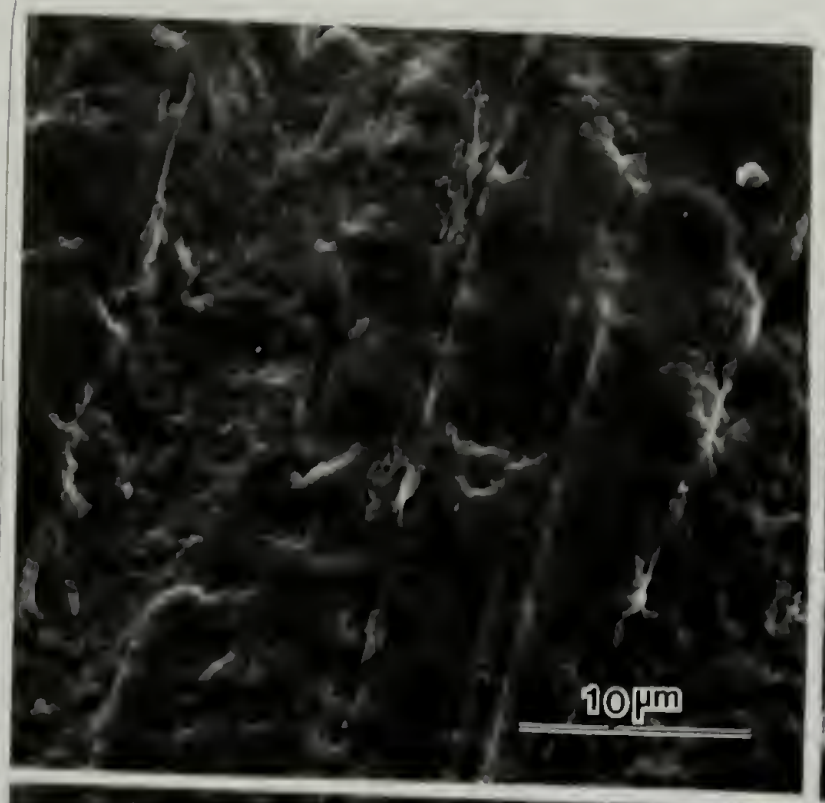
10μm

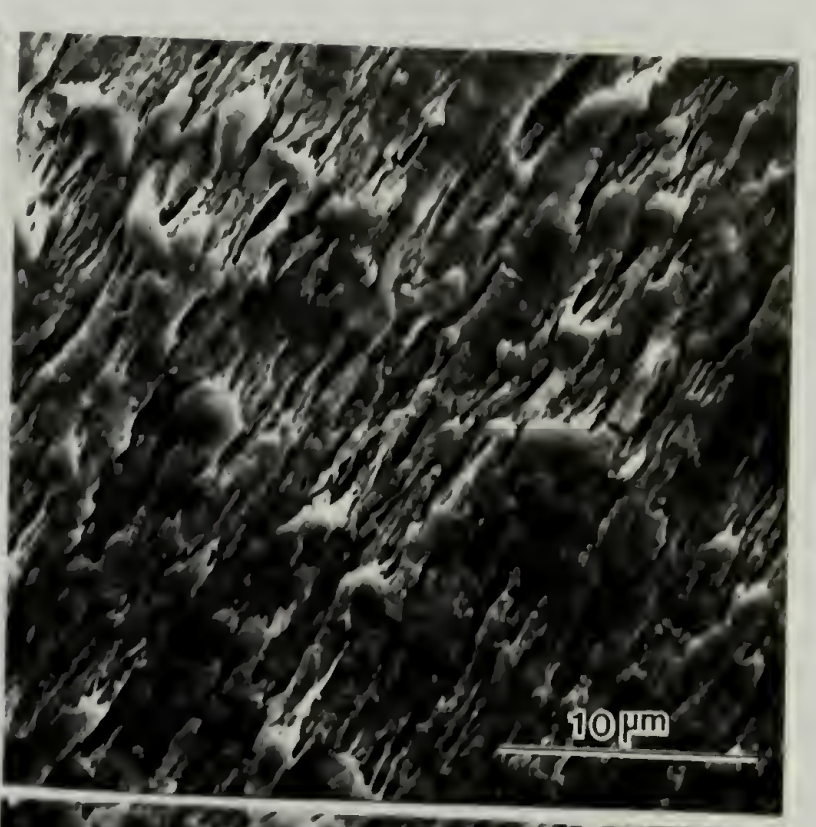
10μm


10μm

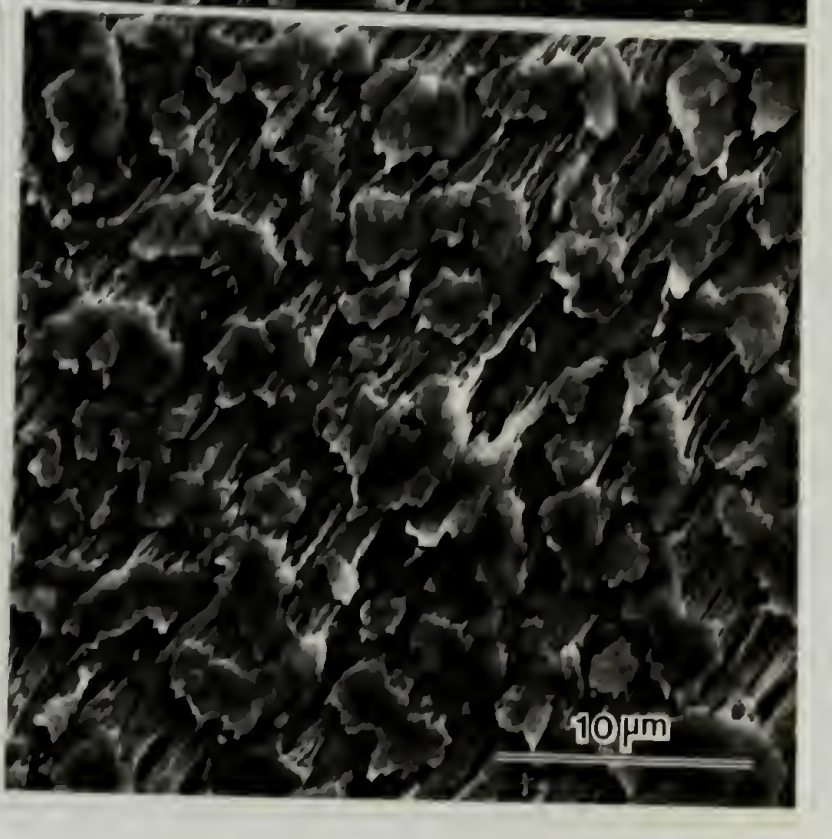
10μm

elongated, a fibrillar morphology results with orientation in the direction of the draw. The analogous experiment on PTFE-C yields micrographs exhibiting patch-like morphology on top of the fibrillar PTFE base. Thus, a new layer of material is formed on reduction, possessing mechanical properties different from those of the PTFE starting material.

Chemical Composition of PTFE-C

The chemical structure of PTFE-C was studied to gain insight into its reactivity. Answers to fundamental questions concerning progress of the reaction, development of the new surface structure, and spectroscopic characterization were sought. The techniques employed in the characterization include both surface analytical methods and bulk methods sensitive to the low concentrations of reduced material present.

Gravimetric Analysis

When PTFE is weighed before and after reaction with benzoin dianion in DMSO, a measurable amount of mass is lost due to loss of fluorine. The reacted layer on the PTFE film can be completely removed by strong oxidants such as $H_2SO_4/KClO_3$, resulting in even greater mass loss. If the initial and final chemical compositions for the reaction sequence (Equation 3.1) are known, then the average depth of reaction can be

calculated from:

$$\text{Depth of reaction} = \frac{M_v - M_o}{2\,(2.10)\,L \cdot W}$$

where M_v and M_o are the masses of the virgin and reduced-then-oxidized PTFE films, respectively; the factor 2 appears in the denominator because both sides of the film sample are reacted; 2.13 is the density of the PTFE film; **l** is the sample length; **w** is the sample width.

As Figure 3.3 indicates, the thickness of the PTFE-C layer can be conveniently controlled with reaction time: PTFE-C samples with reduced layer thicknesses of 150 Å to 20,000 Å have been prepared. Experimental difficulties preclude reaction times of less than 10 minutes which correspond to ~150 Å.

Three points related to the data in Figure 3.3 warrant discussion. First, the reaction depths reported are <u>average</u> depths of reaction. The minimum and maximum depths of reaction are significantly different, as suggested by the SEI micrographs of the reduced-then-oxidized film (Figure 3.1). Second, the data lend support to the corrosive nature of the reduction since the depth of reaction increases with reaction time. This behavior is in sharp contrast to the autoinhibitive reactions of PVF_2 and PCTFE described by Dias[5,6] where reaction depths approach a limiting value with time. Third, the unusually extensive reaction depths

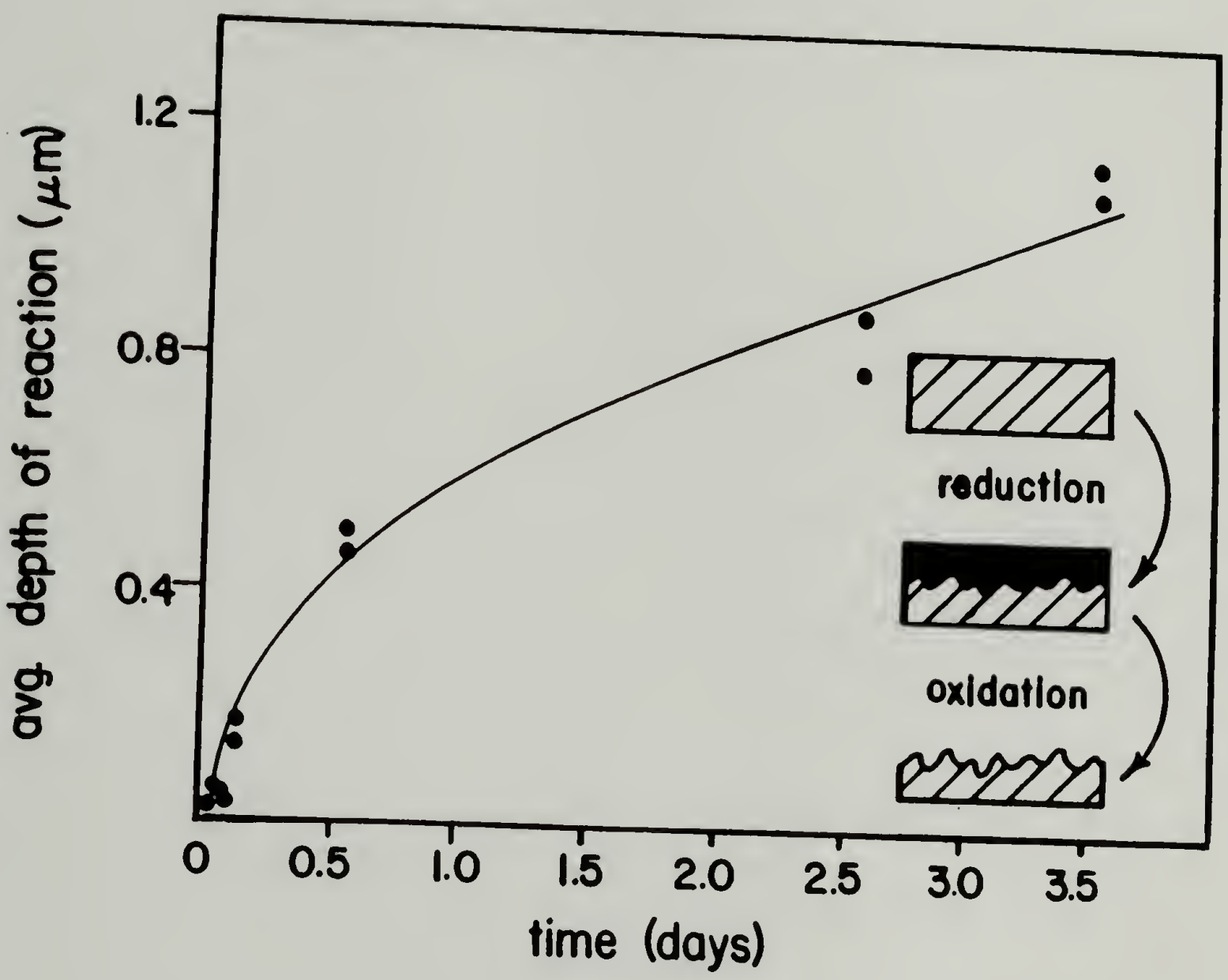

Figure 3.3

Gravimetric analysis: depth of reaction as a function of reaction time.

(> 1 μm) are greater than expected for electron transfer processes which require close contact between donor and acceptor.[7] This result is rationalized when the electronic conductivity (described below) is considered: the product conducts electrons from the solution down to the virgin PTFE. Alternatively, PTFE-C may be permeated by the reaction solution, or autocatalysis resulting from an increased interface area may be operating. It is difficult to draw conclusions from the slope changes of the plot in Figure 3.3: interfacial solvent effects, electron transport rates and autocatalysis may cancel one another in an unpredictable manner.

Quantitative information concerning the stoichiometry of the benzoin dianion reduction can be obtained from the gravimetric analysis of the reactions depicted in equation 3.1. Using the same information (M_v, M_r, and M_o) and assuming that the only source of mass loss is that of fluoride, a mass balance can be calculated. The ratio:

$$\frac{(M_v - M_r)}{(M_v - M_o)}$$

represents the fraction of mass lost by PTFE that reacts to form PTFE-C. If this ratio is expressed as the number of fluorines lost per C_2F_4 monomer unit it can be plotted as a function of the average depth of reaction. (Figure 3.4)

The data indicate that there is incomplete reduction on both a physical and a chemical level. Physical heterogeneity is evident in the

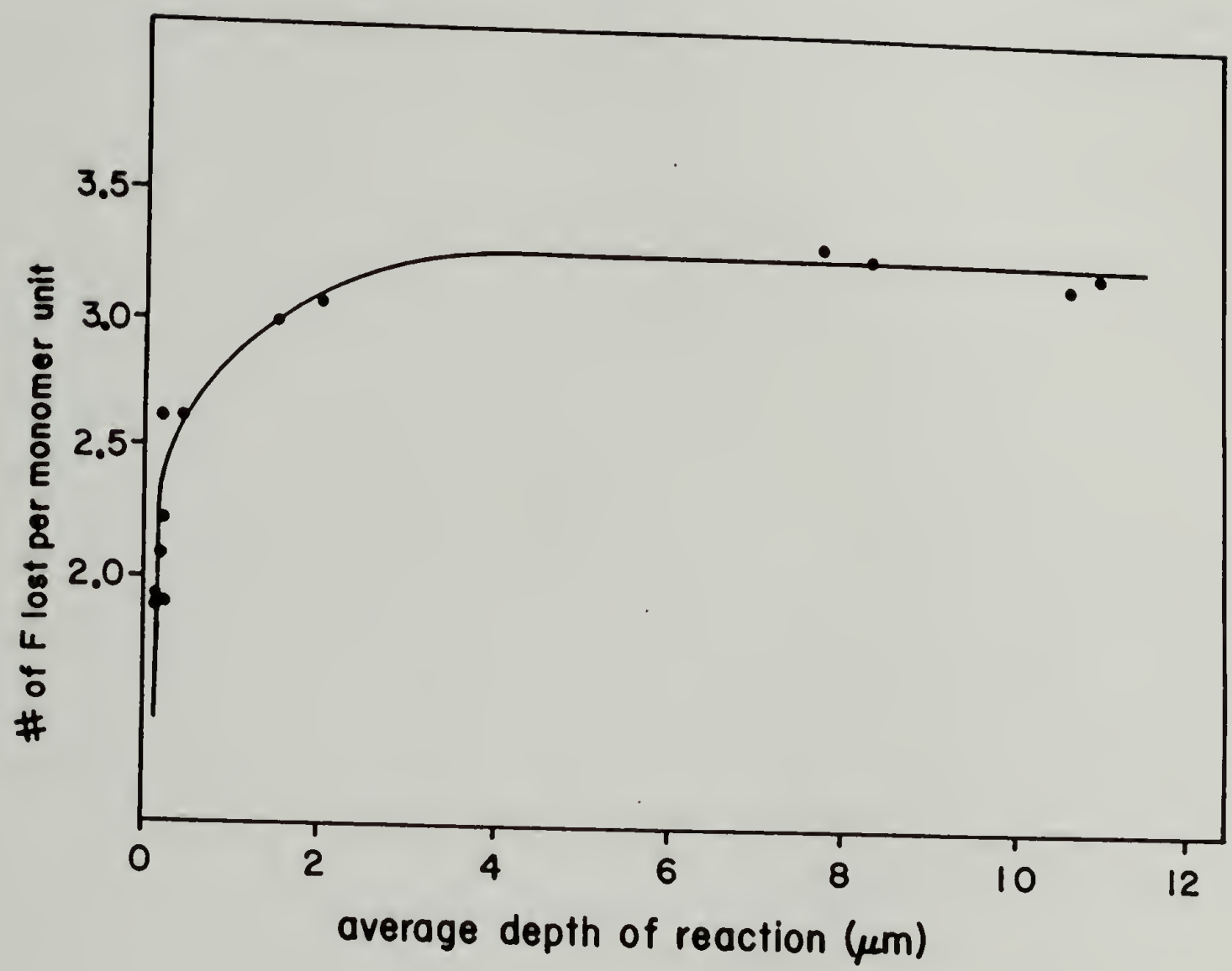

Figure 3.4

Gravimetric analysis: stoichiometry of the benzoin dianion reduction.

unreacted PTFE "islands" depicted in equation 3.1. When the reduced layer containing these islands is removed by $H_2SO_4/KClO_3$, the observed fluorine loss is lower than expected, yielding a larger C:F ratio. Oxidizing solutions from NaOCl oxidation of PTFE-C actually contain white particles which are clearly visible to the eye. Partial chemical reduction of C_2F_4 units also occurs. Figure 3.4 suggests that, after the stoichiometry levels off, approximately 3 fluorines are lost per monomer unit. This implies that the fluorine in the reduced layer (see below) is bound to sp^2 hybridized carbon. The initial values on the plot may indicate partial completion of a two step reduction sequence or may reflect the heterogeneity of the reaction. It is imprudent to draw firm conclusions about the chemical state of the reduced layer or of the reaction mechanism solely on the basis of gravimetric data. However, these data can be used to corroborate hypotheses formed on the basis of other spectroscopic methods such as IR, Raman, EPR and XPS.

XPS Spectra

The XPS spectra for the reaction sequence depicted in Equation 3.1 support the assumptions made in the gravimetric analysis and yield information on the nature of the carbon surface formed. Figure 3.5 shows the F_{1s} and C_{1s} high resolution spectra for the overall reaction sequence. The XPS spectrum for PTFE contains 2 major peaks: one from fluorine (F_{1s}:696 eV) and one from carbon (C_{1s}:293 eV). On reduction, the majority of the surface is carbon, with small amounts of fluorine and oxygen. Oxidation of PTFE-C by NaOCl yields a spectrum identical to that

Figure 3.5

XPS F_{1s} and C_{1s} high resolution spectra for unreacted, reduced, and reduced-then-oxidized PTFE.

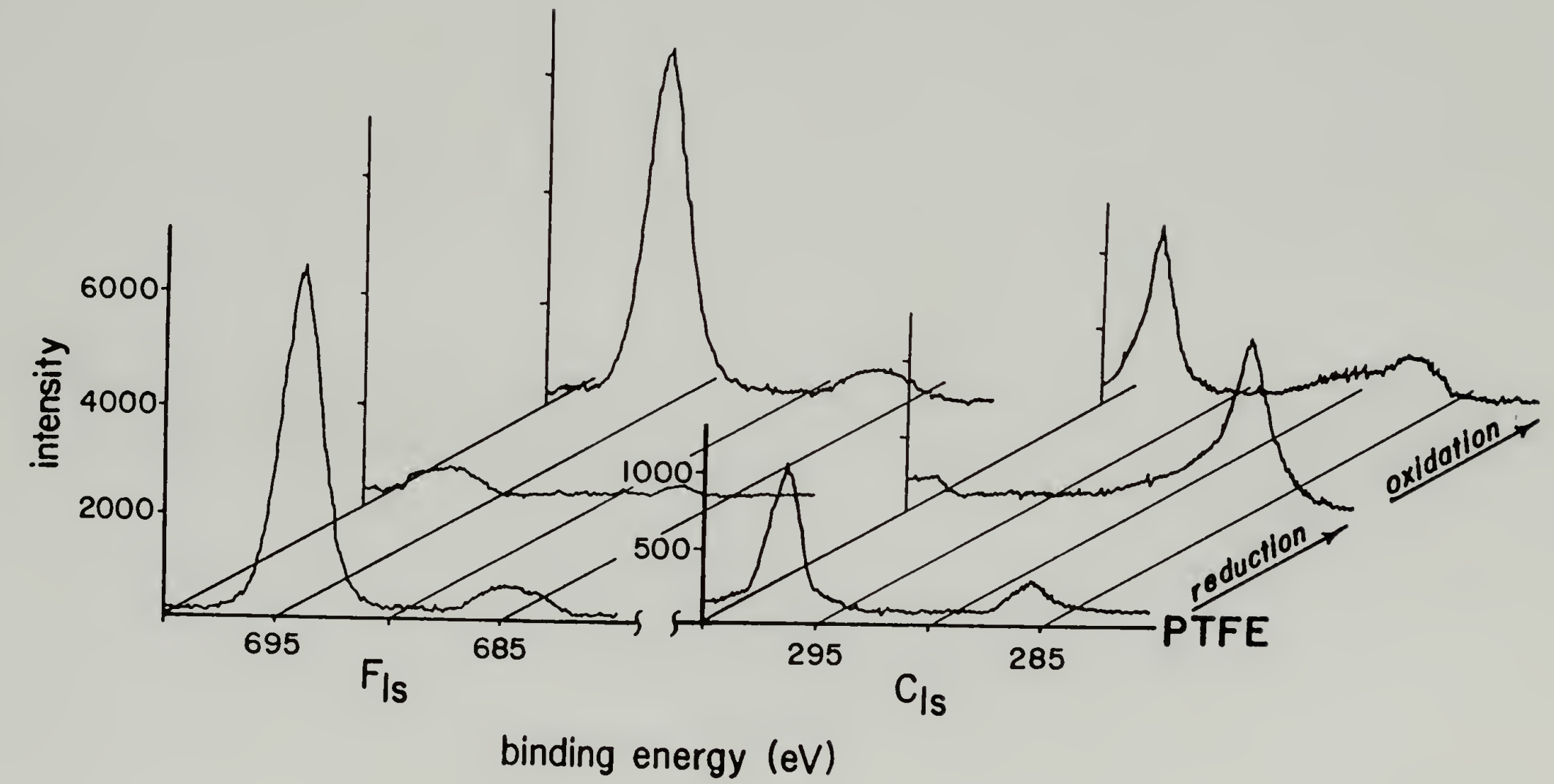
intensity
6000
4000
2000
1000
500
695
685
F_{1s}
295
285
C_{1s}
reduction
oxidation
PTFE
binding energy (eV)

for PTFE, except for a slight trace of oxygen. Samples oxidized in $H_2SO_4/KClO_3$ contain <0.5% oxygen by atomic composition. The C_{1s} high resolution spectrum of PTFE-C shows a shift in the carbon peak from the highly oxidized CF_2 in PTFE (293 eV) to a lower binding energy, less oxidized form of carbon in PTFE-C (286 eV). On oxidation of PTFE-C, a spectrum almost identical to that of virgin PTFE results except for a small shoulder on the high binding energy side of the C_{1s} peak, indicating oxygen-based functionality.

XPS spectroscopy also provides information on the reaction course in the outer ~40 Å with time. Figure 3.6 shows the XPS survey spectra of PTFE (**A**), PTFE-C (10 min reduction (**B**)), PTFE-C (20 min reduction (**C**)), and PTFE-C (24 hr reduction (**D**)). The reaction depths associated with these reaction times are 0 Å, 150 Å, 450 Å, and 6000 Å, respectively. The spectra indicate the gradual loss of fluorine (F_{1s}:696 eV) within the XPS sampling depth as the reaction proceeds. Also noted is the presence of oxygen; this varies somewhat sample-to-sample and is most likely attributed to exposure during sample preparation and analysis, reaction with water in the workup, and/or reaction with t-butoxide during the reduction.

Further information concerning the nature of the carbon is obtained from the high resolution C_{1s} spectra of the same samples. Figure 3.7 indicates that the higher binding energy CF_2 signal (293 eV) of PTFE is gradually replaced by a low binding energy signal (286 eV) due to the less-oxidized carbon in PTFE-C. This implies that PTFE is still present in the ESCA sampling depth (~40Å) even as the reaction proceeds thousands

Figure 3.6

XPS spectroscopy: changes in survey spectra as a function of time. **A**: unreacted PTFE; **B**: 10 minute reduction; **C** 25 minute reduction reduction; **D** 24 hour reduction.

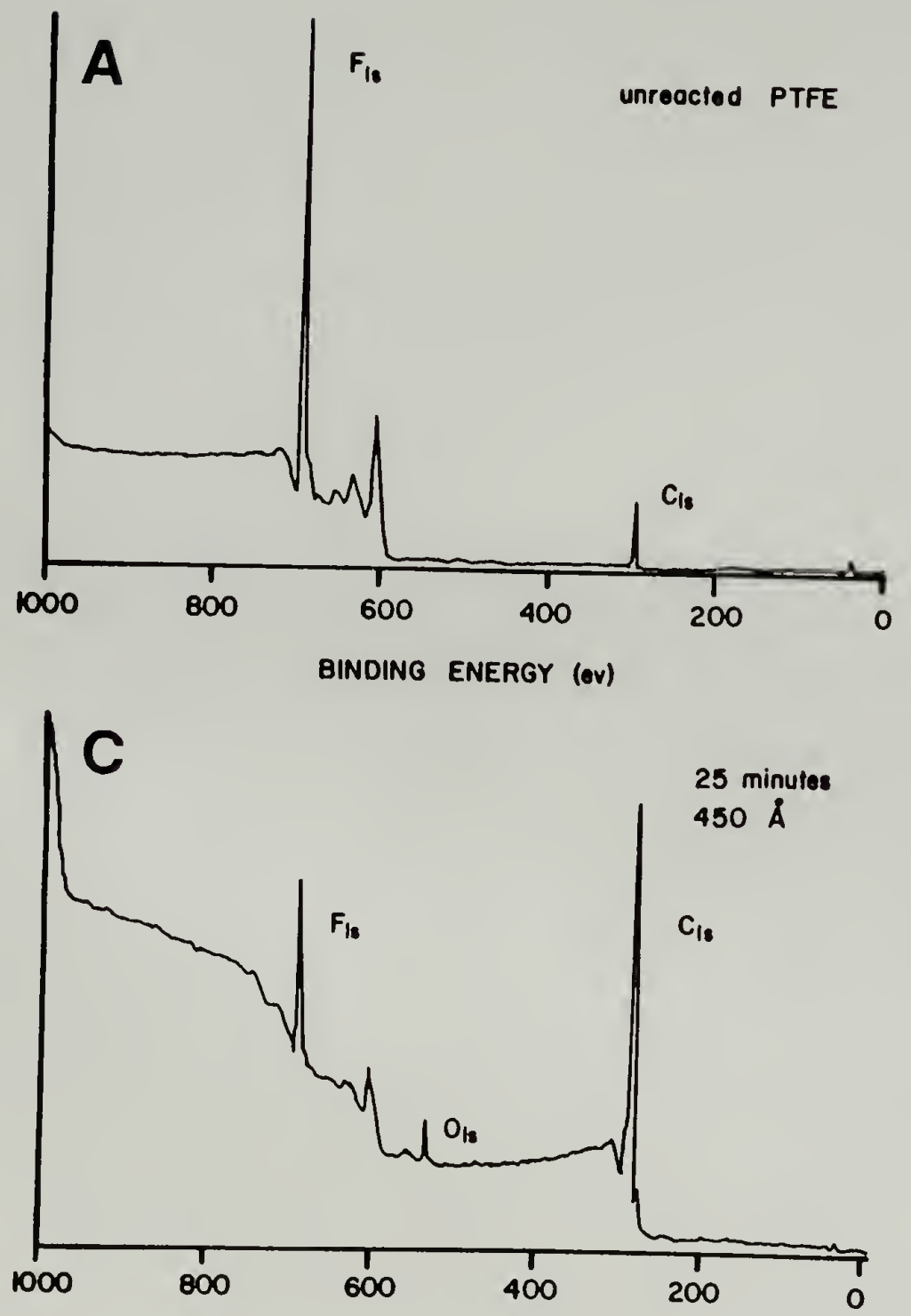
A
unreacted PTFE
F_{1s}
C_{1s}
1000
800
600
400
200
0
B
10 minutes
150 Å
F_{1s}
C_{1s}
O_{1s}
1000
800
600
400
200
0
C
25 minutes
450 Å
F_{1s}
C_{1s}
O_{1s}
1000
800
600
400
200
0
D
24 hours
4500 Å
C_{1s}
F_{1s}
O_{1s}
1000
800
600
400
200
0
BINDING ENERGY (ev)

Figure 3.7

XPS spectroscopy: changes in C_{1s} high resolution region as a function of reaction time. **A**: unreacted PTFE; **B**: 10 minute reduction; **C**: 25 minute reduction; **D**: 24 hour reduction.

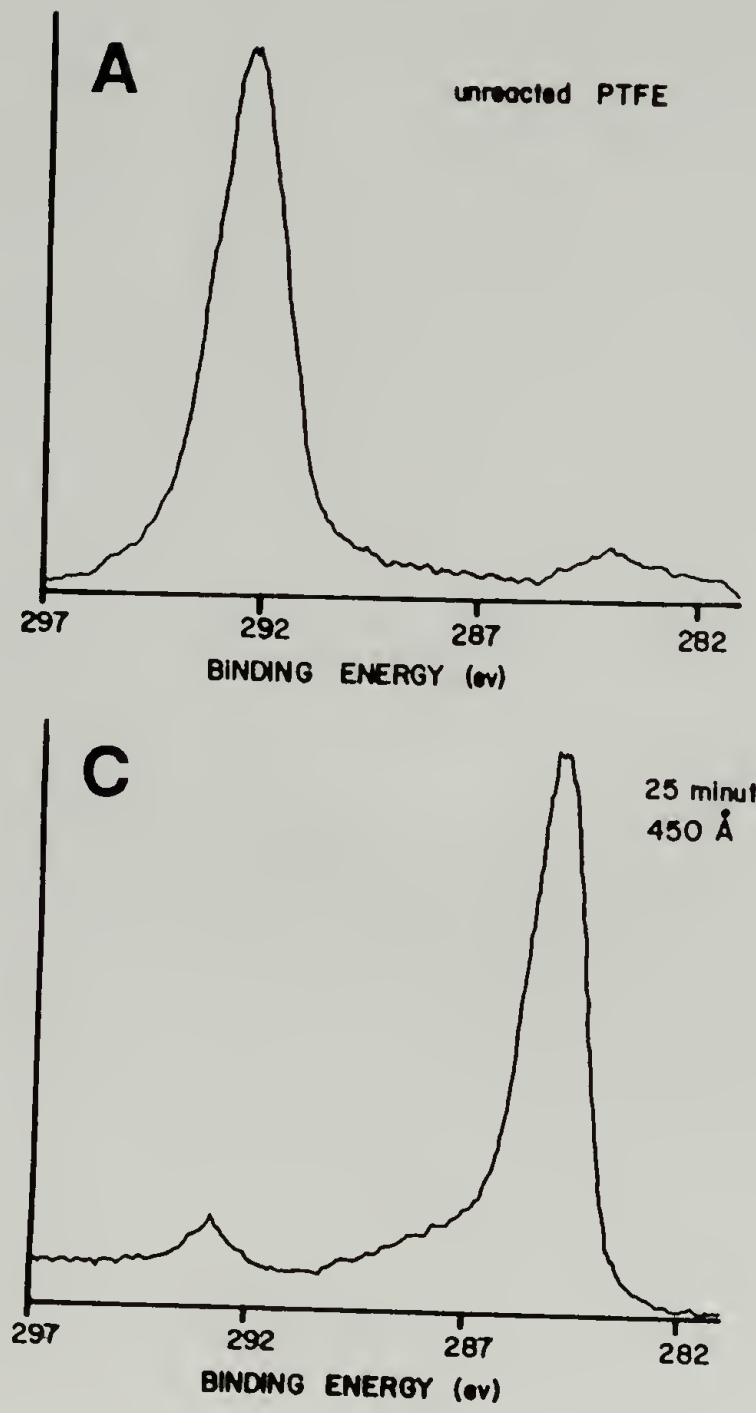
A
unreacted PTFE
297
292
287
282
BINDING ENERGY (ev)

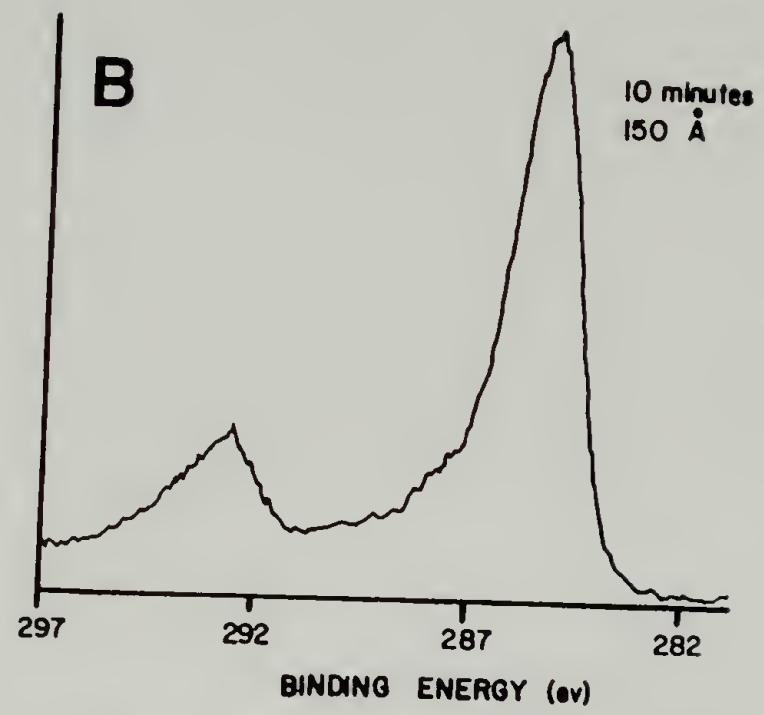
B
10 minutes
150 Å
297
292
287
282
BINDING ENERGY (ev)

C
25 minutes
450 Å
297
292
287
282
BINDING ENERGY (ev)

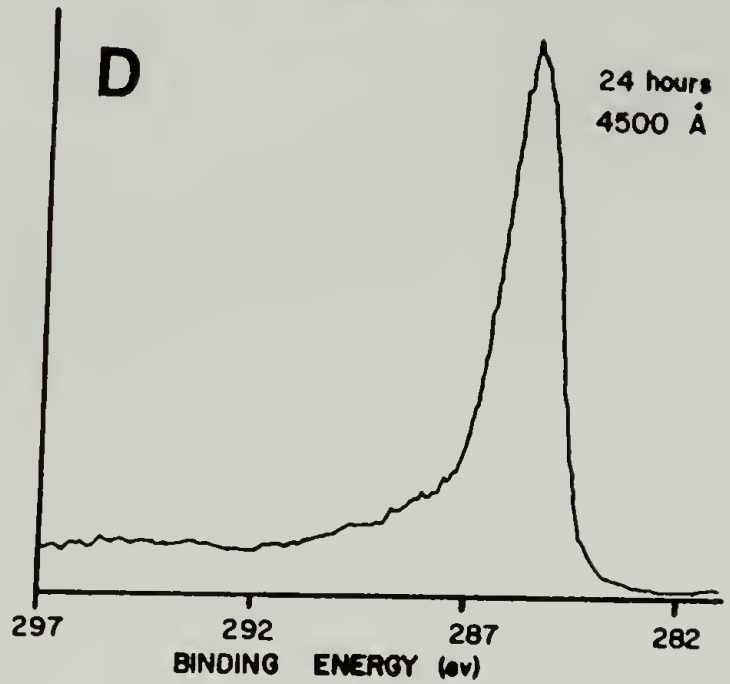
D
24 hours
4500 Å
297
292
287
282
BINDING ENERGY (ev)

of angstroms deep. When the signal due to CF_2 completely disappears at long reaction times, fluorine is still present in the survey spectrum. This remaining fluorine must be present as CF species other than CF_2. The literature suggests that there is not a significant difference in the binding energy values between the major carbon peak and sp^2 carbon bound to fluorine;[8] however, the higher binding energy shoulder to the left of the major carbon peak in Figure 3.7d may be due to fluoroolefin structure. More convincing evidence lies in the high resolution fluorine spectra taken during the reaction course. Figure 3.8 displays F_{1s} high resolution spectra for PTFE (a), PTFE-C (reduced 10 minutes (b)), PTFE-C (reduced 2 hours (c)), and PTFE-C (reduced 24 hours (d)). It is evident from these spectra that as the reaction progresses, changes in C-F structure are occurring. PTFE exhibits a CF_2 peak at 696 eV; after 10 minutes of reaction the peak is slightly broadened. A new fluorine signal is observed (690 eV) with a lower binding energy shoulder (688 eV) after 2 hours of reaction. A complex signal is observed after the 24 hour reaction period. These spectra are consistent with both the survey and C_{1s} high resolution spectra discussed above: the fluorine present must be C-F in some other form than CF_2.

The atomic composition of PTFE calculated for the 24 hour reduced sample (Figure 3.6) is $CF_{0.07}O_{0.07}$. Although hydrogen is present in the sample as evidenced by elemental analysis of extensively reduced samples, we are not able to quantify it at the surface, since XPS can not detect hydrogen.

It is difficult to discern effects of PTFE crystallinity and the

Figure 3.8

XPS spectroscopy: changes in F_{1s} high resolution spectra as a function of reaction time. **A**: unreacted PTFE; **B**: 10 minute reduction; **C**: 2 hour reduction; **D**: 24 hour reduction.

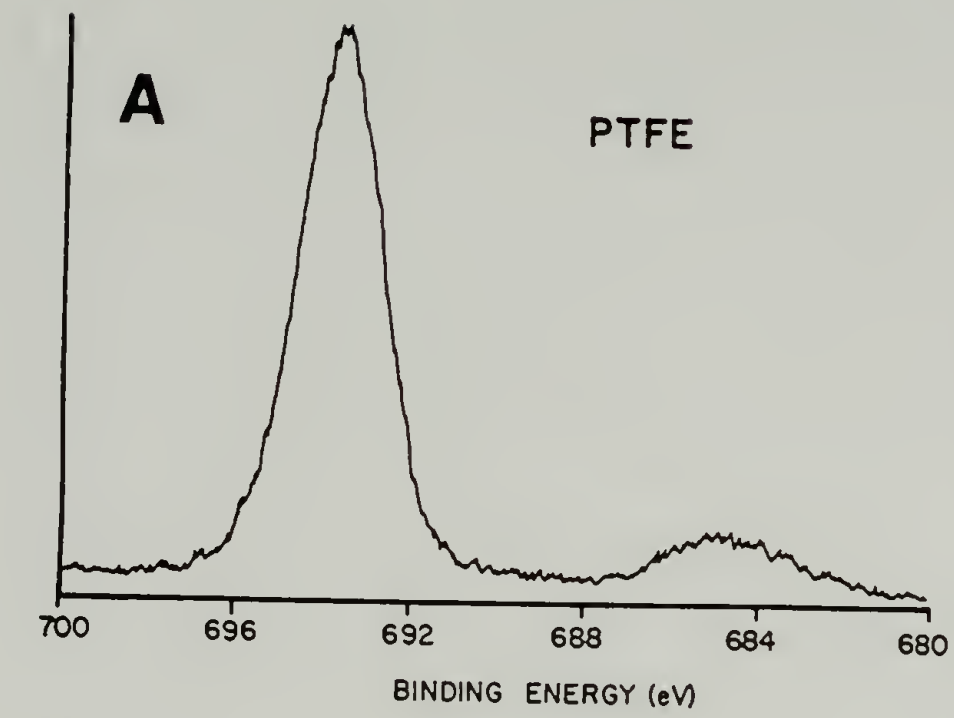
A
PTFE
700
696
692
688
684
680
BINDING ENERGY (eV)

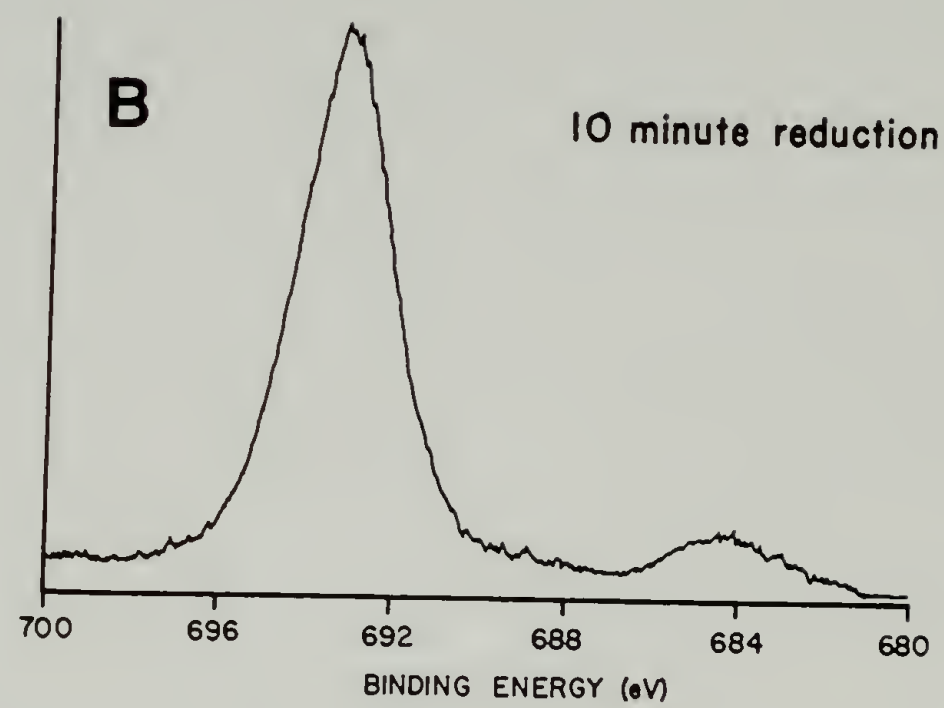
B
10 minute reduction
700
696
692
688
684
680
BINDING ENERGY (eV)

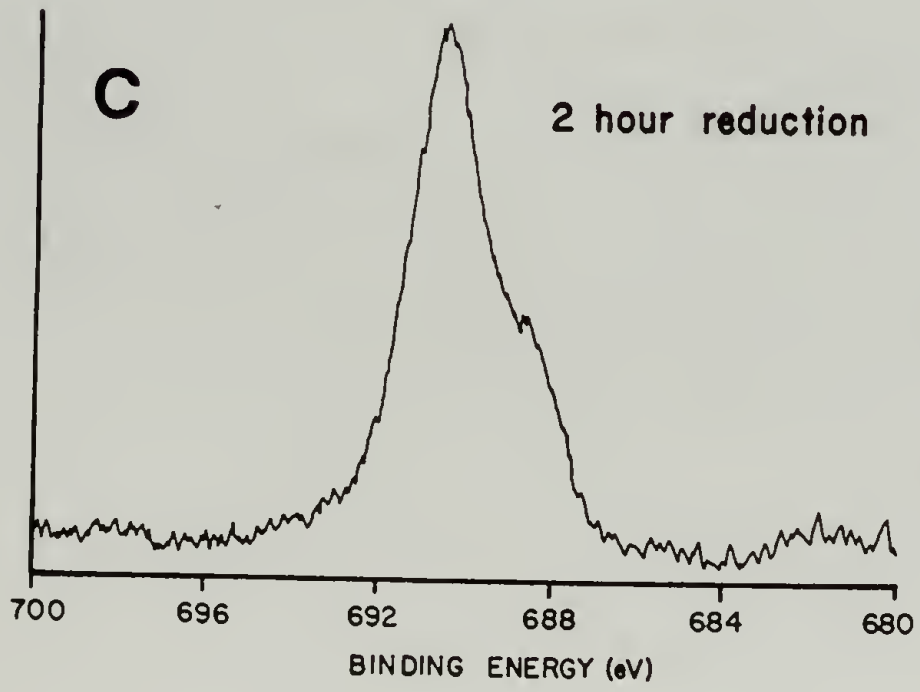
C
2 hour reduction
700
696
692
688
684
680
BINDING ENERGY (eV)

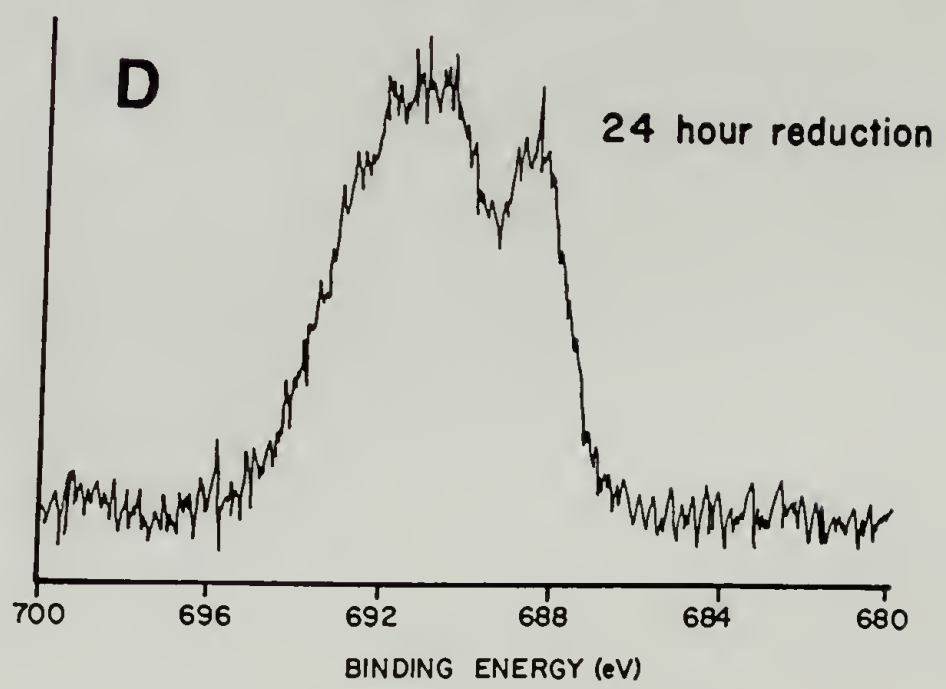
D
24 hour reduction
700
696
692
688
684
680
BINDING ENERGY (eV)

characteristics of the reaction medium on the reaction course. We have observed qualitatively that there is an effect of temperature on the reaction: at lower temperature (below room temperature) the reaction is sluggish. Whether the "room temperature"[9] transition in PTFE is responsible for this behavior is not certain. Solvent wetting of the surface may be important. In the liquid state, DMSO assumes a chainlike structure held together by the alignment of S-O dipoles. This structure suffers partial breakdown between 40°C and 60°C affecting properties of DMSO such as refractive index, density, and viscosity.[10] How this solvent phenomenon affects the reaction is not certain.

UV-Vis Spectroscopy

Further insight into the chemical nature of PTFE-C was obtained by UV-Vis spectroscopy of PTFE-C. The spectrum was obtained with a virgin film in the reference beam (Figure 3.9). The spectrum exhibits a broad absorbance with λ_{max} = 540, possessing little fine structure, consistent with the formation of a highly extended conjugated system.

EPR Spectroscopy

EPR spectroscopy at -196°C of PTFE powder (3 day reduction) indicated the presence of mobile free spins. (Figure 3.10) The PTFE control did not exhibit a signal, but PTFE-C gave a singlet with a Lorenztian line shape and a g value of 2.0030. Diphenylpicrylhydrazyl (DPPH) was used as a reference for the determination of the g value. The g value was determined from the crossover point of the first derivative

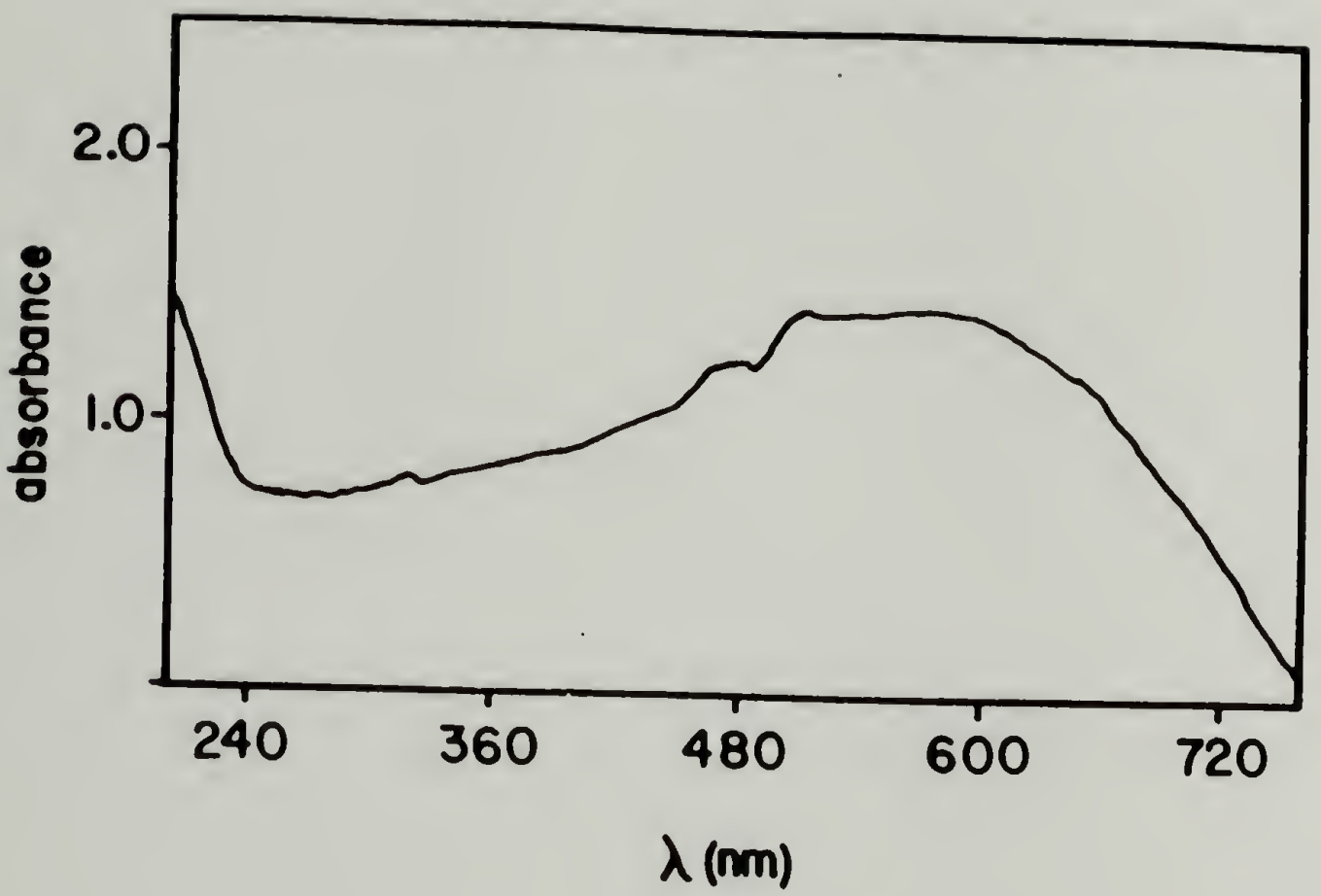

Figure 3.9

UV-vis spectrum of PTFE-C. The spectrum was obtained with a virgin film in the reference beam.

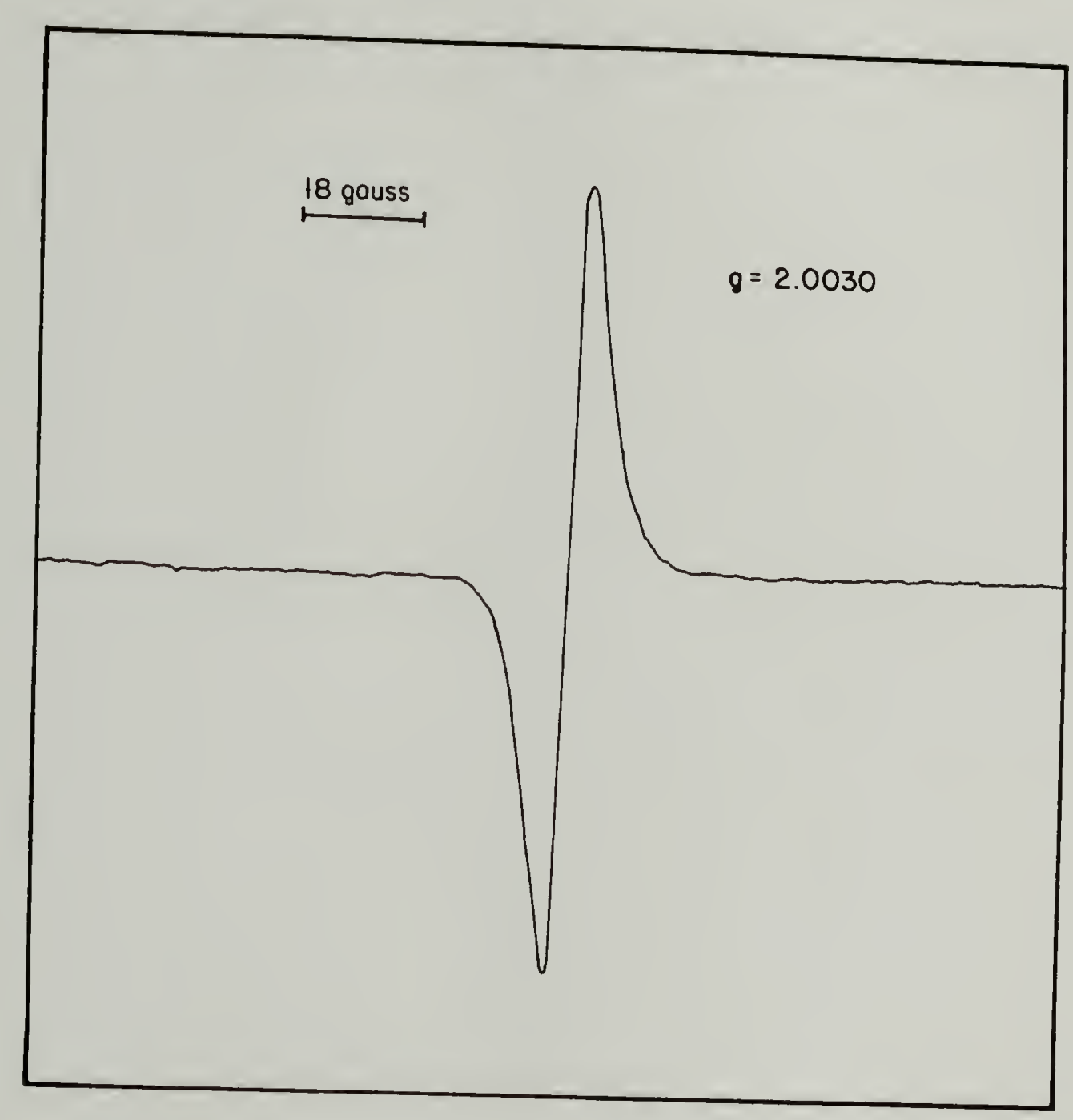

Figure 3.10

EPR spectrum of PTFE-C obtained at -196°C.

spectrum using the relationship

$$g_x H_x = g_s H_s$$

where H is the strength of the magnetic field at the crossover point and x and s represent the sample and standard, respectively. The EPR linewidth, Δ H (9 gauss) was taken as the peak to peak separation of the first derivative spectrum. The relative EPR line intensity was plotted as a function of temperature (Figure 3.11), demonstrating the Boltzmann distribution of electrons in the 2 spin states. No measureable effects of temperature on the linewidth were observed. Signals of this type are observed for highly conjugated polymers such as polyacetylene[11] and poly(paraphenylenevinylene),[12] which contain carbon-based mobile spins.

CPMAS NMR

Several pieces of information were obtained by ^{13}C CPMAS NMR of a PTFE sample reduced for 6 days. Less extensive reaction times did not result in enough material to obtain a suitable signal. Noteworthy is the presence of a signal in the CPMAS NMR, indicating the presence of hydrogen. The spectrum (Figure 3.12) exhibits broad and poorly resolved signals due to sp^3 (δ 29.87), sp^2 (δ 130.36), and sp (δ 80.70) carbons. The broadness of these peaks can be attributed to the presence of paramagnetic species, supported by the EPR data presented above, and dipolar interactions between ^{13}C and ^{19}F nuclei. Broad peaks due to paramagnetic species have been observed in the CPMAS NMR spectra of Iodine-doped polyacetylene[13] and various coals.[14]

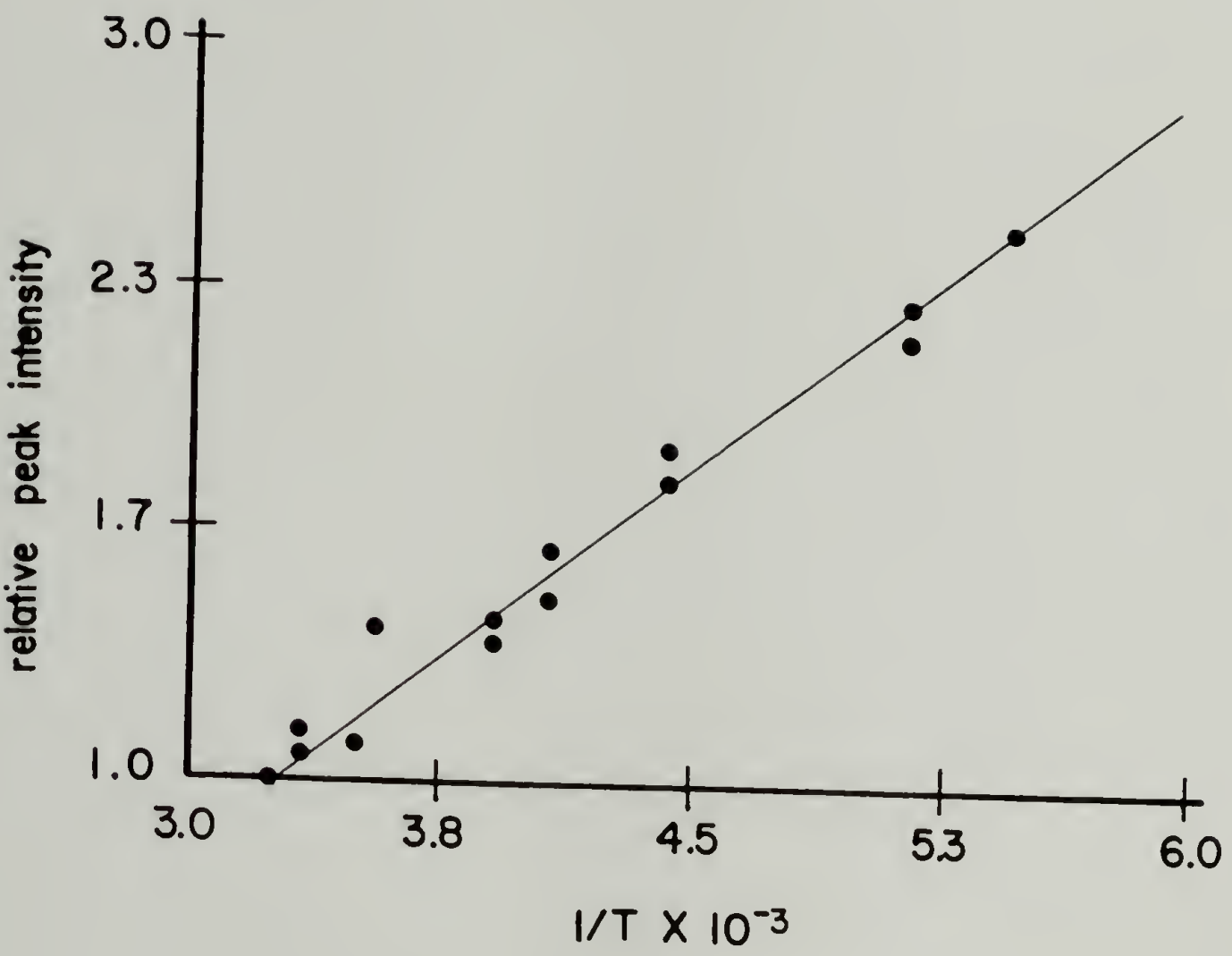

Figure 3.11

Temperature dependence of the relative EPR signal intensity for PTFE-C.

Figure 3.12

Cross polarized magic angle spinning NMR of PTFE-C. Signals due to sp^3 (δ 29.87), sp^2 (δ 130.36), and sp (δ 80.70) are indicated.

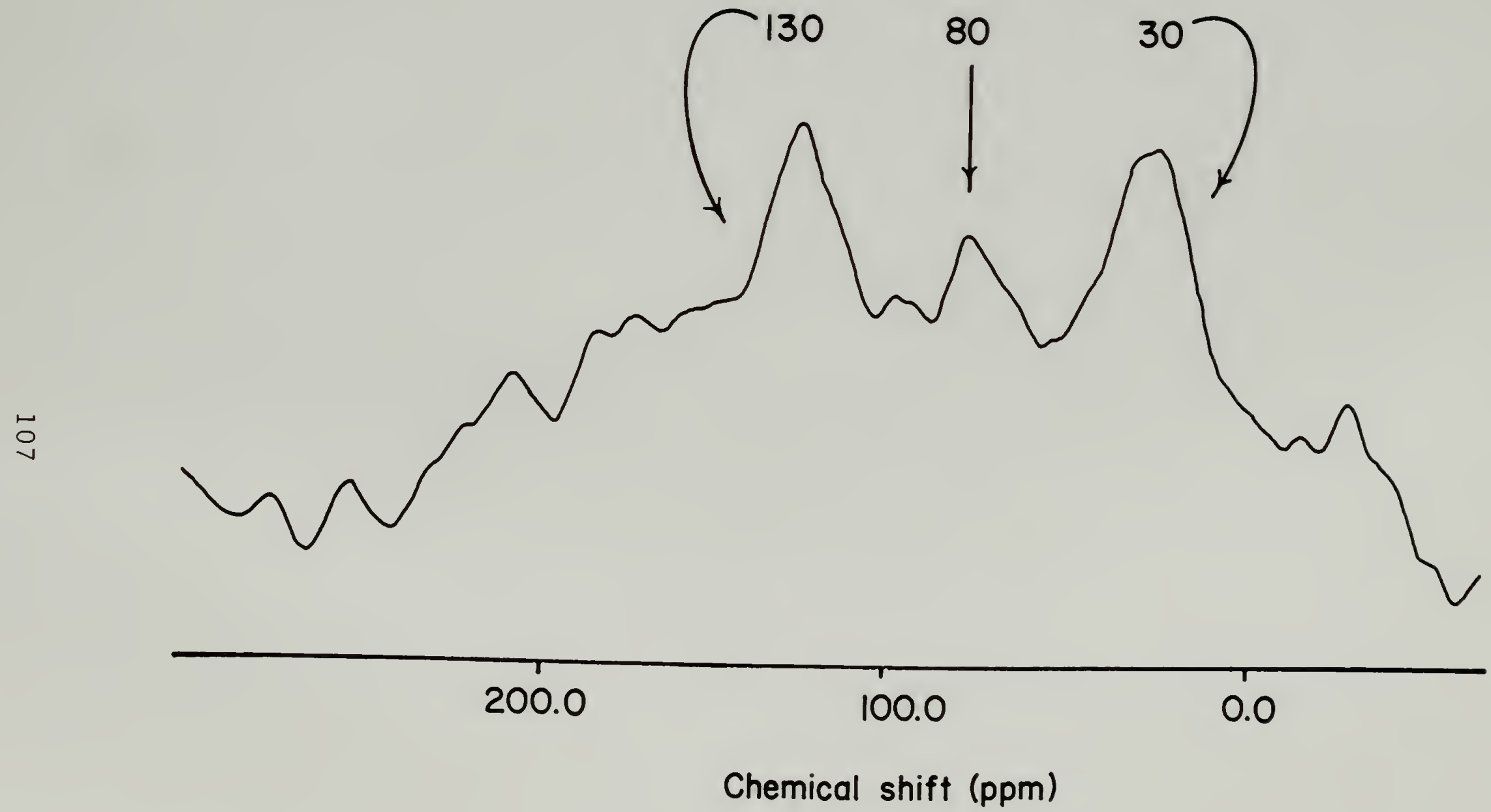
130
80
30
107
200.0
100.0
0.0
Chemical shift (ppm)

Vibrational Spectroscopy

The combination of isotopic labelling and vibrational spectroscopy yielded further structural information on PTFE-C. Samples analyzed by ATR-IR were reduced for 3 days, providing ample material for inspection in the ATR sampling region. Analyses were done using a 45° KRS5 crystal; spectra obtained on a 45° germanium crystal, despite less depth of penetration, exhibited little contrast, probably because of unacceptable matching of refractive index of the crystal (n=4.0) to the polymer (n=1.35). Samples analyzed by Raman spectroscopy were reduced for 2 days to obtain an acceptable signal-to-noise ratio. Although XPS spectra of samples reduced $\geq$ 3 days showed increasing amounts of oxygen in the outer 40 Å, indicating side reactions, the techniques employed here necessitated micron-level thicknesses of PTFE-C for analysis.

Attenuated Total Reflectance Infrared Spectroscopy

Figure 3.13 illustrates baseline and ATR corrected FT ATR-IR spectra of PTFE and PTFE-C. The bands observed in our PTFE specimen agree well with those observed by Starkweather[15] and others.[16,17] On reduction, numerous bands not attributable to PTFE appear. The most prominent absorbances are found in the following regions: 3000-2850; 2300-2100; 1725-1290; 1010-900. Inspection of the spectrum indicates the presence of C-H stretching (3000-2850). In order to explain the origin of this hydrogen and further characterize the structure, the reaction was carried using deuterated reagents and solvents. Figure 3.14 shows FT ATR-IR spectra of **A**: PTFE-C prepared using all hydrogen containing reagents and

Figure 3.13

ATR-IR of PTFE (top) and PTFE-C (bottom) obtained on a 45° KRS5 crystal.

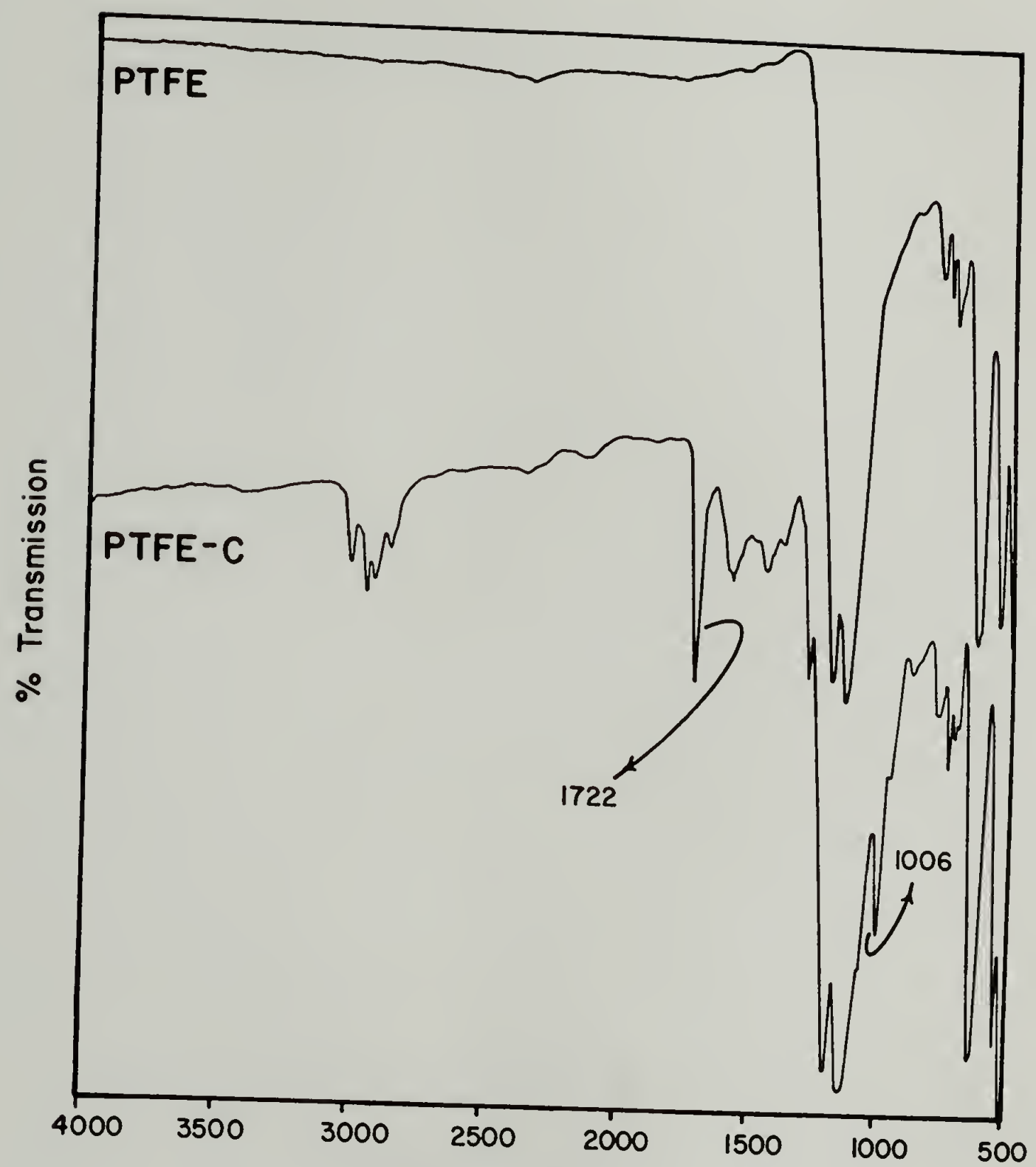
PTFE
PTFE-C
1722
1006
% Transmission
4000
3500
3000
2500
2000
1500
1000
500
Wavenumber (cm⁻¹)

solvents, **B**: PTFE-C prepared as in **A**, except that DMSO-d_6 was used as the reaction solvent, **C**: PTFE-C prepared as in **A** except that D_2O was used in the workup and **D**: PTFE-C prepared as in **A** except benzoin-d_{12} was used as the reagent. Table 3.2 lists the peak positions for all absorbances found in **A–D**. From these spectra, it is obvious that there is no benzoin (or benzil) incorporation in the reduced material. We attribute the absorbances from 2960 to 2860 cm^{-1} present in each spectrum to aliphatic C-H stretching from the only non-deuterated source of protons: potassium t-butoxide. Addition of butoxide ion to fluorinated unsaturation yields t-butyl ether groups on the surface. (Equation 3.2)

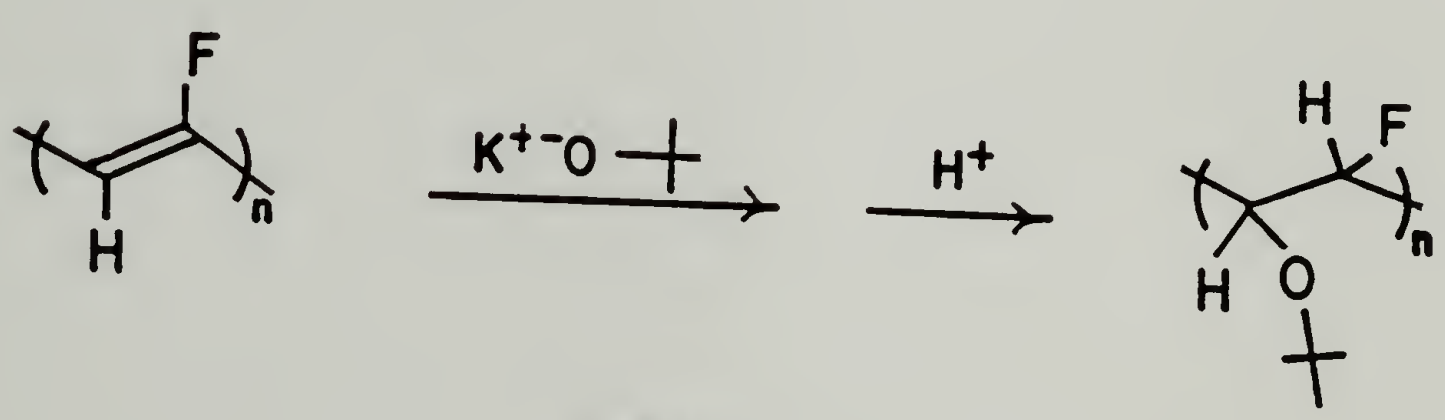

Equation 3.2

The lower intensity of these absorbances in **B** (prepared using DMSO-d_6) suggests the solvent is a major source of hydrogen. The absorbance at 3012 cm^{-1} (v C-H), present in **A** and **C** but absent in **B**, shifts to 2220 cm^{-1} (v-C-D) in **B** suggesting that DMSO is the source of hydrogen. Further evidence for this is found with inspection of the sp^2 C-H out of plane bending vibration in **A** at 1006 cm^{-1}; reaction in DMSO-d_6 causes this peak to shift to 740 cm^{-1}, corresponding to sp^2 C-D out of plane bending. Also noteworthy is the change in intensity of the peak at 1722

Table 3.2

Infrared absorbances in cm^{-1} for deuterated PTFE-C prepared under various conditions

Non deuterated reagents	DMSO-d_6	D_2O	Benzoin-d_{12}
3013	2953	3011	3013
2959	2922	2975	2959
2930	2870	2918	2930
	2856	2856	
2376	2370	2370	2368
2150	2220	2154	2148
1722	1715	1711	1722
1579	1589	1580	1579
1462	1564	1449	1464
1385	1514	1412	1383
	1495	1375	
	1460		
1286	1300	1292	1289
1200	1200	1202	1200
1142	1140	1143	1143
1006		1003	1008
885		883	887
		806	
779	787	771	773
773			
742	740	740	740
719	723	719	719
706	704	704	704

Figure 3.14

ATR-IR of PTFE-C prepared under various deuterated conditions. See text for details.

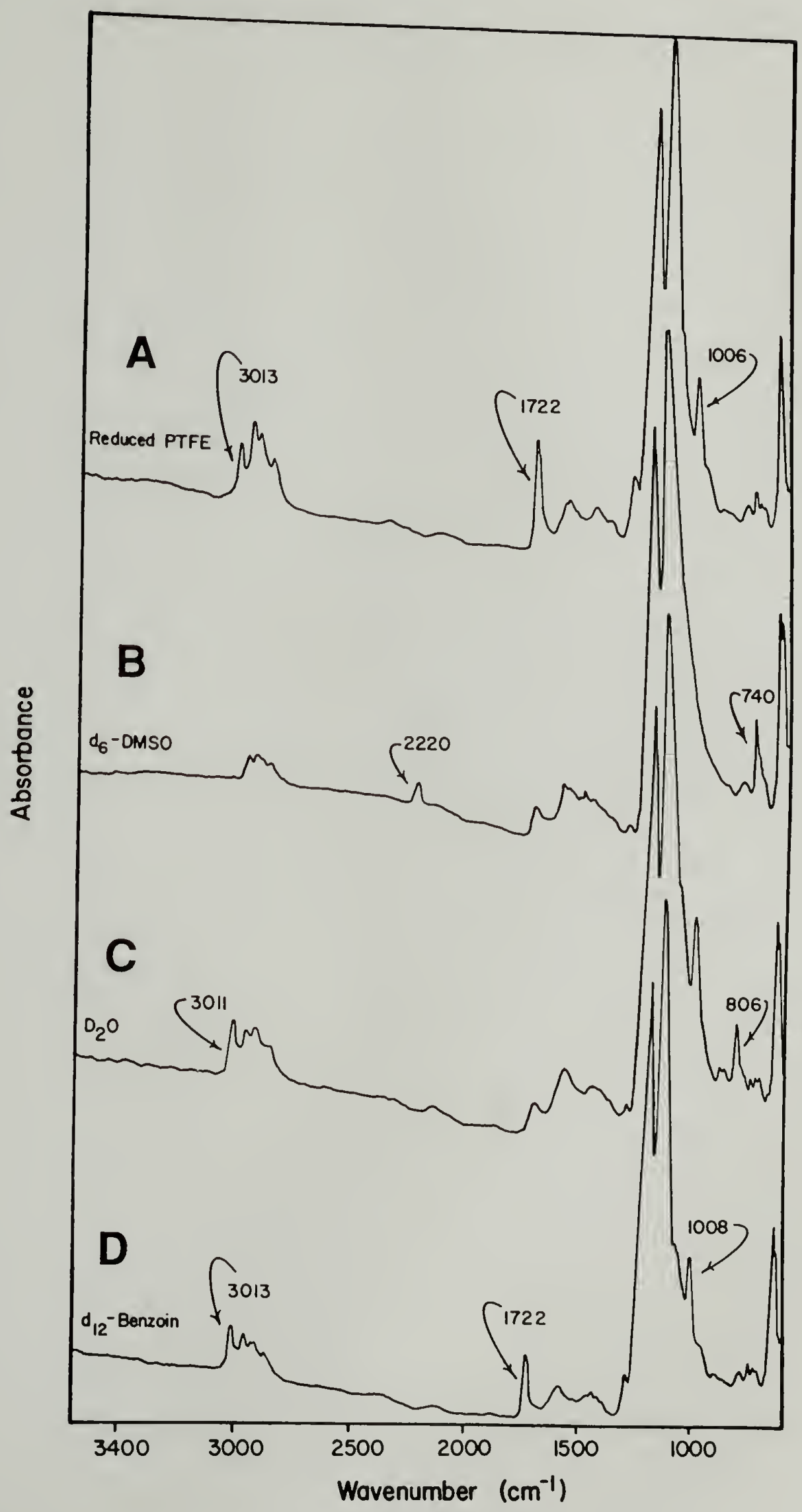
A
Reduced PTFE
3013
1722
1006
B
d_6-DMSO
2220
740
C
D_2O
3011
806
D
d_{12}-Benzoin
3013
1722
1008
Absorbance
3400
3000
2500
2000
1500
1000
Wavenumber (cm^{-1})

and 1286 cm^{-1} on going from **A** to **B.** We tentatively assign the 1722 cm^{-1} absorbance to monofluorinated olefin C==C stretching, based on literature values for this vibration and its deuterated analogues[18,19] The XPS and gravimetric data support its existence. On deuteration, one would expect this absorbance to shift into the 1150-1200 region; unfortunately, PTFE CF_2 stretching absorbances are quite strong in this region. There is sufficient evidence that the 1722 cm^{-1} absorbance is <u>not</u> related to carbonyl C==O stretching, since this absorbance shifts to lower frequency in reactions **A** and **B.** Examination of literature values for $\nu_{C=O}$ of deuterated ketones, aldehydes, and carboxylic acids indicate no shifts in the C==O stretching frequencies on deuteration of the carbon α to the carbonyl[20]. The only other possible assignment for the peak at 1722 cm^{-1} would be a combination or overtone of other absorbances.

Another source of hydrogen is the water used in the workup. On workup in D_2O, the 1722 cm^{-1} peak in **A** decreases in intensity. Although the 1006 cm^{-1} peak in **A** remains intact, a new absorbance at 806 cm^{-1} appears in **C.** This absorbance may be due to C-D out of plane bending but this assignment is suspect as no absorbance due to C-D stretching is observed. As previously mentioned, the importance of protonation by water is obvious visibly: the reduced films are black/purple in color, even after repeated DMSO washing. Only after the water is added, do the films turn gold.

Two other regions of the spectra are not altered when deuterated. The absorbance at 2150 cm^{-1} is assigned to C$\equiv$C stretching; the

absorbances from 1600 to 1400 cm^{-1} are due to skeletal vibrations of condensed aromatic-like carbon.

Raman Spectroscopy

Since the UV-vis spectrum of PTFE-C indicates that it is an extended conjugated system, we exploited the resonance enhancement effect in Raman spectroscopy[21] in order to obtain information on skeletal vibrations. The method permits observation of backbone vibrations of minute concentrations of extended conjugation. Although the effect is not well understood theoretically, it has enjoyed practical application in the study of extended conjugated systems such as polyacetylene[22-24] and polydiacetylene.[25]

The Raman spectrum of PTFE-C using green (5145 Å) excitation is shown in Figure 3.15. The sample fluoresced so intensely at this wavelength (which is close to that where the sample absorbs in the UV-vis region (Figure 3.9), obscuring most of the Raman bands. Only two peaks were discernable: 1500 cm^{-1}, assigned to C==C stretching and a broad absorbance from 2100-2275 cm^{-1} which we assign to C≡C stretching.

More lucid structural information was obtained using red (6328 Å) excitation. It is important to emphasize that the Raman spectrum obtained with red excitation exhibits the structural information of only a small percentage (the most highly conjugated) of PTFE-C. The Raman spectra of PTFE-C and PTFE-C (DMSO-d_6) are shown in Figure 3.16. In agreement with the IR data, the Raman spectra indicate that hydrogen is present in PTFE-C, originating from DMSO. Peak assignments for both spectra are listed in Table 3.3.

Table 3.3

Raman shifts for PTFE-C and PTFE-C (DMSO-d_6)

PTFE-C		PTFE-C (DMSO-d6)	
Peak position (cm-1)	Assignment	Peak position (cm-1)	Assignment
1003	C-H out-of-plane bend	740	C-D out-of-plane bend
1100	C-C stretch	857	C-C stretch
1476	C=C stretch	1197	C-C-D out-of-plane bend
2176	C≡C stretch and 2 (1100)	1382	C=C stretch
2554	1100 +1476	1715	2 (857)
2942	2 (1476)	2058	857 + 1197
		2239	C≡C stretch and 857 + 1382
		2580	1197 + 1382
		2755	2 (1382)

Figure 3.15

Raman spectra of PTFE-C obtained using green (5145 Å) excitation.

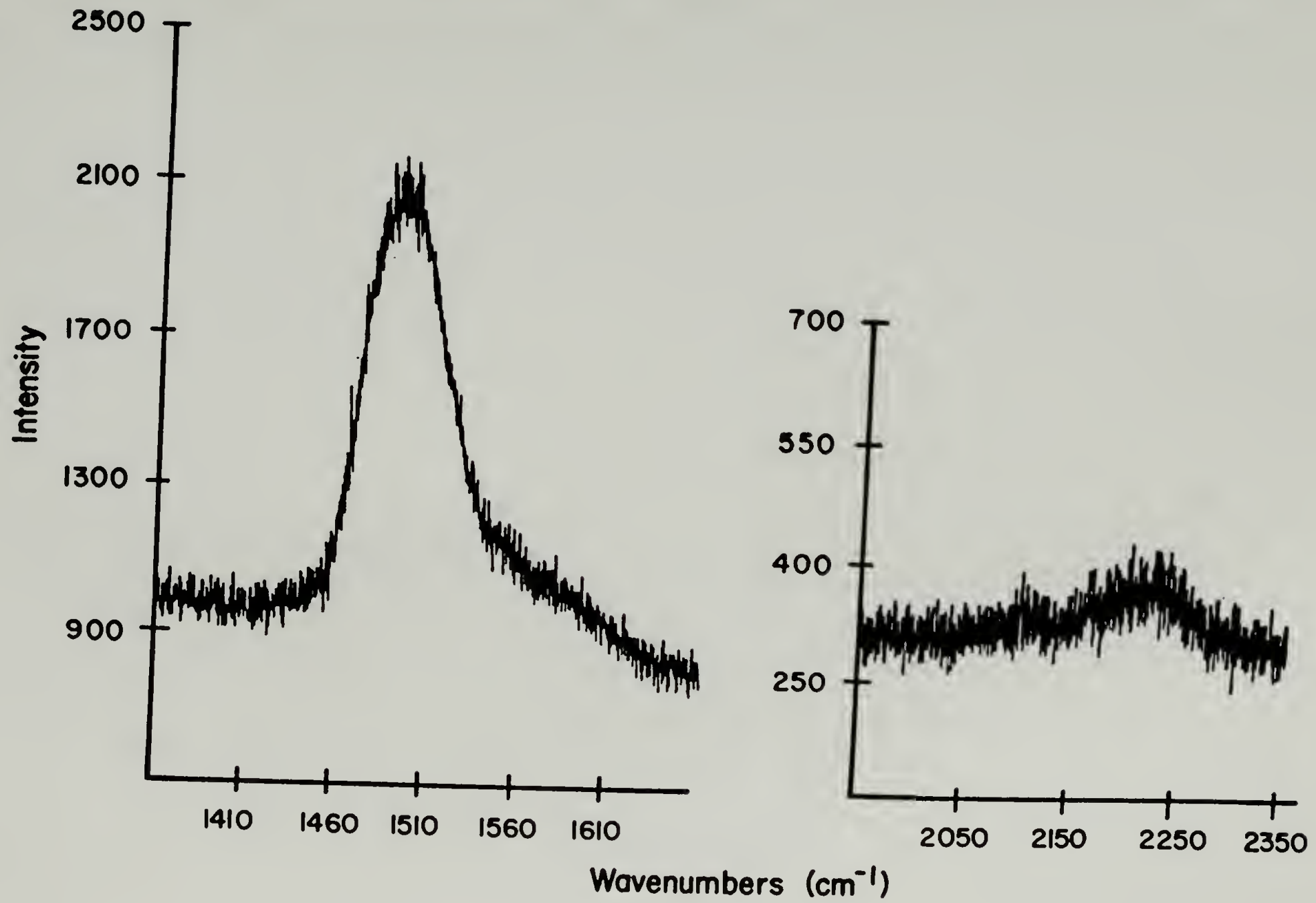
Intensity
2500
2100
1700
1300
900
1410
1460
1510
1560
1610
700
550
400
250
2050
2150
2250
2350
Wavenumbers (cm⁻¹)

Figure 3.16

Raman spectra of PTFE-C and PTFE-C prepared in DMSO-d_6.

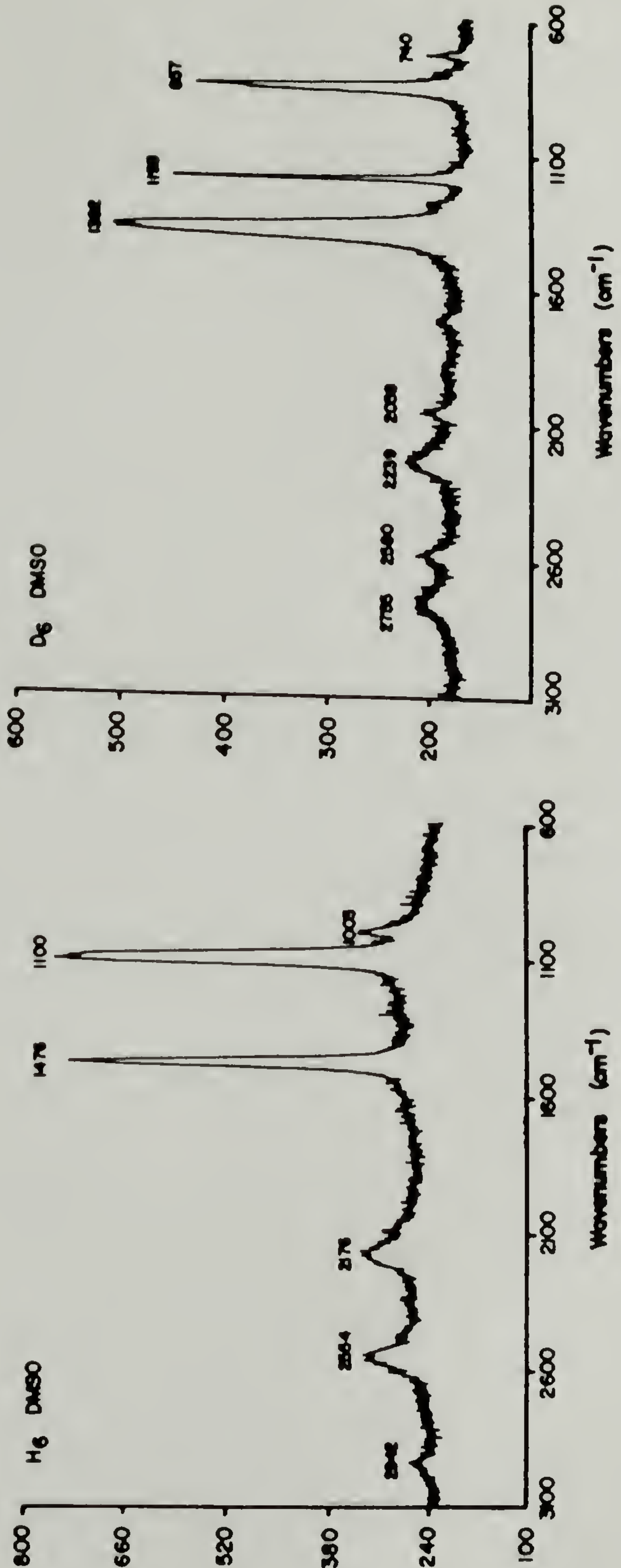
H6 DMSO
D6 DMSO
Wavenumbers (cm-1)
1476
1100
2554
2176
2540
2229

Samples prepared with benzoin-d_{12} or worked up in D_2O exhibited the same Raman spectra as that of PTFE-C run with all hydrogenated solvents and reagents.

The Raman peak positions in PTFE-C and PTFE-C (DMSO-d_6) correspond well with literature values for those found in trans h-polyacetylene and trans d-polyacetylene, respectively;[26] we conclude that there is a polyacetylene-like component of PTFE-C. No quantitative information can be interpreted from this Raman data in light of the unknown magnitude of the resonance enhancement, the excitation used, and the inherent nature of the Raman process.

Composite structure of PTFE-C

A composite structure is given for PTFE-C based on our characterization work (Figure 3.17). It is important to emphasize that this pictorial representation is meant to convey a qualitative image of the major features present: single, double, and triple bonds, extended conjugation, condensed aromatic-like cross-links, fluorine bound to sp^2 carbon, hydrogen bound to polyacetylene-like structure, oxygen (from adventitious sources and as t-butyl ethers) and free mobile spins. Scheme 3.2 depicts the probable sequence of reactions leading to these features. The XPS survey spectra vs. reaction time data presented above suggest a gradient structure of highly reduced carbonaceous material at the surface, less reduced (containing more fluorine) PTFE at greater depths, and virgin (unreacted) PTFE in the bulk.

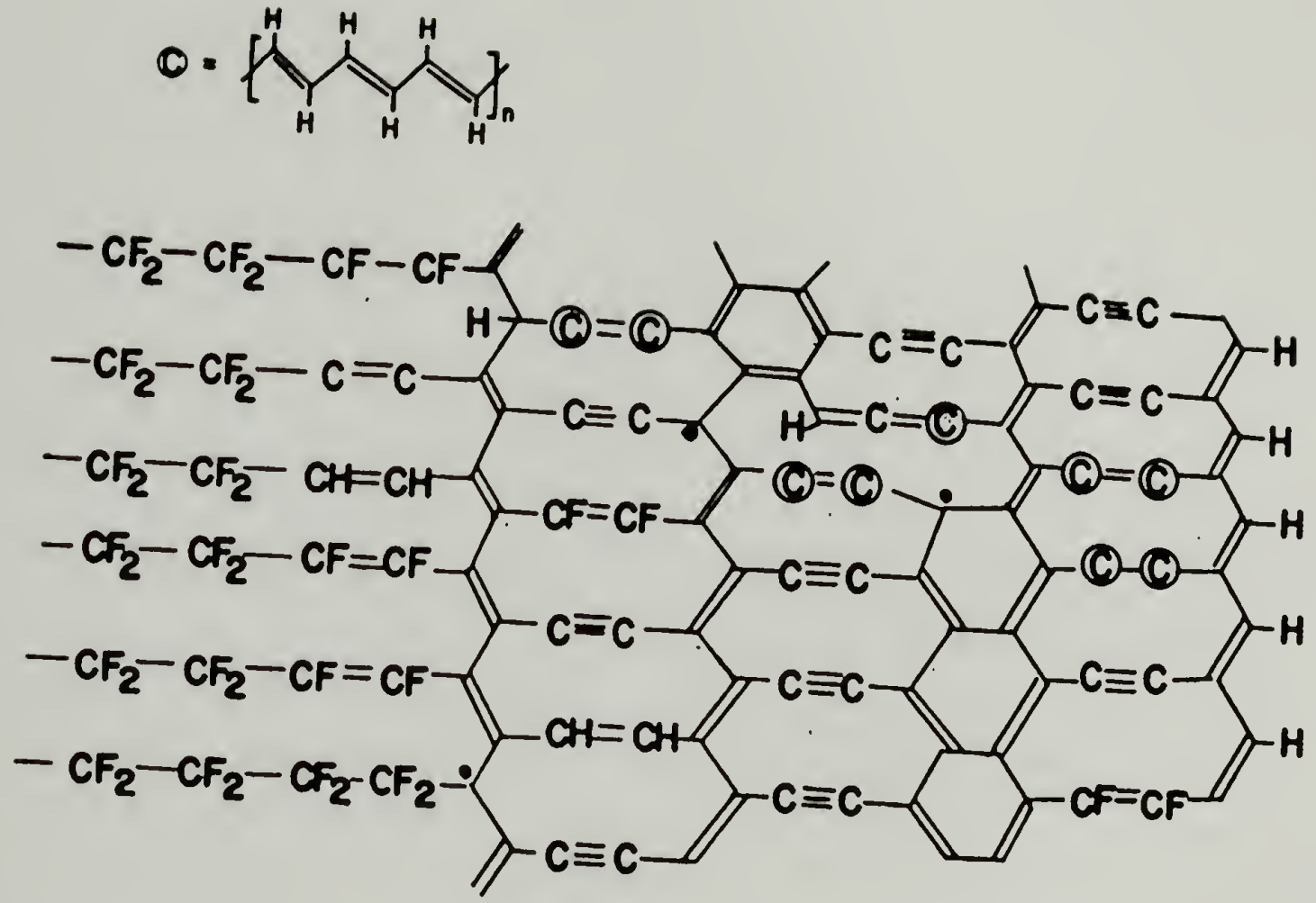

Figure 3.16

Composite representation of PTFE-C.

Scheme 3.2

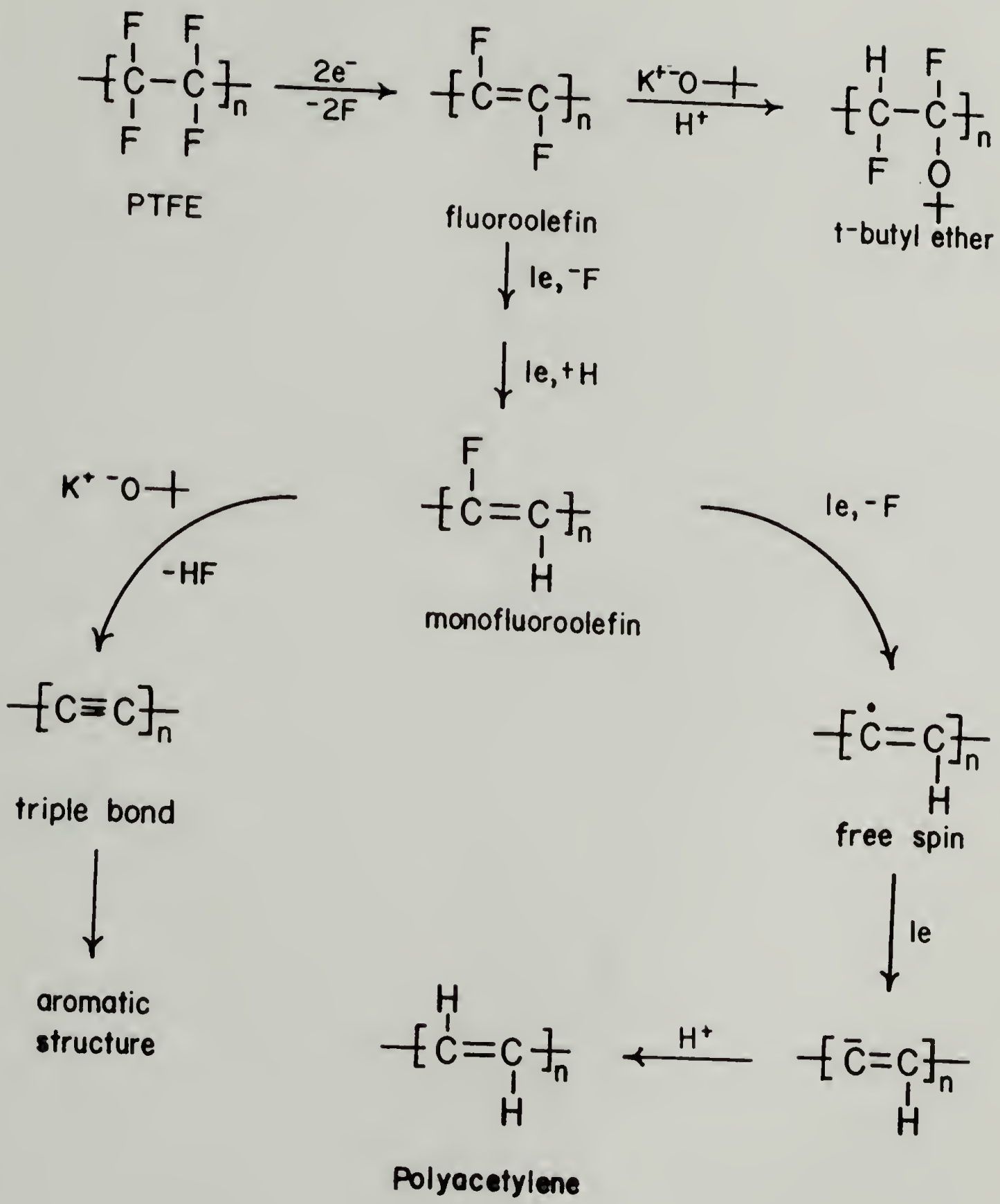
PTFE
2e⁻
-2F
fluoroolefin
K⁺⁻O
H⁺
t-butyl ether
le, -F
le, +H
monofluoroolefin
K⁺ ⁻O
-HF
le, -F
triple bond
free spin
le
aromatic structure
H⁺
Polyacetylene

Electronic Properties

The electronic properties of PTFE-C were investigated. Motivation for this work originated from the chemical characterization results, which indicated that PTFE-C was an extended conjugated system. Pristine PTFE-C exhibits very low conductivity ($\sigma < 10^{-10}\ \Omega^{-1}cm^{-1}$), however, doping with dry iodine induces a dramatic increase to values ranging from 0.3-40 $\Omega^{-1}cm^{-1}$, depending on the depth of reaction. Iodine doped samples generally have a black metallic appearance and are air stable, unlike the undoped material. A sample exhibiting a maximum conductivity of 36 $\Omega^{-1}cm^{-1}$, showed a conductivity of 14$\Omega^{-1}cm^{-1}$ after 12 hours in air. The conductivity was shown to be electronic in nature (not ionic) by passing current at 1V for 6 hours and then reversing the probes of the multimeter: no change in resistance occurred, thus no poling of charge occurred.

Figure 3.18 shows a plot of conductivity vs. thickness of the conductor for the iodine-doped samples. The depth of reaction is obtained gravimetrically, as described above. The points appear scattered; we do not infer any linear relationship, but a general trend implying an inverse thickness-conductivity relationship. There are two possible explanations for this type of behavior: 1) The thickness obtained gravimetrically is an average thickness which is much greater than the minimum thickness. This calculated average thickness may increase faster that the conductivity limiting thickness, yielding measured values that are lower than the intrinsic conductivity of the sample. 2) There may be a reaction which is deleterious to conductivity competing with reduction, diminishing the observed conductivity values.

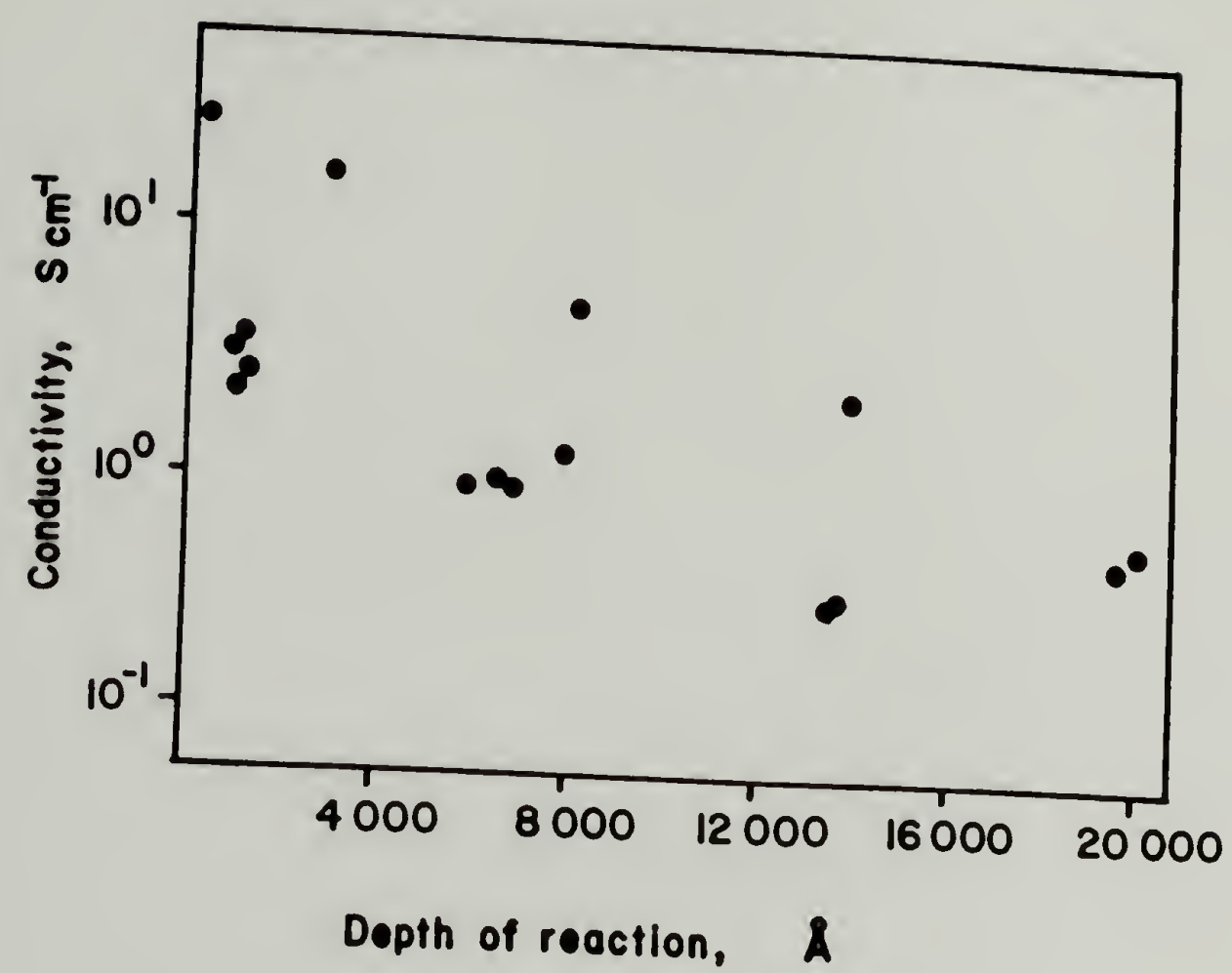

Figure 3.18

Plot of the conductivity of iodine-doped PTFE-C as a function of reaction depth.

The temperature dependence of the conductivity of the I_2-doped samples was investigated. (figure 3.19). The data indicates that the material is a semiconductor with an activation energy of 0.4-0.7 eV over the temperature range studied. The significance of these plots in determining conductivity mechanisms has been reviewed by others.[25]

The EPR spectrum of the iodine-doped PTFE-C (Figure 3.20) recorded at room temperature shows broadening (ΔH = 12 gauss) compared with the undoped sample (ΔH = 9 gauss) (Figure 3.10). It also appears that the signal is split by fluorine.

The C:I ratios in iodine doped PTFE-C films were determined gravimetrically. Table 3.5 lists the values obtained in film samples of PTFE-C reduced for various times. The amount of iodine incorporated is inversely dependent on the amount of reduced material present.

Table 3.4

Iodine uptake experiments: C:I atomic ratios in PTFE-C

C:I ratio	Reduction time (hours)
0.74	3
6.5	4
7.2	7

The electrical conductivity PTFE-C possesses demonstrates the applicability of this reduction as an excellent route to a conducting polymer from a processable precursor: PTFE. In addition the alteration of the surface properties of an excellent insulating material with a low dielectric constant to those of a semiconductor would find use in a wide range of applications.

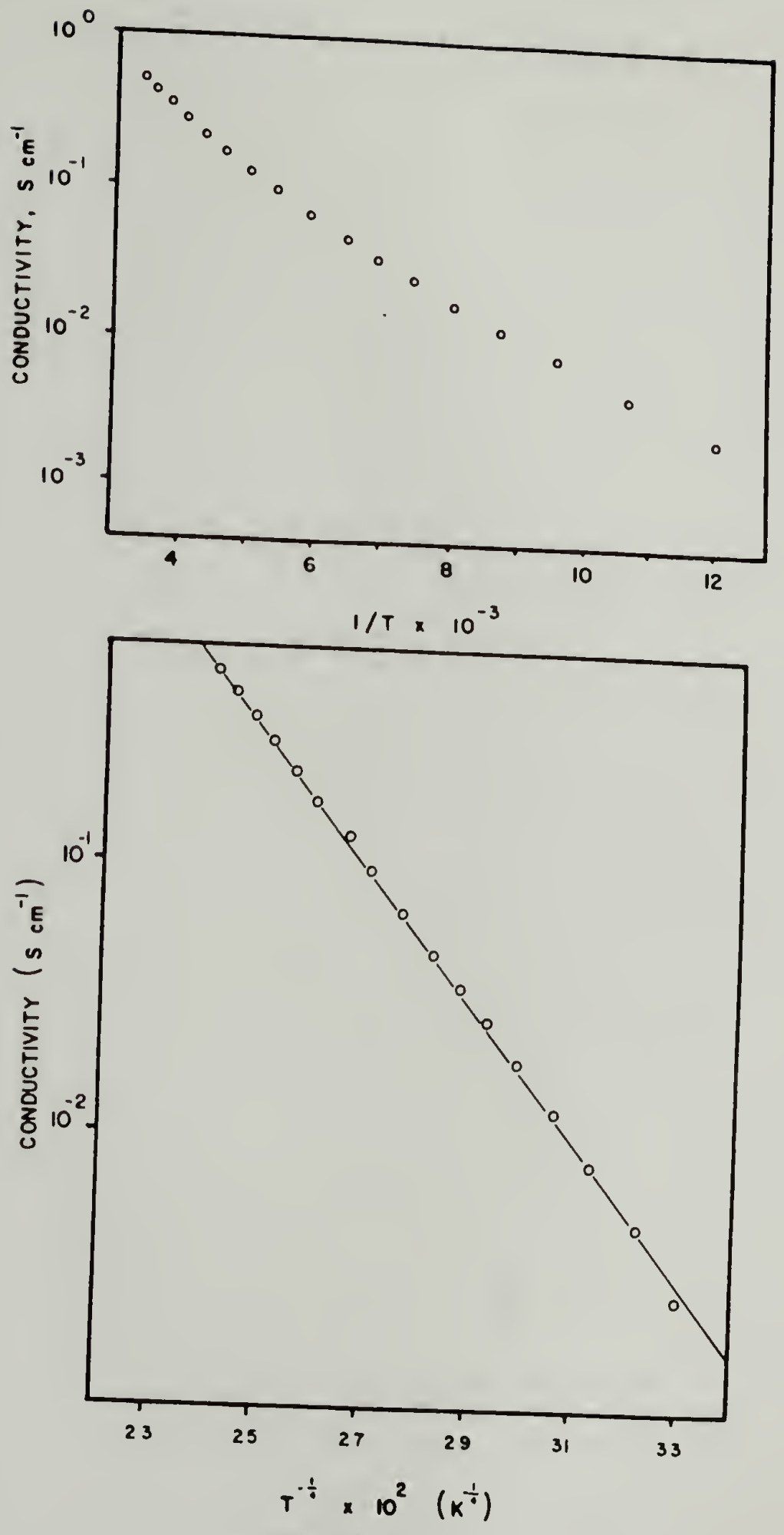

Figure 3.19

Temperature dependence of conductivity of iodine-doped PTFE-C.

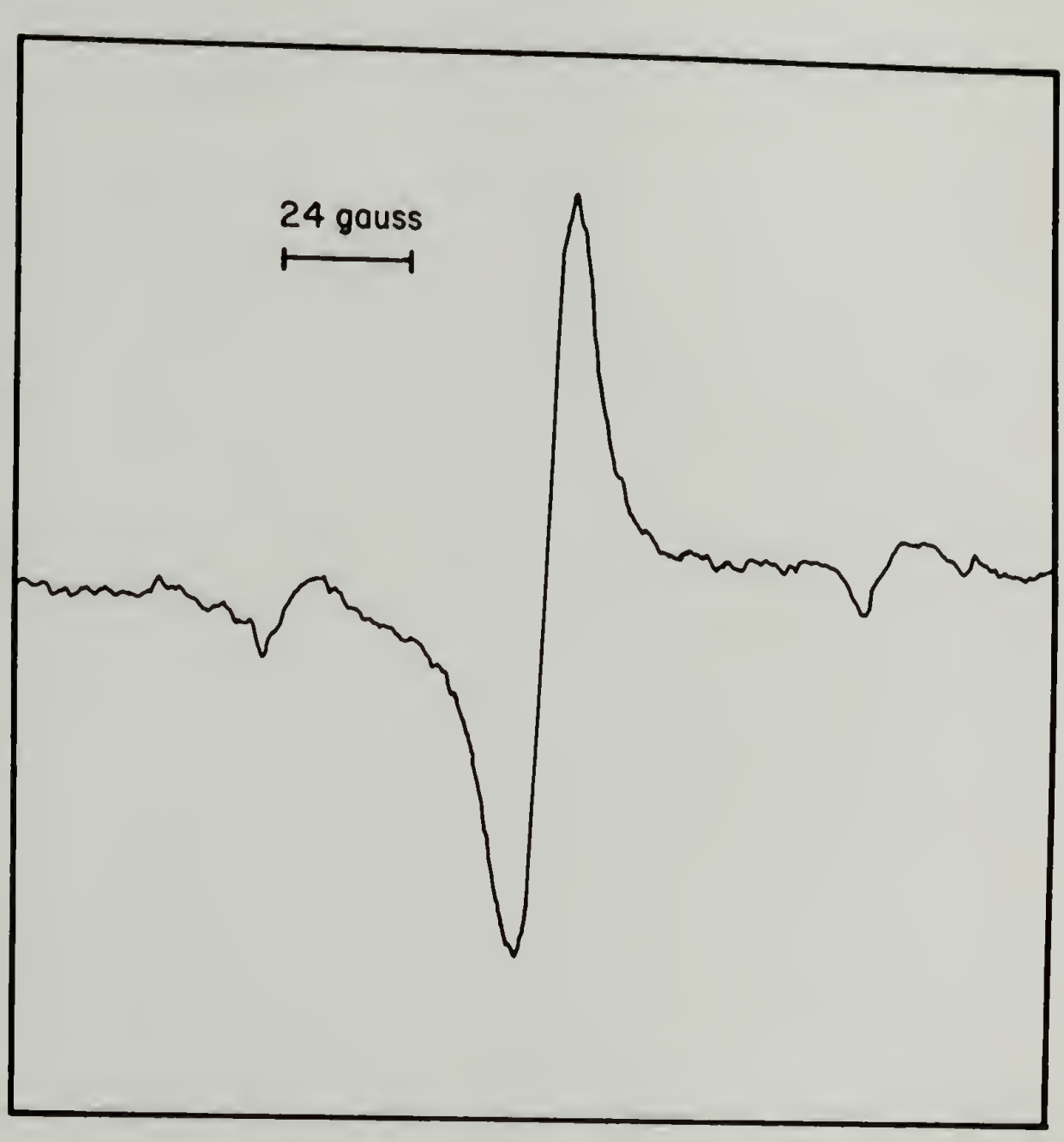

Figure 3.20

EPR spectrum of iodine-doped PTFE-C obtained at room temperature.

Reactions of PTFE-C

The following section of this chapter deals with exploiting the reactivity of PTFE-C to introduce three different organic functional groups to PTFE surfaces: alcohols, carboxylic acids, and amines. The characterization of these derivatized surfaces is not trivial: the insolubility of PTFE prohibits using solution reactions as controls. Fortunately, the depth of reduction can be extensive, depending on the reaction time. Thus, analysis by ATR-IR could be employed to determine the form of functionality introduced. Highly fluorinated XPS labels were used on derivatized samples prepared from extensively reduced PTFE-C. These samples contain no CF_2 to interfere with the highly oxidized C-F present in the labels. Fluorine also exhibits a large photo crosssection (1.0) so that decreases in C:F ratios expected on labelling are easily detected.

Halogenation

Treatment of PTFE-C film samples (10 minute reduction time) with chlorine vapor or Br_2/CCl_4 solution produces changes consistent with C-halogen bond formation. PTFE-Cl is white; PTFE-Br is pale yellow. ATR-IR data on both KRS5 and germanium crystals of PTFE-X (X = Br or Cl) is not informative: C-F stretching and wagging vibrations from PTFE and absorbances due to the crystal backgrounds interfere with expected C-X stretching absorbances in PTFE-X.

Gravimetric data and XPS provided lucid information on the extent of halogenation. PTFE-C film samples gain mass on halogenation. Assuming mass gained on halogenation is due only to gain in halogen and the mass

lost in the reduction is due only to loss of fluorine, it is possible to calculate the C:halogen ratios in PTFE-Cl and PTFE-Br. PTFE-Cl has a C:Cl ratio of 1:1 (net reaction $CF_2 \longrightarrow CCl$). PTFE-Br has a C:Br ratio of 1.6:1 (net reaction $CF_2 \longrightarrow CBr_{0.63}$). Direct surface composition was obtained from XPS, yielding information on the outer 30 Å of material. These data are summarized in Table 3.5. It is clear from the data that chlorination is more extensive than bromination. Quantitative

Table 3.5

Atomic ratios in PTFE-X

	C:X ratio	
Method of analysis	PTFE-Br	PTFE-Cl
Gravimetric	1.6	1.0
XPS	4.7	3.1

differences in values obtained gravimetrically versus those obtained by XPS can be rationalized in two ways: 1) as previously mentioned, a gradient structure for PTFE-C would inply that a different (perhaps more reduced) material exists in the outer 30 Å than is found further in the bulk. This surface material may be less easily halogenated if it is more extensively reduced than the entire reacted layer. 2) The error implicit in gravimetric analysis may have biased the C:X ratio low. PTFE control samples exposed to either bromine or chlorine show slight (0.02%) mass increases but no halogen in their XPS spectrum. Halogenated PTFE-C samples containing unreacted or absorbed halogen, would then exhibit a

lower C:X ratio.

High resolution C_{1s} XPS spectra nicely reflect changes due to halogenation. Figure 3.21 exhibits spectra which show that bromination causes a shift of a component of the carbon peak to higher binding energy (more highly oxidized carbon) and chlorination renders a distinct shoulder on the higher binding energy side (Cl is more electronegative than Br).

Contact angle changes for the reaction sequence given in Table 3.6 are consistent with those expected for PTFE-X; the polymer surface synthesized exhibits lower contact angles than those found in PTFE.

Table 3.6

Contact angle data for PTFE-X synthesis

Sample	θ_a	θ_r
PTFE	121	89
PTFE-C	114	68
PTFE-Br	103	53
PTFE-Cl	108	67

Synthesis of PTFE-OH: Hydroboration and Subsequent Oxidation of PTFE-C

The reactivity of the unsaturation in PTFE-C was further exploited to introduce hydroxyl groups to the PTFE surface. The PTFE-C films undergo hydroboration easily; less extensively reduced films turn from purple to white, while deeply reduced gold films turn purple/pink on treatment with borane/THF. Oxidation of hydroborated films with basic peroxide produces film samples (PTFE-OH) exhibiting spectra and

Figure 3.21

C_{1s} high resolution XPS data illustrating effects of halogenation on PTFE-C (10 minute reduction).

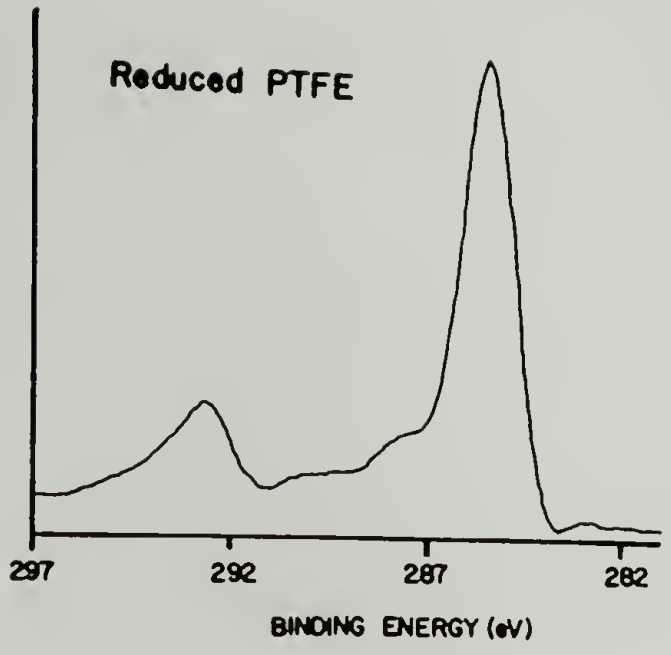
Reduced PTFE
297
292
287
282
BINDING ENERGY (eV)

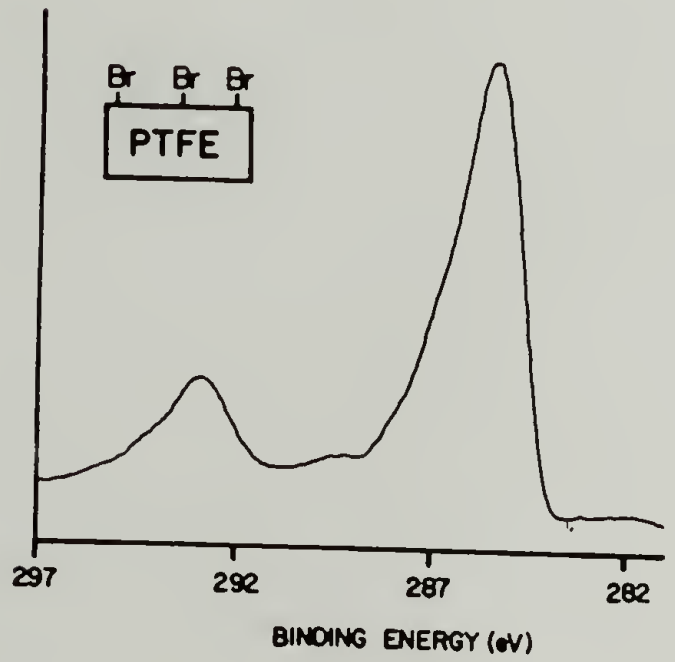
Br Br Br
PTFE
297
292
287
282
BINDING ENERGY (eV)

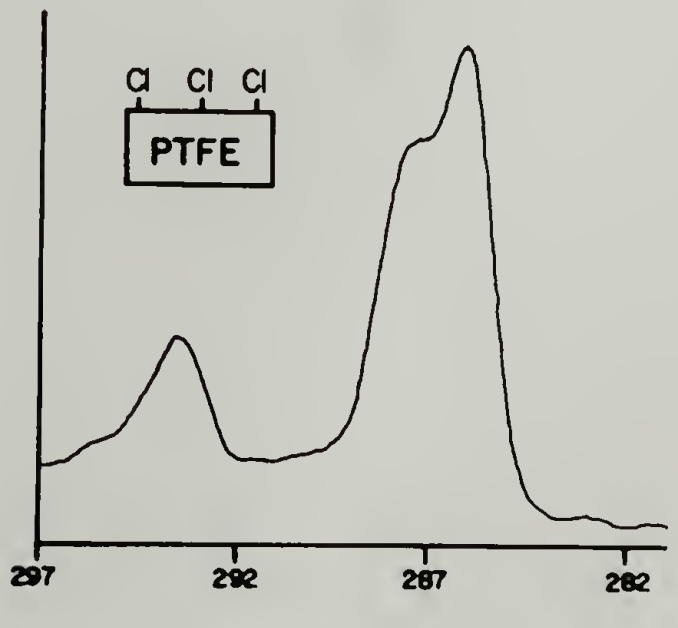
Cl Cl Cl
PTFE
297
292
287
282

properties consistent with the presence of hydroxyl groups. Contact angle changes of water on PTFE-OH are consistent with the presence of polar functionality; Table 3.7 summarizes this data:

Table 3.7

Contact angle data for PTFE-OH synthesis

Sample	θ_a	θ_r
PTFE	121	89
PTFE-C	114	68
PTFE-OH	62	0

Complete wetting (θ_r) is noted in PTFE-OH, reflecting the hydrophillicity of the surface.

In order to gain insight into the nature of this high energy surface, ie. the elements present and their functional form, ATR-IR and XPS labelling experiments were undertaken. The XPS survey spectrum (Figure 3.22) of PTFE-OH prepared from PTFE-C (24 hour reduction) shows an increased level of oxygen, with a calculated atomic composition ratio for C:O of 3.4:1. The functional form of this oxygen was established using fluorinated XPS labelling reagents. PTFE-C is extensively reduced to eliminate the CF_2 peak present in the C_{1s} high resolution spectrum. Reaction of PTFE-OH prepared from this sample with trifluoroacetic anhydride or heptafluorobutyryl chloride yields C_{1s} high resolution spectra consistent with the formation of fluorinated esters (Figure 3.23).

Although these results may be attributed to reaction of carboxylic acid groups present, this is highly unlikely since the reactions:

Figure 3.22

XPS survey spectra for PTFE-C (top) and PTFE-OH (bottom).

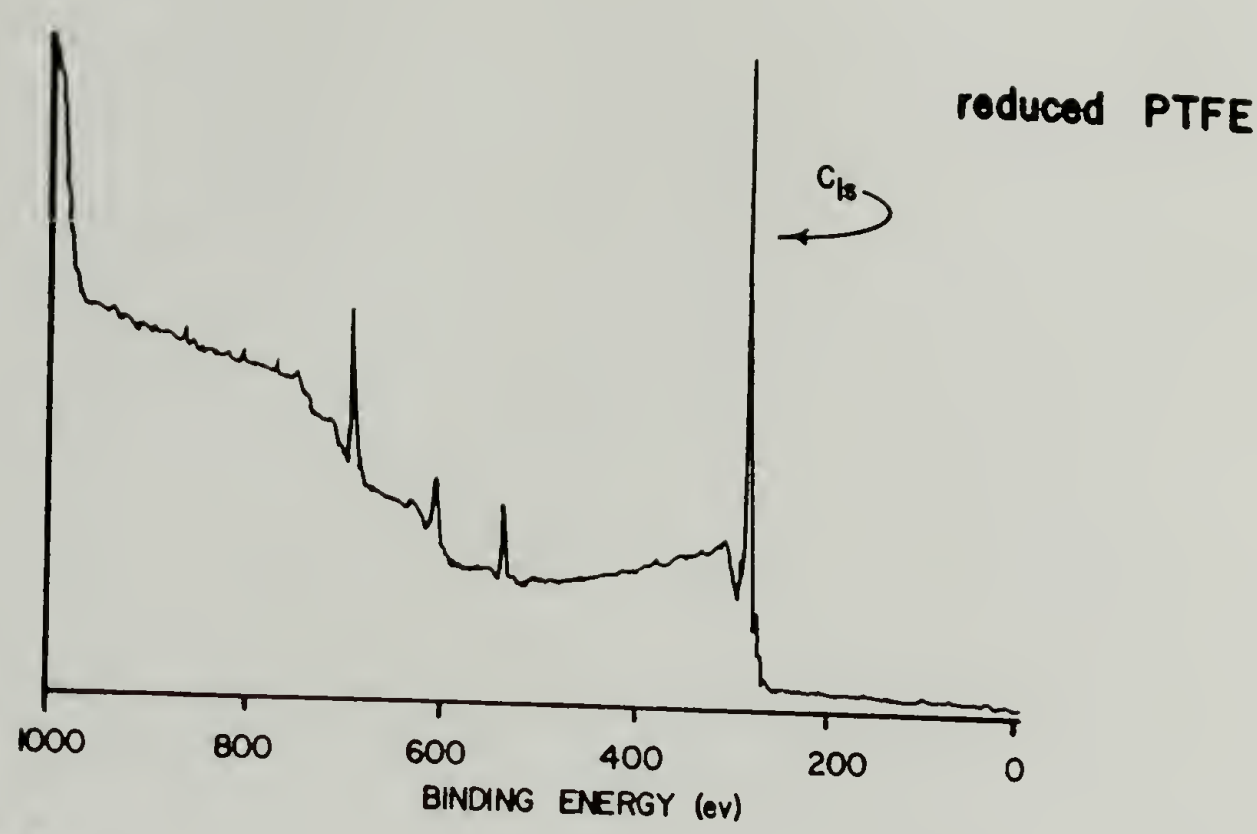
reduced PTFE
C_{1s}
1000
800
600
400
200
0
BINDING ENERGY (ev)

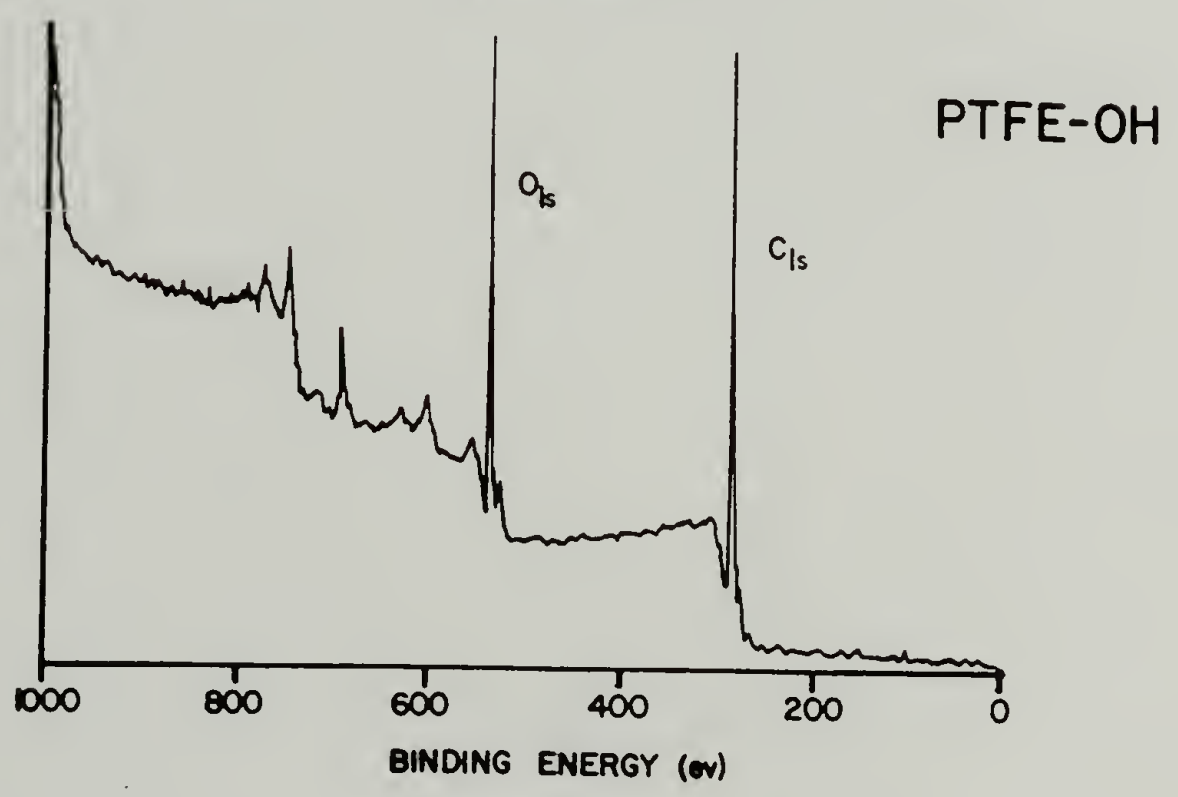
PTFE-OH
O_{1s}
C_{1s}
1000
800
600
400
200
0
BINDING ENERGY (ev)

Figure 3.23

C_{1s} high resolution spectra for PTFE-OH reactions with trifluoroacetic anhydride and heptafluorobutyryl chloride.

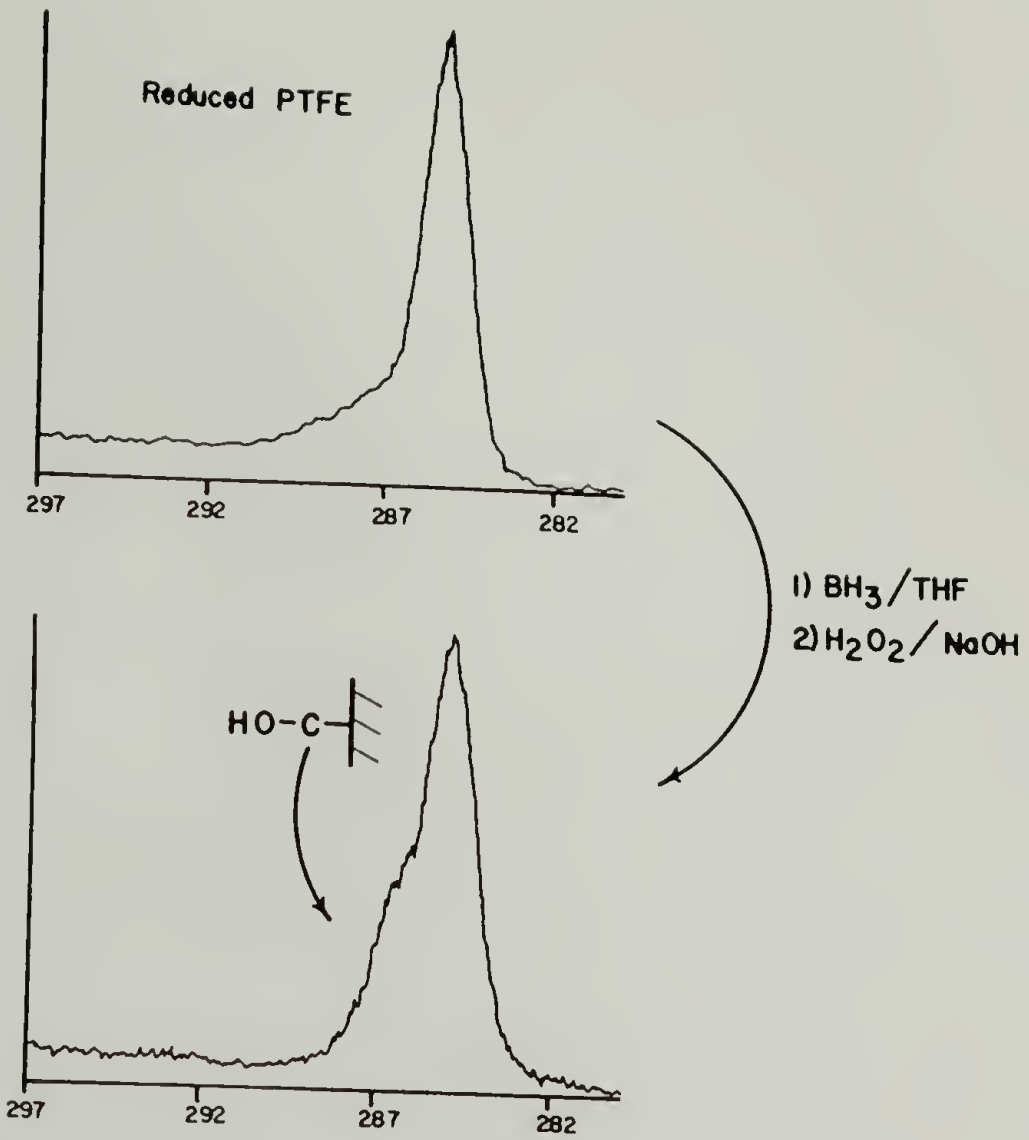
Reduced PTFE
297
292
287
282
1) BH_3/THF
2) H_2O_2/NaOH
HO-C
297
292
287
282

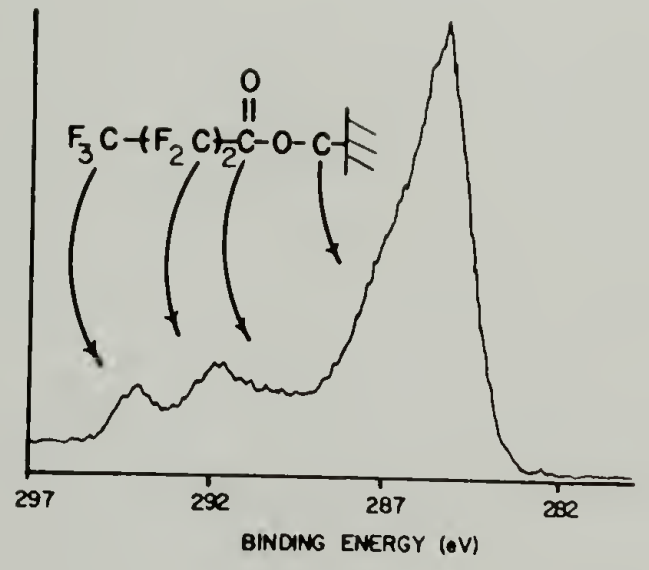
O
$F_3C-(F_2C)_2-C-O-C$
297
292
287
282
BINDING ENERGY (eV)

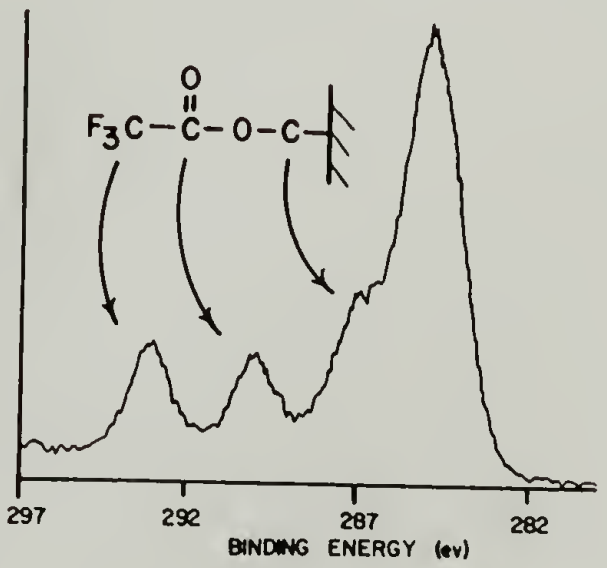
O
$F_3C-C-O-C$
297
292
287
282
BINDING ENERGY (ev)

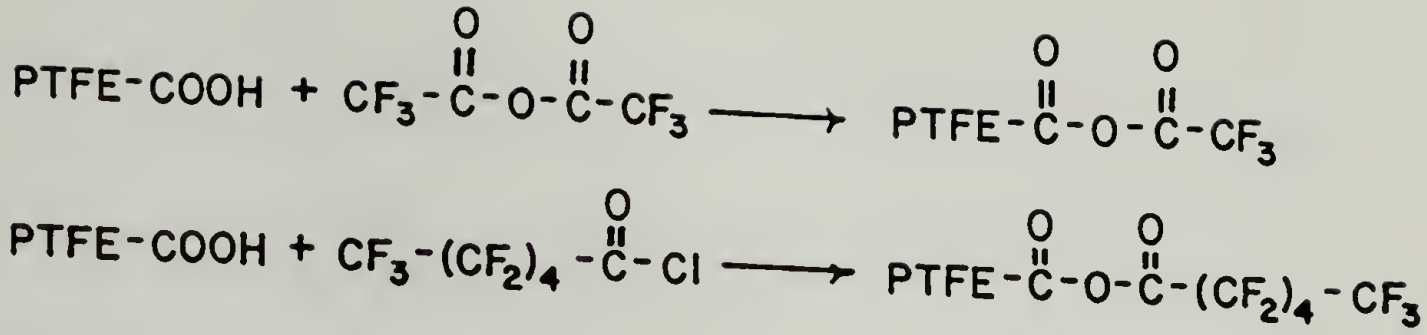

occur only when the acid is present as its carboxylate salt.[26] Since the XPS spectra indicated that sodium counterion was not present, the reaction from carboxylic acids must be negligible.

Additional evidence for hydroxyl group introduction is given by the ATR-IR spectrum (KRS5, 45°) for PTFE-OH prepared from PTFE-C (24 hour reduction). Figure 3.24 illustrates the absorbances in PTFE-OH at 3500 cm^{-1} and 1020 cm^{-1} due to ν_{O-H} and ν_{C-O} respectively. The intensity of these signals suggests that reaction has taken place throughout most of the PTFE-C layer (6000 Å). The ATR-IR spectrum also indicates possible presence of ketonic carbonyl groups ($\nu_{C=O}$ at 1650-1700 cm^{-1}) formed from hydroboration of triple bonds:

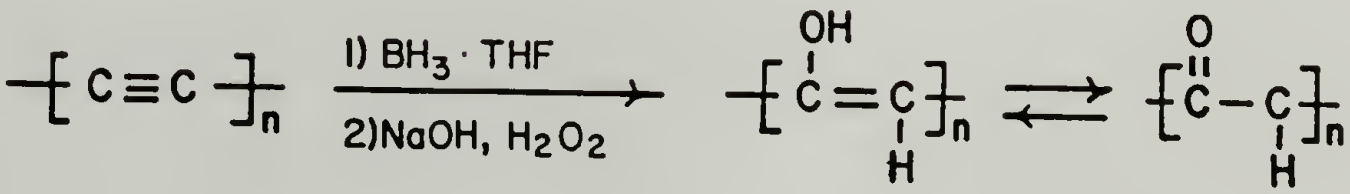

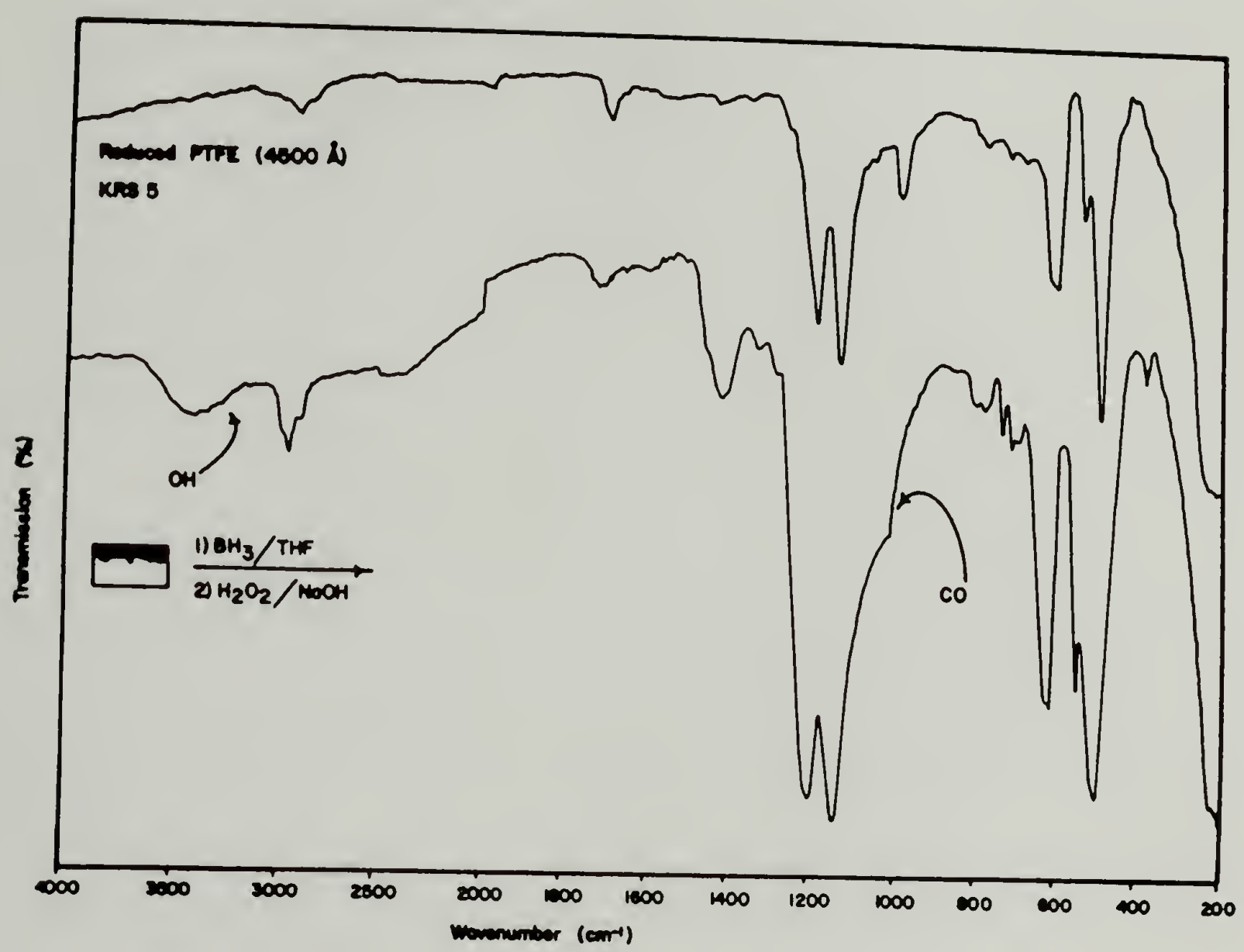

Figure 3.24

ATR-IR spectra of PTFE-C (top) and PTFE-OH (bottom) on 45° KRS5 crystal.

Attempts at labelling these carbonyl groups by the method outlined by Kato[27] using dichlorophenylhydrazine were unsuccessful. This is not positive proof that carbonyl groups are not present; it may merely suggest that DPH is not a good XPS labelling reagent for these functional groups.

XPS labelling of PTFE-OH with trichloroacetylisocyanate yielded superfluous results. A simple reaction to form the urethane did not take place; a N:Cl ratio of 1:1 was obtained instead of the 1:3 value expected from the stoichiometry. Evidently, chlorine to the carbonyl is reactive as well.

Attempts were also made to follow the reaction gravimetrically, quantitating the hydroxyl groups present using heptafluorobutyryl chloride. There was, however, no mass change in repeated experiments on going from PTFE-C to PTFE-OH, suggesting partial cleavage of PTFE-C during hydroboration/oxidation.

Synthesis of PTFE-COOH

Numerous methods were undertaken to introduce carboxylic acids to PTFE. In many cases promising results were obtained but for varying reasons (explained later) the reactions were abandoned. In each attempt,

the reactivity of PTFE-C towards different classes of reagents was evaluated. XPS provided a rapid method for determining whether acid groups were present on the surface. Labelling the acid-containing films

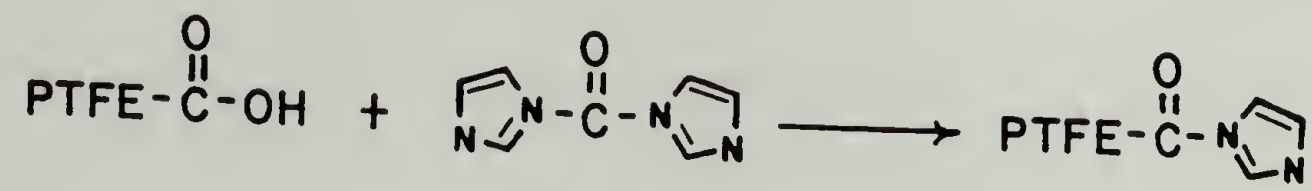

Equation 3.3

with carbonyldiimidazole (equation 3.3) provided a quick check for success of a given reaction. It has been shown[28] that carboxylic acid groups on poly(chlorotrifluoro)ethylene surfaces react with carbonyldiimidazole. The nitrogen in the product is readily detected in the XPS spectrum (N_{1s}:401 eV).

Hydroboration and subsequent oxidation with CrO_3

The reactivity of PTFE-C in hydroboration reactions prompted efforts to utilize the resultant surface alkyl boranes. Reports of CrO_3 oxidation of alkyl boranes[29] producing carboxylic acids motivated further investigation. When PTFE-C was hydroborated, as in the synthesis of PTFE-OH, and treated with 8N CrO_3 at 0°C, large amounts of oxygen were incorporated into the surface by XPS. The oxidant, however, cleaved bonds in the reduced layer. Evidence for this is seen in Figure (3.25) where C:F and C:O ratios are plotted as a function of time of oxidation.

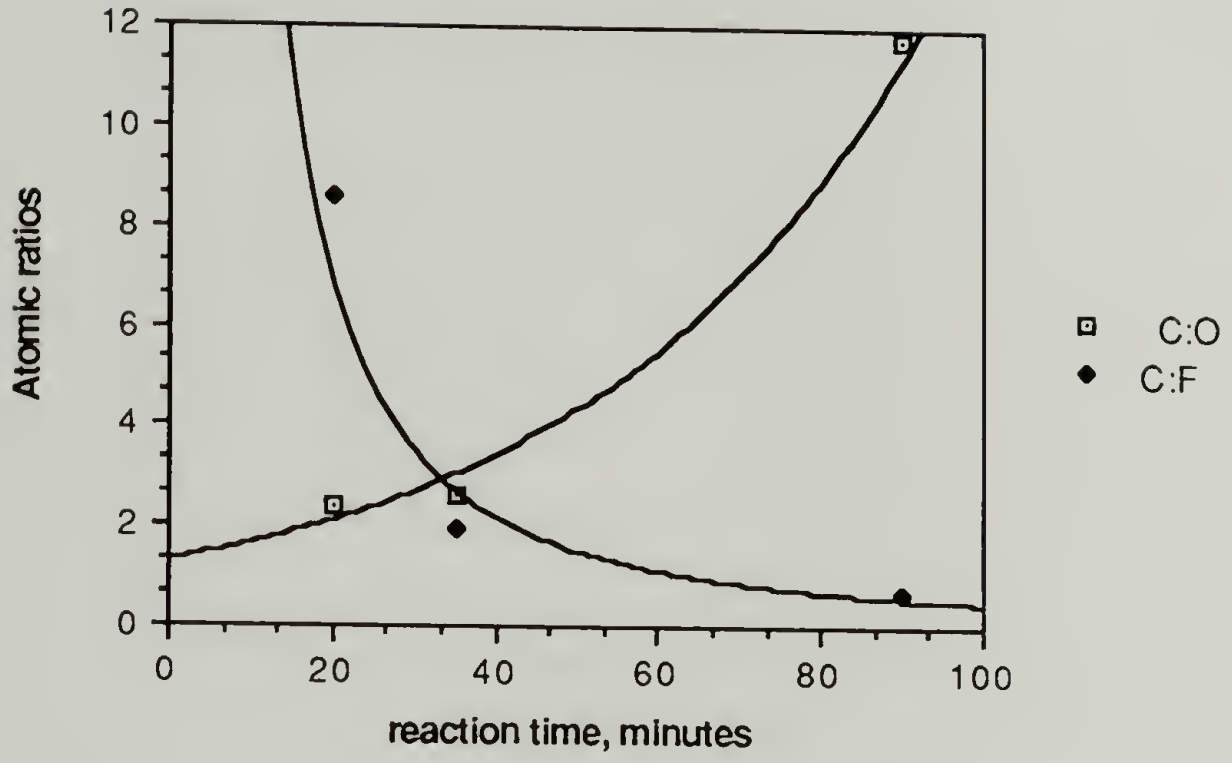

Figure 3.25

Reaction of PTFE-C with borane/THF and subsequent oxidation with CrO_3: atomic ratio data as a function of oxidation time. Reaction temperature is 0°C.

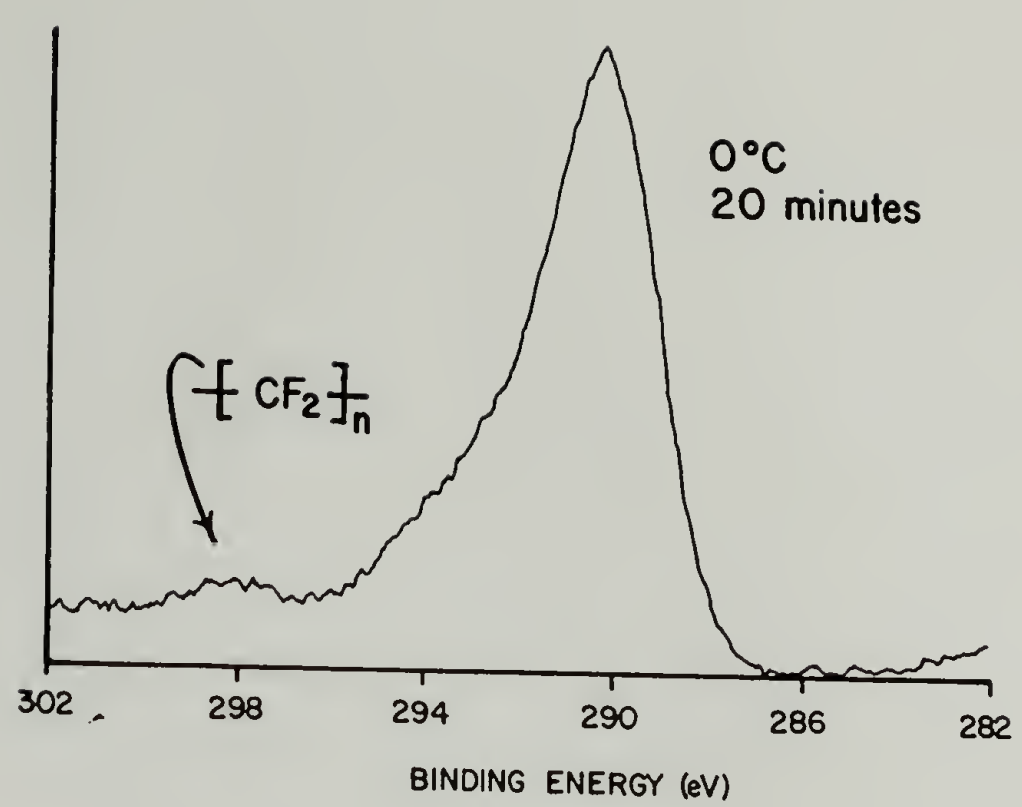

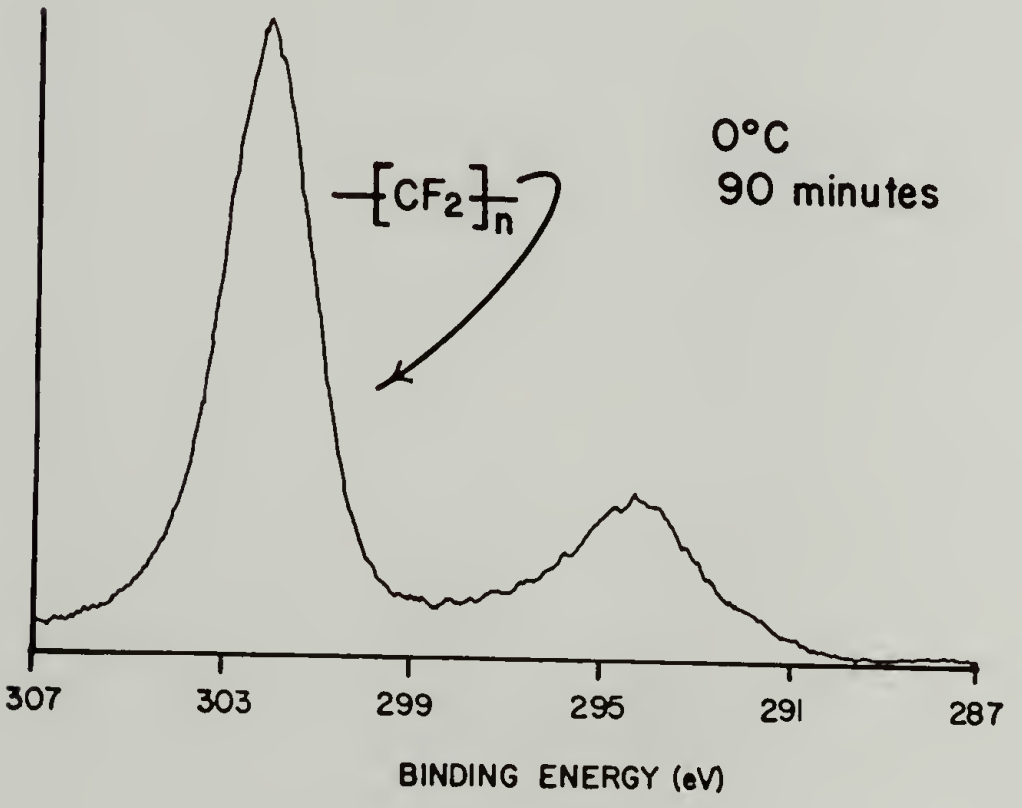

Figure 3.26

Reaction of PTFE-C with borane/THF and subsequent oxidation with CrO_3: XPS C_{1s} high resolution spectra for 20 minute (top) and 90 minute (bottom) oxidation times.

Since the C:F ratio in the original PTFE-C (reduced 12 hours) is 23:1, it is obvious that a highly fluorinated surface has been generated. Inspection of the C_{1s} spectra (Figure 3.26) for the samples oxidized for 20 minutes and 90 minutes, respectively, demonstrates that the fluorine is present as CF_2. Reaction of carbonyldiimidazole with the oxygen present indicated that 13% of the oxygen was present as carboxylic acids.

One major drawback in this method of PTFE-COOH synthesis is the trace amounts of chromium (from CrO_3 and its inorganic esters) and sulfur (from sulfuric acid used to dilute the 8N CrO_3) present, corresponding to high oxygen levels. Despite various workup procedures, these elements could not be removed. This problem and the corrosive nature of the oxidation mentioned above precluded this as a viable method for PTFE-COOH synthesis.

Koch-Haaf carboxylation of PTFE-C

Treatment of PTFE-C with a solution of formic acid in sulfuric acid also renders films with decreased C:O ratios (6.6:1 vs. 23:1 in PTFE-C) expected from the hydrocarboxylation of the unsaturation present.[30] XPS atomic composition data indicated the presence of sulfur, which, once again, was impossible to remove by any workup method tried. The source of this adventitious sulfur is either from addition of H_2SO_4 across unsaturation in PTFE-C or from physisorption of the acid. Although XPS labelling with CDI appeared promising, the reaction was abandoned.

Diels-Alder reactions of PTFE-C

The reactivity of PTFE-C towards maleic anhydride, a good dienophile, in Diels-Alder reactions was investigated. Treatment of PTFE-C film (6 hour reduction time) with a THF solution of maleic anhydride followed by acid catalyzed hydrolysis yielded C:O ratios of 4.82 (average of 4 reactions). 12% of the oxygen present on the surface was labelled as carboxylic acids with CDI. Although the reaction appeared promising, it seemed that under the reaction conditions, the derivatized surface was being dissolved from the PTFE. Large increases in F:C ratios were observed before and after derivitization of PTFE-C. Diels-Alder reaction of maleic acid to directly introduce acid functionality without hydrolysis was attempted, however no significant reaction occurred.

Friedel Crafts acylation of PTFE-C with oxalyl chloride

Reaction of PTFE-C with oxalyl chloride and subsequent hydrolysis were attempted to prepare the acid-functionalized surface. Under the

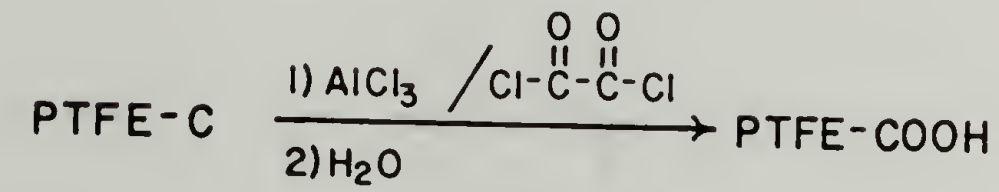

reaction conditions employed, decreased C:O ratios (6.5:1) were obtained, but adventitous nitrogen present from nitrobenzene made it difficult to discern whether subsequent labelling of PTFE-COOH with CDI had occurred.

Radical addition of maleic anhydride and other acids

Acid introduction to PTFE-C was attempted by radical addition of carboxylic acids and maleic anhydride according to Equation 3.4 a-c:

a) PTFE-C + 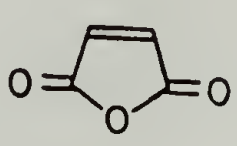 $\xrightarrow[\text{THF}]{\text{AIBN}}$ PTFE-anhydride $\xrightarrow[\text{TFAA}]{H_2O}$ PTFE-COOH

b) PTFE-C + $HO-\overset{O}{\overset{\|}{C}}-H$ $\xrightarrow[\text{THF}]{\text{AIBN}}$ PTFE-COOH

c) PTFE-C + $CH_3-\overset{O}{\overset{\|}{C}}-OH$ $\xrightarrow[\text{THF}]{\text{AIBN}}$ PTFE-CH_2-COOH

Equation 3.4

Of all these attempts, the reaction of PTFE-C with maleic anhydride yielded the most promising results. Irradiation of a solution of maleic anhydride in contact with a PTFE-C film produces changes in the film surface consistent with incorporation of anhydride functionality. Trifluoroacetic acid catalyzed hydrolysis converts this surface to PTFE-COOH. Figure 3.27 exhibits these transformations as observed in XPS survey and C_{1s} high resolution spectra. The XPS survey spectrum of PTFE-COOH indicates the presence of oxygen (the C:O ratio is 6.6:1) and a highly oxidized carbon component in the C_{1s} high resolution spectrum at 290 eV. The presence of carboxylic acid functionality is confirmed by the labelling reaction with CDI, which yielded the expected peak at 401

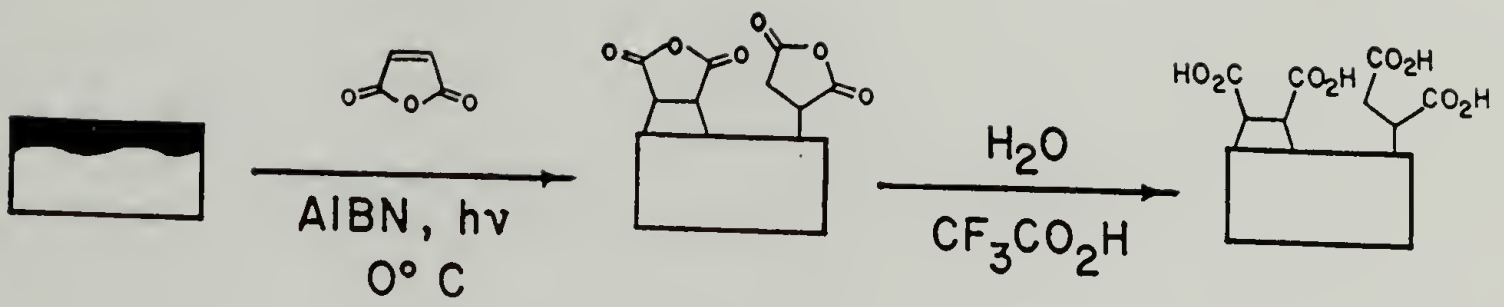

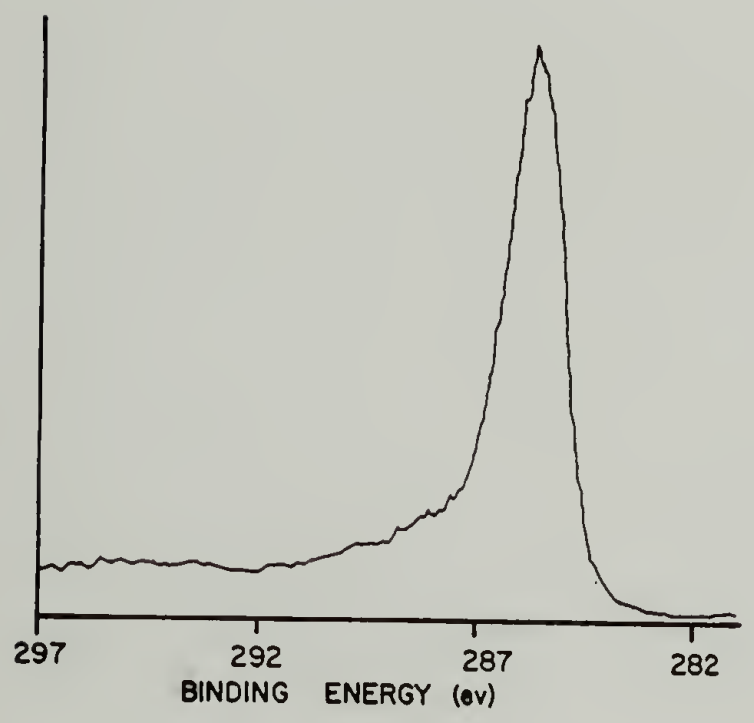

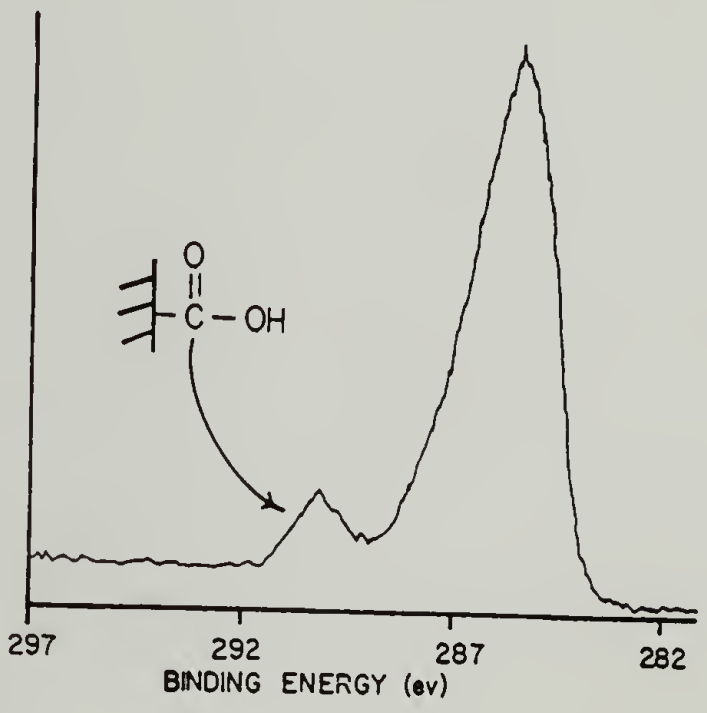

Figure 3.27

Radical reaction of PTFE-C with maleic anhydride and subsequent hydrolysis: C_{1s} high resolution spectra.

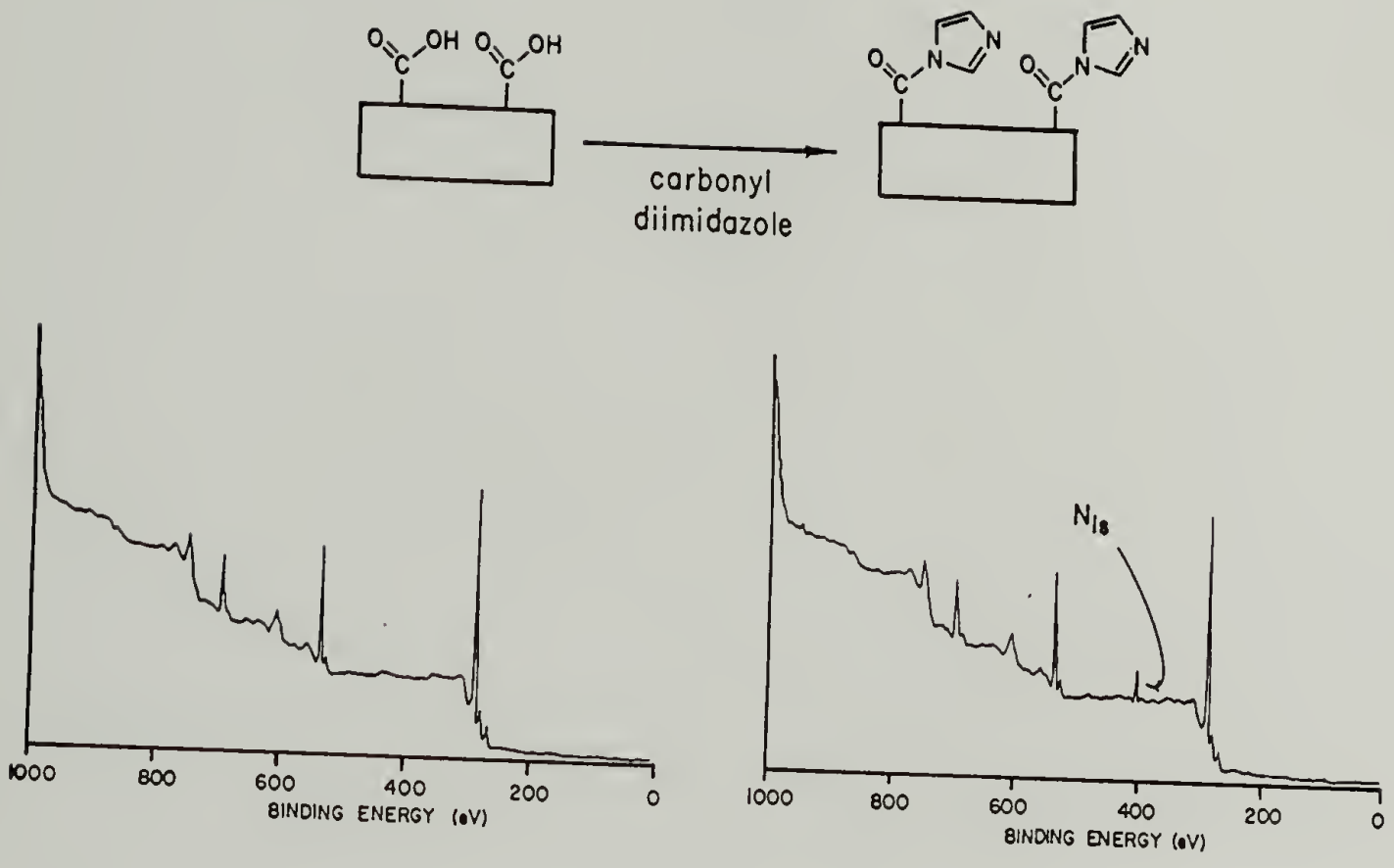

Figure 3.28

XPS survey spectra for the labelling reaction of carboxylic acid groups on PTFE-COOH with carbonyldiimidazole.

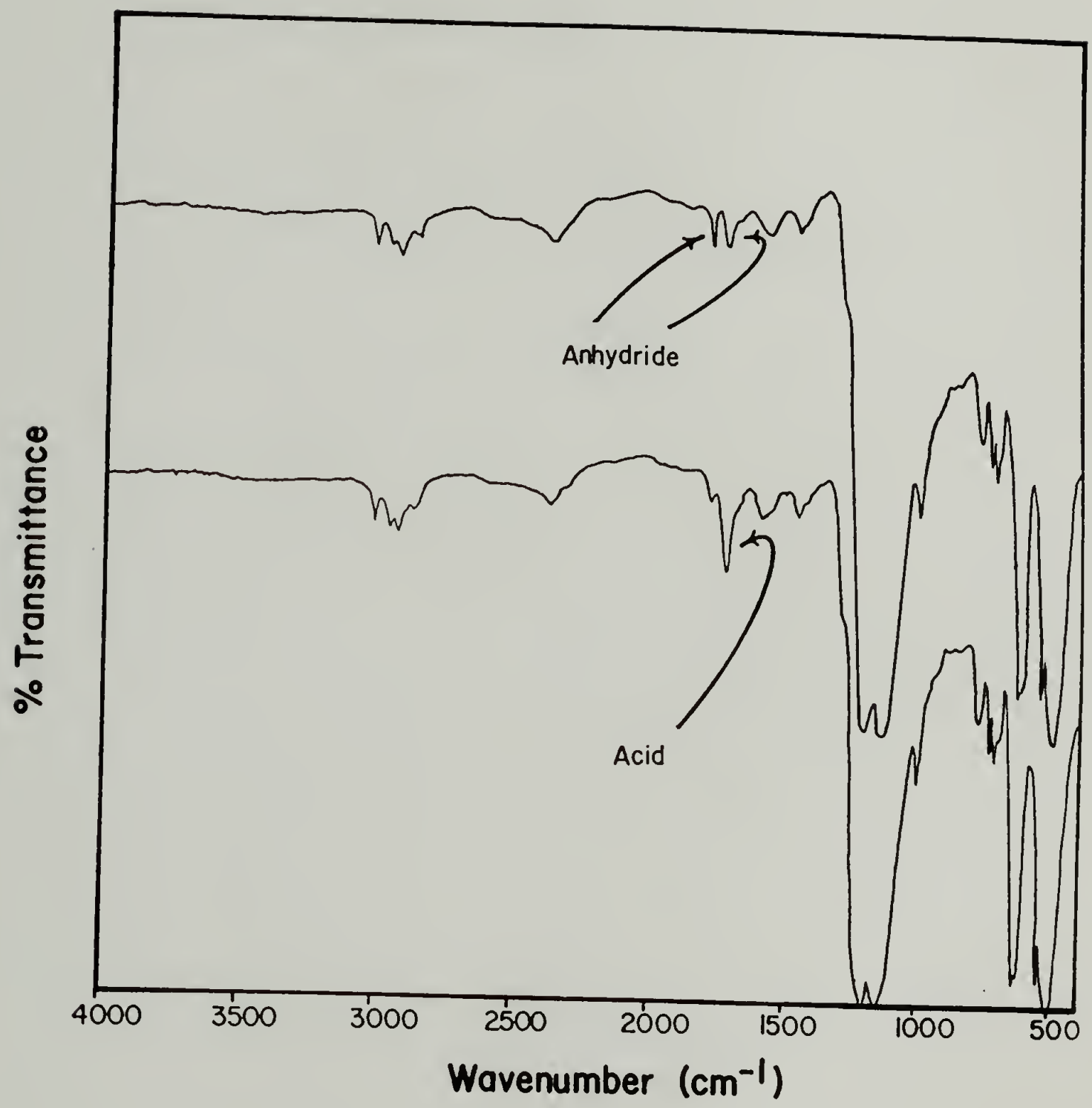

Figure 3.29

ATR-IR spectra for the hydrolysis of PTFE-anhydride to PTFE-COOH.

eV. The ATR-IR spectra (figure 3.29) show the presence of the anhydride (symmetric and assymetric C=O stretching at 1722 cm^{-1} and 1784 cm^{-1}) which can be almost completely hydrolyzed to the carboxylic acid (1723 cm^{-1}). It is clear that maleic anhydride has reacted with and is not merely absorbed or coated onto PTFE-C. The carbonyl peak positions in PTFE-anhydride indicate the presence of acrylic type anhydride structures expected from the reaction:

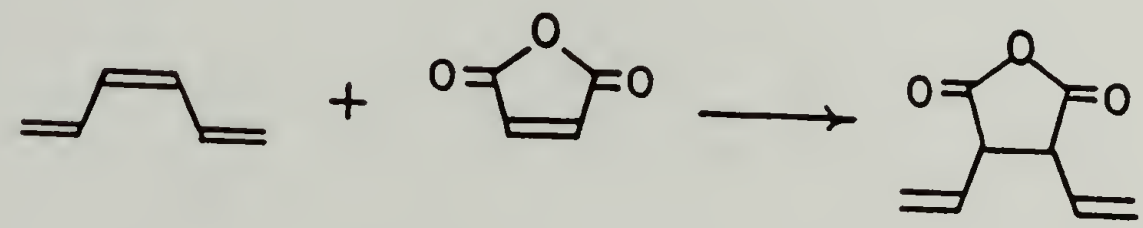

The corresponding absorbances in maleic anhydride are found at higher frequencies (1850 and 1790 cm^{-1}).[31] Also, the fluorine present in PTFE-C remains in the XPS sampling depth.

The mechanism of maleic anhydride incorporation was not examined, but repeated runs indicate that the reaction of AIBN fragments to PTFE-C may also occur; N:C ratios range from 0 to 0.12. Surface confined radicals in PTFE-C may add to maleic anhydride. It is not known whether only one maleic anhydride unit is added or if the maleic anhydride is graft polymerized or oligimerized. It has been shown, for example that maleic anhydride polymerizes under the conditions examined here.[32-34]

The advancing and receding contact angles of PTFE-COOH are 69° and 0°, respectively. These values indicate the increased hydrophilicity upon derivatization.

Synthesis of PTFE-NH_2

Hydroboration followed by workup in $NH_4^+OH^-$/NaOCl

Direct amination of PTFE-C was attempted via hydroboration followed by the reaction of chloramine generated in situ by ammonium hydroxide and

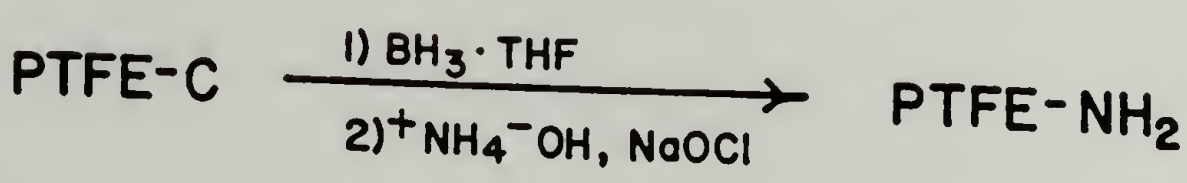

sodium hypochlorite.[35] XPS data indicate introduction of nitrogen, but since oxidation predominated (O:N ratios were 5:1) the reaction was abandoned.

A better route to PTFE-NH_2 was developed using PTFE-Br as a starting material. PTFE-C (1.5 hour reduction time) treated with 0.2N Br_2/CCl_4 (1.0 hour reaction time) yielded suitable PTFE-Br for further reaction. PTFE-Br was then treated with ammonia to prepare a surface containing amino groups. Figure 3.30 shows XPS spectra for this conversion: the bromine photoelectron lines at 256, 189, 182, and 69 eV are replaced by the nitrogen photoelectron line at 401 eV. XPS labelling of amino groups with trichloroacetylchloride yielded the expected Cl_{2p} peak at 200 eV. The validity of this labelling experiment is questionable since trichloroacetylchloride is not an amine-specific reagent. Furthermore, XPS atomic composition data for the same reaction with control samples indicates that the reagent has either reacted or is physisorbed. (Table 3.8)

Figure 3.30

XPS survey spectra for PTFE-C conversion to PTFE-NH_2 and subsequent amine labelling with trichloroacetylchloride.

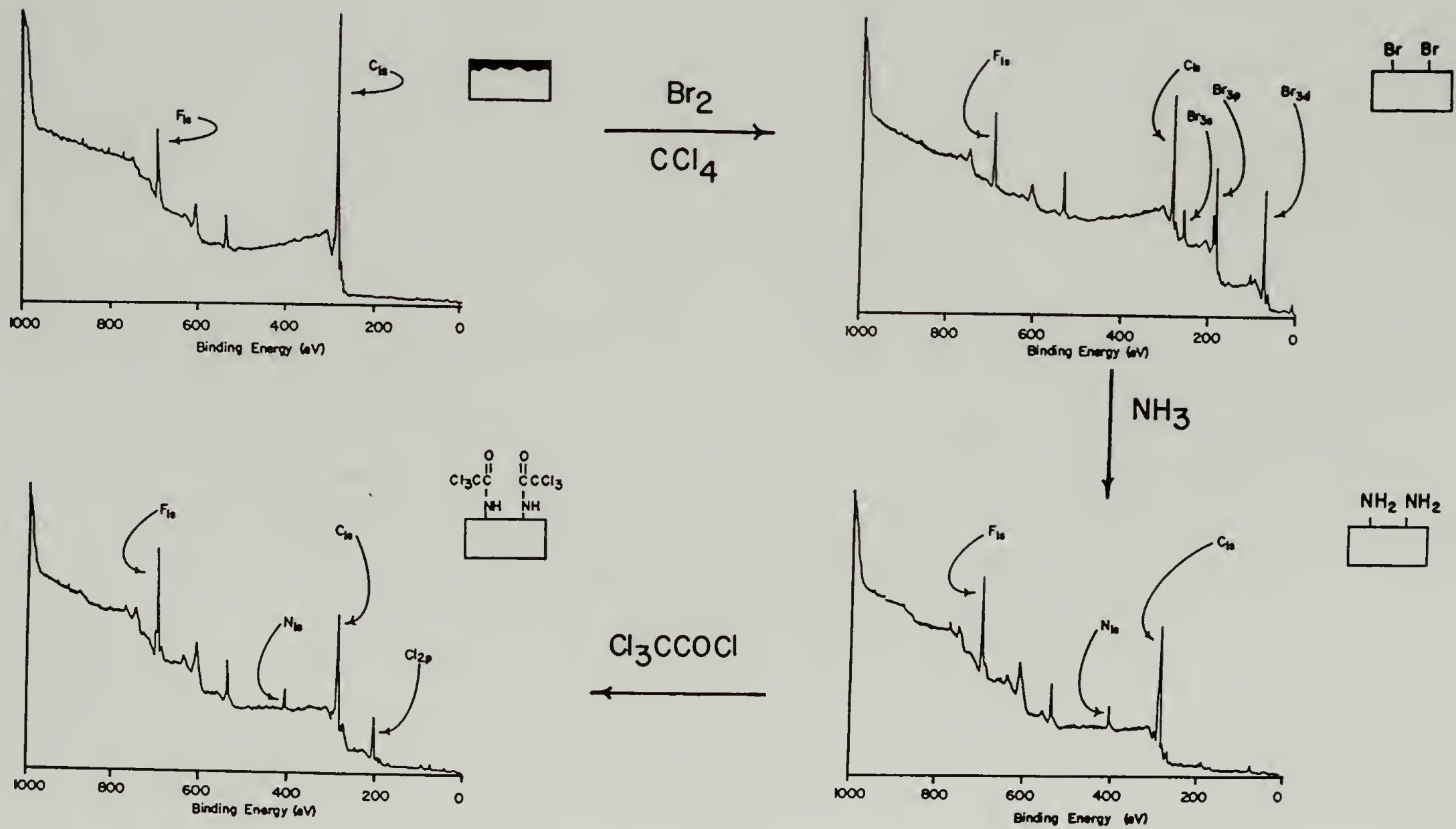
F1s
C1s
1000
800
600
400
200
0
Binding Energy (eV)
Br2
CCl4
Br Br
Br3p
Br3s
Br3d
NH3
NH2 NH2
Cl3CCOCl
Cl3CC
CCCl3
NH
N1s
Cl2p

Table 3.8

Trifluoroacetyl chloride labelling of PTFE-NH_2

Sample	Atomic composition						
	F	O	C	Si	N	Br	Cl
PTFE-NH_2 + TCAC*	13.71	8.03	64.88	0.23	4.54	0.93	7.68
PTFE-Br + TCAC	9.59	4.21	65.50	0.00		16.21	4.49
PTFE-C + TCAC	3.20	5.93	85.74	0.02			5.10

* TCAC = Trichloroacetyl chloride

The C:Cl ratio in the PTFE-NH_2 reacted sample is half of that in either of the controls, indicating that amines are probably present. The amines present on PTFE-NH_2 were also labelled successfully with pentafluorobenzaldehyde (Equation 3.5).

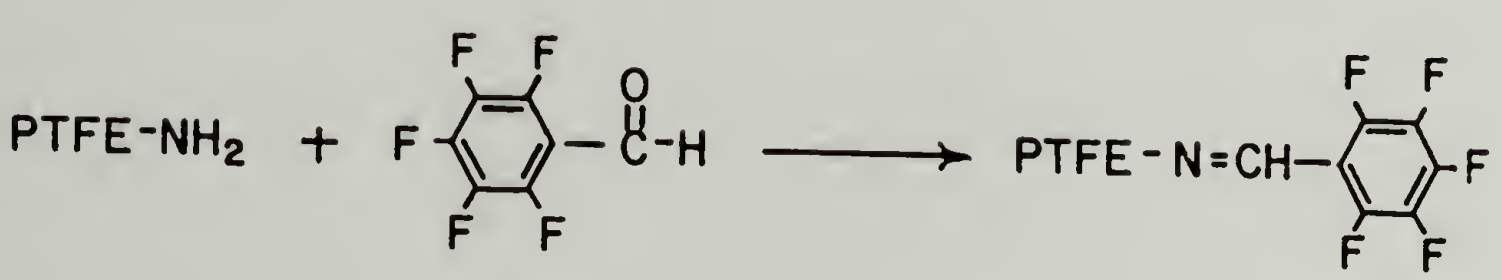

Equation 3.5

Advantages of this reagent are that: 1) it is specific for the labelling of primary amines[36-38] and 2) there is no reaction or absorption of the reagent with the control samples. In addition, the high resolution F_{1s} spectrum of PTFE-NH=C-C_6F_5 shows two fluorine signals: one from the fluorine from PTFE-C and one from the label, respectively (Figure 3.31).

The ATR-IR of PTFE-NH_2 prepared from PTFE-C reduced for 12 hours supports introduction of amine functionality: N-H stretching (3500-3200

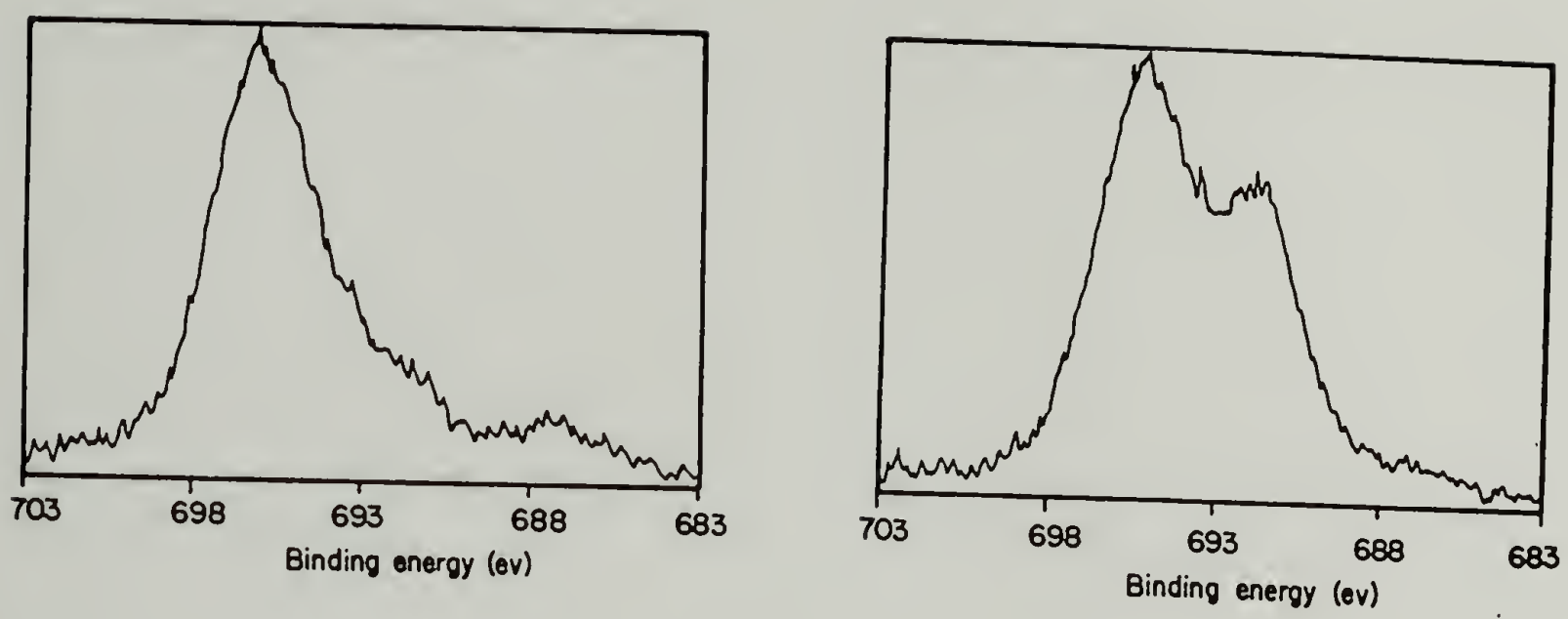

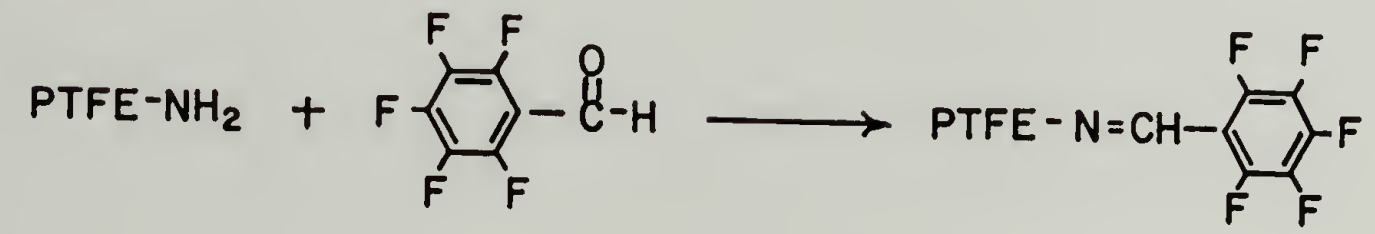

Figure 3.31

XPS F_{1s} high resolution spectra for PTFE-NH_2 and PTFE-N=CHC_6F_5.

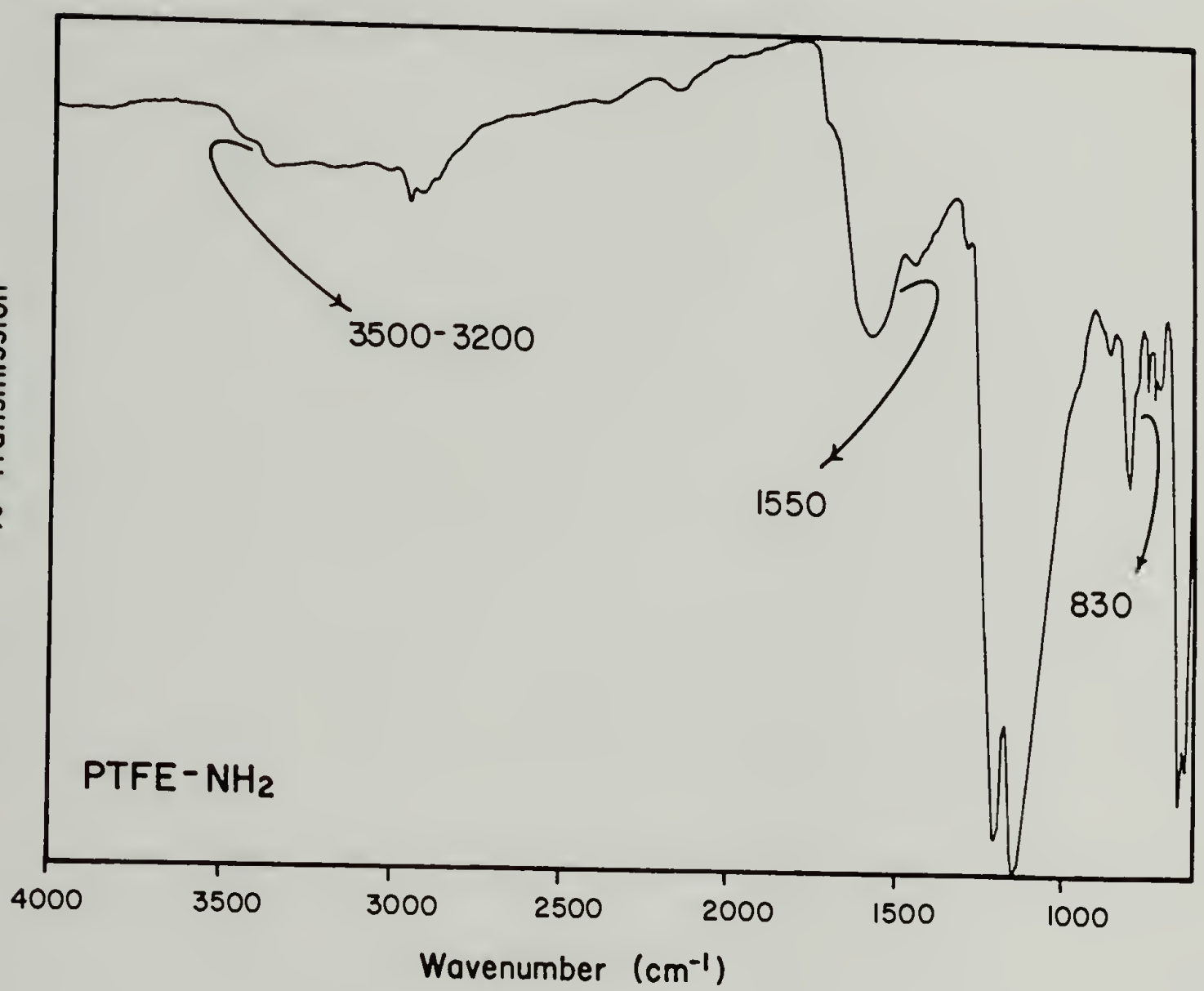

Figure 3.32

ATR-IR spectrum of PTFE-NH_2 on a 45° KRS5 crystal.

cm^{-1} (broad)), N-H bending (1550 cm^{-1}), and N-H wagging (830 cm^{-1}) vibrations are all present (figure 3.32). The expected C-N stretching vibration is hidden by C-F stretching in PTFE. The advancing and receding contact angles for PTFE-NH_2 are 79° and 24°, respectively.

Other reactions of PTFE-C

Diels-Alder reactions

The limited success observed in the Diels-Alder reaction of maleic anhydride with PTFE-C prompted efforts to react other good dienophiles: dimethylacetylenedicarboxylate (DMADC) and tetracyanoethylene (TCNE). Although there was no noticeable reaction of PTFE with DMADC by XPS, the reaction of TCNE yielded XPS data consistent with the introduction of nitrogen to the surface, presumably as nitrile groups (the C:N ratio was 12:1). A shoulder to the left of the main carbon peak at (290 eV) in the C_{1s} high resolution spectrum of PTFE-N provided further evidence for nitrile group presence (Figure 3.33). Reductions of the nitrile groups were were not attempted since amination of PTFE via PTFE-Br was successful.

Reaction of PTFE-C with succinic anhydride

PTFE-C film treated with succinic anhydride in THF solution showed changes in its XPS spectrum that indicated a reaction had taken place. Decreased C:O ratios were noticed. It also appeared that the derivatized layer was THF soluble as the characteristic CF_2 peak in the C_{1s} high resolution spectrum was found in reacted samples. The most probable

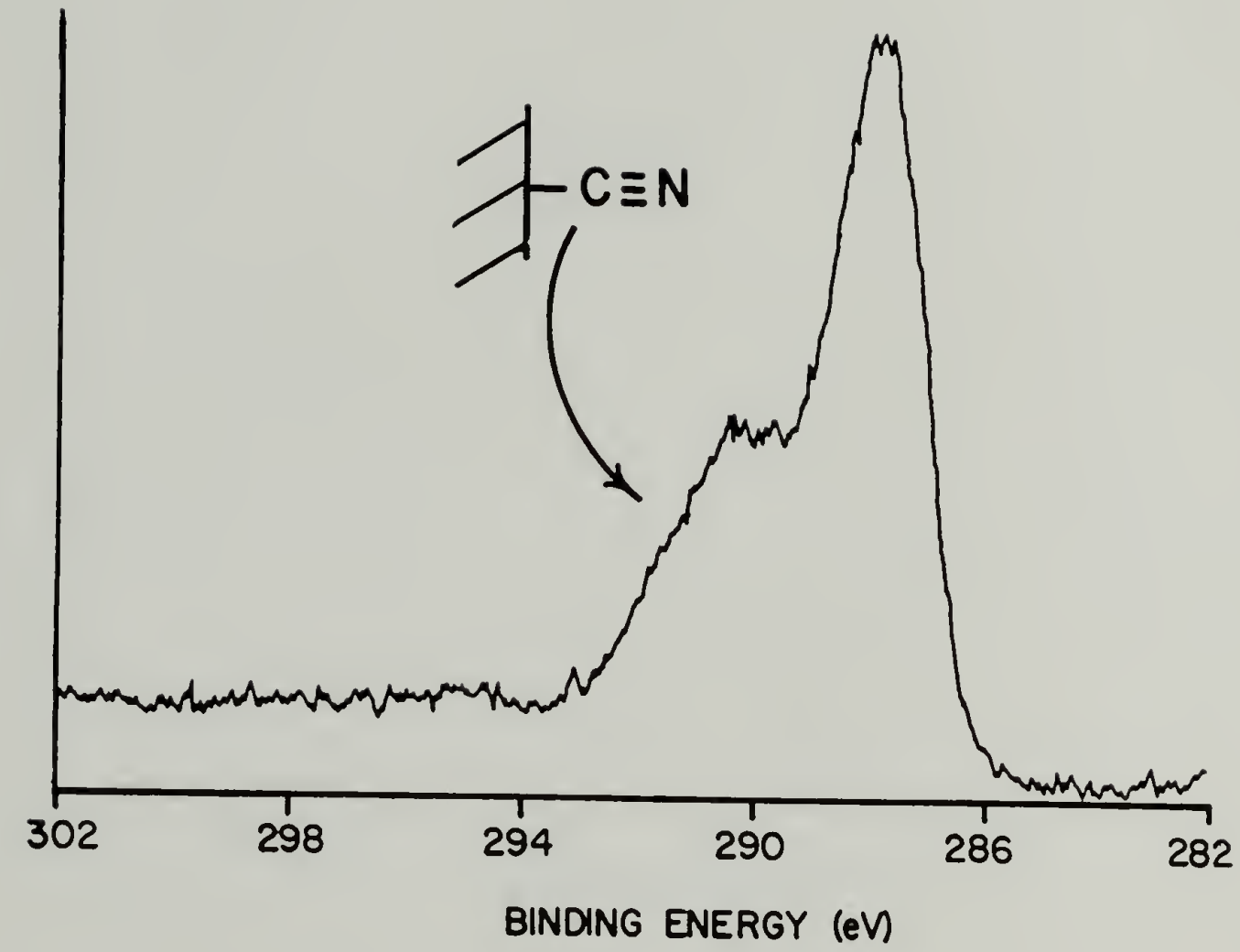

Figure 3.33

C_{1s} high resolution XPS spectrum for the reaction product of PTFE-C with tetracyanoethylene.

reaction path is the free radical addition of the anhydride to PTFE-C. Surface confined radicals in PTFE-C abstract the active hydrogen in the anhydride to form the reactive species which then adds to unsaturation in PTFE-C.

Attempted synthesis of PTFE-polymer interfaces

Two routes to PTFE-polymer interfaces were attempted. In the first case, styrene was radically polymerized in the presence of PTFE-C using AIBN as a radical initiator. Ungrafted homopolymer was extracted from the PTFE-PS surface. Gravimetric analysis indicated a 5 μg increase in mass after grafting, but ATR-IR results were inconclusive concerning the incorporation of polystyrene. The second route involved synthesis of PTFE-polyethylene:

$$\text{PTFE-C} \xrightarrow[\text{2) acetic acid}]{\text{1) } BH_3 \cdot THF} \text{PTFE-Polyethylene}$$

This proved to be unsuccessful as the second step resulted in cleavage of the derivatized surface from the PTFE substrate. XPS data indicated large amounts of CF_2 present in the sampling depth.

Oxidations of PTFE-C:PTFE-O

Reaction of PTFE-C with MCPBA

Reaction of PTFE-C with MCPBA using either ethanol or glacial acetic acid as a solvent yielded ATR-IR spectra consistent with reaction. At the time these experiments were done, a lack of surface analytical tools

existed, but the ATR-IR (Ge crystal, 60°) indicated the presence of carbonyl stretching at 1680-1700 cm^{-1}. Reacted films were white in color. Contact angle measurements were impossible to obtain; the water drop skipped and dragged across the surface.

Air oxidation of PTFE-C

Exposure of extensively reduced PTFE-C (2 day reaction time) to ambient laboratory conditions introduces oxygen in high amounts to the surface (C:O ratio decreases to 6:1). The functionality of the oxygen is difficult to discern: the broad peak at 3000-3500 cm^{-1} in the ATR-IR spectrum (Figure 3.34) may be due to a combination of acid and alcoholic functionality O-H stretching; similarly, the carbonyl stretch present at 1718 cm^{-1} may correspond to both acidic and ketonic functionality. Air exposed PTFE-C appears yellow/brown to white in color depending on the depth of the original PTFE-C.

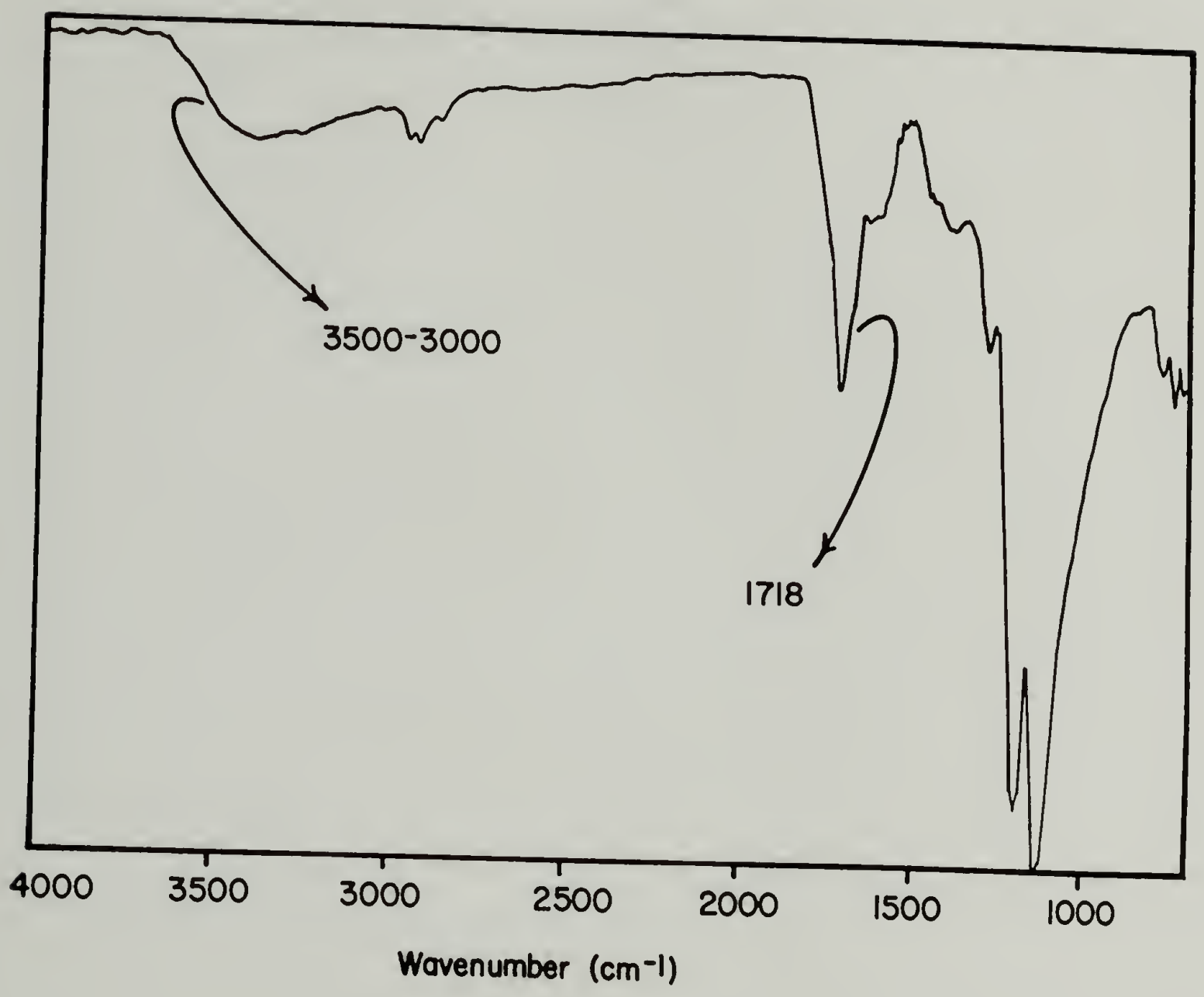

Figure 3.34

ATR-IR spectrum of PTFE-C exposed to ambient laboratory conditions.

Metal Polymer Interfaces

This section deals with the synthesis of a well characterized sulfur-containing PTFE surface. The reactivity of PTFE-C was further defined: radical additions, nucleophilic substitutions and electrophilic additions were among the reactions explored. Some parts of this research were carried out before acquisition of XPS; as a result the work is centered on ATR-IR and gravimetric analysis. In order to detect changes in ATR-IR spectra and gravimetric analysis, the PTFE-C films used were prepared by 12 hour reductions of PTFE. The depths of reaction associated with these reduction times are typically on the micron level (see above). When XPS analysis became routine, less extremely reduced PTFE (<150 Å) was employed.

Reaction of PTFE-C with ethanethiol

When PTFE-C (12 hour reduction) is treated with ethanethiol, a reaction occurs (according to ATR-IR and gravimetric analysis) under some conditions (Table 3.9).

Table 3.9

Addition of ethanethiol to PTFE-C

Reaction	Method	Reaction time	Reaction temperature	Removal of excess reagent by	Overall % mass change
1	acid catalyzed/neat	1 week	ambient	THF extraction	0.0
2	acid catalyzed/DMSO	1 week	ambient	EtOH/THF wash	0.0
3	base catalyzed	1 week	ambient	THF extraction	- 0.0160
4	radical, photochemical	8 hours	0°C	THF wash	+ 0.0144
5	radical, thermal	12 hours	65°C	THF extraction	- 0.208

The data obtained indicate that the functionalized surface is removed in workup by extraction. Films washed, rather than extracted gain weight as expected from the reaction course. ATR-IR spectra of Reactions 1-4 in Table 3.9 were recorded using a 60° KRS5 crystal and are shown in Figure 3.35. The spectrum for **1** indicates the addition of H_2SO_4 to the unsaturation: bands at 1050 and 960 cm^{-1} (S-O-C stretching) and 1430 (SO_2) are present but no evidence for thioether presence is indicated. Diluting the reagents in DMSO depressed the extent of the addition of the acid (**2**) but no thioether was detected. Base catalyzed addition of ethanethiol was not effective: no significant changes in the ATR-IR spectrum (**3**) were found. The most effective method of addition of ethanethiol to PTFE-C was by free-radical initiation; PTFE-C treated with ethanethiol using AIBN in THF at 0° C yielded product with ATR-IR spectrum (**4**) which exhibits a higher frequency shoulder on the PTFE C-F stretch (1250 cm^{-1}), indicative of S-CH_2 wagging. The other peaks necessary for definitive thioether identification are hidden by PTFE absorbances. Since it was difficult to discern exactly what type of functionality was present using the tools at hand, the reaction was abandoned.

Reaction of PTFE-C with elemental sulfur

"Vulcanization" of PTFE-C with elemental sulfur was attempted. When PTFE-C films (24 hour reduction) were refluxed in mesitylene solutions of sulfur, data consistent with the introduction of sulfur to the surface was obtained. Although ATR-IR data (using a KRS5 crystal) of PTFE-S did

Figure 3.35

Addition of ethanethiol to PTFE-C: ATR-IR spectra of reaction products. Spectra are recorded on a 60^{o} KRS5 crystal.

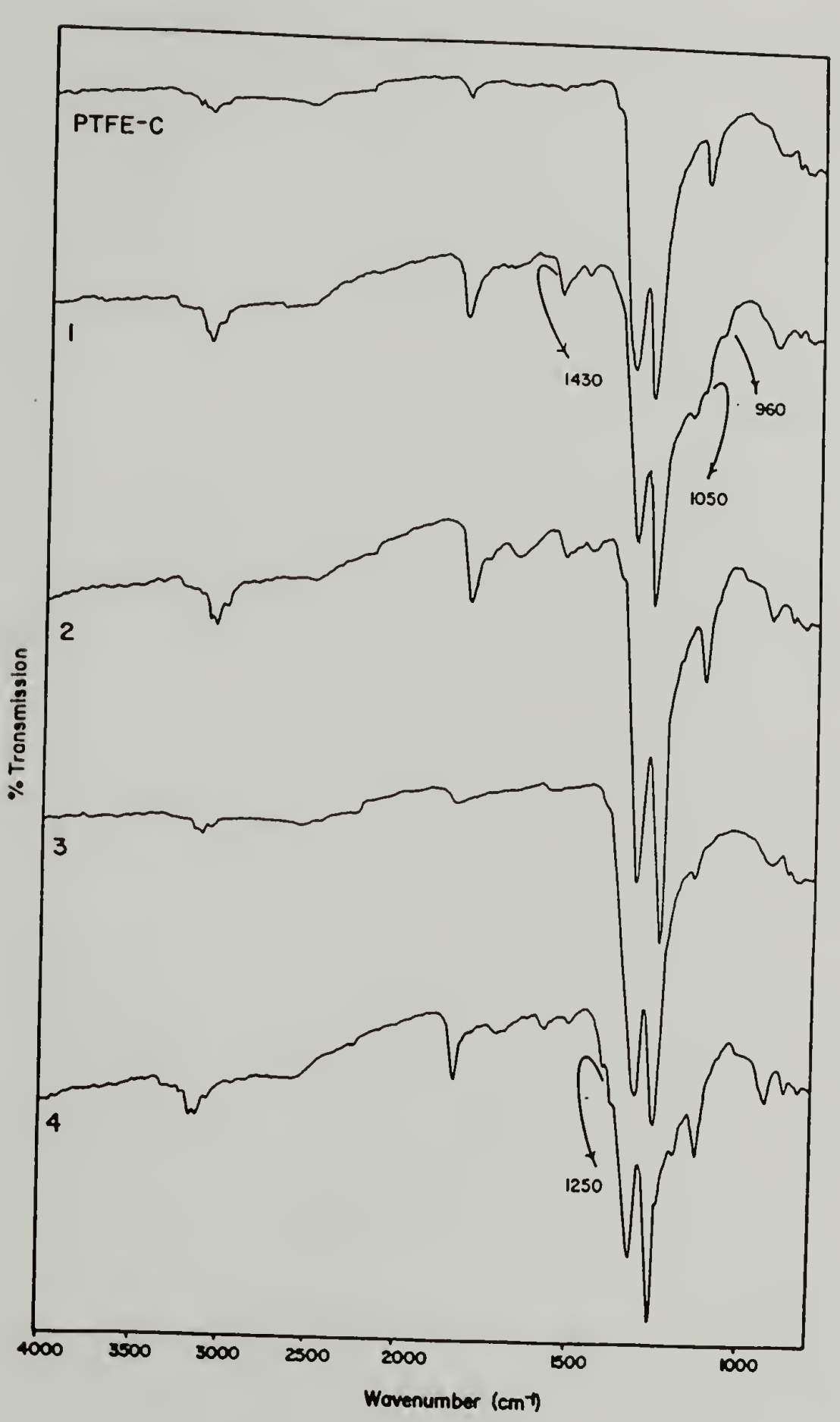
PTFE-C
1
1430
960
1050
2
3
4
1250
% Transmission
4000
3500
3000
2500
2000
1500
1000
Wavenumber (cm⁻¹)

not indicate any significant changes upon reaction, gravimetric analysis and elemental analysis (ion chromatography) indicated that sulfur was present (Table 3.10).

Table 3.10

Sulfur levels determined for PTFE-S

Analytical method	% Sulfur introduced
Gravimetric analysis	0.138
Ion chromatography	0.110

In order to investigate the role of interfacial chemistry in adhesion, we decided to submit these samples for 180° peel force testing of vapor deposited copper ribbons. It should be noted that the samples were reacted inhomogeneously due to experimental difficulties, which affected the reproducibility of the results. The data in Table 3.11 indicate that there is no difference in peel force measurements between

Table 3.11

Peel force results for PTFE-S

Run #	PTFE control	PTFE-C	PTFE-S
1	0.5	13.5	12.6
2	0.6	14.5	13.9
3	0.6	18.6	12.0
Average	0.6	15.3	12.8
Failure mode	adhesive	cohesive	cohesive

PTFE-C and PTFE-S within experimental error. The enhanced adhesion of copper to PTFE-C implied by the data is probably due to formation of the covalent copper-olefin complexes formed.[41] Cohesive failure in PTFE-C and PTFE-S was shown by X-ray and SEM data (obtained by Jae Park at IBM) to occur within the reacted layers, probably due to the extensive depths of reaction in both these samples. Nonetheless, the data illustrated that the chemistry at the metal-polymer interface was influencing adhesion of vapor-deposited copper; that sulfur had any influence, however, was not discerned by this experiment.

Reaction of PTFE-C with CS_2

A PTFE-C film (10 minute reduction) was reacted with atomic sulfur generated from the photolysis of CS_2 at 254 nm. XPS and gravimetric data indicate that a reaction had occurred. PTFE control samples, however, contained sulfur (by XPS) which could not be removed despite repeated extraction in mesitylene or benzene.

Reaction of PTFE-C with SCl_2

The electrophilic addition of SCl_2 to unsaturation yields bridged sulfur compounds.[42] PTFE-C films (10 minute reduction) treated in SCl_2 immediately turn white; inspection by XPS, however, indicated that the surface contains mostly C-Cl and no C-S bonds. Thus chlorine from the equilibrium:

$$2\,SCl_2 \rightleftharpoons S_2Cl_2 + Cl_2$$

chlorinates the unsaturation much faster than SCl_2 adds electrophilically. In order to scavenge the dissolved chlorine, SCl_2 was freshly distilled into flasks containing cyclooctene and PCl_3 and then this mixture was immediately transferred to a PTFE-C film. This strategy met with limited success: C:S ratios decreased substantially, but chlorine still added appreciably, (Figure 3.36) over the temperature range investigated.

Radical addition of thiolacetic acid to PTFE-C (PTFE-$SCOCH_3$)

Based on earlier success with the radical addition of ethanethiol to PTFE-C, the radical addition of thiolacetic acid to PTFE-C was attempted. XPS data for reactions using both benzoyl peroxide and AIBN as radical initiators were consistent with the formation of the thioester from PTFE-C according to Equation 3.6.

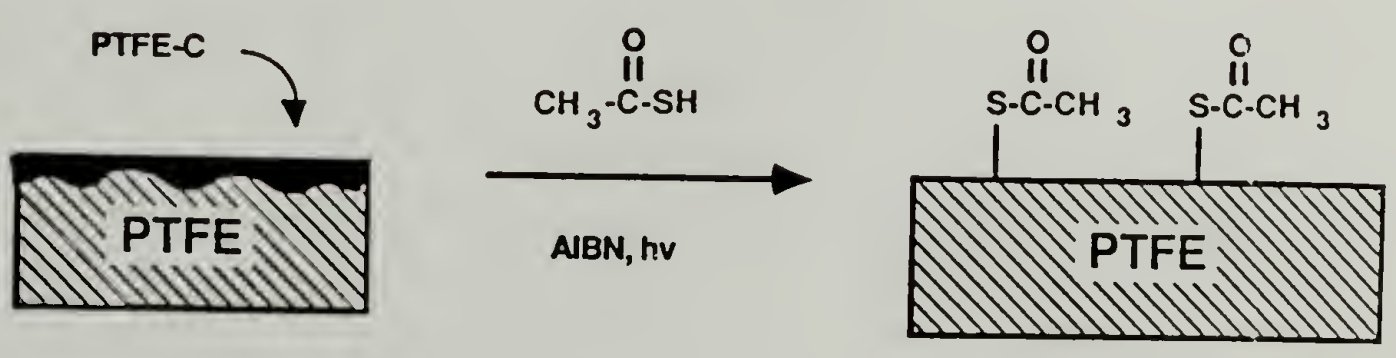

Equation 3.6

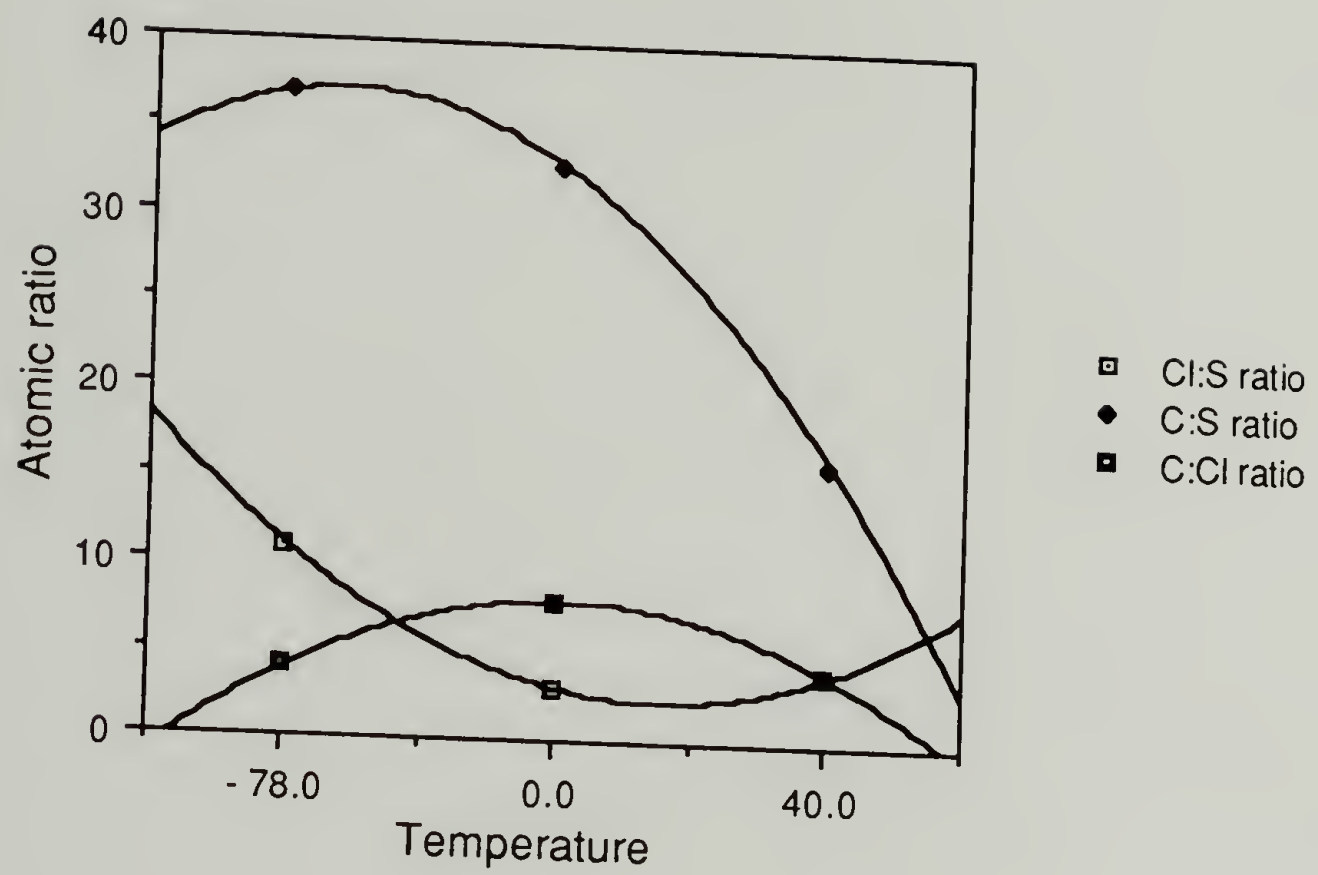

Figure 3.36

Temperature dependence of electrophilic addition of sulfur dichloride to PTFE-C.

Optimization of reaction conditions indicated maximum sulfur incorporation using AIBN photochemically decomposed at 12°C. In general, S:O ratios in PTFE-$SCOCH_3$ agreed well with calculated stoichiometry. AIBN provided a good XPS label for the incorporation of initiator fragments onto PTFE-C. The absence of nitrogen (N_{1s}:401 eV) in XPS survey spectra of reacted samples indicates that initiator fragment addition to PTFE-C did not occur.

Base-catalyzed hydrolysis of PTFE-$SCOCH_3$ yielded samples with XPS spectra which indicate competing hydration of double bonds in PTFE-C. (Figure 3.37). The theoretical stoichiometry predicts decreased O:S ratios on going from PTFE-$SCOCH_3$ to PTFE-SH, but experimental data indicate the incorporation of oxygen at much higher levels than expected. Control experiments for PTFE-C hydrolysis showed increased oxygen levels. Attempted cleavage of the thioether with methyllithium yielded superfluous results.

Phase transfer catalyzed addition of tetrabutylammonium thiolate to PTFE-C

Since direct additions of sulfur to PTFE-C met with limited success, we decided to exploit the reactivity of PTFE-Br and PTFE-Cl towards nucleophilic reagents. When PTFE-Br is treated with an aqueous solution of NaSH and tetrabutylammonium bromide, data consistent with the introduction of sulfur are observed. The reaction apparently involves SN_1 substitution of SH^- for halogen based on knowledge of analogous solution reactions. The overall reaction sequence is depicted in Scheme

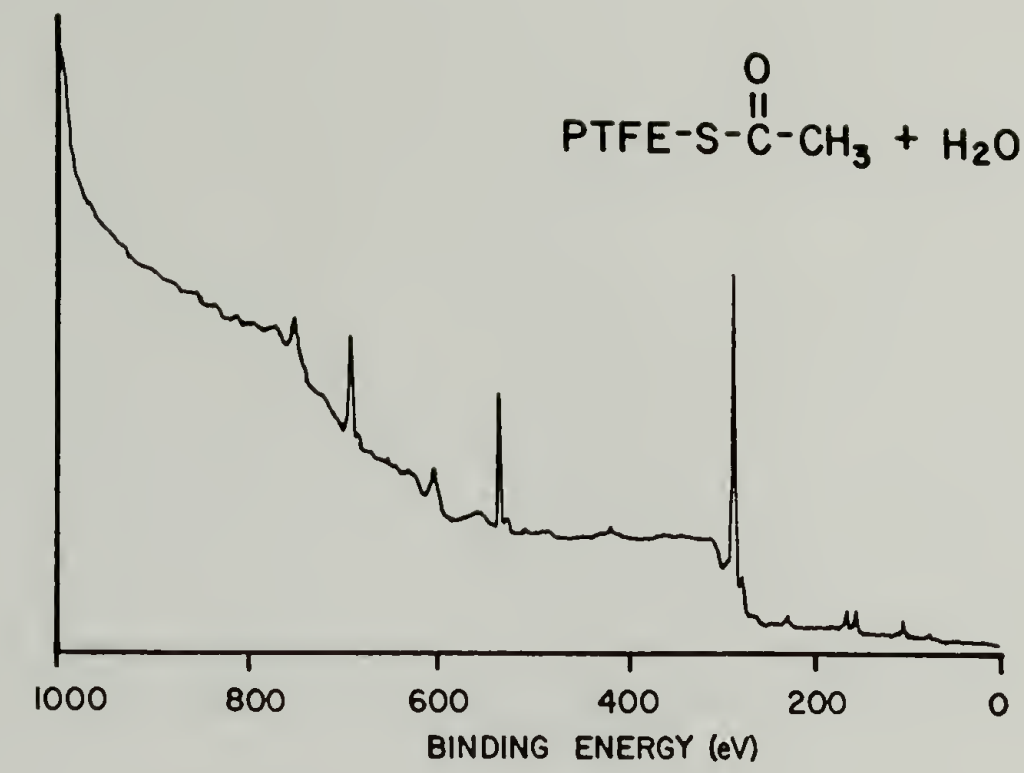

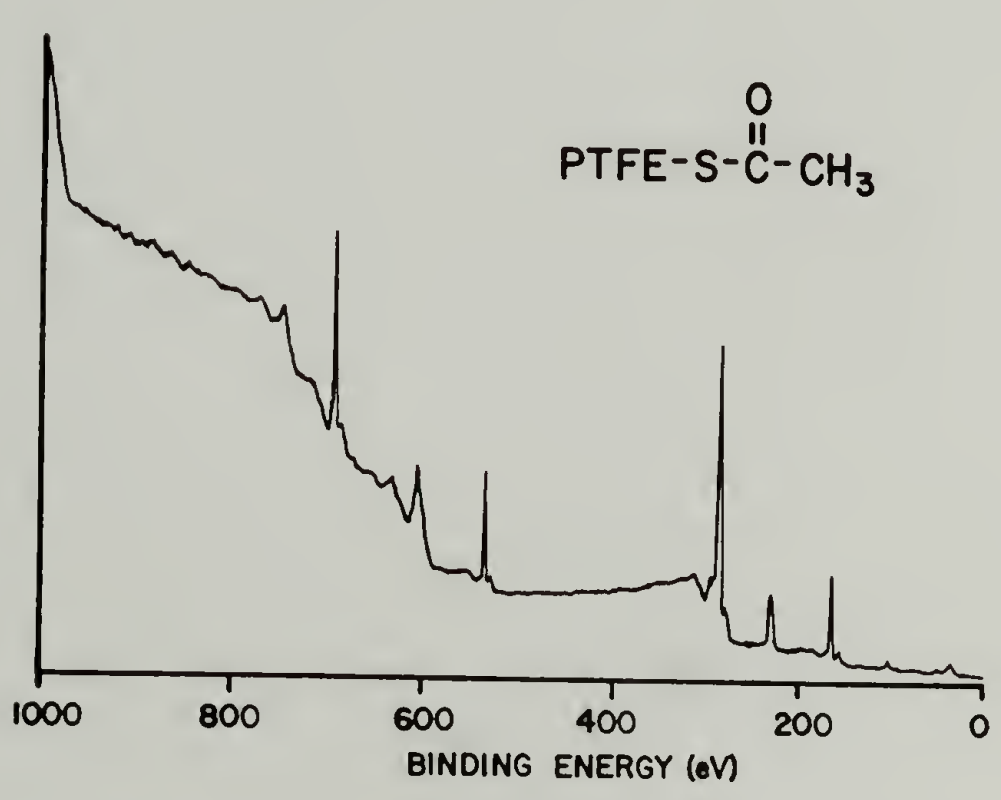

Figure 3.37

XPS survey spectra for the radical addition of thiolacetic acid to PTFE-C and subsequent hydrolysis.

3.3 for PTFE-Br:

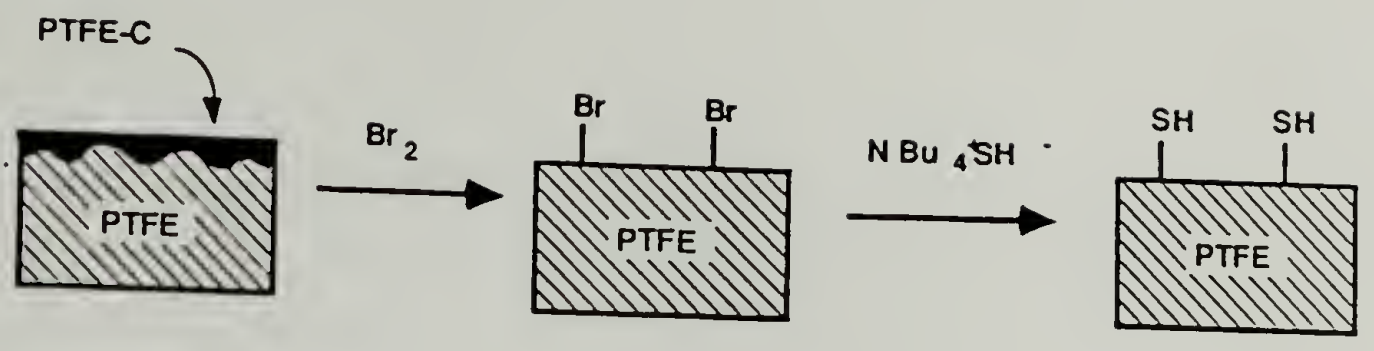

Scheme 3.3

The temperature dependence of the reaction was explored in order to optimize the quantity of SH introduced. XPS atomic ratio data are plotted in Figure 3.38. The data indicate that the lowest C:S ratios are obtained at higher temperature, but oxygen contamination (most likely from hydration of unsaturation in PTFE-C) occurs appreciably.

The analogous reaction of PTFE-Cl with $^{+}N(Bu)_4{}^{-}SH$ at 80°C yielded less oxygen incorporation for the same C:S ratios found in PTFE-SH reacted from PTFE-Br. XPS survey spectra for the sequence of reactions is given in Figure 3.39; the introduction of chlorine results in the appearance of Cl_{2s} (270 eV) and Cl_{2p} (200 eV) photoelectron lines. On treatment with thiolate anion, the chlorine peak intesity is diminished and the peaks corresponding to sulfur (S_{2s}:229 eV; S_{2p}:169 eV) appear. Gravimetric analysis for 2 samples (Table 3.12) indicates that

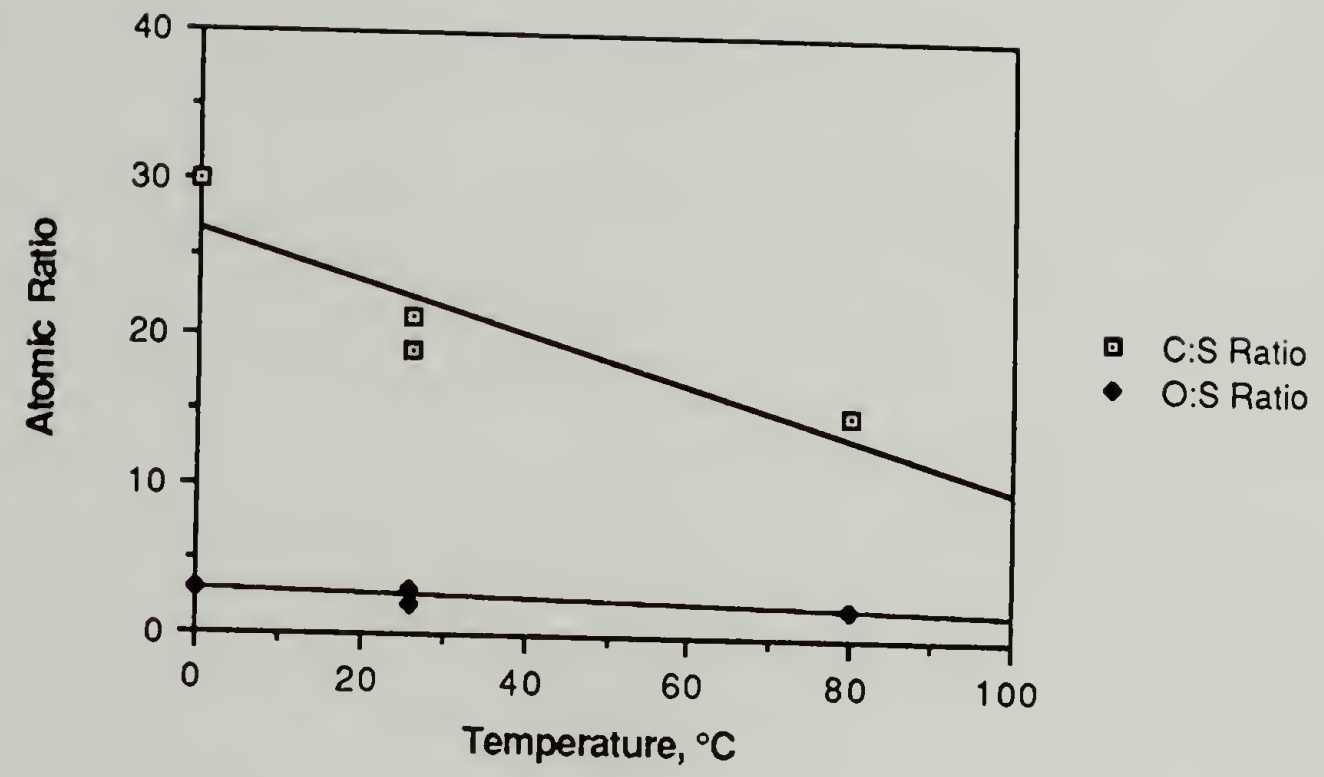

Figure 3.38

Temperture dependence of thiolate anion substitution reaction with PTFE-Br.

Figure 3.39

XPS survey spectra for the conversion of PTFE-C to PTFE-SH.

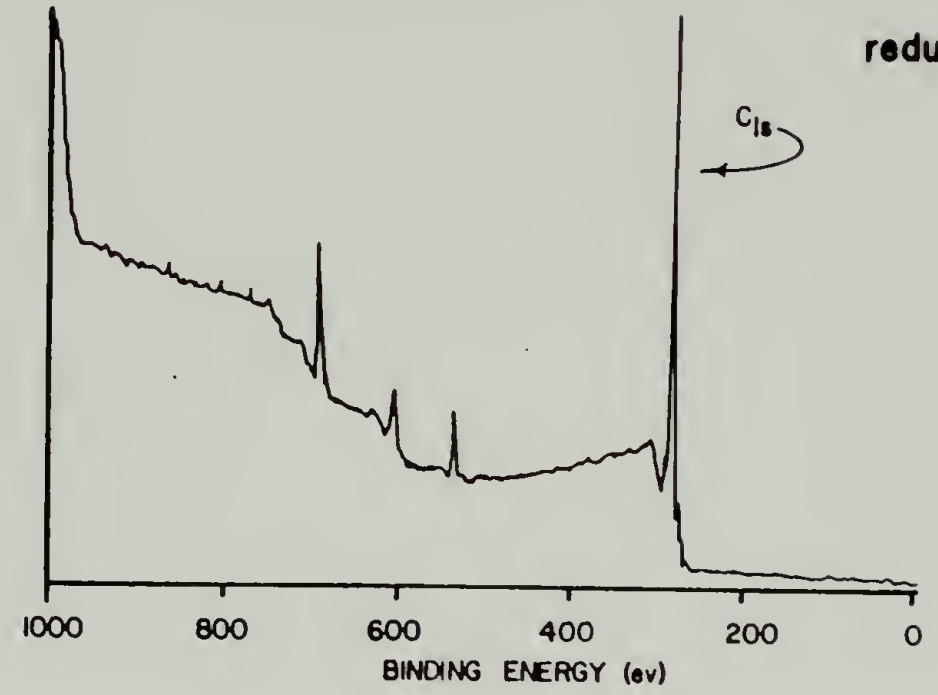

Cl_2
0°C

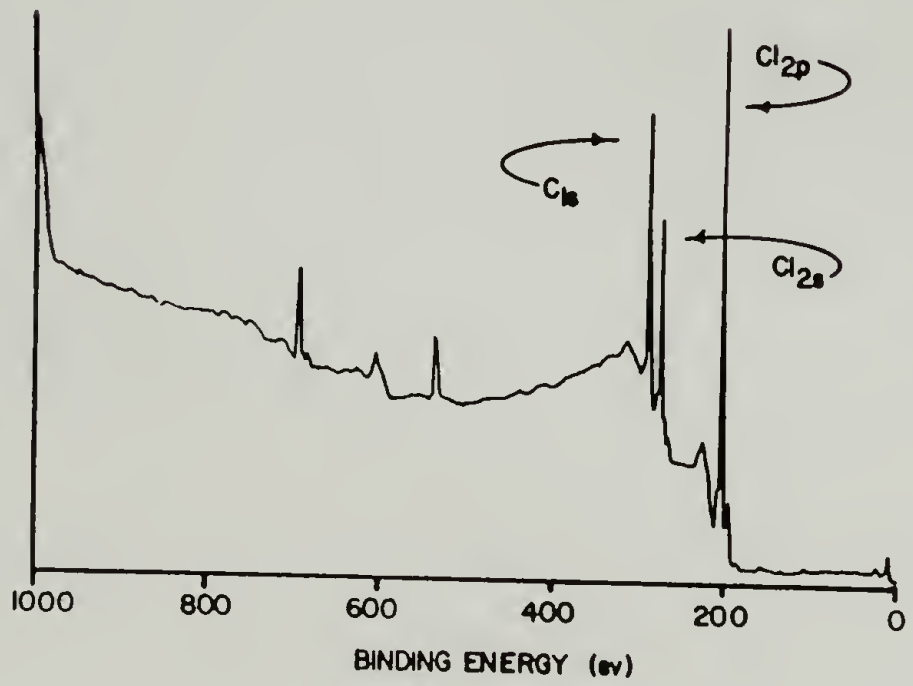

$Bu_4N^+{}^-SH$
80 °C

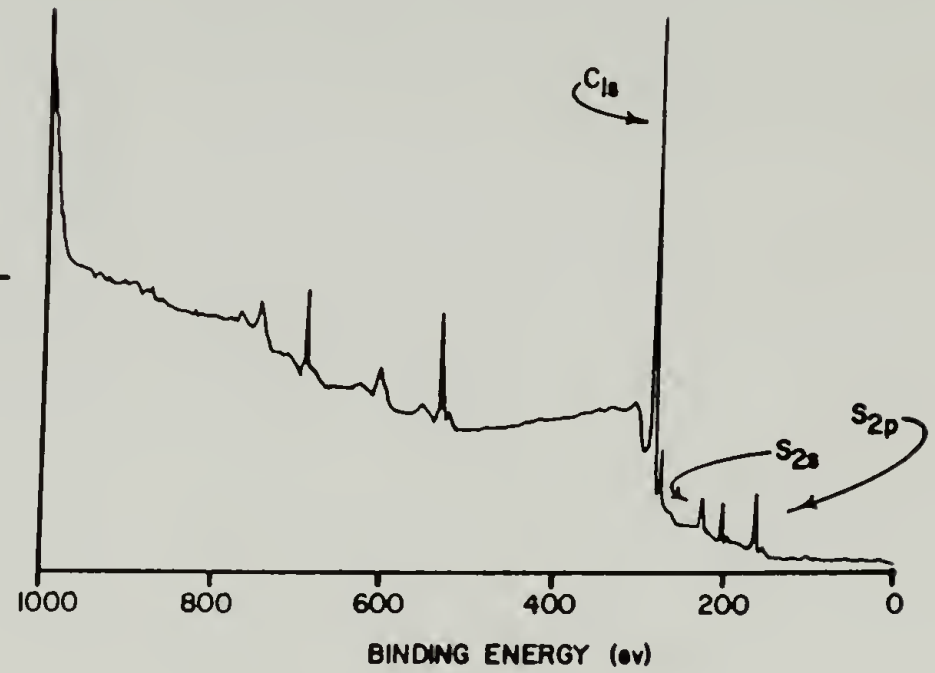

Table 3.12

Gravimetric results for sulfhydryl derivatization of PTFE-C

PTFE --(1)--> PTFE-C --(2)--> PTFE-Cl --(3)--> PTFE-SH

Reaction #	Mass difference (mg) Sample A	Sample B
1	-0.0094	-0.0082
2	+0.0079	+0.0079
3	-0.0034	-0.0035

elimination must occur when PTFE-Cl is treated with $^{+}N(Bu)_4{}^{-}SH$. There should not be significant mass changes on going from PTFE-Cl to PTFE-SH (Cl=35 g/mol; SH=33 g/mol) if only substitution were operative. Competing elimination of Cl^{-} would cause mass loss. XPS atomic composition data also support this: much more chlorine peak area is diminished in making PTFE-SH than predicted solely for substitution by SH^{-}. Also, white-colored PTFE-C films change to purple on reaction with $^{+}N(Bu_4)^{-}SH$ indicating the unsaturation in PTFE-C.

Attempts at labelling thiols present on PTFE-SH for XPS analysis yielded inconclusive results. For this type of work, a good label should uniquely distinguish the functional group. With thiols, this is difficult since their reactivity closely parallels that of the hydroxyl group. Also, establishing good controls is difficult. The XPS labelling reagent may physisorb or chemically react with the controls. For example, when 3,5 dinitrobenzoylchloride (3,5 DNBC) is reacted with PTFE-Cl and PTFE-SH the following XPS composition data (Table 3.13) are obtained:

Table 3.13

Reaction of PTFE-SH with 3,5-dintrobenzoyl chloride

Sample	Atomic composition					
	F	O	C	N	Cl	S
PTFE-SH	22.72	5.72	65.35		1.90	3.77
PTFE-Cl + 3,5-DNBC	6.71	10.95	65.58	3.59	10.91	1.09
PTFE-SH + 3,5-DNBC	6.18	12.61	69.87	4.61	3.01	2.72

Although it seems that PTFE-SH has reacted with 3,5-DNBC, the results obtained for PTFE-Cl indicate that the reagent may be physisorbed or may have reacted with hydroxyl groups present on PTFE-Cl, which result from addition of water found in the chlorine gas to PTFE-C.

A similar XPS labeling experiment was carried out with heptafluorobutyryl chloride (HFBC). The reaction of PTFE-SH with HFBC yielded a sample which shows an increase in F:S ratio from 0.91 in PTFE-SH (prepared from 0.50 hour reduced PTFE-C) to 3.0 in PTFE-$SCOC_3F_7$. The high resolution carbon region also indicates that the reaction has taken place: the characteristic high binding energy C-F peaks due to the heptafluorobutyryl group are present. (Figure 3.40) Although the control samples did not appear to have reacted with HFBC under the reaction conditions, the labeling reaction is not conclusive since HFBC is not specific for thiols. In addition, other analytical techniques did not support the labeling experiments: quantification of thiols present on PTFE-SH by Elman's reagent[43] failed; the ATR-IR spectrum of PTFE-SH does not indicate any S-H stretching. The data suggest that PTFE-SH contains

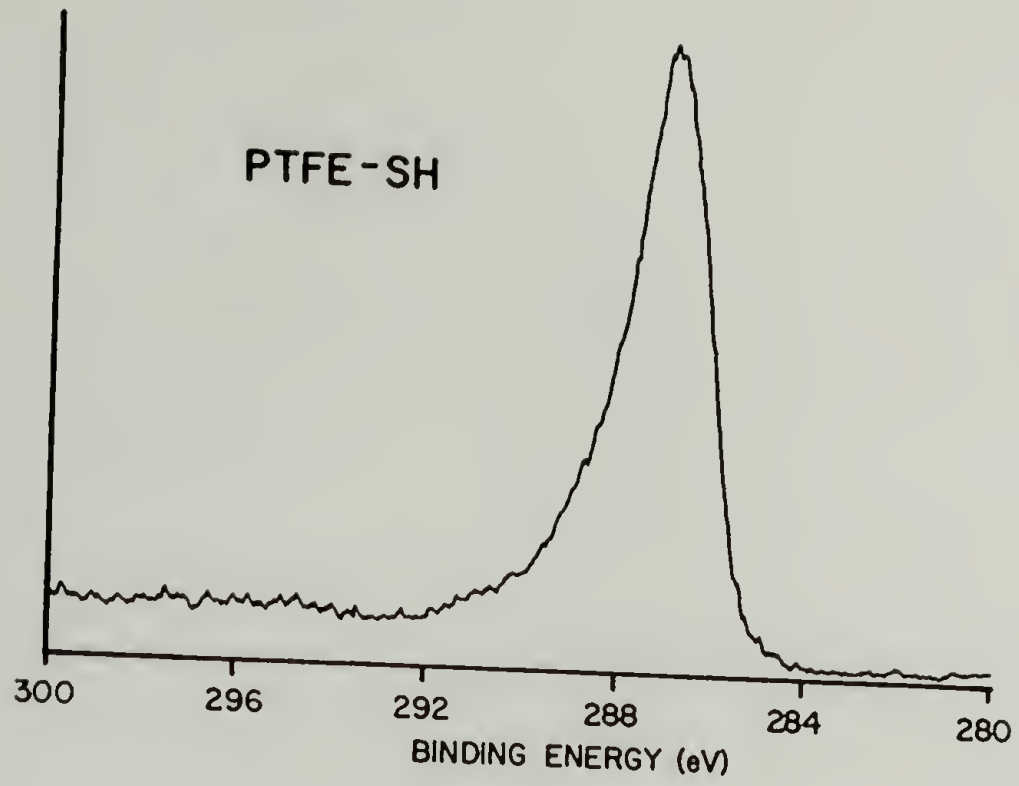

Figure 3.40

XPS C_{1s} high resolution spectra for heptafluorobutyryl chloride tagged thiol groups on PTFE-SH.

few thiol groups; sulfur present on the surface may be present as episulfides or thiocarbonyls resulting from the elimination of Cl^- by two pathways in basic medium:

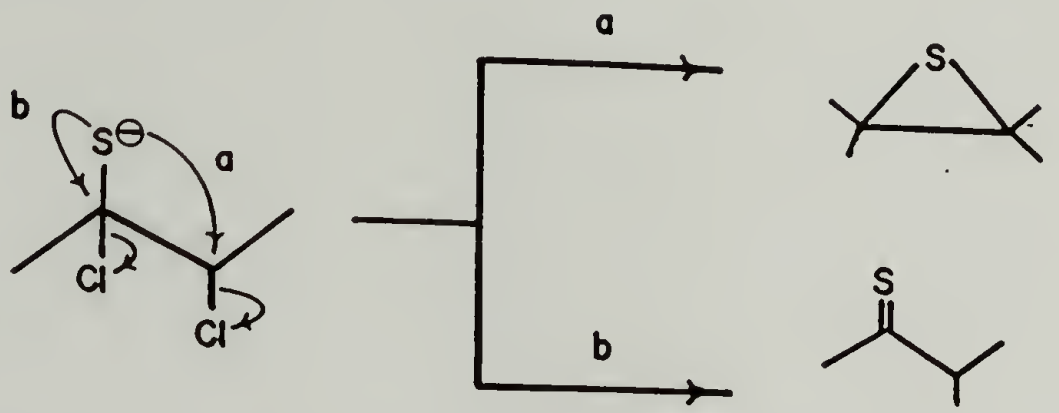

Regardless of the exact nature of the sulfur functionality, this sequence of reactions carried out on PTFE renders a surface with quite different surface properties. Contact angle data (Table 3.14) indicate

Table 3.14

Contact angle data for thiol group introduction to PTFE

Sample	θ_a	θ_r
PTFE	120	89
PTFE-C	114	68
PTFE-Cl	108	67
PTFE-SH	87	16

changes on going from PTFE to PTFE-SH consistent with expected changes in surface free energy.

Peel force data were obtained for samples of PTFE-SH prepared from PTFE-C reduced for 10 minutes. (Table 3.15) The peel strength values for the PTFE control are much higher than observed in the first attempt. (Table 3.11) due to the type of PTFE used: the 1/16" thick sheets were

visually rougher and more homogeneously reacted than the 5 mil thick sheets previously used.

Table 3.15

Peel force results for PTFE-SH

Sample	Peel force (g/mm)
PTFE-Cu	4.1
PTFE-C-Cu	11.9
PTFE-S-Cu	14.1

The data indicate a 2.9 and 3.4 fold increase in peel force for copper deposited on PTFE-C and PTFE-SH, respectively over the control sample. Since the reacted the samples had approximately the same degree of roughness, it can be assumed that the observed adhesion force values are consequences of the chemistry at the interface. The increased peel force measured on PTFE-C-Cu can be ascribed to covalent copper-olefin bonds.[41] Although these experimental results seem to discern the effect of thiol groups on adhesion in PTFE, a major flaw in the investigation remains. The XPS data for PTFE-SH indicates that the surface contains oxygen in addition to sulfur. The source of this contamination is most probably due to hydration of unsaturation (from elimination reactions that compete with substitution of PTFE-Cl) in PTFE-SH. Further work probing specific interactions of copper vapor with PTFE-SH by XPS or UPS is warranted before definitive conclusions can be drawn. The structure-property relationships observed here may be attributed to the oxygen or the unsaturation present in PTFE-SH.

References

1. N.L. Bauld, J. Am. Chem. Soc., **87**, 4788 (1965).

2. E.T. Kaiser, "Radical Ions", Interscience, New York, 1968, p. 87.

3. T. Abe and M. Iwaizumi, Bull. Chem. Soc. Japan, **47**, 2593 (1974).

4. D.I. McCane in "Encyclopedia of Polymer Science and Technology", Vol.13, Wiley, New York, (1970) p. 623.

5. A.J. Dias and T.J. McCarthy, Macromolecules, **17**, 2529 (1984).

6. A.J. Dias and T.J. McCarthy, Macromolecules, **18**, 1826 (1985).

7. H.B. Gray, Chem. Soc. Rev., **15**, 17 (1986).

8. P.K. Ghosh, "Introduction to Photoelectron Spectroscopy", Wiley, New York, (1983) p. 75.

9. C.A. Sperati and H.W. Starkweather, Fortschr. Hochpolym.-Forsch., **2**, 465 (1961).

10. S.W. Jacob, E.E. Rosenbaum, and D.C. Wood, "Dimethyl Sulfoxide", Marcel Dekker, New York, (1971) p. 6.

11. M. Schwoerer, V. Lauterbach, W. Mueller, and G. Wegner, Chem. Phys. Lett., **69**, 359 (1980).

12. G. Wnek, J.C.W. Chien, F.E. Karasz, C.P. Lillya, Polymer, **20**, 1441 (1979).

13. I. Heinmaa, M. Alla, A. Vainrub, E. Lippmaa, M.L. Khidekel, A.I. Kotov, and G.I. Kozub, J. Phys. Coll., **44**, C3-357 (1983).

14. G.E. Macriel and M.J. Sullivan, "NMR Spectroscopy: New Methods and Applications; ACS Symposium 191", American Chemical Society, 1982, p. 319.

15. H.W. Starkweather, R.C. Ferguson, D.B. Chase, and J.M. Minor, Macromolecules, **18**, 1684 (1985).

16. R.E. Moynihan, J. Am. Chem. Soc., **81**, 1045 (1959).

17. C.Y. Lang, S. Krum, J. Chem. Phys., **25** 563 (1956).

18. N.C. Craig and E.A. Entemann, J. Chem. Phys., **36**, 243 (1962).

19. B. Bak and D. Christenson, Spectrochimica Acta, **12**, 355 (1958).

20. C.J. Pouchet, "The Aldrich Library of Infrared Spectra: Edition III", Aldrich Chemical Company, Milwaukee, 1981.

21. B.B. Johnson and W.L. Peticolas, Ann. Rev. Phys. Chem., **27**, 465 (1976).

22. L.S. Lichtmann, A. Sarangi, and D.B. Fitchen, Solid State Commun., **36**, 869 (1980).

23. G. Zannoni and G. Zerbi, J. Mol. Structure, **100**, 485 (1983).

24. A. Peluso, M. See, and J. Ladek, Solid State Commun., **53** 893 (1985).

25. P.N. Batchelder and D. Bloor, J. Phys. Chem.: Solid State Phys., **15** 3005 (1982).

26. See references 20-22.

27. J.C.W. Chien, "Polyacetylene, Chemistry, Physics, and Materials Science", Academic Press, New York, 1984.

28. J. March, "Advanced Organic Chemistry", McGraw-Hill, New York, 1983, p. 369.

29. K. Kato, J. Appl. Poly. Sci., **15**, 2115 (1971).

30. A.J. Dias and T.J. McCarthy, unpublished results, this laboratory.

31. O.S. Bhanot and P.C. Dutta, Chem. Comm., **1968**, 122.

32. W. Haaf, Chem. Ber., **99**, 1149 (1966).

33. K. Nakanishi, "Pratical Infrared Absorption Spectroscopy", Holden-Day, San Fransico, 1962, p. 45.

34. J.L. Lang, W.A. Pavelich, H.D. Cleary, J. Poly. Sci. A, **1**, 1123 (1963).

35. V.D. Braun, I.A. Aziz el Sayad, J. Pomakis, Makromol. Chem., **224**, 249 (1969).

36. N.G. Gaylord, S. Marti, J. Polym. Sci., Poly. Lett. Ed., **11**, 253 (1973).

37. G.W. Kabalka, K.A.R. Satry, G.W. McCollum and H. Yoshioka, J. Org. Chem., **46**, 4296 (1981).

38. A.C. Moffat, E.C. Horning, S.B. Martin, M. Rowland, J. Chromatogr.,

66, 255 (1972).

39. J.C. Lhuguenot and B.F. Maume, J. Chromatogr. Sci., **12**, 411 (1974).

40. D.S. Everhart and C.N. Reilly, Anal. Chem., **53**, 665 (1981).

41. F.A. Cotton and G. Wilkenson, "Advanced Inorganic Chemistry", Interscience, 1972, p. 728.

42. E.J. Corey and E. Block, J. Org. Chem., **31**, 1663 (1966).

43. A.F.S.A. Habeeb, Methods Enzymol., **25**, 457 (1972).

Chapter IV

Conclusions and Suggestions

The work presented in this thesis is an investigation of the surface and interface chemistry of poly(tetrafluoroethylene), a chemically resistant polymer. We have developed a new PTFE surface modification using benzoin dianion solution as a reducing agent, which produces a gold air sensitive carbonaceous layer on PTFE (PTFE-C). We have extended this reaction to address a number of areas: 1) PTFE-surface functionalization 2) electrically conducting polymers and 3) metal-polymer interfaces.

The first part of the research was dedicated to the physical and chemical characterization of PTFE-C. SEI micrographs, gravimetric analysis, and contact angle measurements indicated that the reaction was corrosive in nature. The reaction depth could be controlled from 150 Å to ~1.5 μm, depending on the reaction time. The chemical nature of the product was deduced mainly through spectroscopy. XPS indicated a gradual loss of fluorine with time, until a surface composed of carbon and slight amounts of oxygen and fluorine was present. The EPR spectrum of PTFE-C indicated the presence of mobile carbon-based free spins. The UV-vis spectrum showed a broad absorbance with λ_{max} at 540, supporting a highly conjugated structure. One of the most interesting results of the spectroscopic characterization was that PTFE-C contained hydrogen and that this hydrogen was incorporated by the solvent, DMSO and water used during the workup. Raman spectra of PTFE-C and PTFE-C (prepared in DMSO-d_6) yielded spectra consistent with those found in trans h and d

polyacetylene, respectively. ATR-IR spectra were not consistent with a single trans-polyacetylene component, but also with the presence of triple bonds, monofluroolefins, and aromatic structure. Formation of t-butyl ethers was demonstrated to be one of the major competing deleterious side reactions. With the information that PTFE-C contained hydrogen, cross polarization NMR was attempted and yielded spectra consistent with the presence of sp, sp^2, and sp^3 carbon.

From the chemical characterization results, it was obvious that PTFE-C is quite different from the carbonaceous product obtained from alkali metal reduction of PTFE (PTFE-AMR). PTFE-C is less extensively reduced, containing fluorinated olefins and polyacetylene-like structure, compared to PTFE-AMR, which is graphitic in nature. Thus PTFE-C is more reactive, requiring mild conditions compared to those used for PTFE-AMR. The highly unsaturated PTFE-C is even more reactive towards halogenation, incorporating 4 times as much bromine as PTFE-AMR.

The extended conjugated system formed in this reduction was found to conduct electricity when doped with iodine, achieving conductivities up to $10^2 \Omega^{-1} cm^{-1}$ depending on the depth of reduction. The conductivity was shown to have an inverse relationship to the reaction depth and the iodine-doped material was stable over a 12 hour period. The temperature dependence of its conductivity indicated that it was a semiconductor with an activation energy of 0.4-0.7 eV over the temperature range studied. The conductivity values found for PTFE-C are much higher than the highest values reported for PTFE-AMR. Whereas the conductivity in PTFE-C is due entirely to its organic extended conjugated system, that in PTFE-AMR has been attributed to intercalation of salts produced during the reduction.

The merit in these conductivity results is that this reduction produces an electrically conducting material from a processable insulating precursor. The ramifications of this include not only its potential use as a battery, but also as a capacitor.

The reactivity of PTFE-C was investigated with the objective of introducing alcohols, carboxylic acids, and amines to PTFE surfaces. PTFE-C was easily halogenated with chlorine and bromine. It was also easily hydroborated; subsequent oxidation in basic peroxide yielded ATR-IR spectra and contact angle data consistent with the formation of alcohols. These alcohols were successfully labelled with TFAA and HFBC and characterized using XPS.

Besides electrophilic additions, PTFE-C was also reactive in radical addition reactions. Maleic anhydride was added by free radical initiation and the resulting surface-confined anhydrides were hydrolyzed, yielding carboxylic acids. Thiolacetic acid also added free radically, as did acetic acid and styrene. Diels Alder reactions were also successful, although it is not known whether these additions were truly concerted or whether they occurred through radical intermediates.

The reaction of PTFE-Br with ammonia was used to generate PTFE-NH_2. This amine surface was labelled with PFB, an amine specific XPS label, verifying the presence of amine functionality.

Finally, we synthesized a PTFE-copper interface by introducing sulfur functionality to PTFE-C via substitution reactions on PTFE-Cl and PTFE-Br with tetrabutylammonium thiolate. Although the resulting surface contained minimal sulfhydryl functionality, peel force measurements indicated increased adhesion over control samples.

Many interesting aspects of this work are still unexplored. For example, investigation of the reduction and the application of the reaction in small molecule chemistry is warranted. Reductions done on perfluoroalkanes and analysis of the products would yield information on the distribution of the various kinds of unsaturation present in PTFE-C. In addition, the reactivity of other fluorinated polymers towards benzoin dianion should yield useful information concerning the generality of the reaction. Preliminary investigations on poly(chlorotrifluoroethylene) indicated that the reaction did not produce the same type of carbonaceous layer (see Appendix II). Reactions of poly(tetrafluoroethylene co-hexafluoropropylene) should also yield carbonaceous material. Elimination should predominate in reduction of fluorinated polymers such as poly(vinylidene fluoride), which contain active hydrogens.

The scope of the reactivity of PTFE-C has really only been slightly tapped here. One can imagine numerous reactions to perform on PTFE-C, based on the work presented here, that could be utilized to introduce functional groups to the surface. There are major drawbacks, however. The solubility of reacted surfaces in reaction solvents and subsequent dissolution has been qualitatively observed in this work. Careful choice of reaction conditions, workup, etc. is necessary to avoid this problem. In addition, the large amount of unsaturation present in PTFE-C even after derivitization renders any functionalized surface air sensitive. Reactions on PTFE-C, therefore should occur throughout the reduced layer.

Finally, the work has resulted in means for preparing PTFE surfaces containing specific functionality. Provided new surfaces are

topographically similar, they can be used to derive structure-property relationships in the areas of wetting, adsorption, and adhesion. Preparation of the PTFE-copper interface presented here is the initial step towards reaching this goal. XPS experiments on the specific interactions between the in situ vapor deposited metal and PTFE-SH would yield valuble information on the contribution of sulfur functionality to PTFE-copper adhesion. In addition, the preparation methods developed for PTFE-COOH, PTFE-OH, and PTFE-NH_2, permits investigation of the role of these functional groups on metal-PTFE adhesion.

Appendix 1

Hydroxylated Poly(p-phenylene vinylene) via Benzoin Condensation of Terephalaldehyde

Introduction

Poly(p-phenylenevinylene) 1 exhibits an electronic conductivitiy of $3\Omega^{-1}cm^{-1}$ upon treatment with arsenic pentafluoride.[1]

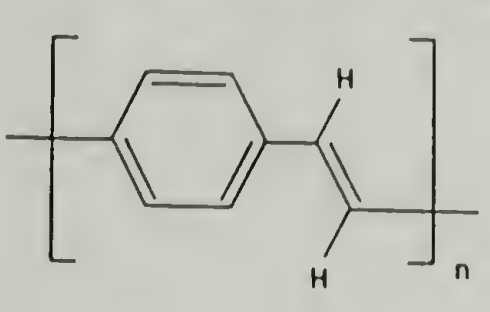

1

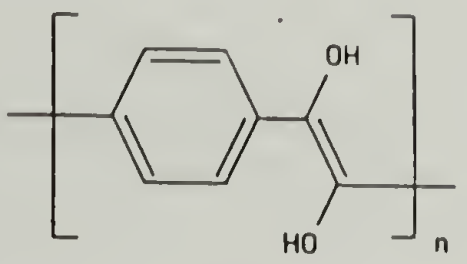

2

Insolubility and infusibility have hindered its (as well as other organic conductor's) application, and research directed at improving processibility by phenylation has been reported.[2,3] The objective of this research was to prepare a hydroxylated derivative 2, which, in addition to enhanced solubility, may exhibit "molecular switch" qualities due to its saturated tautomeric forms 3:

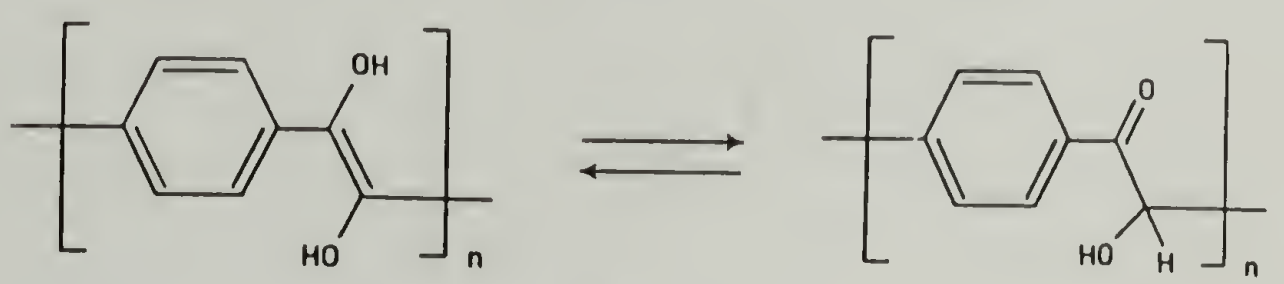

3

Our synthetic strategy was to "benzoin condense" terephalaldehyde and form the hydroxyketone tautomer.

Reports of benzoin condensation of terephalaldehyde are not consistent with regard to the products: Oppenheimer[4] and Kratzer[5] report dimer, Jones and Tinker[6] report an oligomer, which, when kept in an inert atmosphere, exists partially in its ene-diol form, and Wehr[7] reports the formation of a benzoin homopolymer, which is cross-linked at 250°C. None of the products were characterized with regard to structure or molecular weight.

Experimental

Purification and preparation of the starting materials.

Terephthalaldehyde (Aldrich) was recrystallized from water, then from methanol to a constant melting point of 115°C and stored under vacuum. Quartenary ammonium cyanides (tetramethyl and tetraethyl ammonium cyanides) were prepared from the chlorides and sodium cyanide according to the literature procedures.[8,9] N,N-dimethylformamide (Fisher) and dimethylsulfoxide (Aldrich) were distilled from barium oxide at reduced pressure; N-methylpyrrolidone (Eastman) was distilled from phosphorous pentoxide at reduced pressure. Distilled water and methanol (Fisher) were deoxygenated by purging with prepurified nitrogen.

Instrumentation

^{1}H and ^{13}C NMR spectra were obtained at 300 and 75 MHz with a Varian XL300. Infrared spectra were recorded on a Perkin Elmer 283. Gel permeation chromatography was performed on a Waters 150C using N-

methylpyrrolidone as solvent. Elemental analyses were performed by the University of Massachusetts Microanalytical Laboratory and vapor pressure osmometry was performed by the University of Massachusetts Microanalytical Laboratory and Arrolabs. Conductivity was measured at room temperature on films mounted on platinum electrodes with a Fluka multimeter.

Polymerization procedure. (I:47;53;55;57;61;63;67;103, II:19)

Terephthalaldehyde (2.0g, 14.9 mmol) was placed in a Schlenk tube and evacuated and flushed with nitrogen three times on the vacuum line. Solvent (8 ml of DMF, NMP, or DMSO) was introduced via syringe to dissolve the monomer. Tetramethylammonium cyanide (5-20 mg, 0.05-0.20 mmol, 0.3-1.3 mol %) in 2 ml solvent was added via syringe; a deep purple color forms. The Schlenk tube was placed in an oil bath at 80°C for 100-170 hours. During the first 1-5 minutes, depending on the solvent and catalyst level, the purple solution became deep red, then orange. The product was isolated by precipitation using either deoxygenated water or methanol. The polymer was filtered, extracted (Soxhlet extractor) with methanol overnight, and then dried at reduced pressure at 50°C. Yields were typically 60-90%.

Results and Discussion

Treatment of terephthalaldehyde with catalytic amounts (0.3-1.3 mol%) of cyanide in polar aprotic solvents (DMF, NMP, and DMSO) for 4-7 days produces orange solutions which render red-orange powder when precipitated with methanol or yellow powder when precipitated with water.

Each polymer can be redissolved in any of the above solvents and brittle films can be cast from solution at 50°C and 0.05 mm of Hg. Elemental analyses (Table A1.1) indicate nitrogen impurities in all samples, some of which can be attributed to solvent and/or catalyst which is incorporated

Table A1.1

Elemental analysis of polybenzoin synthesized in various solvents

Element	Theoretical weight %	Experimental weight % DMSO	DMF	NMP
Carbon	71.64	71.11	70.91	70.29
Hydrogen	4.48	4.85	4.61	4.34
Nitrogen		0.44	1.25	1.01
Oxygen*	23.88	23.66	23.23	24.36

* obtained by difference

into the polymer. The characterization which is described below was done on the sample polymerized in DMSO at 80°C for 1 week. Both gel permeation chromatography and vapor pressure osmometry were performed in order to determine molecular weight. GPC using columns that can distinguish molecular weights as high as 5 million showed total exclusion. VPO by two commercial laboratories gave values of M_n=600 and

M_n=660. The inherent viscosity was determined to be 0.065-0.16 dl/g[10]. ^{1}H-NMR reveals the absence of an expected aldehyde resonance (δ 9-10) and the presence of an unexpected methyl peak (δ 1.1) (Figure A1.1). The other peaks correspond well with those found in the model compound, benzoin[11]. ^{13}C-NMR reveals, in addition to peaks ascribed to **3**, signals at 142 and 167 ppm which could be due to catalyst incorporation into the polymer in the form of nitriles (Figure A1.2) The infrared spectrum of the polymer also corresponds well with that of the model compound, benzoin (Figure A1.3). It seems then, that the benzoin condensation of terephthalaldehyde proceeds to form low molecular weight oligomers, containing modified (not aldehyde) end groups probably by reaction of catalyst and/or solvent to terminate the reaction.

To test the idea of reversible tautomerization (Equation A1.2), base was added to dilute DMSO solutions of the polymer. Concentrated aqueous sodium hydroxide turned the orange solution initially black and this faded to orange over time. The black color was most likely due to extended conjugation in a partially ionized ene-diol structure **2**.[12] The color most likely faded due to alkaline hydrolysis of the benzoin moiety.[13] When potassium t-butoxide or sodium dimsyl in DMSO was used under nitrogen, a more stable purple-black solution was formed: infrared spectra (Figure A1.4) revealed the loss of O-H and C O absorbances, suggesting ene diolate formation. Acidifying the solutions did not disperse the black color. Oxidation of the ene-diolate yielded a sample whose IR spectra was similar to benzil, except for the absorbance at 2050 cm^{-1}.

None of the samples prepared (including the ene-diolate form

Figure A1.1

300 MHz ^{1}H NMR of polymer from the benzoin condensation of terephthalaldehyde.

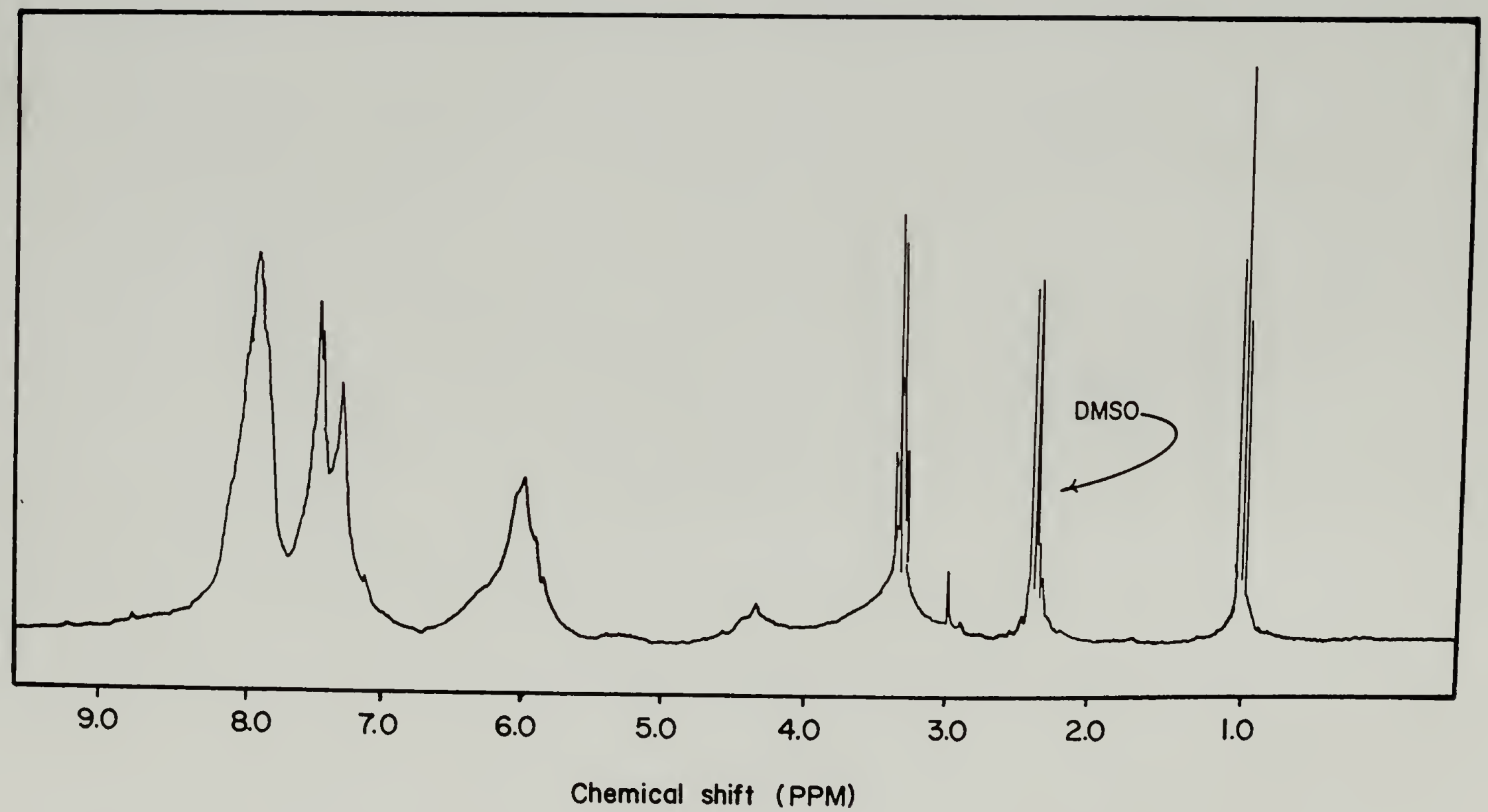
DMSO
9.0
8.0
7.0
6.0
5.0
4.0
3.0
2.0
1.0
Chemical shift (PPM)

Figure A1.2

75 MHz ^{13}C NMR of polymer from the benzoin condensation of terephalaldehyde.

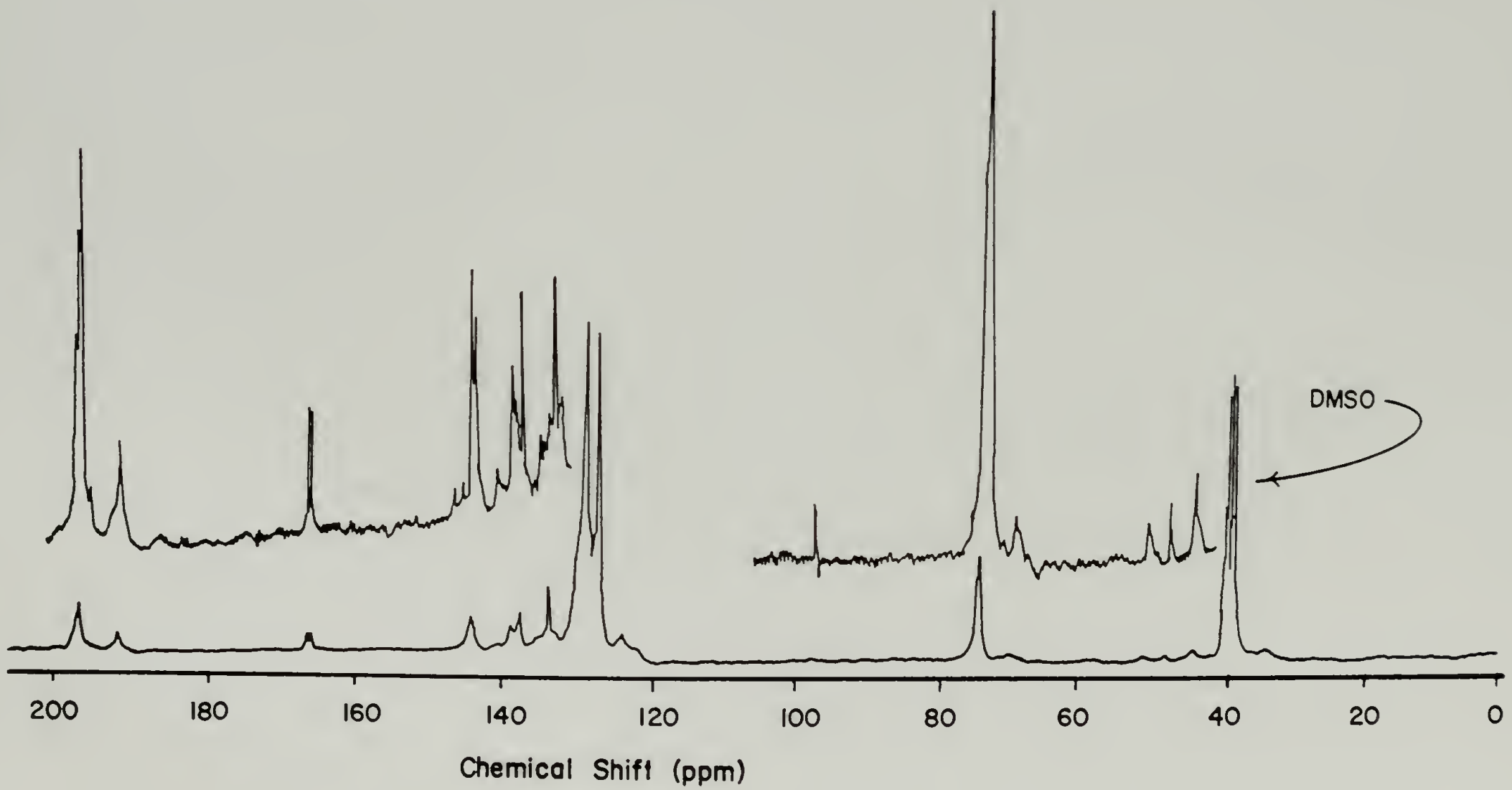
DMSO
200
180
160
140
120
100
80
60
40
20
0
Chemical Shift (ppm)

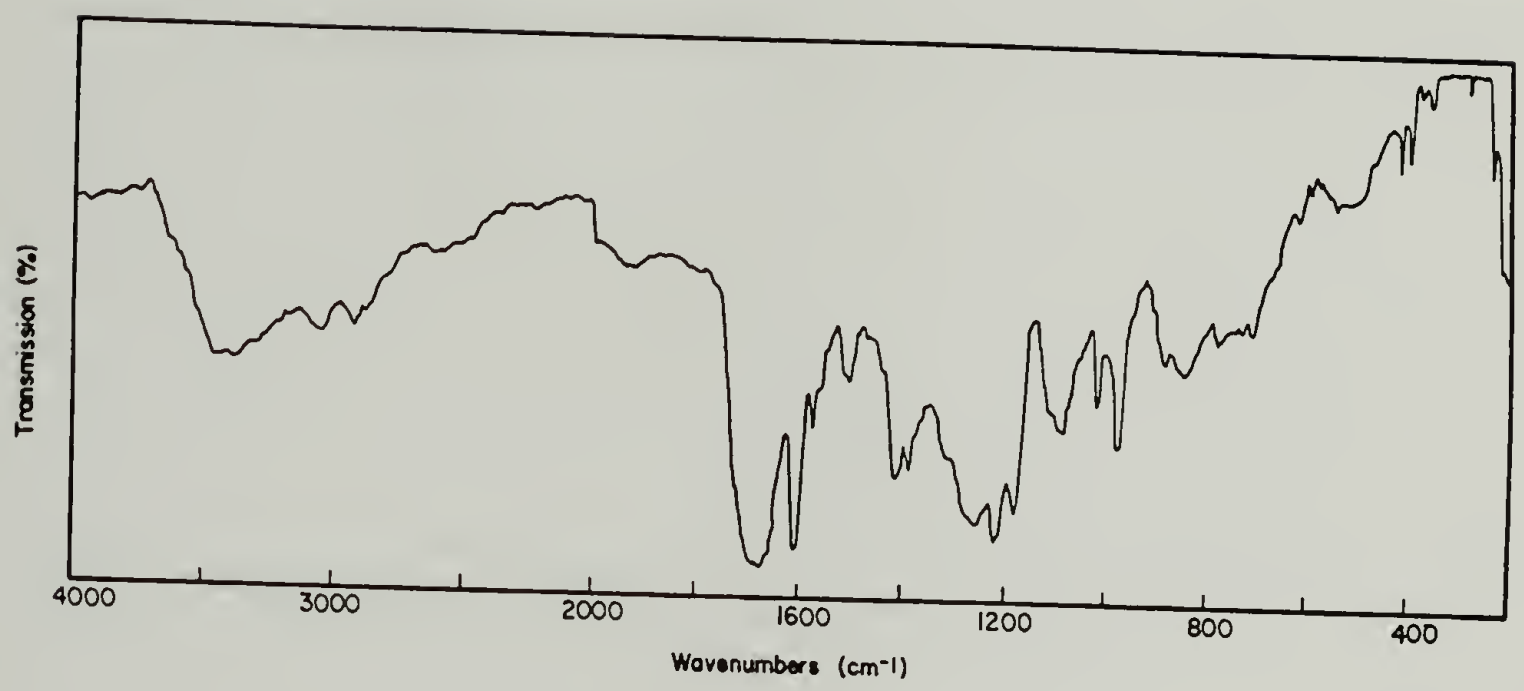

Figure A1.3

IR spectrum (KBr pellet) of polymer from the benzoin condensation of terephalaldehyde.

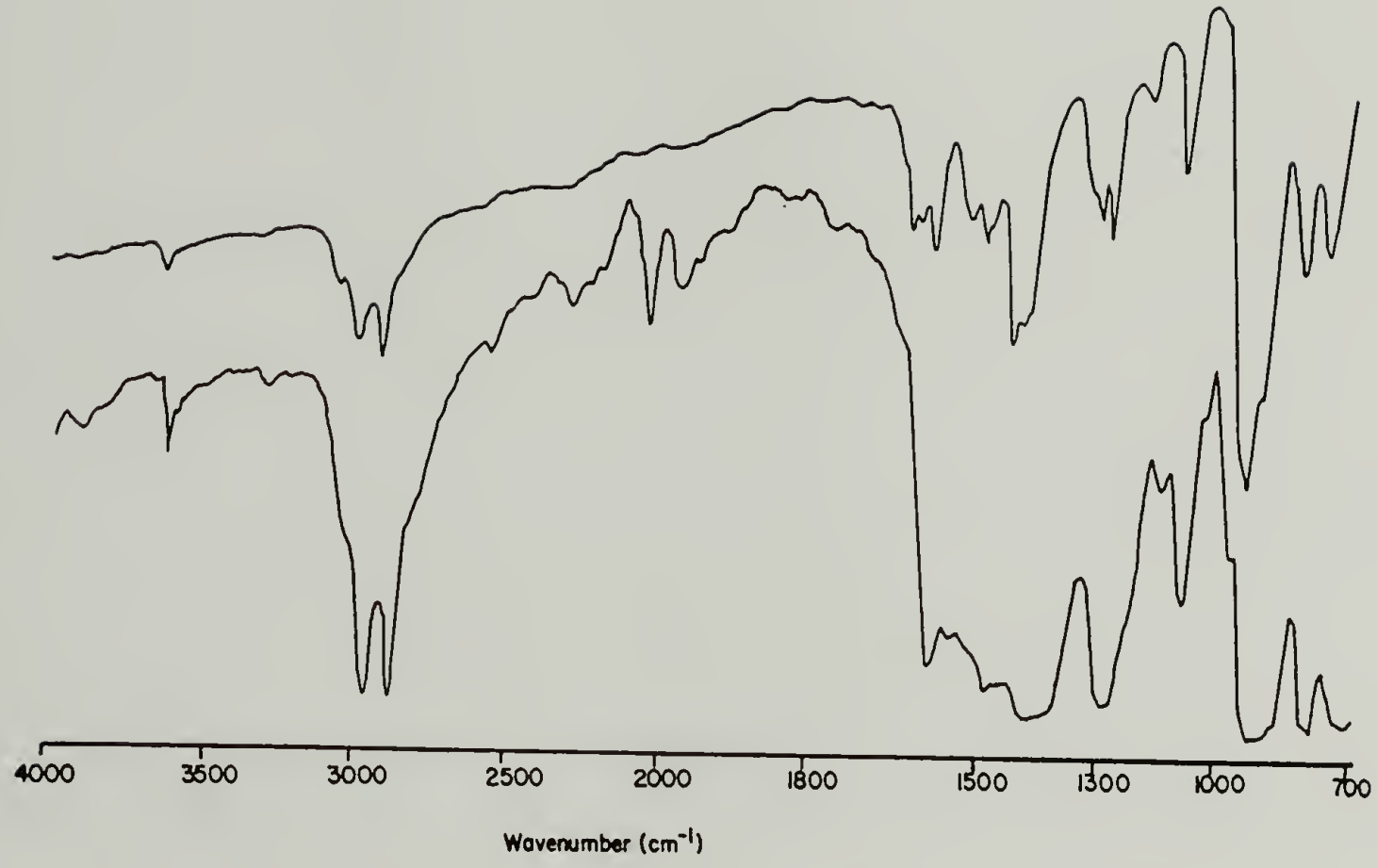

Figure A1.4

IR spectra of ene-diolate and oxidized ene-diolate recorded on sodium chloride plates under nitrogen.

obtained) exhibit conductivity (of films) greater than $10^{-10}\,\Omega^{-1}cm^{-1}$. Sodium and iodine doping were also not effective in imparting conductivity.

In summary, terephthalaldehyde was oligomerized with cyanide ion in polar aprotic solvents; vapor phase osmometry suggested a number average molecular weight consistent with a pentamer. The oligomer could be deprotonated to form an extended-conjugated ene-diolate. Neither the oligomer nor the deprotonated material was or could be doped to a conducting material.

References

1. G.E. Wnek, J.C.W. Chien, F.E. Karasz, and C.P. Lillya, Polymer, **20**, 1441 (1975).

2. W.J. Feast and C.S. Spanomanolis, Polymer Photochemistry, **1**, 285, (1981).

3. W.A. Feld, A. Ganeson, and D.D. Nymberg, A.C.S. Polymer Preprints, **24**, (1), 143 (1975).

4. H. Oppenheimer, Chemische Berichte, **19**, 1814, (1886).

5. R.H. Kratzer, K.L. Paciorek, and D.N. Karle, J. Org. Chem, **41**, (12) 2230, (1976).

6. J.I. Jones, P.B. Tinker, J. Chem. Soc., **1955**, 1286.

7. R. Wehr, U.S. Patent 3,414,466, (1968).

8. O.W. Webster, W. Mahler, and R.E. Benson, J. Am. Chem. Soc., **84**, 3681 (1962).

9. S. Andreades and E.W. Zahnow, J. Am. Chem. Soc., **91**, 4181, (1969).

10. H. Blankenheim, unpublished results from this laboratory.

11. "The Sadtler Standard Spectra", Sadtler Research Laboratories, Inc., Philadelphia, 1971.

12. G.A. Russell, J. Org. Chem., **32**, 353, (1967).

13. D.B. Sharp and E.L. Miller, J. Am. Chem. Soc., **74**, 5643 (1952).

Appendix 2

Reaction of Benzoin Dianion with Polychlorotrifluoroethylene

Introduction

We have reported the reaction of PTFE with benzoin dianion, which produced an extended conjugated carbon system containing carbon-carbon double and triple bonds, free spins, and aromatic structure.[1] Since the suggested mechanism for the reaction involved electron transfer from the dianion, we proposed that it could be generalized to include PCTFE. PCTFE is similar in chemical structure to PTFE except for the presence of a carbon-chlorine bond: it should easily accept an electron from the from the reducing agent.

The reaction of PCTFE with benzoin dianion would represent one of the few reported methods for modification of this polymer. PCTFE is considered a "chemically inert" polymer; however it has been recently modified with by reaction with organometallic reagents.[2-5] Dias has elucidated the mehanism for the reaction of PCTFE with alkyl lithium reagents.[6] This work has been extended to include PCTFE surface reactions using lithium reagents containing protected functional groups. When these surface masked functional groups were deprotected, polar functionality was imparted to the polymer surface.[7]

In addition to the information obtained on the reactivity of PCTFE, the electronic conduction found in PTFE-C prompted investigation of the electrical properties in the product derived from PCTFE reduction.

The objectives of this research are to 1) to investigate the surface

reaction of PCTFE towards the benzoin dianion reducing solution and 2) to determine whether the reaction product is electrically conducting.

Experimental

Purification of starting materials

Polychlorotrifluoroethylene film (5 mil, Aclar 33C, Allied) was extracted in methylene chloride (Soxhlet extractor) and evacuated to a constant weight. All other materials were purified as described in the experimental section of the main body of this thesis.

Instrumentation

Gravimetric analyses were performed with a Cahn 29 electrobalance (no polomium source). XPS spectra were recorded using a MgKα source with a Kratos XSAM 800 spectrometer. ATR-IR spectra were recorded on a Perkin Elmer 283 infrared spectrometer using a 60^{o} germanium crystal. Conductivity was measured at room temperature on samples mounted with silver paste on platinum electrodes with a Fluka multimeter. Iodine was introduced as a vapor from the dry solid.

Reduction Procedure

The reduction procedure was analogous to that used in the reduction of PTFE. Potassium t-butoxide (1.0 g, 8.8 mmol) was dissolved in 30 ml of DMSO and added to benzoin (0.27 g, 1.3 mmol) dissolved in 5 ml DMSO under nitrogen. The dark purple solution was transferred to a Schlenk tube containing a 1 cm x 1 cm PCTFE film sample which was then placed in

a 50°C oil bath where the reaction was allowed to proceed for the desired amount of time. The solution was then transferred from the tube and the film washed with 4 x 10 ml portions of DMSO, 10 x 15 ml portions of water and 5 x 15 ml portions of THF (all under nitrogen). The film was then evacuated at 10^{-3} torr to a constant weight for gravimetric analysis. The films were oxidized (for gravimetric analysis) by submersion into a solution of $H_2SO_4/KClO_3$ (0.5 g in 50 ml) for 24 hours. They were then rinsed in copious amounts of water and THF and evacuated.

Reaction of PCTFE films under control conditions was carried out as follows: DMSO (10 ml) was transferred via cannula onto a PCTFE film in a Schlenk tube which had been evacuated and backflushed with nitrogen (3 times). The tube was placed in a 50°C oil bath and reacted overnight. The following day, it was washed in DMSO, water, and THF and evacuated. Likewise, potassium t-butoxide (1.0 g, 8.8 mmol) was dissolved in 35 ml DMSO, reacted with a PCTFE film overnight, then washed and evacuated.

Results and Discussion

The reaction of PCTFE with benzoin dianion solution yielded data indicative of reaction. Reacted PCTFE films became shiny opaque black in appearance and exhibited contact angle data suggesting surface roughening: extensive skipping and dragging of the water drop across the surface was evident.

The black reacted layer in PCTFE-C could be easily removed by $H_2SO_4/KClO_3$. This oxidation yielded white translucent films which were rough to the naked eye. The XPS survey spectrum of the reduced-then-oxidized material indicated that it was composed of PCTFE. Since the

chemical composition of the starting material and final product were known, the depth of reaction could be determined from Equation A2.1:

$$\text{Depth of reaction} = \frac{M_v - M_o}{2\,(2.10)\,L \cdot W}$$

Where M_v is the mass of the virgin film, M_o is the mass of the reduced-then-oxidized film, **l** is the length, **w** is the width and 2.10 is the density of the PCTFE film used. The reaction depth was easily controlled by reaction time, as was the case with PTFE. Figure A2.1 illustrates the data obtained over reaction periods of up to five days. It is evident that the reaction of PCTFE is more extensive than that of PTFE, proceeding as deep as 4μm over a five day period. The reaction depths achieved were not consequences of the electrical conductivity of the reduced material as in PTFE-C; PCTFE-C showed no conductivity when doped with iodine. The results must be attributed to two transport-related phenomena 1) the diffusion of the reaction solution into the polymer and 2) the increased solubility of the reaction product in the reaction solution. Both effects would lead to extensive reaction.

Gravimetric analysis on control reactions indicated that competing reactions and/or swelling of the polymer by the reaction solvent and reagents were taking place. Table A2.1 lists gravimetric data for control reactions; data for reacted-then-oxidized films are also given.

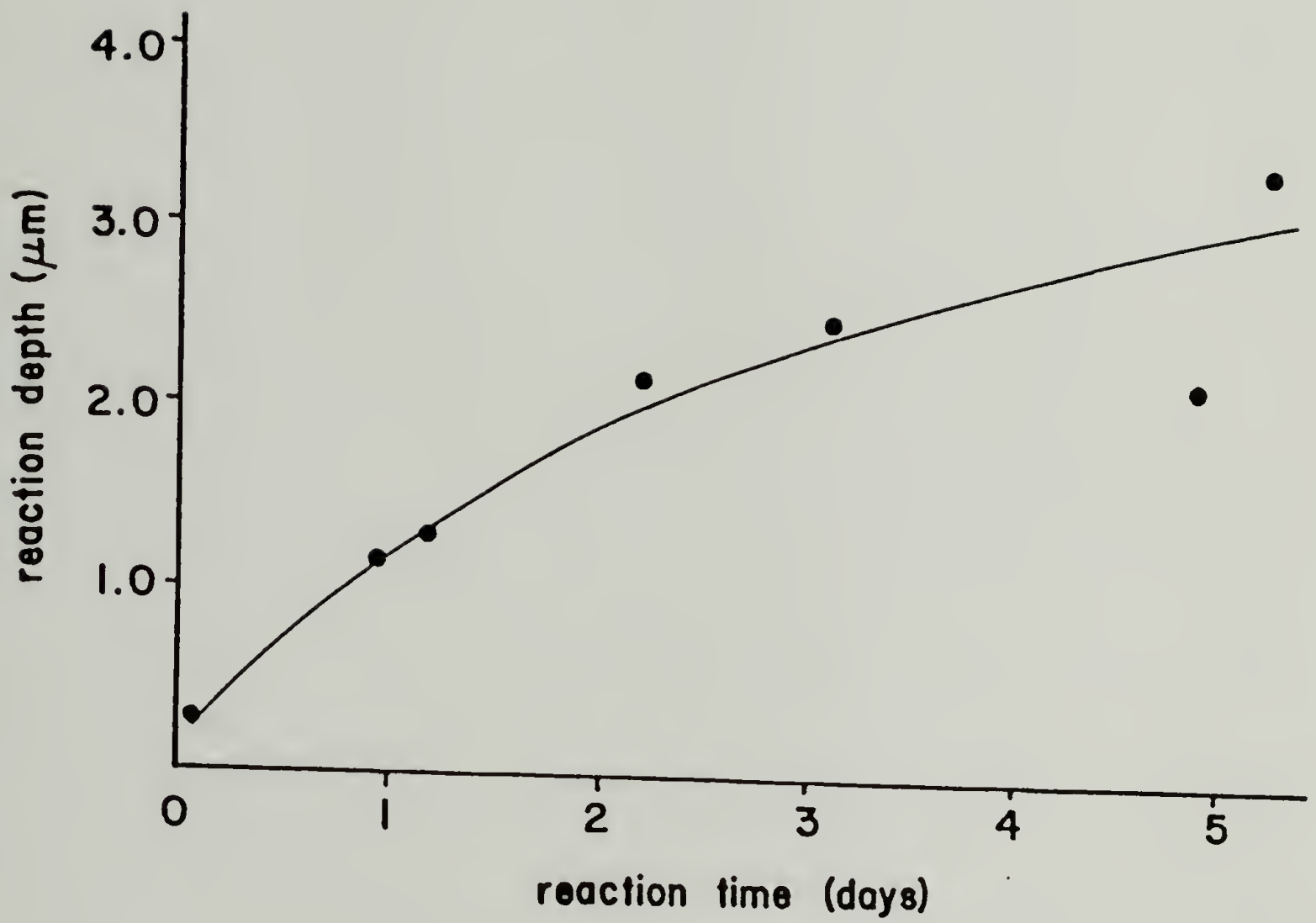

Figure A2.1

Gravimetric analysis: plot of PCTFE reaction depth vs. reaction time.

Table A2.1

Control reactions for PCTFE reductions: Gravimetric results

Reactants used with PCTFE	% Change from initial mass: Reacted Mass	Reacted-then-oxidized-mass
DMSO	+ 0.018	- 0.025
DMSO/Benzoin	+ 0.007	- 0.029
DMSO/Base	- 0.030	-----
$H_2SO_4/KClO_4$	No Change	-----

Visual inspection of the PCTFE film reacted with potassium t--butoxide in DMSO solution substantiated that reaction had taken place: the clear PCTFE film developed a black tint.

XPS spectroscopy also implied that other reactions besides reduction were occurring in this system. Figure A2.2 shows the survey spectra and C_{1s} high resolution spectra for PCTFE, and the reactions of PCTFE with DMSO, DMSO/base, and DMSO/base/benzoin. Reaction and/or swelling of PCTFE with DMSO was apparent: increased area of the O_{1s} peak (535 eV, survey spectrum) and non--CF_2/CFCl carbon peak (288 eV, C_{1s} high resolution spectrum) in addition to appearance of the S_{2p} peak (168 eV, survey spectrum) supported this. The potassium t--butoxide/DMSO solution also reacted with PCTFE; the fluorine and chlorine peaks (696 and 200 eV, respectively, survey spectrum) were almost totally depleted within the XPS sampling depth while a large increase in the O_{1s} peak was observed.

Figure A2.2

XPS survey and C_{1s} high resolution spectra for reactions of PCTFE films with benzoin dianion and control solutions.

survey spectra

high resolution C_{1S}

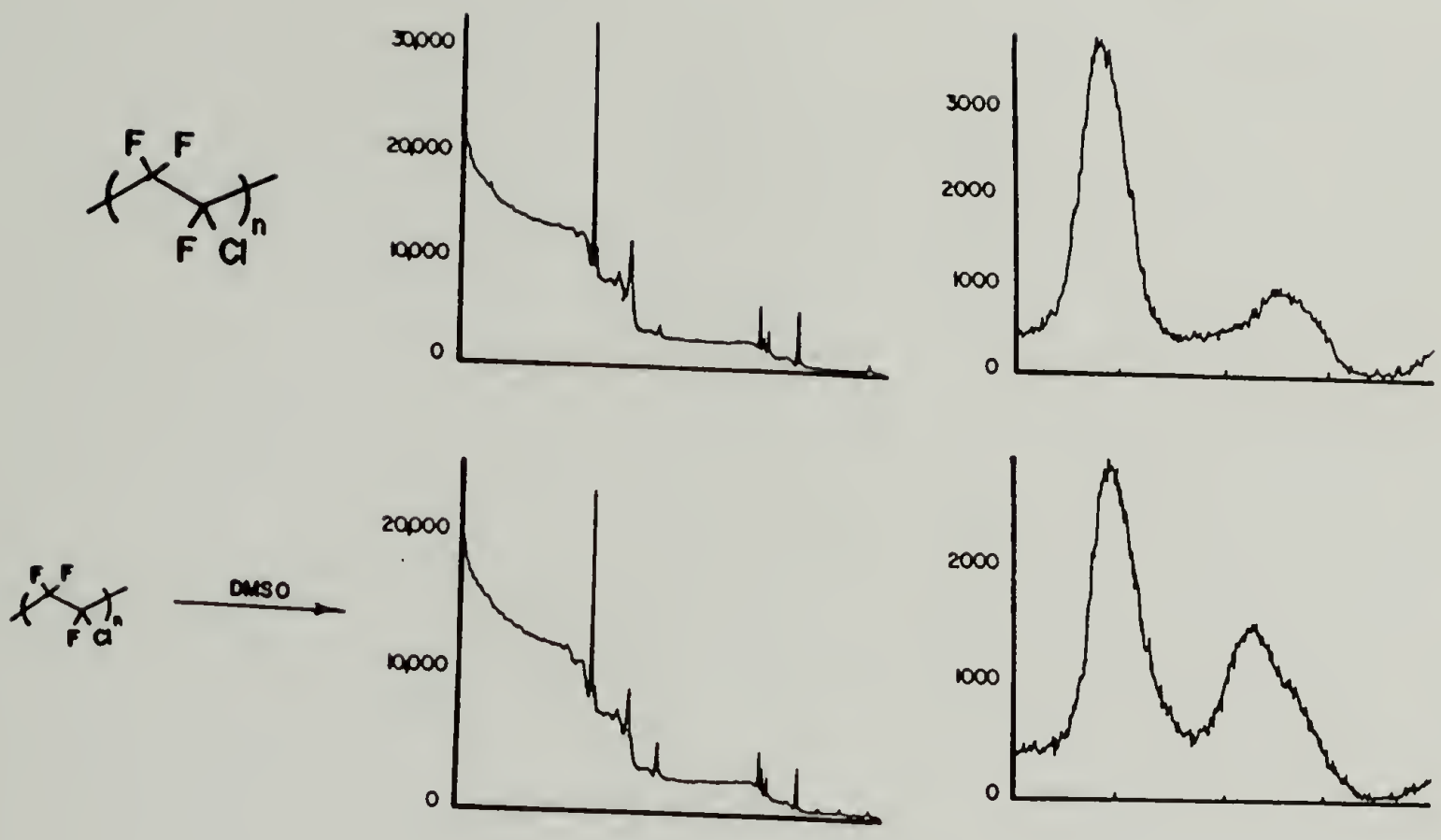

The C_{1s} high resolution spectrum for the base reacted PCTFE film provided lucid information on the nature of the carbon present. The decreased binding energy and lack of fluorine and chlorine found for this sample indicates that a less oxidized (than CF_2) form of carbon existed. A substantial component of this peak must be due to carbon bound to oxygen since the survey spectrum indicated large amounts of oxygen present. Also noteworthy was the small CF_2 peak present from unreacted PCTFE. This suggests that the reaction occurred within the XPS sampling depth or that it is, like the benzoin dianion reduction of PTFE, physically inhomogeneous.

Treatment of PCTFE film with the benzoin dianion solution yielded results similar to those obtained for the reaction in DMSO/base: a surface composed primarily of carbon and oxygen predominated. The C_{1s} high resolution spectrum, however, indicates that all of the CF_2 was depleted in the XPS sampling region. The adventitious fluorine observed in the survey spectrum must be due to fluoroolefin structure present.

ATR-IR spectra substantiated most of the XPS and gravimetric results. Figure A2.3 exhibits spectra obtained on a 45^{o} germanium crystal for **A** PCTFE, **B** reaction of PCTFE with a DMSO solution of potassium t-butoxide , and **C** reaction of PCTFE with the benzoin dianion reducing solution. No changes were observed in the ATR-IR for the reaction of DMSO with PCTFE. Aliphatic C-H stretching (2900-2800 cm^{-1}) and either carbonyl stretching or (fluoroolefin) C=C stretching (1720 cm^{-1}) are apparent in **B**. The spectra obtained for **C** demonstrate the extensive depth of the reaction: PCTFE absorbances are completely absent

Figure A2.3

ATR-IR spectra for reactions of PCTFE films with benzoin dianion and reducing solutions. See text for details.

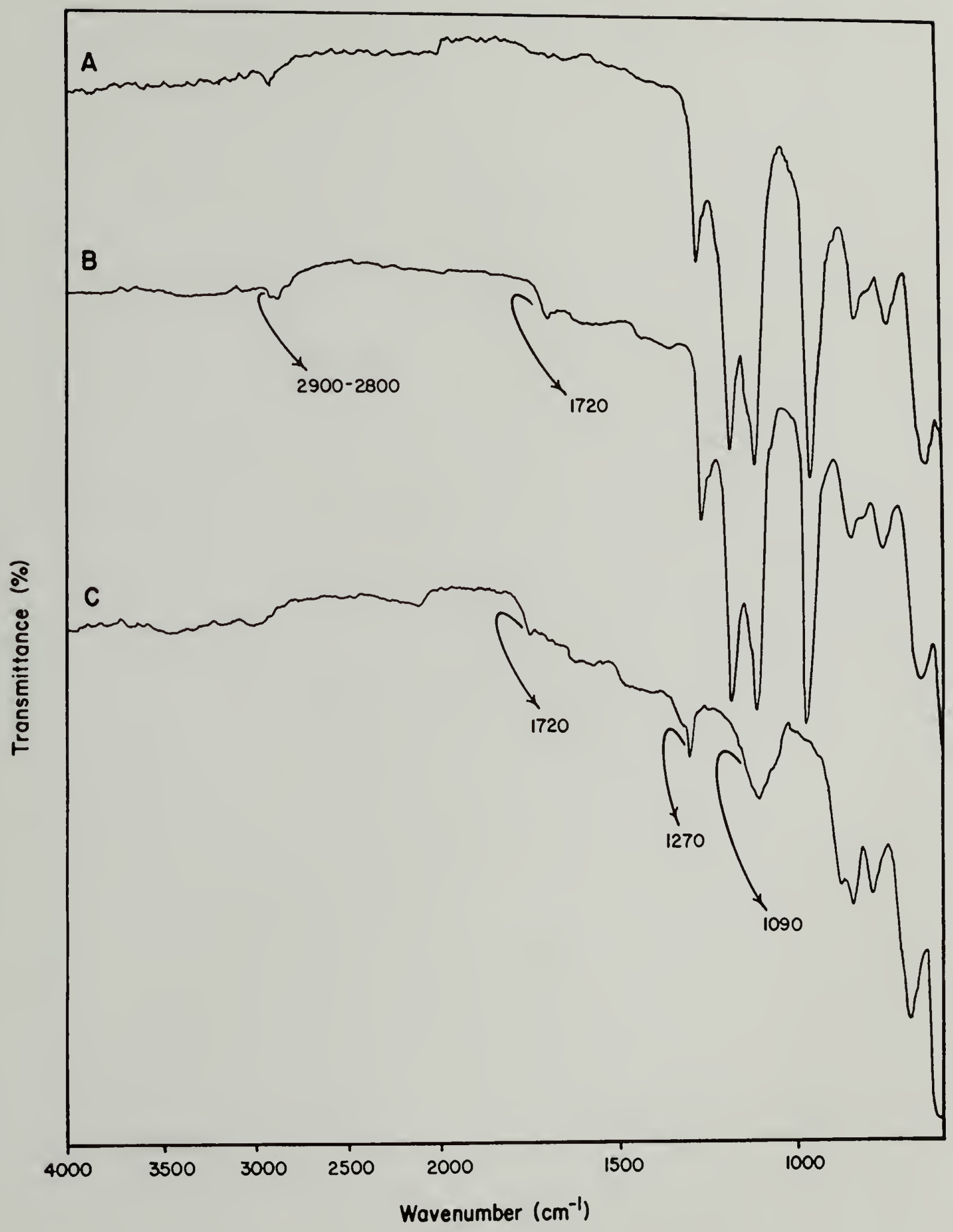
A
B
2900-2800
1720
C
1720
1270
1090
Transmittance (%)
4000
3500
3000
2500
2000
1500
1000
Wavenumber (cm⁻¹)

in the ATR sampling region. Peaks at 1720 cm^{-1} (fluoroolefin C=C stretching and/or carbonyl C=O stretching), 1270 cm^{-1} (C-O-C stretching) and a broad peak at 1090 cm^{-1} (C-O stretching) are consistent with the large amount of oxygen present in the XPS spectrum.

The nature of the reactions occurring in PCTFE under these conditions is difficult to discern. The unexpected reaction of PCTFE with potassium t-butoxide in DMSO has no literature precedence. Although Ashby [8] demonstrated single electron transfer for reaction of lithium t-alkoxide with primary halides, the extension of this chemistry to potassium t-butoxide is questionable.

In conclusion, the reaction of PCTFE with benzoin dianion reducing solution yields a carbon and oxygen containing product quite different from PTFE-C. PCTFE, unlike PTFE reacts with the base/DMSO control solution, providing interesting insight into the reactivity of PCTFE.

References

1. C.A. Costello, T.J. McCarthy, unpublished work, this laboratory.

2. J.A. Huth, N.D. Danielson, Anal. Chem., **54**, 930 (1982)

3. R.W. Siergiej, N.D. Danielson, J. Chromatography Sci., **21**, 362 (1983)

4. R.W. Siergiej, N.D. Danielson, Anal. Chem., **55**, 17 (1983)

5. N.D. Danielson, R.T. Taylor, J.A. Huth, R.W. Siergiej, J.G. Galloway, J.B. Paperman, Ind. Eng. Chem. Prod. Res. Dev., **22**, 303 (1983)

6. A.J. Dias, T.J. McCarthy, Macromolecules, **18**, 1826 (1985)

7. A.J. Dias, T.J. McCarthy, unpublished work, this laboratory.

8. A.E. Ashby, D.H. Bae, W.S. Park, R.N. Depriest, W.Y. Su, Tett. Lett., **25**, (45), 5107 (1984)

Appendix 3

ESCA Data

A list of ESCA data acquired follows. The data are tabulated as follows: 1) esca file number that appears on the disk 2) The relevant notebook reference including page number 3) a short description of the experiment 4) whether the spectrum represents a survey (s) or multiplex (m) scan 5) grazing (g) or normal (n) take-off angle 6) whether or not a high resolution (HRES) spectrum was obtained and 7) the atomic composition for any multiplex scans.

esca file #	notebook reference	description	scan	angle	res	F	O	C	Si	S
esca 001.d		PTFE	s	n						
esca 002.d		PTFE	m	n	HRES					
esca 003.d		PTFE	m	n	HRES					
esca 004.d	CCV 57-1	PTFE-C	s	n						
esca 005.d		PTFE-C	m	n	HRES	12.88	5.26	81.56		
esca 006.d	CCV 57-2	PTFE-C	m	n		11.81	4.88	83.31		
esca 013.d	CCV 59-1	PTFE-C	s	n						
esca 014.d	CCV 59-2	PTFE-C	m	n	HRES	4.29	4.54	89.89	1.30	
esca 015.d	V 61-1	PTFE-sulfur	s	n						
esca 016.d	V 61-2	PTFE-sulfur	m	n	HRES			•		
esca 017.d	V 61-3	PTFE-sulfur	m	n	HRES	•				
esca 018.d	V 61-4	PTFE-sulfur	m	n	HRES					
esca 019.d	V 61-5	PTFE-sulfur	m	n	HRES		•			•
esca 020.d	V 61-6	PTFE-sulfur	m	n	HRES					•
esca 024.d	V 65-1	CS_2 control (Reduced PTFE w/ CS_2 and no hv radiation)								
esca 025.d	V65-2	CS_2 control " "	s	n						
esca 026.d	V65-3	CS_2 control " "	m	n	HRES			•		
esca 027.d	V65-4	CS_2 Control " "	m	n	HRES					
esca 076.d		PTFE control	m	n	HRES	•				•
esca 077.d			s	n						
esca 078.d			m	n						
esca 079.d			m	n						
esca 080.d			m	n		69.39	0.00	30.61		
esca 082.d			s	n						
			m	n		19.73	6.45	73.82	0.00	

esca file #	notebook reference	description	scan	angle	res	F	O	C	Si	S	K2
esca 110.d	V 79-1	thiolacetic acid on rPTFE	s	n							
esca 111.d	V 79-1	thiolacetic acid on rPTFE	m	n		16.96	7.71	66.89	2.70	5.74	
esca 112.d		PTFE control on AIBN/hυ rxn	s	n							
esca 113.d		PTFE control on AIBN/hυ rxn	m	n							
esca 114.d	V 81-1	PTFE control on AIBN/hυ/rxn	m	n	HRES	69.11		30.89			
esca 115.d	V 81-2	thiolacetic acid/ AIBN/hυ on rPTFE	s	n							
esca 117.d	V 81-2	thiolacetic acid/ AIBN/hυ on rPTFE	m	n		18.16	6.65	65.74	3.70	5.74	
esca 118.d	V 81-2	thiolacetic acid/ AIBN/hυ on rPTFE	m	n		37.44		20.43	42.13		
esca 119.d	V 83-1	thiolacetic acid/ thermal/AIBN	s	n							
esca 120.d	V 83-1	thiolacetic acid/ thermal (1000-0)	s	g							
esca 121.d	V 83-1	thiolacetic acid/ thermal 1100-0 survey	s	g							
esca 122.d		thiolacetic acid/ thermal	m	g							
esca 123.d	V 83-1	" AIBN	m	g		15.20	6.15	72.88	2.56	3.21	
esca 124.d	V 83-1	" "	m	n		16.70	2.98	76.84	0.00	3.48	
esca 125.d		PTFE control for thiolacetic acid/Δ	s	n							
esca 127.d	V 83-2	PTFE control for thiolacetic acid/Δ	m	n		69.65	0.00	29.68	0.67	0.00	
esca 4	V 89	PTFE hydrolysis control V 85-1	s	n							
esca 5	V 89	PTFE hydrolysis control V 85-1	m	n		68.72	1.83	29.39			0.07
esca 6	V 89	RPTFE hydrolysis control V 85-1	s	n							
esca 7	V 89	RPTFE hydrolysis control V 85-1	m	n	HRES	16.06	4.19	79.74			
esca.8	V 89	thiolacetic acid,	s	n							

esca file #	notebook reference	description	scan	angle	res	F	O	C	S1	K2	S	Cl	Br
esca 9	V 89	H_2O on rPTFE V 85-1	s	g									
esca 10	V 89	thiolacetic acid, H_2O on rPTFE V 85-1	m	n	HRES	14.92	6.64	73.43		5.01			
esca 11	V 89	thiolacetic acid, H_2O on rPTFE V 85-2	m	g	HRES	19.91	7.23	68.96	0.00	3.89			
esca 14	V 87-1	PTFE control for hyd. rxn (taken all the way thru rxn sequence)	s	n									
esca 15	V 87-1	" "	m	n									
esca 18	V 87-1	RPTFE control for hydrolysis KOH/PTC rxn (taken thru hydrolysis step)	s	n		70.61	2.16	27.23		0.00			
esca 19	V 87-1	" "	m	n									
esca 20	V 87-1	RPTFE/thiolacetic acid/control (for s.o. ratio) for hyd. rxn	s	n		12.34	7.76	76.50	1.96		1.44		
esca 21	V 87-1	" "	m	n									
esca 22	V 87-1	Hydrolysis rxn on thiolacetic acid treated reduced PTFE	s	n		12.77	6.38	76.45	2.53		1.87		
esca 23	V 87-1	"	m	n									
esca 38	V 95-2	Br_2/CCl_4 treated rPTFE	s	n		8.24	10.23	74.55	4.48		2.50		
esca 39	V 95-2	" "	m	n	HRES	29.95	0.95	61.57				0.46	7.44
esca 40	V 95-1	PTFE control for Br_2/CCl_4	s	n									
esca 42	V 95-1	" "	m	n									
esca 49	V 97-2	$Br2_2/CCl_4$/NaSH/DM80 on rPTFE	s	n		68.17	0.50	31.28				0.03	0.00
esca 50	V 97-2	" "	m	n									
esca 51	V 97-3	PTFE control for Br_2 /CCl_4/NaSH/DM80 on rPTFE	s	n	HRES	31.07	4.15	63.13		1.65			0.00
esca 52	V 97-3	" "	m	n									
esca 56		Br_2/CCl_4/NaSH/DM80 on rPTFE 1000-0	s	n		68.70	0.83	30.44		0.03			
esca 57		" 1200-800	s	n									
esca 58	CCV 99-4	" PTC rxn on PTFE-Br	m	n									
esca 59		Brominated control film 1000-0	s	n		18.47	9.32	65.18		2.80			4.20
esca 60	CCV 99-3	" "	m	n	HRES	21.73	9.22	58.81					10.24
esca 63		PTFE control for PTC rxn (esca 50)	s	n									
esca 64		" "	m	n									
esca 65		PTFE control for Br_2/CCl_4 for (ESCA 50)	s	n		68.71	1.14	29.92		0.22			
esca 66		" "	m	n									
esca 75	V 101-2	RPTFE/Br_2/NaSH/PPTC	s	n		69.33	0.27	30.40					0.00

esca file #	notebook reference	description	scan	angle	res	F	O	C	Si	S	Br
esca 76	V 101-2	RPTFE Br_2/CCl_4/NaSH/PPTC	m	n	HRES	18.54	5.81	67.78		2.66	5.20
esca 77	V 101-1	RPTFE Br_2 control for esca 75 and 76	s	n							
esca 78	V 101-1	"	m	n	HRES	23.95	3.44	61.20			11.41
esca 92		PTFE control for Br_2 then NaSH (see esca 75-76)	s	n							
esca 93		" "	m	n		65.42	1.24	33.14		0.14	0.06
esca 112	V 107-1	NaSH/NPTC/35°C	s	n							
esca 113	V 107-1	" "	m	n		7.01	7.86	78.70		4.17	2.21
esca 114	V 107-2	NaSH/reduced PTFE control	s	n							
esca 115	V 107-2	" NaSH on a RPTFE film	m	n		10.00	12.41	75.34		1.56	0.00
esca 116	V 107-3	PTFE control for esca 112,114	s	n							
esca 117	V 107-3	" "	m	n		68.89	2.16	28.43		0.52	0.00
esca 118	V 109-111	NaSH/NPTC/35°C repro of esca 112	s	n							
esca 119	V 109-111	" "	m	n		9.96	6.68	77.94		3.58	1.84
esca 127	V 109-111	NaSH/NPTC/80°C	s	n							
esca 128	V 109-111	" "	m	n		9.95	11.64	72.52		4.82	1.07
esca 129	V 109-111	Br_2 control for NaSH/NPTC/80°C	s	n							
esca 130	V 109-111	" "	m	n		20.58	3.65	61.35		0.03	14.38
esca 131	V 109-111	Br_2 control for NaSH/NPTC/0° + 26°C	s	n							
esca 132	V 109-111	" "	m	n		16.97	4.67	63.14		0.01	15.21
esca 133	V 109-111	NaSH/NPTC/0°C	s	n							
esca 134	V 109-111	NaSH/NPTC/0°C	m	n		19.46	6.00	63.04		2.12	9.39
esca 135	V 109-111	NaSH/NPTC/26°C	s	n							
esca 136	V 109-111	"	m	n		14.19	6.27	73.25		3.87	2.42
esca 137	B 109-111	PTFE control for NaSH/NPTC/26°C	s	n							
esca 138	V 109-111	" "	m	n		66.52	1.14	32.10		0.25	0.00

esca file #	notebook reference	description	scan	angle	res	F	O	C	Si	S	Br	Cl
esca 139	V 109-111	PTFE control for NaSH/NPTC/0°C	s	n								
esca 140	V 109-111	" "	m	n		64.91	0.59	34.47		0.03	0.00	
esca 141	V 109-111	PTFE control for NaSH/NPTC 80°C	s	n								
esca 142	V 109-111	" "	m	n		68.45	1.04	30.39		0.12	0.00	
esca 183	V 115	Cl_2 control for NaSH/NPTC (Rm temp)	s	n								
esca 184	" "	" "	m	n		18.47	5.15	56.11		0.33		19.93
esca 185	" "	" "	m	n	HRES			*				
esca 186	V 115	PTFE control for Cl_2 /NaSH/NPTC (Rm temp)	a	n								
esca 187	" "	" "	m	n		68.49	1.57	29.56		0.22		0.15
esca 188	V 115	NaSH/NPTC Rm temp/2 hrs	s	n								
esca 189	" "	" "	m	n		7.25	8.85	63.94		1.45		18.55
esca 190	" "	NaSH/NPTC (Rm temp) 2 hrs	m	n	HRES			*				
esca 191	" "	" "	s	g								
esca 192	" "	" "	m	g		10.35	8.02	65.00		1.63		15.00
esca 193	" "	" "	m	g	HRES			*				
esca 213	V 115-1	NaSH/Cl_2/NPTC 80°C	s	n								
esca 214	" "	" "	m	n		8.34	6.74	76.61		4.57		3.73
esca 215	" "	" "	m	n	HRES			*				
esca 216	" "	" "	s	g								
esca 217	" "	" "	m	g		10.09	10.00	78.17		3.96		2.78
esca 218	" "	" "	m	g	HRES	*		*				*
esca 219	V 115-2	Cl_2 control for NaSH/NPTC 80°C	s	n								
esca 220	" "	" "	m	n		5.10	5.92	66.26		0.00		22.72
esca 221	" "	" "	m	n	HRES			*				
esca 222	V 115	PTFE control for NaSH/Cl_2/NPTC 80°C	s	n								
esca 223	" "	" "	m	g		68.13	1.63	29.71		0.42		0.11

esca file #	notebook reference	description	scan	angle	res	F	O	C	Si	S	Br	Cl	N
esca 273	V 117	Set #1 Repro Cl_2 control for NaSH/80°C/NPTC	s	n									
esca 274	V 117-1	" "	m	n									
esca 275	" "	" "	m	n		17.79	2.87	60.59		0.07		18.78	
esca 276	" "	Set #1 NaSH/NPTC 80°C Repro	s	g	HRES			*					
esca 277	" "	" "	m	g		6.78	9.60	75.56		3.79		4.27	
esca 278	V 117-2	Repro of NaSH/NPTC 80°C	s	n									
esca 279	V 117-2	" "	m	n		9.05	7.49	75.29		3.50		4.68	
esca 280	" "	" "	m	n	HRES			*					
esca 281	V 117	PTFE control	s	n									
esca 282	" "	" "	m	n		68.47	1.21	30.22		0.09		0.01	
esca 335	V117/V133	NaSH/initial tagging experiment w/DNBC	s	g									
esca 336	" "	" "	m	s		34.55	8.34	32.57		2.09		1.96	0.69
esca 337	" "	" "	s	n									
esca 338	" "	" "	m	n		32.57	5.38	57.41		2.06		1.94	0.63
esca 352	" "	KSH/NPTC 80°C	s	g									
esca 353	" "	" "	m	g		9.78	15.11	59.68	3.25	1.98		6.19	4.01
esca 354	" "	" "	s	n									
esca 355	" "	" "	m	n		13.60	13.42	58.69	3.28	1.81		5.79	3.41
esca 384	V 127	NaSH/NPTC/24 hr/rm. temp. (long time rxn)	s	g									
esca 385	" "	" "	m	g		10.18	7.35	66.18	1.85	2.37		12.08	
esca 386	" "	" "	s	n									
esca 387	" "	" "	m	n		15.25	5.28	64.25	0.54	1.95		12.74	
esca 388	" "	" "	m	n	HRES			*					
esca 389	" "	Cl_2 control for NaSH 24 hr rxn	s	n									
esca 390	" "	" "	m	n		20.84	4.84	55.73	1.77	0.02		16.80	
esca 391	" "	" "	m	n	HRES			*					

esca file #	notebook reference	description	scan	angle	res	F	O	C	Si	S	Br	Cl	N
esca 392	" "	PTFE control 1100-0	s	n									
esca 393	" "	" "	m	n		68.29	0.95	29.77	0.75	0.24		0.00	
esca 394	V 129 (top)	SCl_2/0°C/undistilled	s	n									
esca 395	" "	" "	m	n		12.43	6.79	54.12	2.36	0.16		24.15	
esca 396	" "	" "	m	n	HRES			*					
esca 397	" "	PTFE control for SCl_2/0°C	s	n									
esca 398	" "	" "	m	n		68.43	0.50	30.81	0.19	0.00		0.07	
esca 399	V 129 (bottom)	SCl_2/-78°C distilled	s	n									
esca 400	" "	" "	m	n		15.30	6.53	57.38	2.92	0.75		17.12	
esca 401	" "	" "	m	n	HRES			*					
esca 402	V 131 (top)	SCl_2/-78-0°C w/CO (distilled)	s	n									
esca 403	" "	" "	m	n		15.66	4.47	59.23	2.12	1.59		16.93	
esca 405	" "	PTFE control for SCl_2/-78-0°C/w/CO	s	n									
esca 406	" "	" "	m	n		68.33	0.41	31.13	0.06	0.01		0.06	
esca 407	V 131 (bottom)	SCl_2/PCl3/CO/0°C	s	g									
esca 408	" "	" "	m	g		13.10	9.48	61.19	3.57	2.69		9.24	
esca 409	" "	" "	s	n									
esca 410	" "	" "	m	n		22.87	6.12	59.63	2.44	1.78		7.15	
esca 411	" "	" "	m	n		23.77	6.29	60.21		2.37		7.37	
esca 412	" "	SCl_2/PCl3/CO/-78°C	s	n									
esca 413	" "	" "	m	n		3.24	13.71	72.56		1.59		8.89	
esca 415	" "	" "	m	n		5.16	13.50	64.49	5.54	2.01		9.30	
esca 416	" "	PTFE control rxn for -78°C rxn	s	n									
esca 417	" "	" "	m	n		68.65	0.69	30.41	0.15	0.02		0.09	
esca 418	" "	PTFE control for 0°C rxn	s	n									
esca 419	" "	" "	m	n		67.92	1.44	29.86	0.49	0.25		0.03	

esca file #	notebook reference	description	scan	angle	res	F	O	C	Si	N
esca.g255	VI 83-2	H_3C COOH/AIBN/0 100°C	s	g						
esca.g256	" "	" "								
esca.g257	" "	" "	m	g		7.10	6.77	82.46	0.15	3.52
esca.g258	" "	" "	m	g	HRES			•		
esca.g259	" "	" "	s	n						
esca.g260	" "	" "	m	n		8.08	5.67	82.53	0.02	3.69
esca.g283	VI 83-3	Rm temp TCNE on PTFE-6	m	n	HRES			•		
esca.g284	" "	" "	s	g						
esca.g285	" "	" "	m	g		8.66	10.80	70.80	0.43	9.30
esca.g286	" "	" "	m	g	HRES			•		
esca.g287	" "	" "	s	n						
esca.g288	" "	" "	m	n		10.14	9.44	72.04	0.41	7.98
esca.g289	" "	" "	m	n	HRES			•		
esca.g290	VI 83-2	COI rxn on H_3C COOH/AIBN 100°C	m	g		8.92	01.63	72.18	1.08	7.20
esca.g291	" "	" "	s	g						
esca.g292	" "	" "	m	g		10.01	7.86	77.78	0.23	4.12
esca.g293	" "	" "	s	n						
esca.g294	" "	" "	m	n		10.01	6.73	78.60	0.53	4.14.
esca.g307	VI 85-2	RPTFE w/malic acid/0	m	n	HRES			•		
esca.g308	" "	" "	s	g						
esca.g309	" "	" "	m	g	6.03	10.98	81.81	1.19		
esca.g310	" "	" "	m	g	HRES		•			
esca.g311	" "	" "	s	n						
esca.g312	" "	" "	m	n		7.86	9.11	81.81	1.22	
esca.g313	VI 85-1	repro of 83-3	m	n	HRES		•			
esca.g314	" "	" "	s	g						
			m	g		10.14	9.50	74.80	0.72	4.85

esca file #	notebook reference	description	scan	angle	res	F	O	C	Si	N	Cl
esca.g367	VI87-2	MA/hυ/AIBN/H_2O/TFAA	s	n							
esca.g368	" "	" "									
esca.g369	" "	" "	m	n		8.54	I1.71	79.22	0.32	0.00	
esca.g370	VI 87-1	H_2O/TFAA on esca.g339	m	n	HRES			•			
esca.g371	" "	" "	s	g							
esca.g372	" "	" "	m	g		11.34	20.71	63.90	I.25	2.81	
esca.g373	" "	" "	m	g	HRES		•				
esca.g374	" "	" "	s	n							
esca.g375	" "	" "	m	n		8.80	5.52	73.12	0.56	1.99	
esca.g376	VI 83-3	H_2O/TFAA on TCNE surface	m	n	HRES		•				
esca.g377	" "	" "	s	g							
esca.g378	"	" "	m	g		61.23	13.04	65.96	1.34	3.42	
esca.g379	" "	" "	s	n							
esca.g380	" "	" "	m	n		14.96	10.56	69.13	6.15	5.20	
esca.g406	VI87-2	COI tagging RXN on PTFE COOH (?)	m	n	HRES			•			
esca.g407	" "	" "	s	g							
esca.g408	" "	" "	m	g		6.82	14.75	73.39	1.06	3.97	
esca.g409	" "	" "	s	n							
esca.g410	" "	" "	m	n		5.17	14.82	74.90	0.42	4.39	
esca.g411	VI 872	PTFE control	m	n	HRES			•			
esca.g412	" "	" "	s	g							
esca.g413	" "	" "	m	g		70.77	1.16	27.82	0.25	0.00	
esca.g414	" "	" "	s	n							
esca.g429	VI 91-1	Br_2/Cl_4 treated RPTFE	m	n		70.41	1.14	28.04	0.41	0.00	
esca.g430	" "	" "	s	g							
			m	g		8.19	8.42	61.17	0.00		22.22

esca file #	notebook reference	description	scan	angle	res	F	O	C	Si	S	Bn	Cl	N
esca 428	V1 31 bottom	$SCl_2/PCl_3/CO/40°C$	s	n									
esca 429	" "		m	n									
esca 430	" "	" "	m	n	NRES		16.28	6.14	57.14	3.00	3.64		13.79
esca 431	" "	" "	m	n									
esca 432	" "	PTFE control for $SCl_2/PCl^3/CO/40°C$	s	n						21.80		78.20	
esca 433	" "	" "	m	n		69.26	0.47	30.47	Si	0.00		0.00	
esca 454	V 135	3.5 DNC/pyr/75°C tagging exp.	s	n									
esca 455	" "	" "	m	n		6.18	12.61	69.87	1.59	2.72		3.01	4.61
esca456	" "	" "	m	n	HRES	8.50	11.64	72.25		3.15		1.18	3.27
esca 457	" "	Cl_2 control for 3.5 DNC/pyr 75°C	s	n									
esca 458	" "	" "	m	n		6.71	10.95	65.58	1.27	1.09		10.81	3.59
esca 459	" "	PTFE control for 3.5 DNC/pyr 75°C	s	n									
esca 460	" "	" "	m	n		67.57	1.23	30.70	0.26	0.00		0.04	0.20
esca 462	V 135	SH film for tagging				22.72	0.72	65.35	0.50	3.77		1.90	
esca 463		PTFE extracted film	s	n									
esca 464		" "	m	n		68.59	0.73	29.92	0.35	0.16		0.20	0.00
esca 465	V 137	RPTFE/CH_3-C-SH/AIBN	s	n									
esca 466	V 137	RPTFE/CH_3-C-SH/AIBN	s	n		8.24	8.40	77.15	1.23	4.99			
esca 467	" "	" "	m	n	HRES								
esca 468	" "	RPTFE starting material for esca 465	s	n									
esca469	" "	" "	m	n		10.23	4.13	85.57	0.28	0.00			
esca 470	" "	" "	m	n	HRES			*					
esca 471	" "	MeLi/Rm temp/0.5 h	s	n									
esca 472	" "	" "	m	n		11.71	6.94	78.67	1.18	1.50			
esca 473	" "	" "	m	n				67.64		32.36			
esca 474	" "	" "	m	n	HRES								
esca 475	" "	" "	m	n		90.36				9.64			

esca file #	notebook reference	description	scan	angle	res	F	O	C	Si	S	Cl	N	B
esca 476	" "	PTFE control MeLi/Rm temp/0.5 hr	s	n									
esca 477	" "	" "	m	n		68.29	0.42	31.28	0.00	0.00			
esca 478	V 139	Deep RPTFE heptane washed	s	n									
esca 479	" "	" "	m	n		9.04	4.70	85.83	0.07	0.00	0.37		
esca 480	" "	" "	m	n	HRES			*					
esca 481	" "	" "	m	n		96.60				3.40			
esca 486	V 139	Cl_2 deep reduced PTFE	s	n									
esca 487	" "	" "	m	n		5.17	2.35	59.92	0.23	0.12	32.21		
esca 488	" "	" "	m	n	HRES			*					
esca 489	" "	" "	m	n		100.0				0			
esca 501	V 139	NaSH rxn on deep red PTFE (3M)	s	n									
esca 502	" "	" "	m	n		4.64	8.26	72.41	1.32	5.08	2.10	1.19	
esca 503	" "	" "	m	n	HRES			*					
esca 504	" "	" "	m	n		53.53				46.47			
esca 507	" "	HFBC/pyr/1/hr/rm temp on SH^orxn	s	n									
esca 508	" "	" "	m	n		12.83	7.93	70.69	1.11	4.33	2.43	0.68	
esca 509	" "	" "	m	n	HRES			*					
esca 510	" "	" "	m	n		76.77				23.23			
esca 511	" "	PTFE control for 507	s	n									
esca 512	" "	" "	m	n		67.69	1.19	30.36	0.50	0.09	0.17	0.00	
esca 3	VI-9(top)	$BH_3/NaOH/H_2O_2$ on RPTFE	s	n									
esca 4	" "	" "	s	n									
esca 5	" "	" " U-1100	s	n									
esca 6	" "	" "	m	n		21.06	16.67	60.42					0.78
esca 7	" "	" "	m	n	HRES			*					

esca file #	notebook reference	description	scan	angle	res	F	O	C	Si	Cl	Na	B	
esca 8	VI 9 (top)	PTFE-OH DNBC tagged 1100-0	s	n									
esca 9	" "	" "	m	n									
esca.e10	VI 9 (bottom)	1100-0 BH_3/NaOH/H_2O_2 on RPTFE (12M)/HCl wash	s	n									
esca.e11	" "	1000-0 "	s	n									
esca.e12	" "	" "	m	n									
esca.e13	" "	" "	m	n	HRES			4.63	21.20 *	72.57	0.97		0.00
esca.e14	" "	" " 1000-0	s	g									
esca.e15	" "	" "	m	g									
esca.e27	V 9	12 hr RPTFE used in esca.e 10-15	s	n		4.84		20.27	71.93	0.19		0.48	2.29
esca.e28	" "	" "	m	n									
esca.e29	" "	" "	m	n		3.20		4.51	91.03	1.26			
esca.e30	" "	" "	m	n	HRES				*				
esca.e31	" "	" "	m	n	HRES				*				
esca.e32	V 9	TFAA tagged PTFE-OH $MeCl_2$/heptane wash	s	g	HRES				*				
esca.e33	" "	" "	m	g									
esca.e34	" "	" "	m	g		28.01		18.28	52.16	1.21	0.33		
esca.e35	" "	" "	s	n	HRES				*				
esca.e36	" "	" "	m	n									
esca.e37	" "	" "	m	n		25.76		17.14	56.07	1.03	0.01		
esca.e38	V 9	RPTFE/H_2O_2/NaOH heptane wash (for TFAA tagging)	s	g	HRES				*				
esca.e39	" "	" "	m	g									
esca.e40	" "	" "	m	g		3.40		12.92	81.14	2.55		0.00	
esca.e41	" "	" "	s	n	HRES				*				
esca.e42	" "	" "	m	n									
		*				1.28		11.65	85.71	1.37		0.00	
esca.e53		BH_3.THF on RPTFE	s										

esca file #	notebook reference	description	scan	angle	res	F	O	C	Si	Na	B	Cl
esca.e54		BH_3 on RPTFE	m	g		14.43	16.58	62.78	0.00		6.71	
esca.e55		" "	s	n								
esca.e56		" "	m	n		18.90	13.65	61.10	0.26		6.08	
esca.e57		" "	m	n	HRES			*				
esca.e58		RPTFE control for esca.e53 (pumped 4 days)	s	n								
esca.e59		" "	m	n		20.84	3.19	73.51	1.47		1.00	
esca.e60		" "	m	n	HRES			*				
esca.e61	VI 9	RPTFE/H_2O_2/NaOH tagged (see esca.e38)	s	g								
esca.e62	" "	" "	m	n		21.22	20.86	57.68	1.04			0.00
esca.e63	" "	" "	m	g	HRES			*				
esca.e64	" "	" "	s	n								
esca.e65	" "	" "	m	n	HRES			*				
esca.e66	VI 15	deep RPTFE for tagging study	s	n								
esca.e67	" "	" "	m	g		4.66	5.95	89.20	0.18			
esca.e68	" "	" "	m	g	HRES			*				
esca.e69	" "	" "	s	n								
esca.e70	" "	" "	m	n		5.42	5.12	88.69	0.77			
esca.e71	" "	" "	m	n	HRES	*		*				
esca.e72	VI 15	BH_3/H_2O_2/NaOH treated RPTFE	s	g								
esca.e73	" "	" "	m	n		6.47	20.45	69.43	3.65			
esca.e74	" "	" "	m	g	HRES	*		*				
esca.e75	" "	" "	s	n								
esca.e76	" "	" "	m	n		9.04	19.81	69.12	2.03			
esca.e77	" "	" "	m	n	HRES	*		*				
esca.e86	VI 15-17	deep RPT6FE tagged w/TFAA (pumped 2 days)	s	g								
esca.e87	" "	" "	m	g		9.01	7.49	81.80	1.70			

esca file #	notebook reference	description	scan	angle	res	F	O	C	Si	K	Na
esca.e88	VI15-17	Deep RPTFE tagged w/TFAA pumped 2 days	m	g	HRES	*		*			
esca.e89	" "	" "	s	n							
esca.e90	" "	" "	m	n							
esca.e91	" "	" "	m	n	HRES	9.52 *	6.23	83.21 *	1.07		
esca.e92	V15	TFAA tagged surface (made on pg 17)	s	g							
esca.e93	" "	" "									
esca.e94	" "	" "	m	g							
esca.e95	" "	" "	m	g	HRES	21.81 *	19.77	51.40 *	2.01	0.00	
esca.e96	" "	" "	s	n							
esca.e97	" "	" "	m	n							
esca.e122	VI 20	10 minute RPTFE (HFWashed; 1 day pumped	m	n	HRES	22.99 *	18.08	57.11 *	1.69	0.13	
esca.e123	" "	" "	s	g							
esca.e124	" "	" "	m	g							
esca.e125	" "	" "	m	g	HRES	13.95 *	8.93 *	74.81 *	2.30		0.00
esca.e126	" "		s	n							
esca.e127	" "		m	n							
esca.e134	VI 25	Oxidized(10 min) RPTFE $KClO_3/H_2SO_4$ from esca 122	m	n	HRES	23.86 *	5.88 *	68.94 *	1.32		0.00
esca.e135	" "	" "	s	g							
esca.e137	" "	" "									
esca.e137	" "	" "	m	g							
esca.e138	" "	" "	m	g	HRES	67.74 *	1.74	30.52 *	0.00		
esca.e139	" "	" "	s	n							
esca.e140			m	n							
esca.e141	" "	24 hr RPTFE(pumped 24 hrs)	m	n	HRES	69.42 *	29.67	0.91 *	0.00		
esca.e142	" "	" "	s	g							
esca.e143	" "	" "	m	g							
			m	g	HRES	6.40 *	5.88 *	86.86 *	1.07		
			a	n							

esca file #	notebook reference	description	scan	angle	res	F	O	C	Si	K	Na
esca.e144		24 hr RPTFE (pumped 24 hr)	m	n							
esca.e145		" "	m	n	HRES	6.71 *	4.10 *	88.67 *	0.51		
esca.e155		2 hr RPTFE	s	g							
esca.e156		" "	m	g							
esca.e157		" "	m	g	HRES	3.24 *	6.31 *	88.62 *	1.83	0.00	
esca.e158		" "	s	n							
esca.e159		" "	m	n							
esca.e160		" "	m	n	HRES	7.57 *	3.32 *	88.34 *	0.71	0.06	
esca.e161	VI 25	NaOCl oxidized RPTFE (24 hr red)	s	n							
esca.e162	" "	" "	m	n							
esca.e163	" "	" "	m	n	HRES	61.67 *	2.07 *	36.26 *	0.00		0.00
esca.e247	VI 25	Air oxidized (2 weeks) RPTFE (6 nU	s	g							
esca.e248	" "	" "	m	g							
esca.e249	" "	" "	m	g	HRES	4.17	26.90	68.31	0.62		
esca.e250	" "	" "	s	n							
esca.e251	" "	" "	m	n							
esca.e252	" "	" "	m	n	HRES	2.51	28.17	68.91	0.42		
esca.e257	VI 25	6 hr RPTFE for air oxidation exp.	s	n							
esca.e258	" "	" "	m	n							
esca.e259	" "	" "	m	n	HRES	4.25 *	4.45	90.79 *	0.51		
esca.e276	VI 35	MA rxn w/15 minute RPTFE (Bad film)	s	g							
esca.e277	" "	" "	m	g							
esca.e278	" "	" "	m	g	HRES	14.59 *	17.25 *	67.56	0.06		
esca.e279	" "	" "	s	n							
esca.e280	" "	" "	m	n							
esca.e281	" "	" "	m	n	HRES	28.30	10.46 *	60.63 *	0.06		
esca.e282	" "	" "	m	g	HRES		*	*			

esca file #	notebook reference	description	scan	angle	res	F	O	C	Si	Na	Cl	B
esca.e283		hydrolysis rxn on MA rxn on RPTFE	s	g								
esca.e284		" "										
esca.e285		" "	m	g		8.04	20.96	69.85	1.15			
esca.e286		" "	m	g	HRES		*	*				
esca.e287		" "	s	n								
esca.e288		" "	m	n		14.45	15.58	69.75	0.21			
esca.e289		RPTFE control (15 minute) for rxns	m	n	HRES		*	*				
esca.e290		" "	s	g								
esca.e291		" "	m	g		6.22	8.31	84.26	1.20			
esca.e292		" "	s	n								
esca.e303	VI 39	24 hr RPTFE for C-OH tagging exp.	m	n		11.61	4.21	82.96	1.21			
esca.e304	" "	" "	s	g								
esca.e305	" "	" "	m	g		8.26	6.14	89.58	1.03			
esca.e306	" "	" "	m	g	HRES			*				
esca.e307	" "	" "	s	n								
esca.e308	" "	" "	m	n		3.48	4.25	91.27	1.00			
esca.e309	VI 39	RPTFE (24 hr) $BH_3/H_2O_2/NaOH$	m	n	HRES			*				
esca.e310	" "	" "	s	g								
esca.e311	" "	" "	m	g		3.25	23.40	72.49	0.55	0.00	0.42	
esca.e312	" "	" "	m	g	HRES			*				
esca.e313	" "	" " 1200-900	s	n								
esca.e314	" "	" "	s	n								
esca.e315	" "	" "	s	g								
esca.e316	" "	" "	m	n		4.11	22.24	72.08	0.63	0.14	0.79	
esca.e317	" "	" "	m	n	HRES			*				
esca.e318	" "	" "	m	n		5.11	22.11	72.30	0.23	0.23		
			m	n		5.12	21.74	72.38	0.67	0.09	0.00	

esca file #	notebook reference	description	scan	angle	res	F	O	C	Si	Na	Cl	N
esca.e337	VI 39	C_4 F70 Cl tagged surface from .e300-.e318	s	g								
esca.e338	" "	" "										
esca.e339	" "	" "	m	g		32.18	15.58	51.56	0.41	0.07		
esca.e340	" "	" "	m	g	HRES		*	*				
esca.e341	" "	" "	s	n								
esca.e342	" "	" "	m	n		23.70	17.19	58.82	0.29	0.00		
esca.f22	VI 39	MA RPTFE (24 hr) control	m	n	HRES			*				
esca.f23	" "	" "	s	g								
esca.f24	" "	" "	m	g		4.37	11.23	84.38				
esca.f25	" "	" "	m	g	HRES			*				
esca.f26	" "	" "1100-0	s	n								
esca.f27	" "	" "	s	n								
esca.f28	" "	" "	m	n		3.54	5.67	90.79				
esca.f29	VI 39	RPTFE (15 min) for isocyanate tagging exp.	m	n	HRES			*				
esca.f30	" "	" "	s	g								
esca.f31	" "	" "	m	g		4.53	9.79	84.59	1.09			
esca.f32	" "	" "	m	g	HRES			*				
esca.f33	" "	" "	s	n								
esca.f34	" "	" "	m	n		4.33	6.51	88.13	0.37			
esca.f35	VI 39	$BH_3/H_2O_2/NaOH$ on esca.f29 (isocyanate tag. exp.)	m	n	HRES			*				
esca.f37	" "	" "	s	g								
esca.f38	" "	" "	m	n		8.02	24.20	65.90	1.28	0.00	0.39	0.21
esca.f39	" "	" "	m	g	HRES			*				
esca.f40	" "	" "	s	n								
esca.f41	" "	" "	m	n		9.90	20.81	67.81	0.45	0.09	0.08	0.86
			m	n	HRES							

esca file #	notebook reference	description	scan	angle	res	F	O	C	Si	N	Cl	Na
esca.f45	V 39	isocyanate tagged OH surface	s	g								
esca.f46	" "	" "										
esca.f47	" "	" "	m	g		11.12	20.82	53.26	1.30	5.21	8.28	
esca.f48	" "	" "	m	g	HRES			*				
esca.f49	" "	" "	m	g		15.43	20.11	50.66	0.90	4.78	4.65	?3.47
esca.f50	" "	" "	s	g								
esca.f51	" "	" "	m	n		17.24	18.74	53.85	1.40	4.42	4.35	
esca.f95	V1 43	DCP hydrozine tag on $BH_3/NaOH/H_2O$ on 15 min (control) RPTFE	m	n	HRES			*				
			s	g								
esca.f96	" "	" "										
esca.f97	" "	" "	s	g		6.04	33.89	54.32	1.99	1.03	2.46	0.28
esca.f98	" "	" "	m	g	HRES			*				
esca.f99	" "	" "	s	n								
esca.f100	" "	" "	m	n		9.09	34.49	53.03	1.27	0.00	2.09	0.04
esca.f101	V1 43	2.5 DCPH tagged PTFE-OH	m	n	HRES			*				
esca.f102	" "	" "	s	g								
esca.f103	" "	" "	m	g		42.71	8.35	46.56	1.35	0.65	0.38	0.00
esca.f104	" "	" "	m	n	HRES			*				
esca.f105	" "	" "	s	n								
esca.f106	" "	" "	m	n		55.36	4.28	37.32	1.47	1.28	0.29	0.00
esca.f149	V1 35	MA rxn with RPTFE	m	n	HRES							
esca.f150	" "	" "	s	g	HRES							
esca.f151	" "	" "	m	n		3.91	24.30	70.68	1.11			
esca.f152	" "	" "	m	g	HRES		*					
esca.f153	" "	" "	s	n								
esca.f154	" "	" "	m	n		3.25	23.66	72.49	0.60			
			m	n	HRES							

esca file #	notebook reference	description	scan	angle	res	F	O	C	Si	N	1	S
esca.f155		$H_2SO_4/KC1O_3$ oxidized/extracted (THF) PTFE	s	g								
esca.f156		" "	m	g		67.12	1.12	31.75	0.00			
esca.f157		" "	m	n		68.59	1.03	30.38	0.00			
esca.f158		" "	m	n	HRES			*				
esca.f186	V1 35	P1A tag on esca.f149 NH_2 -1	s	g								
esca.f187	" "	" "	m	g			4.70	23.14	71.22	0.45	0.00	0.49
esca.f188	" "	" "	m	g	HRES			*				
esca.f189	" "	" "	s	n								
esca.f190	" "	" "	m	n		3.00	21.13	73.39	0.97	0.91	0.58	
esca.f191	V1 45	H_2SO_4/HCOOH on 12 hr RPTFE	s	g								
esca.f192	" "	" "	m	g		1.98	15.14	79.84	1.28			1.76
esca.f193	" "	" "	m	g	HRES			*				
esca.f194	" "	" "	s	n								
esca.f195	" "	" "	m	n		2.10	12.33	82.47	1.44			1.66
esca.f196	" "	" "	m	n	HRES							
esca.f258	V1 51	Rxn of 12 hr red PTFE w/MAhu/A1BN	s	g								
esca.f259	" "	" "	m	g		3.40	19.02	74.84	0.10	2.04		
esca.f260	" "	" "	m	g	HRES			*				
esca.f261	" "	" "	s	n								
esca.f262	" "	" "	m	n		3.14	16.37	78.37	78.24	0.76	1.51	
esca.f263	" "	" "	m	n	HRES			*				
esca.f264	V1 45	Rxn of 12 hr RPTFE w/HCOOH/H_2SO_4 40°C	s	g								
esca.f266	" "	" "	m	g		5.26	14.63	76.69	1.80			1.35
esca.f265	" "	" "Check for Kauyr	s	g								
esca.f267	" "	" "	n	g	HRES			*				

esca file #	notebook reference	description	scan	angle	res	F	O	C	Si	S	K2	Cr	N
escaf.268	VI 45	Rxn of 12 hr RPTFE w/$HCOOH/H_2SO_4$ 40°	s	n									
escaf.269	" "	" "	m	n		4.32	10.00	81.59	1.07	1.36	1.71		
esca.f270	" "	" "	m	n	HRES		*						
esca.f274	VI 53	CrO_3 (RT/overnight at 50° pump) 8NO treated RPTFE	s	n									
esca.f275	" "	" "	m	n		68.26	1.57	29.02	1.16				0.00
esca.f281	VI 53	BH_3/ClO_3 treated red PTFE	s	g									
esca.f282	" "	" "	m	g		43.98	9.37	45.81	0.52			0.32	
esca.f283	" "	" "	m	g	HRES			*					
esca.f284	" "	" "	s	n									
esca.f285	" "	" "	m	n		48.92	7.32	42.50	0.84	0.22		0.21	
esca.f286	" "	" "	m	n	HRES			*					
esca.f287	IV 63	$BH_3/NaOH/H_2O_2$ then CrO_3 on RPTFE	s	g									
esca.f288	" "	" "	m	g		66.10	2.78	30.99	0.00	0.13		0.00	
esca.f330	VI 51	PIA tagged MA rxn on RPTFE	s	g									
esca.f331	" "	" "	m	g		4.91	16.50	75.38	1.42				0.54
esca.f332	" "	" "	s	n									
esca.f333	" "	" "	m	n		5.38	15.12	77.58	0.98				0.54
esca.f334	VI 51	MA control (12°C on RPTFE) no hν	s	g									
esca.f335	" "	" "	m	g		4.16	14.73	79.20	1.90				
esca.f336	" "	" "	s	n									
esca.f337	" "		m	n		2.82	13.50	82.49	1.20				
esca.f338	" "	" "	m	n	HRES			*					
esca.f436	VI 59	3 day reduced PTFE Check for IR rxns	s	n									
esca.f437	" "	" "	m	n		2.59	10.04	85.85	1.53				
esca.f438	" "	" "	m	n		*		*					

esca file #	notebook reference	description	scan	angle	res	F	O	C	Si	Cr	Cl	S	N
esca.f439	VI 59	Home made benzoin RPTFE (2 day rxn)	s	g									
esca.f440	" "	" "	m	g		3.39	7.90	87.91	0.89				
esca.f441	" "	" "	s	n									
esca.f442	" "	" "	m	n		2.01	4.47	93.19	0.33				
esca.f443	" "	" "	m	n	HRES	*		*					
ESCA.F444	" "	" "	m	g	HRES	*		*					
esca.f540	CCVI 63-1	RPTFE/BH_3/CrO_3 0°C	s	g									
esca.f541	" "	" "	m	g		23.94	20.07	53.82	0.84	1.33			
esca.f542	" "	" "	m	g	HRES			*					
esca.f543	" "	" "	s	n									
esca.f544	" "	" "	m	n		50.51	16.31	50.50	.39	1.29			
esca.f545	" "	" "	m	n	HRES			*					
esca.f546	VI 63-1	$SOCl_2$ on BH_3/CrO_3/0°C/15 min of esca.f540	m	n	HRES			*					
esca.f547	" "	" "	m	n		49.16	7.35	41.72	0.64		1.14		
esca.f548	" "	" "	m	n	HRES			*					
esca.f582	VI 63-2	BH_3/CrO_3/0°C/15 min on 24 hr RPTFE (see pg. 66)	s	g									
esca.f583	" "	" "	m	g		4.29	30.14	60.86	0.90	1.36		1.82	
esca.f584	" "	" "	m	g	HRES			*					
esca.f585	" "	" "	s	n									
esca.f586	" "	" "	m	n		7.31	26.18	62.56	1.20	1.31		1.44	
esca.f587	" "	" "	m	n	HRES			*					
esca.f600	" "	CDI tag on esca.f582	s	g									
esca.f601	" "	" "	m	g		4.20	24.50	65.45					5.84
esca.f602	" "	" "	s	n									
esca.f603	" "	" "	m	n		6.26	22.69	63.15	0.00	1.21	1.62		5.66

esca file #	notebook reference	description	scan	angle	res	F	O	C	Si	K	S	Cr	Na
esca.f604	CCVI 63-3	PTFE-COOH	s	g									
esca.f605	" "	" "	m	g									
esca.f606	" "	" "	s	n		58.19	3.89	37.22		0.47	0.23	0.00	
esca.f607	" "	" "	m	n									
esca.g1	CCVI6304	PTFE-COOH/BH/BH_3/ CrO_3/0°35 min NO_2 4% wash	s	g		58.89	3.21	37.71		0.00	0.19	0.00	
esca.g2	" "	" "	m	g									
esca.g3	" "	" "	s	n		19.86	22.29	55.47	0.73		0.22	1.73	0.00
esca.g4	" "	" "	m	n									
esca.g5	CCVI 63-3	CRI rxn on PTFE-COOH	s	g		26.22	19.61	50.84	1.27		0.44	1.34	0.28
esca.g6	" "	" "	m	g									
esca.g7	" "	" "	s	n		39.24	11.43	44.74	0.68		0.00	0.52	
esca.g8	" "	" "	m	n									
esca.g9	CCVI 63-4	CDINn on PTFE-COOH (LSCa.g1)	s	g		42.05	10.58	44.07	0.73		0.19	0.47	
esca.g10	" "	" "	m	g									
esca.g11	" "	" "	s	n		14.81	25.96	53.07	0.41		0.25	0.95	
esca.g12	" "	" "	m	n									
esca.g13	CCVI 67-1	DA MN rxn on 5 hr RPTFE(50°C)	s	g		17.58	24.91	52.85	0.06		0.15	0.84	
esca.g14	" "	" "	m	g									
esca.g15	" "	" "	m	g	HRES	3.18	17.45	76.63	2.10				
esca.g16	" "	" "	s	n				*					
esca.g17	" "	" "	m	n									
esca.g18	" "	" "	m	n	HRES	5.13	15.63	77.62	1.62				
esca.g63	CCVI71-1	CDI tagged MA surfaces	g					*					
esca.g64	" "	" "	m	g									
esca.g65	" "	" "	s	n		4.84	14.89	75.31	1.94				
esca.g66	" "	" "	m	n		4.31	13.03	78.54	0.91				

esca file #	notebook reference	description	scan	angle	res	F	O	C	Si	N	Cr	Cl	S
esca.g67	VI 67-2	MA rxn/dilute H+ workup	s	g									
esca.g68	" "	" "	m	g		6.70	16.46	75.58	1.25				
esca.g68	" "	" "	s	n									
esca.g69	" "	" "	s	n									
esca.g70	" "	" "	m	n		4.80	15.89	78.27	1.03				
esca.g77	CCVI 71-1	CrO_3 oxidized	s	g									
esca.g78	" "	" "	m	g		21.23	29.99	45.88	0.17	0.77	0.67	1.29	
esca.g79	" "	" "	s	n									
esca.g80	" "	" "	m	n		20.42	31.02	45.34	0.56	0.83	0.60	12.24	
esca.g82	CCVI 67-2	CDI rxn on MA rxn dilute HCl washed	s	g									
esca.g83	" "	" "	m	g		8.24	17.73	67.09	2.14	4.72		0.08	
esca.g84	" "	" "	s	n									
esca.g85	" "	" "	m	n		6.62	14.93	73.24	1.00	4.16		0.05	
esca.g86	" "	test for x-ray exposure	s	g									
esca.g87	" "	" "	m	g		8.28	16.80	68.5	1.72	4.69		0.00	
esca.g88	VI 71-2	BH_3/THF/NH_4OH NaOCl	s	g									
esca.g89	" "	" "	m	g		12.01	19.32	64.03	0.55	4.08			
esca.g90	" "	" "	s	n									
esca.g91	" "	" "	m	n		13.24	8.55	65.34	0.19	2.68			
esca.g92	VI 71-1	CrO_3 oxidized (washed in HNO_3)	s	g									
esca.g94	" "	red PTFE COI tagged	m	g		48.17	8.87	39.94	1.74	1.23	0.21		0.44
esca.g95	" "	" "	s	n									
esca.g96	" "	" "	m	n		52.18	7.75	37.92	1.09	0.63	0.22		0.21
esca.g97	VI 71-3	MA rxn TFA Acid hydrolysis	s	g									
esca.g98	" "	" "	m	n		30.68	12.28	56.35	0.69				
esca.g99	" "	" "	s	n									
esca.g100	" "	" "	m	n		33.96	10.52	52.35	3.17				
esca.g101	" "	" "	m	n	MRES								

esca file #	notebook reference	description	scan	angle	res	F	O	C	Si	N
esca.g105	CCVI 71-3	CD1 on MA/TFAA/H_2O	s	g						
esca.g102	" "	" "	m	g		19.90	18.02	56.35	2.61	3.13
esca.g103	" "	" "	s	n						
esca.g104	" "	" "	m	n		31.68	9.48	55.27	0.86	2.71
esca.g136	CCVI 75-2	RPTFE thin DMADCs	g							
esca.g137	" "	" "	m	g		18.19	9.95	70.57	1.30	
esca.g138	" "	" "	s	n						
esca.g139	" "	" "	m	n		25.89	6.27	67.27	0.51	
esca.g140	CCVI 75-2	repeat of 136	s	g						
esca.g141	" "	" "	m	g		13.33	13.64	72.48	0.56	
esca.g142	" "	" "	s	n						
esca.g143	" "	" "	m	n		16.74	11.63	70.86	0.77	
esca.g144	CCVI 75-3	10 min RPTFE control for DA MnS	s	g						
esca.g145	" "	" "	m	g		12.51	8.37	76.91	2.21	
esca.g146	" "	" "	s	n						
esca.g147	" "	" "	m	n		15.45	8.20	74.55 *	1.79	
esca.g148	" "	" "	m	n	HRES					
esca.g172	CCVI 75-3	RPTFE/THF (50°C overnight) control for 144	s	g						
esca.g173	" "	" "	m	g		11.31	10.55	77.54 *	0.06	
esca.g174	" "	" "	m	g	HRES					
esca.g175	" "	" "	s	n						
esca.g176	" "	" "	m	n		10.72	10.52	78.76 *	0.00	
esca.g177	" "	" "	m	n	HRES					
esca.g182	V1 79-1	MA/H_2O/TFAA 24 hrs	s	g						
esca.g183	" "	" "	m	g		10.94	15.09	73.12 *	0.85	
esca.g184	" "	" "	m	g	HRES					

esca file #	notebook reference	description	scan	angle	res	F	O	C	Si	N
esca.g185	CCV1 79-1	MA/H_2O/TFAA 24 hrs	s	n						
esca.g186	" "	" "	m	n		10.59	14.79	74.04 *	0.59	
esca.g187	" "	" "	m	n	HRES					
esca.g188	CCVI79-1	CD1 rxn on esca.g182	s	g						
esca.g189	" "	" "	m	g		12.49	12.15	71.41 *	0.51	3.44
esca.g190	" "	" "	m	g	HRES					
esca.g191	" "	" "	s	n						
esca.g192	" "	" "	m	n		11.51	11.90	73.08	0.65	2.79
esca.g193	" "	" "	m	n	HRES					
esca.g206	CCVI 79-2	HCOOH/AIBN/50°	s	g			*			
esca.g207	" "	" "	m	g		10.23	8.39	77.57 *	0.96	2.85
esca.g208	" "	" "	m	g	HRES					
esca.g209	" "	" "	s	n						
esca.g210	" "	" "	m	n		12.04	7.49	77.95 *	0.74	1.77
esca.g211	" "	" "	m	n	HRES					
esca.g212	CCVI79-2	CDI rxn on 13 ca.g206	s	g						
esca.g213	" "	" "	m	g		9.06	8.61	78.81	0.59	2.94
esca.g214	" "	" "	s	n						
esca.g215	" "	" "	m	n		9.95	7.22 *	79.85	0.92	2.06
esca.g216	" "	" "	m	n	HRES					
esca.g217	VI 81-1	HCOOH AIBN/hυ 5°	s	g						
esca.g218	" "	" "	m	g		18.12	7.13	72.21	2.54	
esca.g219	" "	" "	s	n						
esca.g220	" "	" "	m	n		22.48	6.30 *	69.05	2.17	
esca.g221	" "	" "	m	n	HRES					

esca file #	notebook reference	description	scan	angle	res	F	O	C	Si	Al	Cl	N
esca.g222	VI 81-2	$AlCl_3$/ClCOCOCl on highly RPTFE	s	g								
esca.g223	" "	" "	m	g								
esca.g224	" "	" "	m	g	HRES	2.75	14.91	79.00	1.81	0.13	1.40	
esca.g225	" "	" "	s	n			*					
esca.g226	" "	" "	m	n								
esca.g227	" "	" "	m	n	HRES	1.90	12.39	80.87	1.23	1.04	1.10	1.47
esca.g231	VI 81-1	CDI on HCOOH/AIB/hυ	s	g			*					
esca.g232	" "	" "	m	g								
esca.g233	" "	" "	s	n		19.67	6.02	70.01	0.39			3.91
esca.g234	" "	" "	m	n								
esca.g235	" "	" "	m	n	HRES	22.39	5.90	66.44	1.18			4.09
esca.g238	VI 81-2	CDI on $AlCl_3$/ClCOCOCl on RPTFE	s	g				*				
esca.g239	" "	" "	m	g								
esca.g240	" "	" "	s	n		3.14	18.09	69.81	2.02	1.89	0.67	4.39
esca.g241	" "	" "	m	n								
esca.g242	" "	" "	m	n	HRES	3.00	15.61	74.39	1.31	1.70	0.39	2.73
esca.g243	VI 83-1	$CH_3(OOH)$ AIBN/hr 100° on RPTFE	s	g				*				
esca.g244	" "	" "										
esca.g245	" "	" "	m	g								
esca.g246	" "	" "	m	g	HRES	6.58	5.18	84.61	0.84			2.79
esca.g247	" "	" "	s	n			*					
esca.g248	" "	" "	m	n								
esca.g249	" "	" "	m	n	HRES	8.97	4.93	83.08	0.47			2.28
esca.g250	" "	" "	s	g				*				
			m	g		6.40	5.28	84.89	0.93			2.51

esca file #	notebook reference	description	scan	angle	res	F	O	C	Si	N	Cl
esca.g315	VI85-1	repro of 83-3	m	g	HRES			*			
esca.g316	" "	" "	s	n							
esca.g317	" "	" "	m	n		11.31	7.80	77.16	1.14	2.59	
esca.g318	" "	" "	m	n	HRES			*			
esca.g327	VI 85-2	CDI or maleic acid Diels Alden	s	g							
esca.g328	" "	" "	m	g		10.47	15.45	71.93	0.61	1.54	
esca.g329	" "	" "	s	n							
esca.g330	" "	" "	n	n		12.69	11.64	74.57	1.08	0.02	
esca.g331	" "	" "	m	n	HRES			*			
esca.g339	VI 87-1	MA/nυ/AIBN 2 hrs	s	g							
esca.g340	" "	" "	m	g		4.72	22.93	67.58	1.45	3.33	
esca.g341	" "	" "	m	g	HRES			*			
esca.g342	" "	" "	s	n							
esca.g343	" "	" "	m	n		5.60	21.58	69.96	0.99	1.88	
esca.g344		" "	m	n	HRES			*			
esca.g345		PTFE control (THF extracted)	s	n							
esca.g346		" "	m	n		70.75	0.03	29.22	0.00		
esca.g347	VI 83-1	Hydrolysis on TCNE	s	g							
esca.g348		" "	m	g		7.37	3.18	72.90	1.17	4.78	
esca.g349	" "	" "	s	n							
esca.g350	" "	" "	m	n		5.95	10.00	76.13	0.87	6.56	0.50
esca.g351	" "	" "	m	n	HRES			*			
esca.g364	VI 87-2	MAhυ/AIBN/H_2O TFAA	s	g							
esca.g365	" "	" "	m	g		8.12	15.30	74.80	1.40	0.38	
esca.g366	" "	" "	m	g	HRES			*			

esca file #	notebook reference	description	scan	angle	res	F	O	C	Si	N	Br	N	Cl
esca.g431	VI 91-1	Br_2 treated RPTFE	s	n									
esca.g432	" "	" "	m	n									
esca.g433	" "	" "	m	n		13.04	5.63	61.30	0.50	19.53			
esca.g446	V1 91-1	$NaNH_2/NH_3$ on Br_2/CCl_4 RPTFE	m	n	HRES		•						
esca.g447	" "	" "	s	n									
esca.g448	" "	" "	m	n		11.23	13.96	65.64	0.59	0.03	8.40	0.15	
esca.g449	" "	" "	s	n									
esca.g450	" "	" "	m	n		8.01	14.48	68.72	0.68	0.07	7.65	0.39	
esca.g464	V1 91-3	NH_3 MPTFE	m	n	HRES			•					
esca.g465	" "	" "	s	g									
esca.g466	" "	" "	m	g		6.19	5.66	87.68	0.14		0.34		
esca.g467	" "	" "	s	n									
esca.g498	VI 91-2	NH_3 on Br_2/CCl_4 at rxn temp	m	n		6.23	5.03	87.96	0.46		0.31		
esca.g499	" "	" "	s	g									
esca.g500	" "	" "	m	g		11.00	7.78	73.63	0.62	2.14	4.84		
esca.g501	" "	" "	s	n									
esca.g532	V1 93-2	Cl_3-C-C-Cl tag on NH_3/Br_2 at -75°	m	n		10.10	6.75	75.32	0.55	2.48	4.80		
esca.g533	" "	" "	s	g									
esca.g534	" "	" "	m	g		10.17	7.56	64.81	0.25	7.33	2.98		6.89
esca.g535	" "	" "	s	n									
esca.g536	" "	" "	m	n		12.62	6.42	62.65	0.22	7.68	3.97		6.42
esca.g544	V1 93-1	NH_3 on RPTFE	m	n	HRES								
esca.g545	" "	" "	s	g									
esca.g546	" "	" "	m	g		7.30	3.29	88.18	0.47		0.77		
esca.g547	" "	" "	s	n									
			m	g		6.60	4.07	87.77	0.72		0.83		

esca file #	notebook reference	description	scan	angle	res	F	O	C	Si	Cl	Br	Cl
esca.g548	CCVI 95-1	NH_3 on Br_2 RPTFE 25°C	s	g								
esca.g549	" "	" "	m	g		13.20	9.35	70.99	0.55	4.70	1.20	
esca.g550	" "	" "	s	n								
esca.g551	" "	" "	m	n		13.54	8.83	70.68	0.00	5.77	1.18	
esca.g552	" "	" "	m	n	HRES			•				
esca.g561	CCVI 95-2	Br_2 on RPTFE control for $Cl3_3$-C-C-Cl tagging rxn	s	g								
esca.g562	" "	" "	m	g		3.66	13.04	60.54	3.38		19.39	0.00
esca.g563	" "	" "	s	n								
esca.g564	" "	" "	m	n		5.61	01.02	64.88	8.00		19.41	0.09
esca.g575	CCV1 93-1	Cl_3-C-C-Cl on NH_3 RPTFE	s	g								
esca.g576	" "	" "	m	g		6.59	6.88	76.09	6.56	1.93		7.96
esca.g577	" "	" "	s	n								
esca.g578	" "	" "	m	m		5.72	6.52	77.74	0.28	1.57		8.17
esca.g579	CCV1 95-2	Cl_3-C-C-Cl control on Br_2/CCl_4 on RPTFE	s	g								
esca.g580	" "	" "	m	g		7.44	5.27	63.96	0.15		18.67	4.52
esca.g581	" "	" "	s	n								
esca.g582	" "	" "	m	n		9.59	4.21	65.50	0.00		16.21	4.49
esca.g583	VI 95-1	Cl_3-C-C-Cl on NH_3/Br_2 RPTFE	s	g								
esca.g584	" "	" "	m	g		12.79	9.26	64.47	0.52	4.04	0.82	8.05
esca.g885	" "	" "	m	g	HRES			•				
esca.g586	" "	" "	s	n								
esca.g587	" "	" "	m	n		13.71	8.03	64.88	0.23	4.54	0.93	7.68
esca.g588	" "	" "	m	n	HRES		•					
esca.g589	" "	" "	m	n		15.58	12.22	67.22	6.00	4.25	0.76	0.00
esca.g603	VI 97-2	Cl_3-C-C-Cl tag control on RPTFE	s	g								
esca.g604	" "	" "	m	g		3.65	7.39	83.00	0.67			5.30

esca file #	notebook reference	description	scan	angle	res	F	O	C	Si	Cl	N	Bu	Br
esca.g605	VI97-2	Cl_3-C-Cl tag	s	n									
		control on RPTFE											
esca.g606	" "	" "	m	n									
esca.g607	" "	" "	m	n		3.20	5.93	85.74	6.02	5.10			
esca.g612	VI 97-1	MA NN CH_2Cl_2 extracted	a	g	HRES			*					
esca.g613	" "	" "	m	g									
esca.g614	" "	" "	m	g		8.48	17.60	71.07	1.03	0.43	1.39		
esca.g615	" "	" "	s	n	HRES			*					
esca.g616	" "	" "	m	n									
esca.g617	" "	" "	m	n		9.14	16.84	71.82	1.13	2.11	0.91		
esca.g618	VI 97-1	NH_3 on MA/hυ/AIBN	s	g	HRES		*						
		CH_2Cl_2 reacted											
esca.g619	" "	" "	m	g									
esca.g620	" "	" "	s	n		10.62	19.66	65.68	0.28	0.76	3.01		
esca.g621	" "	" "	m	n									
esca.622	" "	" "	m	n		10.98	18.54	67.65	0.07	0.53	2.20	0.04	
esca.g631	VI 99-1	CDI control on RPTFE	s	g	HRES			*					
		washed in THF/heptane											
esca.g632	" "	" "	m	g									
esca.g633	" "	" "	s	n		4.54	4.89	89.80	0.50		0.27		
esca.g634	" "	" "	m	n									
esca.g653	VI99-1	CDI control on RPTFE	s	g		4.97	4.41	88.89	0.13		1.90		
		CH_2Cl_2 extracted											
esca.g654	" "	" "	m	g									
esca.g655	" "	" "	s	n		6.30	8.97	84.06	0.14	0.53	0.00		
esca.g656	" "	" "	m	n									
esca.g687	VI 101-2	NH_3 on Br_2 RPTFE	s	g		5.50	7.56	86.51	0.00	0.43	0.00		
esca.g688	" "	" "	m	g									
esca.g689	" "	" "	s	n		12.99	7.41	71.12	0.12		6.39		1.97
esca.g690	" "	" "	s	n									
esca.g691	" "	" "	m	n	HRES	13.04	7.15	70.98	0.34		6.64		1.84
							*						

esca file #	notebook reference	description	scan	angle	res	F	O	C	Si	B	N	Br	Cl
esca.g692	VI 101-1	BH_3/CH_3 COOH on Red PTFE	s	g									
esca.g693	" "	" "	m	g		36.34	10.88	45.71	0.83	6.25			
esca.g694	" "	" "	s	n									
esca.g695	" "	" "	m	n		48.45	9.49	38.19	0.00	3.87			
esca.g696	VI 101-2	Cl_3-C-C-Cl tagging on	s	g									
		NH_3/Br_2 on RPTFE CH_2Cl_2 extracted											
esca.g697	" "	" "	m	g		11.83	11.44	60.27	1.84		4.24	0.98	9.30
esca.g698	" "	" "	s	n									
esca.g699	" "	" "	m	n		7.45	8.49	66.54	0.92		5.51	1.60	9.43
esca.g700	" "	" "	m	n	UTIL			*					
esca.g701	" "	" "	m	n	HRES			*					
esca.g733	VI 103-1	Cl_3-C-C-N-C=O on RPTFE	s	g									
esca.g734	" "	" "	m	g		13.97	7.99	64.42			1.87		11.76
esca.g735	" "	" "	s	n									
esca.g736	" "	" "	m	n		14.42	6.92	65.43	0.65		6.52		12.07
esca.g737	" "	" "	m	n	HRES			*					
esca.g750	VI 107-1	RPTFE control for SA	s	g									
		tagging exp											
esca.g751	" "	" "	m	g		8.10	3.83	87.55	0.52				
esca.g752	" "	" "	m	g	HRES			*					
esca.g753	" "	" "	s	n									
esca.g754	" "	" "	m	n		8.91	1.88	88.02	0.19				
esca.g766	V 107-2	RPTFE control for PFB	s	g									
		tagging exp.											
esca.g767	" "	" "	m	g		11.24	5.36	83.05	0.34				
esca.g768	" "	" "	m	g	HRES			*					
esca.g769	" "	" "	s	n									
esca.g770	" "	" "	m	n		12.60	5.56	80.65	1.19				
esca.g771	" "	" "	m	n	HRES				*				

esca file #	notebook reference	description	scan	angle	res	F	O	C	Si	Cl
esca.g775	VI 107-1	SA control on Red PTFE extracted CH_2Cl_2	s	g						
esca.g776	" "	" "								
esca.g777	" "	" "	m	g						
esca.g778	" "	" "	m	g	HRES	28.54	4.62	65.39 •	0.68	0.77
esca.g779	" "	" "	s	n						
esca.g780	" "	" "	m	n						
esca.g781	VI 109-1	Red PTFE for SA (washing control)	m	n	HRES	31.92	3.96	63.46 •	0.00	0.65
esca.g782	" "	" "	s	g						
esca.g783	" "	" "	m	g						
esca.g784	" "	" "	m	g	HRES	7.43	3.73	88.30 •	0.55	
esca.g785	" "	" "	s	n						
esca.g786	" "	" "	m	n						
esca.g792	VI 107-2	PFB tagged RPTFE	m	n	HRES	10.79	2.18	86.74 •	0.29	
esca.g793	" "	" "	s	g						
esca.g794	" "	" "	m	g						
esca.g795	" "	" "	m	g	HRES	9.03	7.76	82.86 •	0.35	
esca.g796	" "	" "	s	n						
esca.g797	" "	" "	m	n						
esca.g798	V 109-1	SA tagged RPTFE	m	n	HRES	9.22	7.38	83.16 •	0.24	
esca.g799	" "	" "	s	g						
esca.g800	" "	" "	m	g						
esca.g801	" "	" "	m	g	HRES	10.66	4.47	8.187 •	0.00	
esca.g802	" "	" "	s	n						
esca.g803	" "	" "	m	n						
esca.g804	V 109-2	RPTFE for THF control	m	n	HRES	16.56	7.34	76.09 •	0.01	
esca.g805	" "	" "	s	g						
esca.g806	" "	" "	m	g						
			m	g	HRES	4.19	3.26	92.27 •	0.28	

esca file #	notebook reference	description	scan	angle	res	F	O	C	Si	N	Cl	Br
esca.g807	VI 109-2	Red PTFE Control for THF	s	n								
esca.g808	" "	" "	m	n								
esca.g809	" "	" "	m	n	HRES	4.28	4.28	91.26 •	0.18			
esca.g820	VI 109-2	RPTFE/24 hr/RT control	s	g								
esca.g821	" "	" "	m	g								
esca.g822	" "	" "	m	g	HRES	4.15	6.31	88.33 •	1.21			
esca.g823	" "	" "	s	n								
esca.g824	" "	" "	m	n								
esca.g825	" "	" "	m	n	HRES	5.86	5.60	87.89 •	0.65			
esca.g84844	CCVI 111-1	MA/AIBN/H_2O/grazing	s	g								
esca.g84815	" "	" "	m	g								
esca.g846	" "	" "	m	g	HRES	9.40	20.31	67.23 •		1.30	1.43	
esca.g847	" "	" "	s	n								
esca.g848	" "	" "	m	n								
esca.g849	" "	" "	m	n	HRES	7.16	18.71	70.22 •	0.35	1.73	1.83	
esca.g857	CCVI 105-1	PFB tag on Br_2/NH_3/RPTFE	s	g								
esca.g858	" "	" "	m	g								
esca.g859	" "	" "	m	g	HRES	15.11	18.85	62.31 •	0.40	2.54		0.79
esca.g860	" "	" "	s	n								
esca.g861	" "	" "	m	n								
esca.g862	" "	" "	m	n	HRES	18.56	14.55	60.86 •	0.79	4.04		1.19
esca.g863	VI 103-2	PFB tag on RPTFE Br_2/NH_2	s	g								
esca.g864	" "	" "	m	g								
esca.g865	" "	" "	s	n		18.14	16.50	60.53 •	0.79	3.27		0.77
esca.g866	" "	" "	m	n								
esca.g867	" "	" "	m	n	HRES	17.62	12.91	64.01 •	0.08	4.12		1.26

esca file #	notebook	description	scan	angle	res	F	O	C	Si	N	Cl	Br
esca.g870	CCVI 111-1	CDI tag on MA/AIBN/hυ CH_2Cl_2 extracted	s	g								
esca.g871	" "	" "	m	g								
esca.g872	" "	" "	m	g	HRES	11.35	19.34	62.26 •	0.15	3.25	3.15	
esca.g873	" "	" "	s	n								
esca.g874	" "	" "	m	n								
esca.g875	" "	" "	m	n	HRES	11.04	18.79	61.99 •	0.78	3.87	3.52	
esca.g881	VI 111-2	dry Br_2/CCl_4 on RPTFE	s	g								
esca.g882	" "	" "	m	g								
esca.g883	" "	" "	m	g	HRES	12.26	3.94	51.78 •	0.00	1.95	7.11	22.97
esca.g884	" "	" "	m	g		no check						
esca.g885	" "	" "	m	g		no check						
esca.g887	" "	" "	m	n		11.73	4.36	59.58	0.00	2.88	2.20	19.25
esca.g888	" "	" "	s	g								
esca.g889	" "	" "	s	n								
esca.g890	" "	" "	m	n								
esca.g891	" "	" "	m	n	HRES	15.39	5.06	60.12 •	0.00	1.46	0.94	17.04
esca.g892	" "	" "	m	g		15.73	4.71	62.85	0.00	1.19	0.00	15.52
esca.g893	VI 112	NH_3 on Br_2/CCl_4 RPTFE	s	g								
esca.g894	" "	" "	m	g								
esca.g895	" "	" "	m	g	HRES	13.08	7.79	69.23 •	0.67	6.38	1.79	1.07
osca.g896	" "	" "	s	n								
esca.g897	" "	" "	m	n								
esca.g898	" "	" "	m	n	HRES	14.56	5.21	69.85 •	0.00	6.30	2.85	1.24
esca.g899	VI 113-1	NH_3 on Br_2 rPTFE	s	g								
esca.g900	" "	" "	m	g								
esca.g901	" "	" "	m	g	hRES	16.04	8.87	68.11 •	0.13	5.68	0.08	1.08

esca file #	notebook reference	description	scan	angle	res	F	O	C	Si	Br	N	Cl
esca.g902	VI 113-1	NH_3 on Br_2-PTFE	s	n								
esca.g903	" "	" "	m	n								
esca.g904	" "	" "	m	n	HRES	13.76	6.48	71.68 •	0.94	1.07	60.07	0.00
esca.g910	VI 113-1	PFB on NH_3/Br_2 RPTFE	s	g								
esca.g911	" "	" "	m	g								
esca.g912	" "	" "	m	g	HRES	20.62	9.32	63.39 •	0.95	0.75	3.71	1.26
esca.g913	" "	" "	s	n								
esca.g914	" "	" "	m	n								
esca.g915	" "	" "	m	n	HRES	21.54	8.49	63.80 •	0.80	0.90	4.46	0.00
esca.g916	VI 115-1	MA/AIBN/hυH_2O/TFAA	s	g								
esca.g917	" "	" "	m	g								
esca.g918	" "	" "	m	g	HRES	10.35	21.65	67.43 •	0.00		0.56	
esca.g919	" "	" "	s	n								
esca.g920	" "	" "	m	n								
esca.g921	" "	" "	m	n	HRES	9.52	18.76	70.91 •	0.00		0.82	
esca.g922	" "	" Au Au_2 Si	m	n								
esca.g923	" "	" other side	m	g		13.60	16.90	67.04	0.88		1.51	
esca.g924	" "	" "	s	m								
esca.g925	" "	" "	m	n		12.34	15.09	72.38	0.19		0.00	
esca.g926	" "	" "	s	g								
esca.g927	VI 115-1	CDI tag on MA/AIBN/H_2O/TFAA	m	g								
esca.g928	" "	" "	m	g	HRES	4.94	15.86	75.92 •	0.63		2.65	
esca.g929	" "	" "	s	n								
esca.g930	" "	" "	m	n		5.28	12.72	77.58	0.94		3.48	
esca.g931	" "	" "	m	n		4.15	13.14	80.19	0.18		2.34	
esca.g932	" "	" (x-ray closer)	m	n	HRES			•				
esca.g933	" "	" "										

esca file #	notebook reference	description	scan	angle	res	F	O	C	Si
esca.h39		air oxidized (many months) RPTFE	s	g					
esca.h40	" "	" "	m	g		3.61	35.78	59.42	1.20
esca.h41	" "	" "	s	n					
esca.h42	" "	" "	m	n		1.75	38.72	58.91	0.62

Bibliography

T. Abe and M. Iwaizumi, Bull. Chem. Soc. Japan, **47**, 2593 (1974).

A.W. Adamson, "Physical Chemistry of Surfaces 4th, Edition", Wiley-Interscience, New York, 1982, p. 341.

J.D. Andrade and V. Hlady, Adv. Poly. Sci., **79**, 1 (1986).

S. Andreades and E.W. Zahnow, J. Am. Chem. Soc., **91**, 4181 (1969).

A.E. Ashby, D.H. Bae, W.S. Park, R.N. Depriest, N.Y. Su, Tett. Lett., **25**, (45), 5107 (1984).

B. Bak and D. Christenson, Spectrochimica Acta, **12**, 355 (1958).

G.L. Baker and F.S. Bates, Macromolecules, **17**, 2619 (1984).

D.J. Barker, D.M. Brewis, R.H. Dahm, and L.R.J. Hoy, Polymer, **19**, 856 (1978).

D.J. Barker, D.M. Brewis, R.H. Dahm, and L.R.J. Hoy, J. Mat. Sci., **14**, 749 (1979).

P.N. Batchelder and D. Bloor, J. Phys. Chem.: Solid State Phys., **15**, 3005 (1982).

F.S. Bates and G.L. Baker, J. de Physique, Colloque, **C3**, supplement au no. 6 Tome **44**, (1983).

N.L. Bauld, J. Am. Chem. Soc., **87**, 4788 (1965).

R. Baumhardt-Nito, S.E. Galembeck, I. Joekes, and F. Galembeck, J. Poly. Sci.: Chem. Ed., **19**, 819 (1981).

K.L. Berry and J.H. Peterson, J. Am. Chem. Soc., **73**, 5195 (1951).

K.L. Berry and H.K. Starkweather, Adv. Poly. Sci., **2**, 465 (1961).

O.S. Bhanot and P.C. Dutta, Chem. Comm., **1968**, 122.

J.J. Bikermann, J. Appl. Phys., **28**, 1484 (1957).

J.J. Bikerman, "The Science of Adhesive Joints", Academic Press, New York, (1961) p. 182.

J. A. Bonafini, A. J. Dias, Z.A. Guzdar, and T.J. McCarthy, J. Poly. Sci.: Poly. Lett. Ed., **23**, 33 (1985).

V.D. Braun, I.A. Aziz el Sayad, J. Pomakis, Makromol. Chem., **224**, 249 (1969).

V.H. Brecht, F. Mayer, and H. Binder, Die Angew. Makro. Chem., **33**, 89 (1973).

D.M. Brewis, R.H. Dahm, and M.B. Konieczko, Die Angew. Makro. Chem., **43**, 191 (1975).

D.M. Brewis, R.H. Dahm, and M.B. Konieczko, Makromol. Chem., **43**, 191 (1975).

J.M. Burkstrand, J. Vac. Sci. Tech., **16**, 1072 (1979).

J.M. Bukstrand, Appl. Phys. Lett., **33**, 5 (1978).

H.J. Busscher, A.W.J. Van Pelt, P. DeBeer, H.P. DeJong, and J. Arends, Colloids and Surfaces, **9**, 319 (1984).

O. Cada and J. Spasova, Adhaesion, **23**, 18 (1979).

D.I. Cane in "Encyclopedia of Polymer Science and Technology", Vol. 13, Wiley, New York, (1970) p. 623.

J.C.W. Chien, "Polyacetylene, Chemistry, Physics, and Materials Science", Academic Press, New York, (1984).

J.C.W. Chien, G.E. Wnek, F.E. Karasz, J.A. Hirsch, Macromolecules, **14**, 479 (1981).

N.J. Chou, D.W. Dong, J. Kim, and A.C Liu, J. Elec. Soc., Solid State Tech., **131**, 2335 (1984).

N.J. Chou and C.H. Tang, J.Vac. Sci. Tech., **A2**, 751 (1984).

D.T. Clark and W.J. Feast, "Polymer Surfaces", Wiley-Interscience, New York, (1978).

E.J. Corey and E. Block, J. Org. Chem., **31**, 1663 (1966).

C.A. Costello and T.J. McCarthy, Macromolecules, **17**, 2942 (1984).

C.A. Costello and T.J. McCarthy, Macromolecules, **18**, 2087 (1985).

F.A. Cotton and G.F. Wilkenson, "Advanced Inorganic Chemistry", Interscience, New York, (1972) p. 906.

N.C. Craig and E.A Entemann, J. Chem. Phys., **36**, 243 (1962).

N.D. Danielson, R.T. Taylor, J.A. Huth, R.W. Siergiej, J.G. Galloway, J.B. Paperman, Ind. Eng. Chem. Prod. Res. Dev., **22**, 303 (1983).

A.J. Dias, T.J. McCarthy, Macromolecules, **18**, 1826 (1985).

A.J. Dias and T.J. McCarthy, Macromolecules, **17**, 2529 (1984).

A.J. Dias and T.J. McCarthy, Macromolecules, **18**, 1826 (1985).

W. Deits, P. Cukor, M. Rubner, and H. Japson, Poly. Prep. Am. Chem. Soc., Div. Poly. Chem., **22**, 197 (1981).

W. Deits, P. Cukor, M. Rubner, and H. Japson, Syth. Metal, **4**, 199 (1982).

J.H Edwards and W.J. Feast, Polymer, **21**, 595 (1980).

J.H. Edwards, W.J. Feast, and D.C. Bott, Polymer, **25**, 395 (1984).

D.S. Everhart and C.N. Reilly, Anal. Chem., **53**, 665 (1981).

W.J. Feast and C.S. Spanomanolis, Polymer Photochemistry, **1**, 285 (1981).

W.A. Feld, A. Ganeson, and D.D. Nymberg, A.C.S. Polymer Preprints, **24**, (1), 143 (1975).

F. Galembeck, J. Poly. Sci. Poly. Lett., **15**, 107 (1977).

M.E. Galvin and G.E. Wnek, Mol. Cryst. Liq. Cryst., **117**, 33 (1985).

N.G. Gaylord, S. Marti, J. Polym. Sci., Poly. Lett. Ed., **11**, 253 (1973).

P.K. Ghosh, "Introduction to Photoelectron Spectroscopy", Wiley, New York, (1983) p. 75.

H.B. Gray, Chem. Soc. Rev., **15**, 17 (1986).

W. Haaf, Chem. Ber., **99**, 1149 (1966).

A.F.S.A. Habeeb, Methods Enzymol., **25**, 457 (1972).

R.H. Hansen and H. Schonhorn, Polymer Letters, **4**, 203 (1966).

S.R. Hanson, L.A. Harker, B.D. Rattner, and A.S. Hoffman, J. Lab. Clin. Med., **95**, 289 (1980).

N.J. Harrick, J. Opt. Soc. Amer., **55**, 851 (1965).

N.J. Harrick, "Internal Reflection Spectroscopy", Harrick Scientific Corporation, New York, 1979.

F.F. He and H. Kise, J. Poly. Sci., Poly. Chem. Ed., **21**, 1729 (1983).

I. Heinmaa, M. Alla, A. Vainrub, E. Lippmaa, M.L. Khidekel, A.I. Kotov, and G.I. Kozub, J. Phys. Coll., **44**, C3-357 (1983).

P.S. Ho, P.O. Hahn, J.W. Bartha, G.W. Rubloff, F.K. Leboues, and B.D. Silverman, J. Vac. Sci. Tech., **A3**, 739 (1985).

S.R. Holmes-Farley, R.H. Reamey, T.J. McCarthy, J. Deutch, and G.M. Whitesides, Langmuir, **1**, 725 (1985).

J.A. Huth, N.D. Danielson, Anal. Chem., **54**, 930 (1982).

S.W. Jacob, E.E. Rosenbaum, and D.C. Wood, "Dimethylsulfoxide", Marcel Dekker, New York, (1971) p. 6.

J. Jansta and F.P. Dousek, Carbon, **24**, 61 (1986).

J. Jansta and F.P. Dousek, Electrochemical Acta, **18**, 673 (1973).

R.E. Johnson and R.H. Dettre, "Surface and Colloid Science", Vol. 2, (Matijevic, ed.), Wiley-Interscience, New York, 1969.

B.B. Johnson and W.L. Peticolas, Ann. Rev. Phys. Chem., **27** 465 (1976).

J.I. Jones, P.B. Tinker, J. Chem. Soc., **1955** 1286.

G.W. Kabalka, K.A.R. Satry, G.W. McCollum and H. Yoshioka, J. Org. Chem, **46**, 4296 (1981).

E.T. Kaiser, "Radical Ions', Interscience, New York, (1968) p. 87.

H.E. Kambic, S. Murabayashi, and Y. Nose, Chem. Eng. News, **15**, 31 (April 14, 1986).

F.E. Karasz, J.D. Capistran, D.R. Gagnon, and R.W. Lenz, Mol. Cryst. Liq. Cryst., **118**, 327 (1985).

K. Kato, J. Appl. Poly. Sci., **15**, 2115 (1971).

L. Kavan, Z. Bastl, F.P. Dousek, and J. Jansta, Carbon, **22**, 77 (1984).

L. Kavan and F.P. Dousek, Carbon, **24**, 61 (1986).

L. Kavan, J. Klima, and M. Pseidlova, Carbon, **18**, 433 (1980).

G.P. Koo and R.D. Andrews, Poly. Eng. Sci., **9**, 268 (1969).

R.H. Kratzer, K.L. Paciorek, and D.N. Karle, J. Org. Chem., **41**, (12), 2230 (1976).

C.Y. Lang, S. Krum. J. Chem. Phys., **25**, 563 (1956).

J.L. Lang, W.A. Pavelich, H.D. Cleary, J. Poly. Sci. A, **1**, 1123 (1963).

J.C. Lhuguenot and B.F. Maume, J. Chromatogr. Sci., **12**, 411 (1974).

L.S. Lichtmann, A. Sarangi, and D.B. Fitchen, Solid State Commun., **36** 869 (1980).

J. March, "Advanced Organic Chemistry", McGraw Hill, New York, p. 28.

G.E. Marcriel and M.J. Sullivan, "NMR Spectroscopy: Newer Methods and Applications; A.C.S. Symposium 191", American Chemical Society, (1982) p. 319.

D.I. McCane in "Encyclopedia of Polymer Science and Technology", Vol. 13, Wiley, New York (1970) p. 623.

R. Michael and D. Stalik, J. Vac. Sci. Tech., **A4**, 1861 (1986).

F.M. Mirambella, J. Poly. Sci.: Poly. Phys. Ed., **20**, 2309 (1982).

K.L. Mittal, J. Vac. Sci. Tech., **13**, 19 (1976).

A.C. Moffat, E.C. Horning, S.B. Martin, M. Rowland, J. Chromatogr., **66**, 255 (1972).

I. Murase, T. Ohnishi, T. Noguchi, M. Hirooka, and S. Murakami, Mol. Cryst. Liq. Cryst., **118**, 333 (1985).

K. Nakanishi, "Practical Infrared Absorption Spectroscopy", Holden-Day, San Francisco, (1962) p. 45.

E.R. Nelson, T.J. Kilduff, and A.A Benderly, Ind. Eng. Chem., **50**, 329 (1958).

F.S. Ohuchi and S. Frielich, J. Vac. Sci,. Tech., **A4**, 1039 (1986).

H. Oppenheimer, Chem. Ber., **19**, 1814 (1886).

L.S. Penn and B. Miller, J. Coll. Int. Sci., **77**, 574 (1980).

C.J. Pouchet, "The Aldrich Library of Infrared Spectra: Edition III", Aldrich Chemical Company, Milwaukee, (1981).

C.J. Powell, Surface Science, **44**, 29 (1974).

R.F. Roberts and H. Schonhorn, Am. Chem. Soc. Div. Poly. Chem. Prep., **16**, 146 (1975).

R.J. Roser and F.R. Whitt, J. Appl. Chem., **10**, 229 (1960).

G.A. Russel, J. Org. Chem., **32**, 353 (1967).

M. Schwoerer, V. Lauterbach, W. Mueller, and G. Wegner, Chem. Phys. Lett., **69**, 359 (1980).

A.K. Sharma and H. Yasuda, J. Vac. Sci. Tech., **21**, 994, (1982).

D.B. Sharp and E.L. Miller, J. Am. Chem. Soc., **74**, 5643 (1952).

G.M. Sessler, J.E. West, F.W. Ryan, and H. Schornhorn, J. Appl. Poly. Sci, **7**, 3199 (1973).

B.A. Sexton and G.L. Nyberg, Surface Science, **165**, 251 (1986).

R.W. Siergieri and N.D. Danielson, Anal. Chem., **55**, 17 (1983).

R.W. Siergiej and N.D. Danielson, J. Chromatogr. Sci., **21**, 362 (1983).

C.A. Sperati and H.W. Starkweather, Fortschr. Hochpolym.-Forsch., 2, 465 (1961).

H.W. Starkweather, R.C. Ferguson, D.B. Chase, and J.M. Minor, Macromolecules, **18**, 1684 (1985).

E. Tsuchida, C. Shih, I. Shinohara, and S. Kambara, J. Poly. Sci.: Pt. A, **2**, 3347 (1964).

A.J. Varma, J.P. Jog, and V.M. Nadkarni, Makromol. Chem. Rapid Comm., **1983**, 715.

C.D. Wagner, W.M. Riggs, L.E. Davis, J.F. Moulder, and G.E. Muilenberg (Editor), "Handbook of X-ray Photoelectron Spectroscopy", Perkin Elmer Corporation, Eden Prairie, Minnesota, (1979).

L.A. Wall, "Fluoropolymers", Wiley-Interscience, New York, (1972).

O.W. Webster, W. Mahler, and R.E. Benson, J. Am. Chem. Soc., **84**, 3681 (1962).

R. Wehr, U.S. Patent 3,414,466, (1968).

R.A. Wessling and R.G. Zimmerman, U.S. Patents, 3,401,152 and 3,706,677.

D.R. Wheeler and S.V. Pepper, J. Vac. Sci. Tech., **20**, 442 (1982).

D.R. Wheeler and S.V. Pepper, J. Vac. Sci. Tech., **20**, 226 (1982).

G.E. Wnek, J.C.W. Chien, F.E. Karasz, and C.P. Lillya, Polymer, **20**, 1441 (1975).

M. Yasaka, Japan Kokai Tokkyo Koho, JP 7953173 (1979).

K. Yoshino, S. Yanagida, T. Sakai, T. Azuma, Y. Inuisha, and H. Sakurai, Jpn. J. Appl. Phys., **21**, L301 (1982).

G. Zannoni and G. Zerbi, J. Mol. Struc., **100**, 485 (1983).